Salahutdin N. Nuritdinov
Alexey S. Rastorguev

EXACT MODELS OF SPHERICAL SELF-GRAVITATING SYSTEMS AND THEIR INSTABILITIES

Moscow, 2023

Salakhutdin N. Nuritdinov and Alexey S. Rastorguev

EXACT MODELS OF SPHERICAL SELF-GRAVITATING SYSTEMS AND THEIR INSTABILITIES

Moscow 2023

The book presents for the first time the possibilities of analytical modeling of the early evolution of galaxies, methods for constructing their nonlinear phase models and studying the stability of nonlinear nonequilibrium states of spherical self-gravitating systems. Accordingly, a number of nonlinear models of the early stage of galaxy evolution are constructed for the first time. A modal analysis of the types of instabilities of nonlinear rotating models of pulsating spherical self-gravitating systems is performed. The problem of detecting instabilities of collapsing states with rotation requires the construction of nonlinear pulsating models that sufficiently cover all possible cases of early stages of evolution in the world of galaxies and individual collisionless self-gravitating systems, in particular, to consider separately the once collapsing or expanding limiting states of their evolution. Classical relaxation problems related to the physical foundations of stellar dynamics are also considered The theoretical results given in the book are obtained mainly by its authors.

УДК 524.6-1/-7:001.891.57
ББК 22.67в643

ISBN 978-5-4499-4038-4

CONTENTS

PREFACE

The modern era of astronomy and astrophysics is primarily the era of extragalactic astronomy, which literally every year brings a lot of amazing discoveries in the world of galaxies and a lot of surprises in the large-scale structure and evolution of the Universe. For today's extragalactic astronomy and cosmology, where there is a clear uncertainty in the choice of one or another model of the Universe, it is extremely important to study the early stages of the evolution of galaxies located at distances of billions of light-years. Today, researchers of the Universe, using large telescopes and powerful computers, are moving to ever greater distances in search of precisely the early stages of the evolution of its building blocks – galaxies. Now the states of cold and hot proto-galaxies, collapsars in their nuclei, active phases of the evolution of galaxies, in particular, quasars, radio galaxies, etc. – all this is today's reality. All this is a very, very long chain of unique states with many branches and parallels. Today we clearly observe many traces of the early global unsteadiness of galaxies. For example, the bends of the optical and gas disks of S and separate SO galaxies, the regularity of the density profile of E - galaxies, well explained by the mechanism of collisionless relaxation, the presence of powerful corona, anomalous manifestations in the form of ring–shaped (with or without a central core) and ϒ-shaped shapes, the variable activity of quasars and radio galaxies etc. All these phenomena, despite their different nature, are the result of global non-stationary processes with significant nonlinearity. However, until now, galactic physics theorists have mainly solved evolutionary equations by linearizing them near the equilibrium state, that is, considering non-stationarity as a small correction to the stationary model. They intensively studied the above phenomena using numerical experiments on powerful computers. That is why there is a need to create an attempt at an analytical theory of some of these phenomena in order to identify patterns and identify nonlinear effects that cannot be detected in any way by direct numerical modeling.

At working on the design of the text one of the authors (S.N.) was helped by PhD students A. Omonov and S. Turaev. We express our gratitude to professor V. A. Antonov for the discussion of some chapters of the book.

The authors would be grateful to readers for comments and suggestions that will be useful in the next edition of the book.

Authors

Introduction

In recent decades, the problems of the unsteady stage of the evolution of collisionless self-gravitating systems and the formation of a large-scale structure of the Universe have been very intensively solved using numerical experiments on computers (see, for example, [1-4]), setting at the initial moment a different degree of non-stationarity. However, during numerical experiments, fundamental questions often remain unnoticed and unclear, for example: what nonlinear effects and phenomena “worked,” whether instability occurred, what is the dependence of evolution on the physical parameters of the nonstationary system and on the degree of nonlinearity, and others. It is clear that solving of such issues is impossible without an analytical approach to such essentially non-linear problems. Without building the foundations of a nonlinear theory, a numerical experiment by itself will not be able to lead to the required success. The author of the book, without denying the great role of numerical and experimental research, believes that each of these problems should be solved in the interaction of both approaches.

In this book, we are primarily interested in the following questions: is it possible to construct analytically solvable models of collapsing galaxies; how to solve the problem of studying the stability of such nonlinear nonstationary configurations in order to identify new types of instability during collapse, and not under conditions close to it; what are the initial conditions necessary at the moment of the collapse to form different types of galaxies, etc. The direct construction of the models we need for one or another nonequilibrium state by solving the system of Boltzmann-Jeans and Poisson differential equations is complicated primarily by the mathematical complexity of the problem, where it is necessary to take into account both instability and nonlinearity. From the physical point of view, the problem is complicated by the real heterogeneity of the observed self-gravitating systems, the need to keep in mind the rotation, the dispersion of the velocities of the "particles" and the specific setting of the degree of non-uniformity. It should be noted that in the analytical formulation of the problem, it is still very difficult to create nonlinear nonequilibrium models of mixed systems of stars and gas (and yet we managed to construct analytically stationary mixed models [7]).

For a comprehensive theoretical study of the problems of the origin of large-scale structures, to clarify the possible stages of the evolution of a non-stationary system, to identify the corresponding types of instabilities under the background of a non-equilibrium state, we need exactly solvable nonlinear models of various states that are sufficiently far from equilibrium. Therefore, without fully considering the nonstationary evolution of a nonlinear nonequilibrium system, we identify typical, realizable states and, accordingly, build exactly solvable nonlinear

models of them in the phase description. At the early stage of the evolution of galaxies, one of these states is the collapsing, gravitationally compressed or nonlinear pulsating state of the system as a whole. We are talking about the states of non-dissipative and collisionless collapses.

Note the following two important points:

1) If we take only a model of continuous collapse as the initial state, then without any expansion, its instability is only power-law in nature, manifests itself weakly and occurs very slowly [6]. Considering this fact and also the fact that in reality the process of collapse of proto-galaxies containing dark matter or young stars and proto-stars is still forced to change to some kind of expansion (even if it is weak and for a short time), it is possible to come to the conclusion that it is necessary to consider in the initial state some pulsating models.

2) Let this pulsating model be described by the phase density function $\Psi\left(\vec{r},\ \vec{v},\ \mathrm{t},\ \lambda\right)$, where $\vec{r}$ is the radius vector, $\vec{v}$ is the velocity vector, t is the time, λ is the nominal amplitude of the pulsation, which characterizes the physical state at the moment of the collapse. Note that this pulsating state cannot actually serve as an exact model of a collapsing galaxy, and a system with a distribution function $\Psi_0 + \delta\Psi$, where $\delta\Psi$ is some evolving small perturbation, should be considered as a real evolutionary model. In this book, a number of functions Ψ_0 are constructed and certain classes of perturbations $\delta\Psi$ are studied, which are responsible for the formation of specific large-scale and small-scale structural formations under the background of a nonlinear nonequilibrium model.

We also discuss the classical problem of logarithmic divergence arising during the calculations of the diffusion coefficients and give the solution of the problem based on the factor that effectively cuts of collective influence of distant field stars.

This book represents only the first step towards solving the problem of analytical modeling of the early stage of the evolution of galaxies and spherical clusters, since only one of the possible research methods is indicated for the first time and the first theoretical results are obtained analytically.

Chapter I. CONSTRUCTION OF NONLINEAR NONEQUILIBRIUM PHASE MODELS

§1. General statement of the problem

The following statement of the problem is **common to all the models constructed in the Chapters I-V,** because each time we deal with the phase density function of the system as the main function $\Psi(\vec{r}, \vec{v}, t)$.

It has the meaning of the number of particles at time t- in the unit element of the volume of phase space in the vicinity of the point $(\vec{r}, \vec{v})$ and satisfies the system of Boltzmann-Poisson equations

$$\frac{\partial \Psi}{\partial t} + \vec{v} \cdot \frac{\partial \Psi}{\partial \vec{r}} + \frac{\partial \Phi}{\partial \vec{r}} \cdot \frac{\partial \Psi}{\partial \vec{v}} = 0, \tag{1.1}$$

$$\Delta \Phi = -4\pi G \rho, \tag{1.2}$$

where Δ is the Laplace operator, $\rho = \int \Psi \, d\vec{v}$ is the density of the system in ordinary space, and the masses of the particles are considered to be the same and equal to one.

If, when constructing purely stationary models, it is sufficient to find the corresponding integrals of the motion of equation (1.1), in the case of this $\partial \Psi / \partial t \neq 0$ approach in direct application is not convenient. For example, the difficulty lies in the fact that the integral of the particle's energy $E = \vec{v}^2/2 - \Phi$ is not conserved if the gravitational potential also depends on time. Really,

$$dE/dt = v_x \cdot dv_x/dt + v_y \cdot dv_y/dt + v_z \cdot dv_z/dt -$$
$$-(\partial \Phi/\partial t + + v_x \cdot \partial \Phi/\partial x + v_y \cdot \partial \Phi/\partial y + v_z \cdot \partial \Phi/\partial z) = -\partial \Phi/\partial t \neq 0. \tag{1.3}$$

But, unlike (1,3), the conservation condition holds for the angular momentum vector of a particle $\vec{L} = \vec{r} \times \vec{v}$, if the nonstationary system is spherically symmetric. For a rotationally symmetric system, only the value is preserved $L_z = xv_y - yv_x$, since in the value field $\Phi((x^2 + y^2)^{1/2}, z, t)$

$$dL_z/dt = x \cdot \partial \Phi/\partial y - y \cdot \partial \Phi/\partial x = 0. \tag{1.4}$$

Below we do not use the methods of motion integrals to construct nonlinear phase models and solve this problem in a different way.

As for global invariants, for an arbitrary system, regardless of its nonstationarity and symmetry, the complete energy of the system

$$0.5 \cdot \iiint (\mathrm{v}^2 - \Phi)\rho \mathrm{dxdydz} \tag{1.5}$$

and values

$$\int L_x \rho d\vec{r}, \quad \int L_y \rho d\vec{r}, \quad \int \mathrm{L}_z \rho \mathrm{d}\vec{\mathrm{r}}, \tag{1.6}$$

representing the components of the rotational moment of the system, remain constant. Obviously, the total mass of the system is also conserved. Note that, when considering nonstationary processes and studying the stability of nonequilibrium states, we further assume that the external source of oscillations is "switched off," i.e., in other words, we are interested in fundamentally nonlinear models of isolated systems.

Considering that at the initial stages of the development of gravitating systems, a special place is occupied by nonlinear pulsations, which inevitably arise and determine the beginning of the path of evolution (see Introduction), among the possible non-stationary models, we must be able to describe, first of all, pulsating states and build the corresponding exact models. And this question can be solved, based, in particular, on the available stationary models, making them pulsate. This idea comes to mind very simply, but, unfortunately, not all known stationary models lend themselves to this approach, especially if we want to achieve something in theoretical terms.

Obviously, the analysis must begin with spatially homogeneous models with finite dimensions, for which the corresponding distribution functions in the stationary state are known Ψ_0. There are few such models in the stationary case, but nevertheless, when generalizing them to the non-stationary variant and identifying the conditions of its instability, as will be seen from the following, a very wide front of work opens up with interesting prospects.

Note that the corresponding objects observed now, if we do not take into account the model of the Universe itself, probably do not have a very large magnitude of the pulsation amplitude.λ. But it is not known what was at an early stage of their evolution. Now, after we have performed an extensive analysis of the process of formation of collapsing galaxies, we can confidently assert that, in principle, for individual objects, the value of this parameter can take on a fairly large value (see Chapter 2). Therefore, from the point of view of future applications in such problems, it is desirable not to put any restrictions on λ, but to consider it an arbitrary value. And this, in turn, greatly complicates a rigorous theoretical analysis. But at any pulsation amplitude, nonlinear oscillations can be studied by passing to Lagrangian coordinates, which has justified itself long ago in other problems [9–11].

In the method we use, in each case, the coordinates and velocities of an arbitrary particle of the perturbed system are represented in vector form:

$$\vec{r} = \alpha(t) \cdot \vec{r}_0 + \beta(t) \cdot \vec{v}_0, \tag{1.7}$$

$$\vec{v} = \dot{\alpha}(t) \cdot \vec{r}_0 + \dot{\beta}(t) \cdot \vec{v}_0, \tag{1.8}$$

where $\vec{r}_0$ and $\vec{v}_0$ are, respectively, the radius vector and the velocity vector in the main stationary state, $\alpha(t)$ and $\beta(t)$ are unknown functions determined from the equation of motion, and the points above them mean the time derivative.

The vectors $\vec{r}_0$ and $\vec{v}_0$ can be expressed inversely in terms of $\vec{r}$ and $\vec{v}$. In this case, it is necessary to take into account the fact that the Jacobian of the transformation $(\alpha\dot{\beta} - \beta\dot{\alpha})^k$, where the k-dimension of the model does not depend on time according to the Liouville theorem. In what follows, we will consider it equal to unity, otherwise subjecting the stationary model used for comparison to some similarity transformation.
Therefore, at

$$\alpha\dot{\beta} - \beta\dot{\alpha} = 1 \tag{1.9}$$

from (1.7) and (1.8) we obtain

$$\vec{r}_0 = \beta(t) \cdot \dot{\vec{r}} - \beta(t) \cdot \vec{v}, \tag{1.10}$$

$$\vec{v}_0 = -\alpha(t) \cdot \dot{\vec{r}} + \alpha(t) \cdot \vec{v}. \tag{1.11}$$

Now let's start building specific models separately.

§2. Nonlinearly pulsating generalizations of Einstein's equilibrium model

Let us take as a basis the stationary model of Einstein's sphere [12-14] with radius R_0, where all particles move only in circular orbits. Obviously, they are kept in circular orbits if the exact equality of gravitational attraction and centrifugal force is satisfied. In this case , the value of the velocity vector $\vec{v}_0$ in the equilibrium state is equal to

$$v_0 = \Omega_0 r_0, \quad \Omega_0 = [(4/3) \cdot \pi G \rho_0]^{1/2}, \tag{1.12}$$

where Ω_0 is the angular velocity of rotation of the star, ρ_0 is the density.

To build a nonlinear model, it is necessary to have a configuration that is completely stable in the linear approximation. Therefore, we consider the model in

the form of a homogeneous Einstein ball, since in an inhomogeneous system, under radial perturbations, generally speaking, intersections of layers can occur, which leads to instability already in the case of linear oscillation amplitude.

Einstein's stationary model is extremely anisotropic in terms of velocities, since in it the radial component of the energy of motion is strictly zero. This model is stable with respect to small asymmetric perturbations [13]. But it is clear that when the pecular velocities are included in it, various instabilities may occur. To find out at what values this is possible, we first need to build a non-linearly pulsating model.

Let the states of pulsation and stationarity depend on each other according to (1.7) and (1.8). Since there are no radial motions in the Einstein ball in the initial state, $\vec{r}_0 \cdot \vec{v}_0 = 0$ then squaring (1.7), taking into account (1.12), we easily find

$$r = \Pi(t) \cdot r_0, \qquad \Pi(t) = (\alpha^2 + \Omega_0^2 \beta^2)^{1/2}. \tag{1.13}$$

The latter means that we really have a stretching of the ball with the preservation of similarity at time t by a factor of Π.

In this case, the density changes, $\rho(t)$ obviously, proportionally Π^{-3}, more precisely

$$\rho(t) = \rho_0 \cdot (\alpha^2 + \Omega_0^2 \beta^2)^{-3/2}. \tag{1.14}$$

Therefore, from the Poisson equation it is easy to determine the potential in the state of pulsation. Then the characteristic equations, compiled according to the Boltzmann equation, give

$$\ddot{\vec{r}} = -\Omega_0^2 \vec{r} / (\alpha^2 + \Omega_0^2 \beta^2)^{3/2}. \tag{1.15}$$

Substituting expression (1.7) here, we obtain equations for two unknown functions α and β:

$$\ddot{\alpha} = -\Omega_0^2 \alpha / [\Pi(t)]^3, \quad \ddot{\beta} = -\Omega_0^2 \beta / [\Pi(t)]^3. \tag{1.16}$$

As expected, the integral of motion of these equations is the expression (1.9) Let's get the equation for the function $\Pi(t)$. To do this, having differentiated Π^2 from (1.13) once and squaring $\Omega_0^2(\alpha\dot{\beta} - \beta\dot{\alpha})^2$, we add and subtract from the result. Then we get

$$\Pi^2 \dot{\Pi}^2 + \Omega_0^2 = (\dot{\alpha}^2 + \Omega_0^2 \dot{\beta}^2)\Pi^2. \tag{1.17}$$

On the other hand, equations (1.16) have the energy integral

$$(\dot{\alpha}^2 + \Omega_0^2 \dot{\beta}^2)/2 - \Omega_0^2/\Pi(t) = E, \tag{1.18}$$

which in combination with (1.17) gives

$$(1/2)\cdot\dot{\Pi}^2 + \Omega_0^2[(1/2)\cdot\Pi^{-2} - \Pi^{-1}] = \mathrm{E}. \tag{1.19}$$

Obviously, in (1.19) the constant E<0, otherwise the function $\Pi(t)$ will grow with time, which is unacceptable for us.

Differentiating (1.19) with respect to t once, we find the corresponding differential equation for $\Pi(t)$ in the form

$$\ddot{\Pi} + \Omega_0^2(\Pi^{-2} - \Pi^{-3}) = 0. \tag{1.20}$$

To find the pulsation law for a nonlinear model, it is necessary to solve (1.20). To this end, we first make a change of variable, more precisely, we move from t to ψ :

$$\psi = q\cdot\int_0^t \Pi^{-1}dt, \tag{1.21}$$

where q- is the proportionality factor associated with the energy integral E $(\mathrm{q} = (-2\mathrm{E})^{1/2})$.

Then instead of (1.20) we have

$$\Pi''(\psi) + \Pi(\psi) = \Omega_0^2/q^2. \tag{1.22}$$

Here and below, the prime denotes differentiation with respect to ψ (we will keep the dot as the sign of differentiation with respect to t). From (1.22), taking into account (1.19), we obtain the following solution

$$\Pi(\psi) = (\Omega_0^2/\mathrm{q}^2)(1 + \lambda\cos\psi), \qquad \lambda = [1 - (\mathrm{q}^2/\Omega_0^2)]^{1/2} \tag{1.23}$$

which satisfies the condition t=0, $\dot{\Pi}$=0 (which corresponds to the moment of greatest expansion). Thus, we have found the expansion coefficient Π of the Einstein ball during its pulsation. The value λ plays the role of the pulsation amplitude and takes values in the interval [0,1].

In the system of differential equations (1.16), we also pass from t to ψ and solve it according to the usual rules for the functions α and β, taking into account (1.23), which leads us to the expressions:

$$\alpha(\psi) = \mathrm{c}_{11}\sin\psi + \mathrm{c}_{12}(\lambda + \cos\psi), \tag{1.24}$$

$$\beta(\psi) = c_{21}\sin\psi + c_{22}(\lambda + \cos\psi) \tag{1.25}$$

with unknown constants c_{ij}. Note that we can always consider β=0 when ψ=0, since we have one trivial degree of freedom associated with the possibility of numbering particles differently. Then from (1.25) it follows that c_{22}=0. The remaining three coefficients can be easily found from the connection between α and β in relation (1.13), substituting (1.23) - (1.25) there.

We finally get that

$$\alpha(\psi) = (\Omega_0^2 / q^2)\cdot(\lambda + \cos\psi), \quad \beta(\psi) = q^{-1}\sin\psi. \tag{1.26}$$

Further, to construct a nonlinearly pulsating model, we must know the radial and transversal components of the star's velocity in a perturbed state.

According to (1.7) - (1.9), we have $\vec{r}\times\vec{v} = \vec{r}_0\times\vec{v}_0$. This implies, what $rv_\perp = r_0 v_{\perp 0} = \Omega_0 r_0^2$ or

$$v_\perp = \Omega_0 r_0 / \Pi(\psi) = \Omega_0 r / \Pi^2(\psi) \equiv v_b. \tag{1.27}$$

Since $\vec{r}\cdot\vec{v} = (\alpha\dot{\alpha} + \Omega_0^2\beta\dot{\beta})r_0^2 = rv_r$, taking into account (1.13) and (1.26) we have

$$v_r = -\Omega_0\lambda(1-\lambda^2)^{-3/2}\sin\psi\cdot(1+\lambda\cos\psi)^{-2} r \equiv v_a. \tag{1.28}$$

Now we can write an expression for the phase density of a **nonlinearly pulsating version** of the Einstein model in the form

$$\Psi(r, v_r, v_\perp, t) = \rho(t)[2\pi v_b(t)]^{-1}\delta(v_r - v_a)\delta(v_\perp - v_b)\chi(R_0\Pi - r), \tag{1.29}$$

where χ is Heaviside function, δ is the Delta Dirac function.

The non-stationary model (1.29) pulsates with the period

$$P(\lambda) = q^{-1}\cdot\int_0^{2\pi}\Pi(\psi)d\psi = (2\pi/\Omega_0)\cdot(1-\lambda^2)^{-3/2}. \tag{1.30}$$

In this case, the individual particles of the system describe, obviously, elliptical orbits with a focus at the center of the system (Fig. 1.1). It is easy to find out what angle the star has time to go through in azimuth φ during the change of Ψ from 0 to 2π. To do this, we integrate the equation

$$\dot{\varphi} = v_\perp / r = \Omega/\Pi(t) \tag{1.31}$$

having previously passed from t to ψ. We get φ=2π, i.e. all stellar orbits in model (1.29) are closed. It is also easy to find the velocity dispersion components of the nonlinear model: $\sigma_r^2 = 0$, $\sigma_\perp^2 = v_b^2$.

Finally, we calculate the components of the kinetic energy of the pulsating motion

$$T_r = (M/2)\cdot\overline{v_r^2}, \qquad T_\perp = (M/2)\cdot\overline{v_\perp^2}, \tag{1.32}$$

where M is the total mass of the system, and the overline means averaging over the phase space. In particular,

$$\overline{v_r^2} = M^{-1}\cdot\iint v_r^2\,\Psi\, d\vec{r}\, d\vec{v} = (3/5)\cdot(R_0 q\lambda\sin\psi)^2\cdot(1+\lambda\cos\psi)^{-2}. \tag{1.33}$$

In a similar way, we calculate such a quantity from the transversal component

$$\overline{v_\perp^2} = (3/5)\cdot(1-\lambda^2)\cdot(R_0 q)^2\cdot(1+\lambda\cos\psi)^{-2}. \tag{1.34}$$

In what follows, when comparing the results of the analysis of the stability of individual nonlinear models, the values of the ratio of the values averaged over the pulsation period in (1.32) will be of interest, i.e. an anisotropy parameter

$$\nabla(\lambda) = 2<T_r>/<T_\perp> = 2[1-(1-\lambda^2)^{1/2}]\cdot(1-\lambda^2)^{-1/2}. \tag{1.35}$$

At the same time, the averages over the components themselves are equal

$$\left\langle T_\perp \right\rangle = (2\pi)^{-1}\cdot\int_0^{2\pi}(1+\lambda\cos\psi)T_\perp d\psi = (3/10)\cdot MR_0^2 q^2(1-\lambda^2)^{1/2}, \tag{1.36}$$

$$<T_r> = (3/10)\cdot MR_0^2 q^2[1-(1-\lambda^2)^{1/2}]. \tag{1.37}$$

The sum of the last expressions exactly satisfies the virial theorem, which is already valid for the energy components averaged over the period (see (1.56) and (1.57)). At $\lambda = \sqrt{5}/3 \approx 0.745$ parameter ∇=1 and we have an average velocity isotropic nonlinear model. It is important to note that the pulsating model (1.29) can be made rotating by analogy with the stationary model [15]. Despite the fact that the phenomenon of rotation in spherical clusters of stars and galaxies is still considered debatable, the study of the problem of large-scale structure and the early stage of evolution requires non-equilibrium phase models of rotating subsystems with nonlinear pulsations.

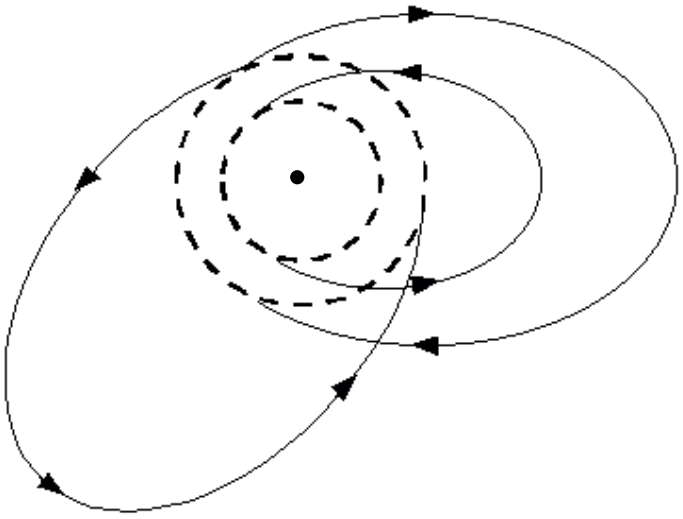

Fig. 1.1. Orbits of particles in the pulsating model (1.29). The center of the system coincides with one of the foci of the ellipse. Dashed lines are circular orbits in equilibrium.

Expression (1.29) can be generalized to the case of solid rotation [16, 17]

$$\Psi_{rot} = [1 + \mu(xv_y - yv_x)]\Psi \ , \qquad (1.38)$$

where μ plays the role of the angular rotation velocity of the disk, and $|\mu| \le 1$, (when μ>1 (1.38) is physically unacceptable). Note that although the Einstein's equilibrium model is very unnatural, the pulsating rotating model (1.38) constructed by us on its basis is quite interesting and useful. In (1.38)

$$L_z = xv_y - yv_x = v_\phi \cdot (x^2 + y^2)^{1/2}$$

(1.39)

is the integral of motion. Obviously

$$L_z = r \cdot v_\perp \cdot \sin\theta \cdot \sin\eta, \qquad (1.40)$$

where $\sin\theta = (x^2 + y^2)^{1/2}/r$, $\eta = \mathrm{arctg}(v_\varphi / v_\theta)$, v_φ and v_θ are the azimuth and meridional components $v_\perp$.

The question arises: is it of interest to know the Ostriker-Peebles parameter [18] $t_{O\Pi} = T_{rot}/|U|$ to determine the instability criterion for the nonstationary model (1.38). The answer is no and here's why. In this case, the potential energy of the

pulsating model (1.38)

$$U = -(3GM^2/10) \cdot \int_0^\infty (R^2 + s)^{-3/2} ds = -3GM^2/[5R(t)], \qquad (1.41)$$

and the kinetic energy of rotation of the system

$$T_{rot} = \varpi^2 J/2 = M\varpi^2 R^2/5, \qquad R = \Pi(\psi) \cdot R_0. \qquad (1.42)$$

Therefore, for the model (1.38)

$$t_{O\Pi} = \mu^2(1 - \lambda^2)/[12(1 + \lambda\cos\psi)]. \qquad (1.43)$$

It is easy to see that during the pulsation period this parameter takes values from $\mu^2(1-\lambda)/12$ to $\mu^2(1+\lambda)/12$ and the Ostriker-Peebles criterion is not satisfied for the non-stationary model, since near the moment of greatest compression $t_{O\Pi} > 0.14$, if $\lambda > (1.68/\mu^2) - 1$.

Thus, one can qualitatively establish the region of instability of model (1.38) with respect to ellipsoidal perturbations. In fact, this is very conditional and requires specific analysis (see Chapter 2). Note that although the value (1.43) averaged over the oscillation period satisfies the Ostriker-Peebles stability criterion

$$< t_{O\Pi} >= \mu^2(1-\lambda^2)/12 < 0.14,$$

but the pulsating model at a certain value of λ, as will be seen below, is necessarily unstable.

Obviously, the result of the nonlinear evolution of a nonequilibrium system primarily depends on the degree of its non-stationarity in the initial state.

The latter can be characterized by the value of the virial ratio $(2T/|U|)_0$ at t=0, which, in turn, uniquely depends on λ. Indeed, from (1.32)-(1.34), taking into account (1.41), we have

$$(2T/|U|)_0 = (1+\lambda\cos\psi)|_{\psi=0} = 1-\lambda \ , \qquad (1.44)$$

where $T = T_r + T_\perp$. Substituting here the critical value of the pulsation amplitude λ^* for both the nonrotating model (1.29) and the rotating model (1.38), we can determine the corresponding instability criterion in the form

$$2T/|U| < (2T/|U|)_0 = 1-\lambda^* . \qquad (1.44')$$

For the sake of interest, a curious inequality should be noted: the average value of the virial parameter for non-stationary models (1.29) and (1.38) is less than unity

$$< 2T/|U| >= 1-\lambda^2/2 < 1,$$

which was not obvious beforehand, since the collisionless relaxation still leads $2T/|U|$ to tending to unity.

For the rotating model (1.38) its global characteristics (1.32) -(1.37) remain the same as for the model (1.29).

§3. Non-stationary version of The Camm equilibrium model

We are talking about the possibility of generalizing to the case of nonlinear pulsations the well-known equilibrium Camm model [19] with the phase density

$$\Psi_0 = c\cdot[\Omega_0^2\cdot(R_0^2 - r_0^2) - v_{0\perp}^2\cdot(1 - r_0^2/R_0^2) - v_{0r}^2]^{-1/2}\cdot\chi(R_0 - r_0), \qquad (1.45)$$

where c is some constant, v_{0r} and $v_{0\perp}$ are the radial and transversal components of the velocity vector v_0. In contrast to the Einstein equilibrium sphere , model (1.45) contains stellar orbits with arbitrary ellipticity, including circular ones, and the center of the system coincides with the center of these orbits. However, model (1.45), just like Einstein's equilibrium ball, is homogeneous and has a quadratic gravitational potential.

For the considered fluctuations (1.7), the quadratic property of the potential is preserved, and the density function $\rho(t)$ of the nonlinear model will be described by formula (1.14), according to (1.49). Consequently, the equation of motion of an individual star in a state of pulsation has the form (1.15). This means that model (1.45) has been generalized to the nonstationary case with the pulsation law (1.23). To this end, we substitute (1.7) and (1.8) into the equation of the phase boundary of the original model (1.45)

$$v_0^2 + \Omega_0^2 \cdot r_0^2 - (\vec{r}_0 \times \vec{v}_0)^2 / R_0^2 = \Omega_0^2 \cdot R_0^2 \tag{1.46}$$

Then, taking into account (1.9), we have

$$(\dot{\alpha}^2 + \Omega_0^2 \dot{\beta}^2) r^2 - 2(\alpha\dot{\alpha} + \Omega_0^2 \beta\dot{\beta})\, \vec{r} \cdot \vec{v} + \Pi^2(t) v^2 - (\vec{r} \times \vec{v}) \cdot R_0^{-2} = \Omega_0^2 \cdot R_0^2. \tag{1.47}$$

In (1.47) we divide the speed into its components $(v_r, v_\perp)$ and transform it into the form

$$\Pi^2 [v_r - (\alpha\dot{\alpha} + \Omega_0^2 \beta\dot{\beta})\Pi^{-2} r]^2 + (\Pi^2 - r^2 / R_0^2) \cdot (v_\perp^2 - \Omega_0^2 R_0^2 / \Pi^2) = 0. \tag{1.48}$$

This shows that the largest admissible value of r, at which

$$v_r - (\alpha\dot{\alpha} + \Omega_0^2 \beta\dot{\beta}) \cdot r / \Pi^2 = 0,$$

is

$$R(t) = \max r = R_0 \Pi. \tag{1.49}$$

Passing in (1.48) from t to ψ, taking into account (1.23) and (1.26), one can easily write **the phase density of the pulsating model**

$$\Psi(r, v_r, v_\perp, t) = \rho \Pi^4 / (\pi^2 R^2 \Omega_0^2) \cdot f^{-1/2} \cdot \chi(f), \tag{1.50}$$

where

$$f = (1 - r^2 / R^2) \cdot (\Omega_0^2 R^2 / \Pi^4 - v_\perp^2) - \{v_r + \Omega_0 \lambda \cdot \sin\varphi \cdot r / [(1 - \lambda^2)^{1/2} \cdot \Pi^2]\}^2. \tag{1.51}$$

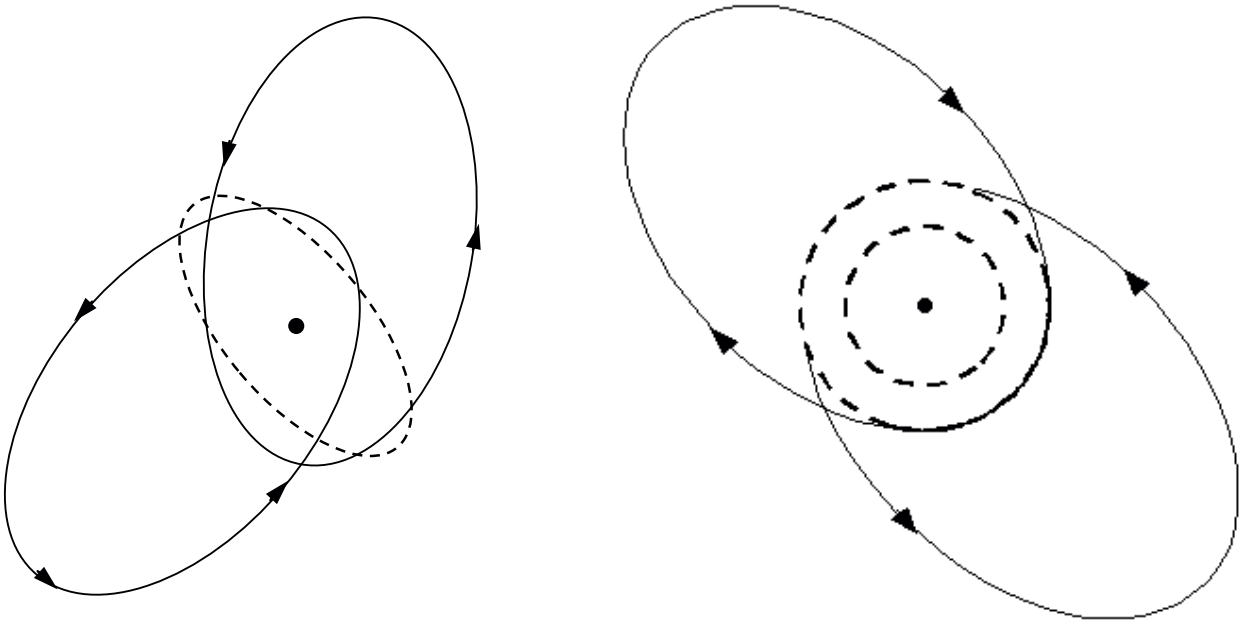

Fig. 1.2. In the pulsating model (1.50), the center of the system may not be at the focus of the ellipse (a), and for the original circular orbit it may coincide with the focus of the elliptical orbit (b).

Function (1.50) satisfies the condition $\rho = \int \Psi d\vec{v}$. In model (1.50), the trajectory of each star, in contrast to (1.45), is only elliptical, if the energy of radial oscillations is less than the parabolic limit. In this case, the center of the system can be in the focus of an elliptical orbit, if the initial orbit (λ=0) is not circular (Fig. 1.2). Indeed, let the particle be in the initial state, for example, in the plane (x_0, y_0), i.e. $\vec{r}_0 = r_0(x_0, y_0, 0), \quad \vec{v}_0 = v_0(0, v_0, 0).$

Then using the relations

$$x = \alpha x_0 = (1-\lambda^2)^{-1} \cdot (\lambda + \cos\psi) \cdot x_0, \qquad y = \alpha y_0 + q^{-1} \sin\psi \cdot v_0$$

we get the following orbit equation

$$[(1-\lambda^2)\cdot x\cdot x_0^{-1}-\lambda]^2+(\Omega_0/v_0)^2\cdot(1-\lambda^2)\cdot(y-y_0x_0^{-1}x)^2=1. \qquad (1.52)$$

This shows that at $\lambda\neq 0$ the center of the orbit is displaced relative to the origin of coordinates. Further, passing in (1.52) from (x,y) to polar coordinates (r, φ), the quadratic equation for r, whose discriminant is equal to

$$(\Omega_0^2y_0^2/v_0^2+1)\cdot\cos^2\varphi/x_0^2-\Omega_0^2y_0\cdot\sin 2\varphi/(x_0v_0^2)+\Omega_0^2\cdot\sin^2\varphi/v_0^2.$$

In the general case, it is impossible to extract the root from the last expression to derive the known dependence r(φ) in the form of an equation of a conic section. In order to obtain such an equation, in (1.52) it is necessary to shift the focal point relative to the center of the system. However, this shift does not need to be performed for the pulsating state (1.29) of the Einstein ball, which in the equilibrium state in the plane (x_0, y_0) contains only a circular orbit: $v_0=\Omega_0\cdot x_0$ and $y_0=0$.

The existence of all possible elliptical orbits in model (1.50) is due to the fact that the transversal velocity component $v_\perp$ at each point does not take a specific value, as in the case of the Einstein model, but fills the whole interval

$$0\le v_\perp^2\le\Omega_0^2R_0^2/\Pi^2(t)\equiv v_m^2 \qquad (v_m=\max v_\perp). \qquad (1.53)$$

But the average value of the radial component of the particle velocity, as can be seen from (1.51), coincides with the corresponding value (1.28) for the previous model (1.29) and is equal to

$$v_a=-\Omega_0\lambda(1-\lambda^2)^{3/2}\sin\psi\cdot r/(1+\lambda\cos\psi)^2.$$

It is easy to calculate the velocity dispersion components for the constructed model

$$\sigma_r^2=\frac{1}{4}\cdot v_m^2\cdot(1-r^2/R^2), \qquad \sigma_\perp^2=v_m^2/2. \qquad (1.53')$$

Let us find an expression for the anisotropy parameter ∇(λ). It is convenient to first calculate the transversal component of the pulsation energy

$$T_\perp=(M/2)\cdot\overline{v_\perp^2}=(1/2)\cdot\int dr\iint v_\perp^3\psi dv_r dv_\perp=(M/4)\cdot v_m^2. \qquad (1.54)$$

and its average over the period, taking into account (1.53)

$$< T_{\perp} >= (1/4) \cdot M \cdot \Omega_0^2 \cdot R_0^2 \cdot (1-\lambda^2)^{3/2}. \qquad (1.55)$$

And the radial component is $< T_r >$ easier to find using the virial theorem

$$< T_r >= -(1/2) \cdot < U > - < T_{\perp} >, \qquad (1.56)$$

where the potential energy averaged over the oscillation period in accordance with (1.41), (1.30) and (1.49) is equal to

$$< U >= -3GM^2 \cdot (5R_0 P)^{-1} \cdot \int_0^p [\Pi(t)]^{-1} dt = -(3/5) M R_0^2 \Omega_0^2 (1-\lambda^2). \qquad (1.57)$$

Substituting (1.55) and (1.57) into (1.56), we find

$$< T_r >= (1/20) \cdot M \cdot \Omega_0^2 \cdot R_0^2 \cdot (1-\lambda^2) \cdot [6 - 5(1-\lambda^2)^{1/2}]. \qquad (1.58)$$

The validity of (1.58) can be verified by preliminarily calculating T_r by analogy with (1.54), which gives

$$T_r = (1/20) \cdot M \cdot \Omega_0^2 \cdot R_0^2 \cdot \Pi^{-2} \cdot [1 + 6\lambda^2 \sin^2 \psi / (1-\lambda^2)]. \qquad (1.58')$$

Therefore, the desired parameter

$$\nabla(\lambda) = 2 < T_r > / < T_{\perp} >= 0{,}4 \cdot [6 - 5(1-\lambda^2)^{1/2}] / (1-\lambda^2)^{1/2}. \qquad (1.59)$$

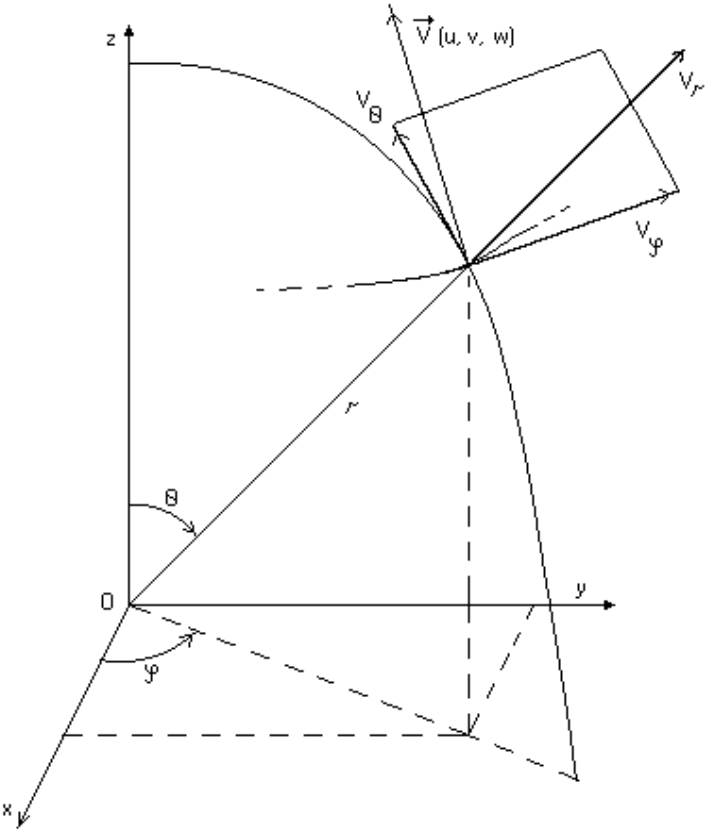

Fig.2. Coordinate systems used in calculations

If we consider the behavior of the components themselves $< T_r >$ and $< T_\perp >$ depending on the pulsation amplitude, then it is easy to see that for $\lambda=3/5$ the nonlinear model (1.50) is isotropic on average in terms of velocities.

Therefore, in the interval $0<\lambda<3/5$, the non-stationary system with phase density (1.50) in terms of the parameter ∇ occupies an intermediate position between the non-linear pulsating model (1.29) and the indicated isotropic model with the value $\nabla=1$. It should be noted that if the non-stationary model (1.29) can be divided, in principle, into synchronously pulsating spherical shells, then this cannot be done in (1.50) due to the existence of radial residual velocities. Nevertheless, relations (1.44) and (1.44') are also valid for model (1.50).

By analogy with the pulsating version of Einstein's ball, one can generalize the nonlinear model (1.50) to the case of rotation. Let us write the phase density of the rotating model in the form

$$\Psi_{rot} = \rho(t)\Pi^4(\pi R\Omega_0)^{-2} f^{-\frac{1}{2}}\chi(f)\cdot\left[1+\mu r v_\perp \sin\theta\cdot\frac{\sin\eta}{\Omega_0 R_0^2}\right], \qquad (1.60)$$

where again $|\mu|\le 1$, $rv_\perp \le R(t)\cdot v_m = \Omega_0 R_0^2$. It should be noted that it is not desirable to include the effect of rotation in the way indicated here in the case of the Einstein model, since there it leads to a differential rotation. The latter requires a completely different approach, and due to its complexity, we do not touch on it here.

Let us calculate the rotation speed of the model (1.60), i.e.

$$\overline{v_\varphi} = \rho^{-1}\iiint v_\perp^2 \sin\alpha\cdot\Psi_{rot}\,dv_r\,dv_\perp\,d\eta = (1/4)\mu\Omega_0\Pi^{-2}(x^2+y^2)^{1/2}. \qquad (1.61)$$

It follows from this that the angular velocity of solid-body rotation is equal to

$$\varpi(t) = \mu\cdot\Omega_0/(4\Pi^2) \qquad (1.62)$$

As can be seen, the maximum value (1.62) is two times less than the corresponding value $\varpi(t)$ in the model (1.38). Therefore, for model (1.60), the value of its moment of rotation is $K = \mu\cdot\Omega_0 R_0^2\cdot M/10$, and the Ostriker-Peebles parameter is equal to

$$t_{O\Pi} = (1/48)\cdot\mu^2(1-\lambda^2)\cdot(1+\lambda\cos\psi)^{-1}. \qquad (1.63)$$

It is easy to see that the model (1.60) constructed by us, in contrast to (1.38), completely satisfies the Ostriker-Peebles stability criterion, since even at the moment of the greatest compression of the system $\max(t_{O\Pi}) < 0.14$. Physically, this is due to the fact that the centrifugal force in model (1.60) is 4 times less than in model (1.38). However, the Ostriker-Peebles criterion does not take into account possible non-linear non-equilibrium and resonant phenomena, and therefore, as will be seen from what follows, it does not work here. Recall that another pulsating model is known in the literature, which was constructed in [20] on the basis of a generalization of the equilibrium rotating Freeman configuration to the case of pulsation, using our results [14, 21] with the pulsation law (1.23).
Note that the mixed model is also of some interest (see Chapter 5)

$$\Psi = (1-\nu)\cdot\Psi_{\mu_1} + \nu\cdot\Psi_{\mu_2}, \qquad (0<\nu<1) \tag{1.64}$$

composed using a superposition of nonlinear models (1.38) and (1.60) or the Freeman model just noted, taking different values of the rotation parameter μ_1 for each of them. Then the new model (1.64) depends in general on the following four parameters: λ, μ_1, μ_2 and ν.

Finally, it should be emphasized that in the future it is necessary to take into account the presence of a corona [22] of galaxies. This is important for the subsequent stages of their nonstationary evolution. Unfortunately, it has not yet been possible to analytically construct a nonlinear nonstationary model of a collapsing galaxy with an exact nonequilibrium law in the presence of a corona.

§4. Expanding or collapsing phase models with finite radius

In order to visualize the physical state of a singly expanding or contracting model, let us turn to the formula for the physical boundary of a pulsating system:

$$R = R_0(1+\lambda\cos\psi)/(1-\lambda^2).$$

From here we find the minimum and maximum values of the radius of the pulsating system for an arbitrary λ

$$R_{min} = R_0/(1+\lambda), \qquad R_{max} = R_0/(1-\lambda). \tag{1.65}$$

As can be seen, the value R_0 can be varied somewhat, since, generally speaking, it is arbitrary. Consider separately the possible options.

1. If for the above considered pulsating models from the very beginning we take $R_0 \propto (1-\lambda)$; then for $\lambda \to 1$, according to (1.65), the value R_{max} remains constant, and the value of $R_{min} \to 0$.

Consequently, in this case we have a model shrinking from a finite size, which is the limiting state of non-rotating configurations (1.29) and (1.50). The latter at $\lambda=1$ coincide and can describe the process of compression to a point, and therefore cannot have a rotating analogue in this case. Let us construct the phase density of this model.

Let at the initial moment of time t=0 we have a ball with radius R_0 and density ρ_0=const, and all its particles are at rest.

Then it shrinks under the influence of its own gravity (due to loss of equilibrium after global star formation or other processes). The equation of motion of a particle located on the surface of a contracting ball has the form

$$\ddot{R}(t) = -G \cdot M / R^2(t), \qquad (M = (4\pi/3)\rho_0 R_0^3). \tag{1.66}$$

Hence it follows that

$$(\dot{R})^2 = 2G \cdot M(R^{-1} - R_0^{-1}) \tag{1.67}$$

The solution of equation (1.67) can be found in the following parametric form

$$R(t) = (1/2)R_0(1+\cos\psi), \quad g \cdot t = \psi + \sin\psi, \quad g = (8G \cdot M / R_0^3)^{1/2} \tag{1.68}$$

The dependence of ψ on t , given in (1.68) corresponds to the case $\lambda=+1$ in (1.21). Consequently, during the collapse, the similarity is preserved and the density remains uniform in space, but depends on time. More precisely, based on (1.68), we have the following density of the contracting system

$$\rho(t) = \rho_0[\cos(\psi/2)]^{-6}, \qquad (0 \le \psi < \pi). \tag{1.68'}$$

Let us write the equation of motion of an arbitrary particle

$$\ddot{\vec{r}} = -G \cdot M \cdot \vec{r} / R^3(t), \qquad \left|\vec{r}\right| = (x^2 + y^2 + z^2)^{1/2}. \tag{1.69}$$

Passing here from t to the argument ψ, we have

$$(1+\cos\psi) \cdot d^2\vec{r}/d\psi^2 + \sin\psi \cdot d\vec{r}/d\psi + \vec{r} = 0. \tag{1.70}$$

Note that the vector equation (1.70) turned out to be linear in itself, without special linearization, and it is applicable over the entire compression period. Particular solutions (1.70) are

$$\vec{r} = (1+\cos\psi) \cdot \vec{r}_0/2, \qquad \vec{r} = \sin\psi \cdot \vec{r}_0. \tag{1.71}$$

The first solution just corresponds to the above initial condition. Comparing it with (1.7), in particular, we find that

$$\alpha = (1+\cos\psi)/2, \qquad \dot{\alpha} = -0.5g\cdot\sin\psi/(1+\cos\psi). \tag{1.72}$$

In this model $v_\perp$=0, and in accordance with (1.28)

$$v_r = \dot{\alpha}\cdot r/\alpha = -g\cdot r\sin\psi/(1+\cos\psi)^2, \tag{1.73}$$

which is zero at ψ=0, and when $\psi\to\pi$ v_r tends to $(-\infty)$. Now it is possible to write the function of the phase density, constructed here contracting from the finite size of the model, in an explicit form

$$\Psi(r, v_r, v_\perp, t) = (\rho/\pi)\cdot\delta(v_\perp^2)\cdot\delta[v_r + g\cdot r\cdot\sin\psi/(1+\cos\psi)^2]\cdot\chi(R-r), \tag{1.74}$$

where again is the Heaviside χ-function. Obviously, expression (1.74) cannot be generalized to the case of rotation, since this model completely lacks transversal motions and, in connection with this, it collapses to a point where a singularity takes place. However, if we consider a process, for example, inverse-expansion, but starting from a finite radius, a rotating model can also be built.

Note that until now the physical picture in pulsating models for the values of λ from the intervals [0,1] and [-1,0] was exactly the same, i.e., a negative value did not change the pulsation pattern, but only shifted ψ by π. Now, when constructing the limiting states of non-stationary models, these two intervals λ can be physically distinguished and therefore we will further consider the case $\lambda\to(-1)$. In this case, instead of (1.65) we have

$$R_{min} = R_0/(1-\lambda), \qquad R_{max} = R_0/(1+\lambda), \tag{1.75}$$

2. Let R_0=const. Then with $\lambda\to(-1)$ we get $R_{min} = R_0/2$, $R_{max}\to\infty$, which corresponds to the mentioned case-extension from a finite size, when the rotation factor may initially exist.

This means that on the basis of pulsating models with rotation (1.38) and (1.60), excluding the singularities present there, it is possible to construct the corresponding two rotating models.

For this purpose, in all formulas of the indicated rotating models, we will replace

$$\psi \to (1-\lambda^2)^{1/2}\psi. \tag{1.76}$$

Revealing the singularities, we obtain in the limit

$$\lambda\cdot\sin\psi/(1-\lambda^2)^{1/2} \to (-\psi),$$

$$\Pi(\psi) = (1+\psi^2)/2 = \Pi_1, \qquad 6\Omega_0 t = \psi^3 + 3\psi. \tag{1.77}$$

At the same time, we assume that $(1-\varepsilon^2)^{1/2} = 1-\varepsilon^2/2$, where $\varepsilon = (1-\lambda^2)^{1/2}$. Therefore,

$$R(\psi) = R_0(1+\psi^2)/2 = R_1, \quad \rho(\psi) = 8\rho_0(1+\psi^2)^{-3} = \rho_1 \tag{1.77'}$$

and from (1.38) we obtain the corresponding model

$$\Psi_{rot}^{(1)} = \rho_1 \delta(v_r - v_{a1})\delta(v_\perp - v_{b1})\chi(R_1 - r)(1 + \mu r \cdot v_\perp \sin\theta \cdot \sin\eta) \tag{1.78}$$

and $v_{a1} = \psi \cdot v_{b1}$, $v_{b1} = \Omega_0 r / \Pi_1^2$.

With the same notation, based on the pulsating model (1.60), one can write a new model with rotation

$$\Psi_{rot}^{(2)} = \rho_1 \Pi_1^4 f^{-1/2}\chi(f)[1 + \mu \cdot r \cdot v_\perp \sin\theta \cdot \sin\eta / (R_0^2\Omega_0)]/(\pi R_1 \Omega_0)^2, \tag{1.79}$$

where

$$f = (1 - r^2/R_1^2)(\Omega_0^2 R_1^2/\Pi_1^4 - v_\perp^2) - (v_r - \Omega \cdot r \cdot \psi/\Pi_1^2)^2.$$

We note that here, by analogy with (1.64), it also makes sense to consider the case of a mixed model using the new models (1.78) and (1.79).

3.There is also a “cosmological variant” in the Newtonian approximation, when $R_{min} \to 0$, and $R_{max} \to \infty$. This is the case, assuming $R_0 \propto \left(1-\lambda^2\right)^{1/2}$. In this case, we have the phenomenon of expanding the model from a singular state to infinity or vice versa. Consequently, the rotation factor here again has no physical meaning, just as in (1.74). But the corresponding phase model can be constructed exactly.

The stated physical situation again requires the replacement (1.76), but, unlike the previous case, now $(1-\varepsilon^2)^{1/2} = 1$.

Then instead of (1.77) we have

$$\Pi(\psi) = \psi^2/2, \qquad \psi = (6\Omega_0 t)^{1/3}. \tag{1.80}$$

Consequently,

$$R_2 = (36G \cdot M)^{1/3} t^{2/3}/2, \qquad \rho_2 = 8\rho_0/\psi^6. \tag{1.81}$$

Therefore, the phase density of such a nonlinear model is equal to

$$\Psi = (\rho_2 / \pi)\delta(v_r - v_{a2})\delta(v_\perp^2)\chi(R_2 - r), \tag{1.82}$$

where $v_{a2} = 4\Omega_0 r / \psi^3$. The models (1.73), (1.78), and (1.79) constructed by us in this section are new, and (1.82) is a Newtonian case of the Fridman model [103]. The stability of the latter model was studied in [107]. However, (1.82) is a special case of the more general model (1.74).

§5. Method for constructing a multi-parameter non-stationary model

Above, we have constructed several nonlinear models that depend mainly on one or two physical parameters (this $(2T/|U|)_0$ and μ) and therefore are necessary primarily for the development of a nonlinear theory. But from the point of view of direct application to real objects, it would be interesting to construct a nonlinear model taking into account the parameters responsible for the large-scale structure. It is clear that the more parameters, the more accurately we can determine the physical conditions at an early stage in the evolution of observed objects. Among the possible ways, we point out one of them, which can be implemented on the basis of the analytical results available in this book and is associated with a preliminary finding of the exact form of natural oscillations of a nonequilibrium model.

The idea of the method is as follows [23]. Obviously, any nonlinear model constructed by us, before its application to other problems, must necessarily be investigated for stability with respect to small perturbations of various types. Only then can the conditions for the emergence of individual observable large-scale or small-scale structures be revealed. In this case, the latter are characterized, for example, by the azimuthal wave number m, the number of the spherical harmonic n and the radial wave number N-n (N is the main index of the entire perturbation), since the small perturbation imposed on the non-stationary background expands into a specific harmonic series.

As will be seen below from other chapters, in some cases it is possible to find the exact form of eigenoscillations $\delta\Phi_{mnN}$, performed in a free manner after the "switching off" of the source of small perturbations.

If it is possible to find the corresponding responses of the densities $\delta\rho$ and $\delta\Psi$ using the Boltzmann and Poisson equations, then we can consider that a new phase model of the type

$$\Psi(\vec{r}, \vec{v}, t, \lambda, \mu) + \delta\Psi(\vec{r}, \vec{v}, t, \lambda, \mu, m, n, N). \tag{1.83}$$

It, in contrast to the previous one (when it was $\delta\Psi=0$), in principle, can take into account density inhomogeneity and other observable features for which the meaning of one or another parameter is physically clear to us in advance.

If the exact form of natural oscillations $\delta\Phi_{mnN}$ in general form is known, we find the corresponding expression for $\delta\rho$ from the Poisson equation

$$\delta\rho = -(4\pi G)^{-1}\Delta\delta\Phi_{mnN}. \tag{1.84}$$

The situation is much more complicated with the calculation of $\delta\Psi$. Let us proceed to its definition in the case of the known Ψ for a non-stationary spherical model with a gravitational potential

$$\Phi(r,t) = 0.5\cdot\Omega_*^2(t)\cdot(3R^2 - r^2), \qquad \Omega_*^2(t) = \Omega_0^2/\Pi^3(t). \tag{1.85}$$

Substituting in (1.1) $\Psi+\delta\Psi$ and $\Phi+\delta\Phi$ instead of Ψ and Φ, respectively, we again obtain a linear equation for $\delta\Psi$:

$$\partial\delta\Psi/\partial t + [\delta\Psi, E] = [\Psi, \delta\Phi] \equiv F, \tag{1.86}$$

where [...] are Poisson brackets, $F=F(t,x,y,z,v_x,v_y,v_z)$. In order not to clutter up the pages with long formulas, let's do a little calculation on the x coordinate, and then generalize the result to the spatial case. From (1.86) one can compose, in particular, the characteristic equation

$$dt = dv_x/(\partial\Phi/\partial x) = dx/v_x = ... = d\delta\Psi/F. \tag{1.87}$$

Hence, taking into account (1.85), in particular, the equation follows

$$\ddot{x}(t) + \Omega_0^2 x/\Pi^3(t) = 0. \tag{1.88}$$

As is known, if $x_1(t)$ and $x_2(t)$ are particular solutions of an equation of type (1.88), then $J_{ix} = x_i\dot{x} - \dot{x}x_i$, will be invariants. Let's pass in (1.88) from t to ψ according to the formula (1.21). Then, taking into account (1.23), equation (1.88) takes the form

$$(1+\lambda\cos\psi)\cdot x'' + \lambda\cdot\sin\psi\cdot x' + x = 0. \tag{1.89}$$

Since (1.89) has particular solutions ($\lambda+\cos\psi$) and $\sin\psi$, then the expressions

$$J_{1x} = -q\Pi^{-1}x\cdot\cos\psi + \sin\psi\cdot v_x, \quad J_{2x} = q\Pi^{-1}x\cdot\sin\psi + (\lambda+\cos\psi)\cdot v_x \tag{1.90}$$

are the desired integrals of motion.

The remaining four integrals of motion J_{1y}, J_{2y}, J_{1z}, J_{2z} have a similar form.

Further, it is easy to find the coordinates and velocity components of the particle in the model $\Psi+\delta\Psi$. For example,

$$x = \Omega_0^2 q^{-3}[\sin\psi J_{2x} - (\lambda + \cos\psi)J_{1x}],$$
$$v_x = (\sin\psi J_{1x} + \cos\psi J_{2x})/(1 + \lambda\cos\psi). \qquad (1.91)$$

Therefore, the final solution for $\delta\Psi$ can be represented in the form

$$\delta\Psi = \int_0^t F(\tau; x(\tau, \vec{J}); y(\tau, \vec{J}); ...; v_z(\tau, \vec{J}))d\tau + C(\vec{J}), \qquad (1.92)$$

Where $C(\vec{J})$- is an arbitrary function of invariants, $\vec{J} = (J_{1x}, J_{2x}, ..., J_{2z})$.

Formula (1.92) is also applicable to two-dimensional models with the pulsation law (1.23). Obviously, the constructed multi-parameter model is not of the most general nature, since it is itself based on a certain law of nonlinear pulsations.

CHAPTER II. INSTABILITIES OF PULSITING MODELS BASED ON AN EINSTEIN SPHERE

§ 6. Basic relations and equations

It is physically clear that the non-stationary models constructed by us, under certain conditions, contain various kinds of instabilities. To study the nature of possible types of instabilities and determine the corresponding states, it is necessary to impose a small, in the general case, asymmetric perturbation on the nonstationary model. Then instead of the equation of motion (1.15) we have

$$\ddot{\vec{r}} = -\Omega_0^2 \vec{r} / \Pi^3(t) + \mathrm{grad}(\delta\Phi). \tag{2.1}$$

Where $\delta\Phi$ - is the perturbation of the potential, which is a function of the perturbed components of the vector $\vec{r} + \delta\vec{r}$, where $\delta\Phi$ is the perturbation of the potential as a function of perturbed components of $\vec{r} + \delta\vec{r}$ vector. Therefore, $\delta\Phi$, in (2.1) is a non-linear function of $\delta\vec{r}$. Linearizing (2.1), we find the equation of asymmetric oscillations for an individual particle

$$\ddot{\delta\vec{r}} + \Omega_0^2 \delta\vec{r} / \Pi^3(t) = \mathrm{grad}(\delta\Phi), \qquad \delta\vec{r} = (\delta x, \delta y, \delta z) \tag{2.2}$$

and now $\delta\Phi$ it is taken at the unperturbed point (x, y, z). Let's pass from t to the argument ψ using formula (1.80). Then (2.2) takes the form

$$\Lambda\delta\vec{r} = \left(\Omega_0^4 / q^6\right) \cdot (1 + \lambda\cos\psi)^3 \cdot [\partial(\delta\Phi) / \partial\vec{r}], \tag{2.3}$$

where operator

$$\Lambda = (1 + \lambda\cos\psi) \cdot d^2 / d\psi^2 + \lambda\sin\psi \cdot d / d\psi + 1. \tag{2.4}$$

Obviously, the deviation of the particle at the current moment depends on the state of the field at previous moments $\psi_1 \in [-\infty, \psi]$, and, since our goal is to search for instability, at $\psi_1 = -\infty$ we assume $\delta x = \delta y = \delta z = 0$.

At each point at the current moment ψ there are particles with different velocities, therefore, to calculate the density perturbation or deformation of the

system boundary, one should proceed to the centroid displacement $(\overline{\delta x}, \overline{\delta y}, \overline{\delta z})$, averaging Eq. (2.3) over the velocity space. Therefore, for $\overline{\delta \vec{r}}$ one can write an integral representation

$$\overline{\delta \vec{r}} = \left(\Omega_0^4 / q^6\right) \cdot \int_{-\infty}^{\psi} (1 + \lambda \cos\psi_1)^3 \cdot S(\psi, \psi_1) \cdot \overline{[\partial(\delta\Phi)/\partial\vec{r}]}\, d\psi_1, \qquad (2.5)$$

where $S(\psi,\psi_1)$ is the Green's function and is compiled in the standard way from solutions of the homogeneous equation in (2.3)

$$S(\psi, \psi_1) = \left[\sin\psi \cdot (\cos\psi_1 + \lambda) - \sin\psi_1 \cdot (\cos\psi + \lambda)\right] / (1 + \lambda\cos\psi_1)^2. \qquad (2.6)$$

Note that the limits of the integral in (2.5) can also be taken from 0 to ψ, assuming the inclusion of a small perturbation only for a moment at the moment t=0. But then it is necessary to add to it some solution of the homogeneous equation corresponding to (2.3). Since in what follows we return to differential equations in the analysis of specific modes, it is convenient to use the notation in the form (2.5). Since under the integral in (2.5) the time associated with ψ is past, it is necessary to connect the current coordinates with the past ones included in (2.6) through $\partial(\delta\Phi)/\partial\vec{r}$. According to (1.10), the coordinates and velocities in the nominal state

$$\vec{r}_0 = \beta\, \dot{\vec{r}}(\psi) - \beta\, \vec{v}(\psi), \quad \vec{v}_0 = -\alpha\, \dot{\vec{r}}(\psi) + \alpha\, \vec{v}(\psi) \qquad (2.7)$$

On the other hand, it is clear that $\vec{r}(\psi_1) = \alpha(\psi_1)\vec{r}_0 + \beta(\psi_1)\vec{v}_0$. Substituting (2.7) here, we find the desired relation formula

$$x(\psi_1) + iy(\psi_1) = [x(\psi) + iy(\psi)]H_\alpha + [u(\psi) + iv(\psi)]H_\beta. \qquad (2.8)$$

Here u, v- are the velocity components in x and y, respectively,

$$H_\alpha = \alpha(\psi_1)\dot{\beta}(\psi) - \beta(\psi_1)\dot{\alpha}(\psi), \qquad H_\beta = \alpha(\psi)\beta(\psi_1) - \alpha(\psi_1)\beta(\psi),$$

where again the dot above means that the differentiation is done with respect to t. Substituting (1.26) here, taking into account (1.80), we have

$$\begin{aligned} H_\alpha &= [\cos\psi(\lambda + \cos\psi_1) + \sin\psi \sin\psi_1]/(1 + \lambda\cos\psi), \\ H_\beta &= (\Omega_0^2 / q^3)[\sin\psi_1(\lambda + \cos\psi) - \sin\psi(1 + \lambda\cos\psi_1)]. \end{aligned} \qquad (2.9)$$

The spatial homogeneity of the nonlinear models constructed by us in Chapter I allows us to take $\delta\Phi$ in the general form

$$\delta\Phi = (x + iy)^n \cdot (a_0 r^{N-n} + a_1 r^{N-n-2} + ...) \tag{2.10}$$

in the same way as in the case of stationary systems [13], but unlike the latter, the coefficients $a_0, a_1, \ldots.$ in (2.10) depend on the time t. Recall that in (2.10) N- is the main perturbation order, and n -is the main index of the spherical harmonic, which is equal to the azimuthal wave number m for sectorial perturbations. Although in the most general case $\delta\Phi$ should contain three wave numbers, when deriving the dispersion relation of the model stability problem, it is quite sufficient to represent $\delta\Phi$ in the form (2.10), as always when considering vibrations of spherically symmetric bodies.

Further, by analogy with the theory of stability of stationary models [13], it is necessary to clearly distinguish between "surface" and "volumetric" types of perturbation, and to find the dispersion equations, it suffices to restrict ourselves to one leading term in (2.10). In the case of "surface" perturbations N=n and we proceed from the expression

$$\delta\Phi = a_0(\psi) \cdot (x + iy)^n \tag{2.11}$$

Consequently,

$$\partial(\delta\Phi)/\partial x = n a_0(\psi) \cdot (x + iy)^{n-1} = -i[\partial(\delta\Phi)/\partial y], \quad \partial(\delta\Phi)/\partial z = 0, \tag{2.12}$$

those $\overline{\delta z} = 0$. The latter means that the equation for the component δz can only have a periodic solution, and the growing solution vanishes. From (2.12) for surface perturbations, the identity $\delta y = i\delta x$, also follows, which entails the equality to zero (see (2.14)) of the density perturbation $\delta\rho$, so that the effect of potential perturbation (2.11) is expressed only in the curvature of the outer surface of the pulsating models. In the case of "volumetric" perturbations $N \neq n$ and $\delta\Phi$ it is enough to take in the form [24]:

$$\delta\Phi = a_0(\psi) \cdot r^{N-n} (x + iy)^n \tag{2.13}$$

At the same time, it is noteworthy that deformations of the system boundary affect only the terms of the lowest degree in the expansion for $\delta\Phi$ and are not essential in recognizing the exponential or periodic nature of oscillations superimposed on the main pulsation. The volume density perturbation value is now different from zero and is equal to

$$\delta\rho = -\rho(\psi) \cdot [\partial(\overline{\delta x})/\partial x + \partial(\overline{\delta y})/\partial y + \partial(\overline{\delta z})/\partial z]. \tag{2.14}$$

Thus, substituting separately (1.11) and (2.13) into (2.5) and introducing the notation

$$E(\psi,\psi_1) = (\Omega_0^4 / q^6)\cdot(1+\cos\psi_1)^3 \cdot S(\psi,\psi_1)\cdot a_0(\psi) \tag{2.15}$$

you can write the corresponding components of the displacement vector $\delta\vec{r}$ for each type of perturbation.

I. For “surface” perturbations:

$$\overline{\delta x} = -i\overline{\delta y} = n\cdot\int_{-\infty}^{\psi}\overline{(x_1+iy_1)^{n-1}}E(\psi,\psi_1)d\psi_1, \tag{2.16}$$

where $x_1=x(\psi_1)$ и $y_1=y(\psi_1)$.

II. For “volumetric” perturbations:

$$\overline{\delta x} = \int_{-\infty}^{\psi}E(\psi,\psi_1)[n\cdot\overline{(x_1+iy_1)^{n-1}r_1^{2k}} + (N-n)\overline{x_1(x_1+iy_1)^{n-1}r_1^{2k-2}}]d\psi_1,$$

$$\overline{\delta y} = \int_{-\infty}^{\psi}E(\psi,\psi_1)[i\,n\cdot\overline{(x_1+iy_1)^{n-1}r_1^{2k}} + (N-n)\overline{y_1(x_1+iy_1)^{n}r_1^{2k-2}}]d\psi_1,$$

$$\overline{\delta z} = (N-n)\int_{-\infty}^{\psi}E(\psi,\psi_1)\overline{z_1(x_1+iy_1)^{n}r_1^{2k-2}}d\psi_1, \tag{2.17}$$

Here $r_1=r(\psi_1)$, $k=(N-n)/2$. From (2.16) and (2.17) it can be seen that when calculating the components of the displacement vector $\overline{\delta\vec{r}}$ averaging, for example, expressions of the form $(x_1+iy_1)^{\tau}$, according to (2.8), is reduced to averaging different members of the type $(u+iv)^{\tau}$ over the velocity space for the current moment of pulsation, taking into account a specific expressions for the phase density function.

§ 7. “Surface” perturbations against the background of nonlinear pulsations

We begin our analysis of the stability of pulsating states with respect to surface perturbations with the case of a non-rotating model (1.29), and then in Section 9 we generalize the results to the case of a rotating model (1.38). We will

proceed similarly in the future, in the case of volume perturbations and analysis of other models. In this case, each time we will try to apply different, most appropriate methods to derive the appropriate dispersion relation in order to develop rigorous methods for analyzing the stability of nonequilibrium models.

7a. Non-stationary dispersion equation (NDR)

It can be seen from (2.16) that in the case of N=n the problem is reduced to averaging only one expression $(x_1 + iy_1)^{n-1}$. Therefore, we expand it into Newton's binomial, taking into account the connection formula (2.8). Then we have

$$\overline{(x_1 + iy_1)^{n-1}} = \sum_{\tau=0}^{n-1} \frac{(n-1)!}{\tau!\,(n-\tau-1)!}[(x - iy)H_\alpha]^{n-\tau-1} H_\beta^\tau \overline{(u+iv)^\tau} \tag{2.18}$$

Here for model (1.29)

$$\overline{(u+iv)^\tau} = (2\pi v_b)^{-1} \iiint (u+iv)^\tau \delta(v_r - v_a)\delta(v_\perp - v_b)\,du\,dv\,dw. \tag{2.19}$$

In (2.19), we turn to integration over $(v_r, v_\perp, \eta)$ and take into account that in spherical coordinates (r,θ,φ)

$$u + iv = (v_r \sin\theta - v_\perp \cos\theta \cos\eta + iv_\perp \sin\eta)\cdot e^{i\varphi} \tag{2.20}$$

Substituting (2.20) into (2.19) and calculating the integrals over v_r and $v_\perp$, we find

$$\overline{(u+iv)^\tau} = A(\psi)\cdot(x+iy)^\tau \tag{2.21}$$

where

$$A(\psi) = (2\pi r^\tau)^{-1} \int_0^{2\pi} (v_a + iv_\perp \cos\xi)^\tau \, d\xi, \tag{2.22}$$

and the notation

$$(-\cos\theta\cdot\cos\eta + i\sin\eta)/\sin\theta = i\cos\xi, \tag{2.22'}$$

and the value $v_\perp$ in this case is determined by the formula (1.27). It is possible to prove even a slightly more general averaging formula than (2.21), namely

$$\overline{(e_1 u + e_2 v + e_3 w)^\tau} = A(\psi)\cdot(e_1 x + e_2 y + e_3 z)^\tau \tag{2.23}$$

for any complex numbers e_1, e_2 and e_3 satisfying the relation $e_1^2 + e_2^2 + e_3^2$. Indeed, in the particular case x=y=0, z=r we have

$$\overline{(\mathrm{ev})^{\tau}} = (2\pi)^{-1}\int_0^{2\pi}[v_{\perp}(e_1^2+e_2^2)^{1/2}\cos\xi + e_3 v_r]^{\tau}\mathrm{d}\xi =$$

$$=\left(\mathrm{e}_3^{\tau}/2\pi\right)\cdot\int_0^{2\pi}(\mathrm{v_r}+\mathrm{iv}_{\perp}\cos\xi)^{\tau}\mathrm{d}\xi..$$

Hence, taking into account the equality $\mathrm{v_r} = \mathrm{v_a}$, we are convinced of the validity of formula (2.23). The function A(ψ), taking into account (1.27), (1.28) and (1.23), has the form

$$\mathrm{A}(\psi) = (2\pi)^{-1}(-\mathrm{q}^3/\Omega^2)^{\tau}(1+\lambda\cos\psi)^{-2\tau}\int_0^{2\pi}[\lambda\sin\psi - \mathrm{i}(1-\lambda^2)^{1/2}\cos\xi]^{\tau}\,\mathrm{d}\xi \qquad (2.24)$$

Substituting (2.21) and (2.24) into (2.18), we have

$$\overline{(\mathrm{x}_1+\mathrm{iy}_1)^{\mathrm{n-1}}} = \frac{(\mathrm{x+iy})^{\mathrm{n-1}}}{2\pi}\int_0^{2\pi}\{\mathrm{H}_{\alpha} - \mathrm{H}_{\beta}\frac{\mathrm{q}^3[\lambda\sin\psi - \mathrm{i}(1-\lambda^2)^{1/2}\cos\xi]}{\Omega^2(1+\lambda\cos\psi)^2}\}^{\mathrm{n}-1}\mathrm{d}\xi \qquad (2.25)$$

Taking into account the expressions for H_{α} and H_{β} in (2.9) and opening the square bracket in (2.25), we represent the result obtained as a Newton binomial in powers of $\sin\psi_1$. Then

$$\overline{(\mathrm{x}_1+\mathrm{iy}_1)^{\mathrm{n-1}}} = \mathrm{C}_{\mathrm{n-1}}(\psi,\psi_1)\cdot(\mathrm{x}+\mathrm{iy})^{\mathrm{n-1}} \qquad (2.26)$$

where

$$\mathrm{C}_{\mathrm{n-1}}(\psi,\psi_1) = \sum_{\tau=0}^{\mathrm{n-1}}\frac{(\mathrm{n-1})!}{\tau!\,(\mathrm{n-\tau-1})!}\frac{\sin^{\tau}\psi_1(\lambda+\cos\psi_1)^{\mathrm{n}-\tau-1}}{(1+\lambda\cos\psi)^{2\mathrm{n}-2}}\mathrm{h}_{\tau}(\psi) \qquad (2.27)$$

moreover

$$\mathrm{h}_{\tau}(\psi) = (2\pi)^{-1}\int_0^{2\pi}[\lambda+\cos\psi-(\lambda^2-1)^{1/2}\sin\psi\cos\xi]^{\mathrm{n}-\tau-1}\cdot$$
$$\cdot[(1-\lambda^2)\sin\psi+(\lambda^2-1)^{1/2}(\lambda+\cos\psi)\cos\xi]^{\tau}\,\mathrm{d}\xi \qquad (2.28)$$

According to (2.16), we find the desired

$$\overline{\delta\mathrm{x}} = -\mathrm{i}\overline{\delta\mathrm{y}} = \Theta(\psi)\cdot(\mathrm{x}+\mathrm{iy})^{\mathrm{n-1}}, \qquad (2.29)$$

where

$$\Theta(\psi) = n \int_{-\infty}^{\psi} E(\psi, \psi_1) \cdot C_{n-1}(\psi, \psi_1) d\psi_1 \ . \qquad (2.30)$$

Knowing (2.29), it is also easy to determine the displacement of a surface point along the radius and the corresponding perturbation of the potential

$$\overline{\delta r} = (x \cdot \overline{\delta x} + y \cdot \overline{\delta y}) = \Theta(\psi)(x + iy)^n / R, \quad \delta\Phi = 4\pi G \cdot \rho \cdot R \cdot \overline{\delta r} / (2n + 1). \qquad (2.31)$$

Comparing the found expression for $\delta\Phi$ with the theoretically given one (2.11), we obtain

$$a_0(\psi) = \frac{3}{2n+1} \Omega_0^2 \Theta(\psi) [\Pi(\psi)]^{-3} \qquad (2.32)$$

Substituting (2.30) into (2.32), taking into account (2.27) and by analogy with the connection between (2.3) and (2.5), we have

$$\Lambda l_\tau(\psi) = a_0(\psi)(1 + \lambda \cos\psi)^3 (\lambda + \cos\psi)^{n-\tau-1} (\sin\psi)^\tau \qquad (2.33)$$

where τ=0, 1, 2, . . ., n-1 and the notation

$$l_\tau(\psi) \equiv \int_{-\infty}^{\psi} a_0(\psi_1)(1 + \lambda \cos\psi_1)^3 S(\psi, \psi_1)(\lambda + \cos\psi_1)^{n-\tau-1} (\sin\psi_1)^\tau \, d\psi_1 \qquad (2.34)$$

and now [14]

$$a_0(\psi) = \frac{3n}{2n+1} (1 + \lambda \cos\psi)^{-(2n+1)} \sum_{\tau=0}^{n-1} \frac{(n-1)!}{\tau!(n-\tau-1)!} h_\tau(\psi) l_\tau(\psi). \qquad (2.35)$$

Thus, (2.33)-(2.35) are a non-stationary analogue of the dispersion equation of the stability problem for the nonlinear model (1.29). In what follows, for brevity, such an equation will be called the nonstationary dispersion equation (NDE).

In principle, this system of equations can be reduced to a single integral equation. To do this, (2.25) must be expressed in terms of the Legendre polynomial $P_{n-1}(\cosh^*)$ by introducing the notation

$$H_\alpha + v_a H_\beta / r = W \cdot \cosh^*, \quad v_b H_\beta / r = W \cdot \sinh^* \qquad (2.36)$$

Then, substituting (2.36) into (2.25), after some transformations we find

$$C_{n-1}(\psi, \psi_1) = W^{n-1} P_{n-1}(\cosh^*),$$

$$\cosh^* = \frac{(\lambda+\cos\psi)(\lambda+\cos\psi_1)+(1-\lambda^2)\sin\psi\sin\psi_1}{(1+\lambda\cos\psi)(\lambda+\cos\psi_1)}. \qquad (2.37)$$

Everything else remains the same and as a result we get the following equation

$$\Pi^3(\psi)\cdot a_0(\psi)=\frac{3n}{2n+1}\cdot\int\limits_{-\infty}^{\psi}\Pi^3(\psi_1)\cdot a_0(\psi_1)\cdot S(\psi,\psi_1)\cdot C(\psi,\psi_1)d\psi_1 \qquad (2.38)$$

However, this integral form of the NDE is difficult for practical analysis and it is easier to deal with its differential representation (2.33)-(2.35).The special case λ=0 corresponds to the imposition of asymmetric perturbations on the equilibrium model without pulsations. Wherein $v_a=0, v_b=\Omega_0 r$, W=1, Π=1,

$$H_\alpha=\cos(\psi-\psi_1),\quad S=\sin(\psi-\psi_1),\quad H_\beta=S/\Omega_0. \qquad (2.39)$$

and the system of equations (2.33)-(2.35) is easily reduced to the equation

$$a_0(\psi)=\frac{3n}{2n+1}\cdot\int\limits_{-\infty}^{\psi}a_0(\psi_1)\cdot\sin(\psi-\psi_1)\cdot P_{n-1}[\cos(\psi-\psi_1)]d\psi_1 \qquad (2.40)$$

Being interested in the exponential solution of the form $a_0(\psi_1)\propto\exp(i\omega\psi_1)$, we obtain the following dispersion relation

$$\int\limits_0^\infty e^{-i\omega\aleph}\sin\aleph\cdot P_{n-1}(\aleph)d\aleph=\frac{2n+1}{3n},\quad \aleph=\psi-\psi_1. \qquad (2.41)$$

This case λ=0 was first studied in [25]. Our calculation coincides with his result and shows the complete stability of the equilibrium model. The latter can be easily proved if we pass from (2.41) to the multiplicative notation.

7b. Large -Scale Modes

Let's pass to the analysis (2.33)-(2.35) with arbitrary λ. When n=1, we are dealing with a trivial displacement of the system as a whole, which does not cause any instability. Indeed, considering in (2.33) n=1, we have only one equation, the integration of which gives

$$l_0(\psi)=\psi+\lambda\sin\psi+\text{const},\quad a_0(\psi)=l_0(\psi)/(1+\lambda\cos\psi)^3 \qquad (2.42)$$

Of great interest is the large-scale oscillation mode with a value of n=2, under the instability of which the pulsating ball takes an elliptical shape. In this case

$$a_0(\psi)=1.2\gamma(\psi)/(1+\lambda\cos\psi)^5,\quad \gamma(\psi)=(\lambda+\cos\psi)l_0+(1-\lambda^2)\sin\psi\, l_1 \qquad (2.43)$$

Substituting (2.43) into (2.33), we now have two equations

$$\Lambda l_0(\psi) = (6/5)(\lambda + \cos\psi)(1 + \lambda\cos\psi)^{-2}\gamma(\psi) \tag{2.44}$$

$$\Lambda l_1(\psi) = (6/5)\sin\psi(1 + \lambda\cos\psi)^{-2}\gamma(\psi) \tag{2.45}$$

Hence, we note that for an arbitrary function $l(\psi)$ we have the identity

$$U_\tau\{l\} \equiv M'_\tau(\psi)\cdot\Lambda l(\psi) = \frac{d}{d\psi}[(1+\lambda\cos\psi)l'\cdot M'_\tau + l\cdot M_\tau] \tag{2.46}$$

(τ=0; 1), where the following designations are introduced

$$M_0(\psi) = \sin\psi/(1+\lambda\cos\psi), \quad M_1(\psi) = \cos\psi/(1+\lambda\cos\psi) \tag{2.47}$$

Composing the sum $U_0\{l_1\}+U_1\{l_0\}$ and using (2.44) and (2.45), we obtain the relation of the first derivatives

$$\sin\psi\cdot l'_0 - (\lambda+\cos\psi)\cdot l'_1 = \sin\psi\cdot l_1 + \cos\psi\cdot l_0 \tag{2.48}$$

Further, forming a difference of the form $U_0\{l_0\}-(1-\lambda^2)U_1\{l_1\}$, taking into account (2.44) and (2.45), we obtain

$$\frac{d}{d\psi}[(\gamma'+2H)/(1+\lambda\cos\psi)] = (6/5)\gamma(\psi)/(1+\lambda\cos\psi)^2 \tag{2.49}$$

and $H\equiv\sin\psi\cdot l_0(\psi)-(1-\lambda^2)\cdot\cos\psi\cdot l_1(\psi)$.Using relation (2.48), we can find the relationship between the functions $\gamma(\psi)$ and $H(\psi)$ in the form

$$\frac{d}{d\psi}[H(\psi)/(1+\lambda\cos\psi)] = [(2-\lambda\cos\psi)\gamma + \lambda\sin\psi\cdot\gamma']/(1+\lambda\cos\psi)^2 \tag{2.50}$$

Then equation (2.49), taking into account (2.50), takes the following form:

$$(1+\lambda\cos\psi)\cdot\gamma'' + 3\lambda\sin\psi\cdot\gamma' + (14/5 - 2\lambda\cos\psi)\gamma = 0 \tag{2.51}$$

Thus, instead of two equations (2.44) and (2.45), one equation was obtained, which is easier to analyze further by analytical methods.

According to the theory of stability of motions [26] described by a second-order differential equation, a periodic solution of equation (2.51) must exist at the critical point of loss of instability. An appropriate search for such a 2π-periodic solution shows that it is equal to

$$\gamma(\psi) = \cos\psi + (15/14)\cdot\lambda, \tag{2.52}$$

if only at the same time

$$\lambda^2 = 21/25, \quad \lambda = 0.9165 \equiv \lambda^*_{22}. \tag{2.52'}$$

Since we analytically found only one critical value of the pulsation amplitude λ_{22}^{*} , we must also prove that there are no other 2π-periodic solutions for $\lambda \neq \lambda_{22}^{*}$. This rigorous proof is given by us in the appendix of [24]. Therefore, ellipsoidal instability occurs if $\lambda > \lambda_{22}^{*}$, which is equivalent to the condition

$$(2T/|U|)_0 < 1 - (21/25)^{1/2} = 0.084 \qquad (2.53)$$

This result is in very good agreement with the numerical experimental conclusions of the authors [4, 27, 28] obtained much later without knowing about our publications [14, 21, 24].

In accordance with the same well-known theory [26], equation (2.51) can also have 4π-periodic solutions limiting on the scale λ a certain instability zone of a different nature. Since the analytical search for exact solutions with a period of 4π is a difficult task, we carried out a numerical solution of the differential equation (2.51) and, using the method of stability of periodic solutions, found an instability zone in the region $\lambda < \lambda_{22}^{*}$, namely, it fills the interval [75] $\lambda \in (0.611; 0.873)$. In this case, characteristic equations were solved, composed of solutions (2.51) at the point $\psi = 2\pi$ for various $\lambda \in (0, \lambda_{22}^{*})$. The values of the instability growth rate Inc and the characteristic time (t_2) of doubling the magnitude of the disturbance growth amplitude were calculated using the following formulas:

$$\mathrm{Inc} = [\ln(\|k_{max}\|)]/P(\lambda), \qquad t_2 = (\ln 2)/\mathrm{Inc}, \qquad (2.54)$$

where $\|k_{max}\|$ - is the value of the largest modulus of the root of the characteristic equation. The table below shows the calculation results for Inc and t_2 , as well as the corresponding values of the anisotropy parameter ∇ for the instability regions.

Tab. 2.1

λ	Inc$[10^{-2}\Omega_0]$	t_2	$\nabla/2$	$(2T/\|U\|)_0$
0.611	0	0	0.526	0.389
0.66	3.172	21.852	0.662	0.34
0.70	3.710	18.683	0.400	0.30
0.78	3.359	20.365	0.598	0.22
0.84	2.054	33.746	0.843	0.16
0.92	82.276	0.842	1.551	0.08
0.95	285.77	0.303	1.931	0.05
0.98	495.49	0.140	4.025	0.02

Calculations show that, under condition (2.53), an aperiodic instability sets in. It is clearly seen from the values of the instability increment that the detected second instability zone corresponds to the values $(2T/|U|)_0 \in (0.127;\ 0.389)$ and is not inferior to (2.53). The second zone of instability, on the one hand, according to the calculations, has an oscillatory nature, and on the other hand, it seems to be associated with the 2:3 resonance phenomenon between the oscillations of individual particles and the collective motions of the N=n=2 oscillation mode. Indeed, the frequency of collective oscillations of the ellipsoidal mode $\sqrt{14/5}$ is close to 3/2. For the corresponding equilibrium model [29], where stability analysis leads to differential equations with constant coefficients, this resonance obviously cannot manifest itself in any way, since there is no exact commensurability of frequencies. And for equilibrium systems, generally speaking, the conditions for the occurrence of resonance are somewhat weakened. In addition, it should be noted that, on average, the velocity-isotropic nonlinear model with $\nabla=1$ also belongs to the indicated zone of vibrational-resonant instability, which covers the segment (0.526; 2.100) on the scale of the anisotropy parameter.

Returning to the above critical value of the pulsation amplitude (2.52'), we note that it is not very close to the oscillatory-resonant zone of instability. In this case, the corresponding value of the anisotropy parameter $\nabla(\lambda=\lambda^*_{22})$ is exactly 3. It is clear that the instability physics in the region $(2T/|U|)_0<0.084$ is clearly related to the Newtonian collapse from an almost "cold" state and the presence of a sharp anisotropy in the radial and transversal energy components movement. Consequently, under such conditions, the instability of almost radial motions occurs, which is confirmed by numerical experiments. Among the numerical-experimental works, the possibility of instability of radial orbits was first indicated in the article by V.L. Polyachenko 1981, but it did not set the task of determining the exact criterion for this instability. Analytical proof of the existence of instability of radial orbits for equilibrium systems was first strictly shown by V.A.Antonov in 1973, and here we study this instability for nonequilibrium systems.

Let us dwell briefly on the case of N=n=3 ("triangular perturbations") (1,30), although it could equally well be attributed to small-scale and large-scale perturbations. In this case, the nonstationary dispersion equation (2.33) takes the following form

$$\begin{aligned}
&\Lambda l_\tau = (9/7)\sin^\tau\psi(\lambda+\cos\psi)^{2-\tau}(1+\lambda\cos\psi)^{-4}\cdot\\
&\cdot\{[(\lambda+\cos\psi)^2-0.5(1-\lambda^2)\sin^2\psi]\cdot l_0+\\
&+3(1-\lambda^2)\sin\psi(\lambda+\cos\psi)\cdot l_1+\\
&(1-\lambda^2)[(1-\lambda^2)\sin^2\psi-0.5(\lambda+\cos\psi)^2]\cdot l_2\},
\end{aligned} \tag{2.55}$$

(τ=0,1,2). This system of differential equations of the 6th order is not amenable to theoretical analysis and therefore it was studied numerically on a computer. Calculations show that again there is an "island" of vibrational instability, and the corresponding region is five times narrower than in the case of the ellipsoidal vibration mode, and is located in the interval $0.762<\lambda<0.819$,, i.e. $0.181<(2T/|U|)_0<0.238$. The corresponding values of the anisotropy parameter ∇ are in the interval $1.088<\nabla<1.486$. It turns out that, on average, the pulsating model with ∇=1, isotropic in terms of speed, is in the stability region. Another zone of instability of the nonequilibrium model is located in the region of almost radial motions

$$\lambda > 0.834 = \lambda_{33}^{*}, \qquad (2T/|U|)_0 < 0.166, \tag{2.56}$$

what do the values $\nabla>1.624$ correspond to. Interestingly, at n=3 in the zones of instability, literally all the roots of the characteristic equation are only complex conjugate, i.e. instabilities are of an oscillatory nature, and, unlike ellipsoidal instability, they arise in the region $\nabla>1$.

§ 8. Volume types of perturbations

Let us turn to the analysis of the behavior of such asymmetric perturbations against the background of pulsations, the instability of which gives rise to global density inhomogeneities in the system [24]. Now it is already n≠N and, in contrast to surface oscillations, where the volume density perturbation is strictly equal to zero, here the process of inhomogeneity generation is also accompanied by some curvature of the outer boundary of the system, which is less significant if it is required to obtain NDR for arbitrary n and N of the same parity. This equation makes it possible to consider limiting and any cases.

8a. Output of the complete NDE

In this case, just as in the previous paragraph, we can use the method of binomial expansion and averaging over the velocity space. Then, according to (2.17), it is necessary to separately derive averaging formulas for the expressions $\overline{u(u+iv)^{\tau}}$, $\overline{v(u+iv)^{\tau}}$, $\overline{w(u+iv)^{\tau}}$. The direct derivation of these formulas, which solve the problem posed and may also be useful in similar problems on the oscillations of other dynamical systems, is given in detail in the Appendix of [24]. Here we will show the possibility of another method, namely, we will use the well-known fact - the spherical symmetry of the pulsating model, taking into account

the regular appearance of terms of the same degree in coordinates as before averaging over velocities. Then, as a result of averaging the corresponding expressions in (2.17), we must have

$$\begin{aligned}
\overline{\delta x} &= B_1 r^{2k}(x+iy)^{n-1} + B_2 r^{2k-2} x(x+iy)^n, \\
\overline{\delta y} &= iB_1 r^{2k}(x+iy)^{n-1} + B_2 r^{2k-2} y(x+iy)^n, \\
\overline{\delta z} &= B_2 r^{2k-2} z(x+iy)^n,
\end{aligned} \tag{2.57}$$

and knowledge of one formula (2.26) is sufficient. Indeed, we define the unknown coefficients B_1 and B_2, which are a function of ψ, composing from (2.57) the following combinations

$$\overline{\delta x} + i\overline{\delta y} = B_2 r^{2k-2}(x+iy)^{n+1}, \tag{2.58}$$

$$x\cdot\overline{\delta x} + y\cdot\overline{\delta y} + z\cdot\overline{\delta z} = (B_1 + B_2) r^{2k}(x+iy)^n. \tag{2.59}$$

On the other hand, from (2.17), taking into account relation (2.8), which can be represented in the form

$$\vec{r}(\psi_1) = \vec{r}(\psi) H_\alpha + \vec{v}(\psi) H_\beta \tag{2.60}$$

we get

$$\overline{\delta x} + i\overline{\delta y} = (N-n)\int_{-\infty}^{\psi} r_1^{2k-2} E(\psi,\psi_1)\overline{(x_1+iy_1)^{n+1}}\, d\psi_1, \tag{2.61}$$

$$\begin{aligned}
x\cdot\overline{\delta x} + y\cdot i\overline{\delta y} + z\cdot\overline{\delta z} &= n(x+iy)\int_{-\infty}^{\psi} r_1^{2k}\overline{E(x_1+iy_1)^{n-1}}\, d\psi_1 + \\
&+ (N-n)\int_{-\infty}^{\psi} r_1^{2k-2}(H_\alpha r^2 + H_\beta r v_r)\overline{E(x_1+iy_1)^n}\, d\psi_1,
\end{aligned} \tag{2.62}$$

According to (2.60), in (2.61) and (2.62) the quantity r_1^{2k} is equal to

$$r_1^{2k} = \tilde{H}_k\cdot[r(\psi)]^{2k}, \quad \tilde{H}_k \equiv [(H_\alpha + H_\beta v_r/r)^2 + (H_\beta v_\perp/r)^2]^k \tag{2.63}$$

and it is taken out of the averaging sign, since in model (1.29) $v_r = v_a$ and $v_\perp = v_b$, are fixed for the given $r(\psi)$. Using (2.26) and (2.63) in (2.61) and (2.62), we compare the obtained results with (2.58) and (2.59), respectively. We have

$$B_1 = n\int_{-\infty}^{\psi}\tilde{H}_k E\cdot C_{n-1}\, d\psi_1 + (N-n)\int_{-\infty}^{\psi}\tilde{H}_{k-1}E\cdot(H_\alpha + H_\beta v_r/r)C_n\, d\psi_1 - B_2 \tag{2.64}$$

$$B_2 = (N-n)\int_{-\infty}^{\psi} \tilde{H}_{k-1} E \cdot C_{n+1} d\psi_1, \quad (k = \frac{N-n}{2}). \tag{2.65}$$

Note that the direct method of averaging over velocities, which we presented in the appendix of [24], gives the same results.

Next, we calculate the volume density perturbation

$$\delta\rho = -\rho(\partial\overline{\delta x}/\partial x + \partial\overline{\delta y}/\partial y + \partial\overline{\delta z}/\partial z), \tag{2.66}$$

moreover, $\rho=3\Omega^2/(4\pi G\cdot\Pi^3)$ - is the density of the non-linear pulsating configuration. Substituting (2.57) into (2.66), we obtain

$$\delta\rho = -\frac{3\Omega^2}{4\pi G\Pi^3} r^{2k-2} (x+iy)^n [2kB_1 + (2k+n+1)B_2]. \tag{2.67}$$

On the other hand, calculating the Laplace operator from expression (2.13), from the Poisson equation we find the corresponding theoretical relation

$$\delta\rho = -\frac{k}{2\pi G}(2k+2n+1) r^{2k-2} (x+iy)^n a_0(\psi). \tag{2.68}$$

Comparing (2.68) with (2.67) and taking into account (2.64) and (2.65), we obtain the desired non-stationary dispersion equation for volume perturbations imposed on a nonlinearly pulsating spherical model (1.29)

$$\begin{aligned} a_0(\psi) = \frac{3\Omega^2}{(2k+2n+1)\Pi^3} \int_{-\infty}^{\psi} [n \cdot \tilde{H}_k C_{n-1} + \\ + (n+1)\tilde{H}_{k-1} C_{n+1} + 2k \cdot \tilde{H}_{k-1} (H_\alpha + H_\beta v_a / r) C_n] E d\psi_1. \end{aligned} \tag{2.69}$$

The integrand in (2.69) can be substantially simplified. For this, we note that, according to (2.36), (2.9), (1.28), and (1.27), the function

$$\tilde{H}_k(\psi, \psi_1) = W^{2k} = [(1+\lambda\cos\psi_1)/(1+\lambda\cos\psi)]^{2k}. \tag{2.70}$$

Using (2.37), (2.70) and the recurrent formula for the Legendre polynomials, from (2.69) we find that

$$\Pi^3(\psi) a_0(\psi) = 3\Omega^2 \int_{-\infty}^{\psi} W^{2k-1} C_n(\psi, \psi_1) \cos 1 \cdot E d\psi_1. \tag{2.71}$$

Finally, it is necessary to move from the integral form of writing to the differential. For this purpose, we use formula (2.27). Then, taking into account (2.36) and (2.70), we have

$$\Pi^3(\psi) a_0(\psi) = \frac{3}{(1+\lambda\cos\psi)^{N+n}} \Gamma(\psi), \tag{2.72}$$

where

$$\Gamma(\psi)=\sum_{\tau=0}^{n}\frac{n!}{\tau!(n-\tau)!}h_{\tau}(\psi)[(\lambda+\cos\psi)\Gamma_{\tau}^{(1)}(\psi)+(1-\lambda^{2})\sin\psi\cdot\Gamma_{\tau}^{(2)}(\psi)], \tag{2.73}$$

and $h_\tau(\psi)$ is expressed by formula (2.28) with n replaced by n+1, and functions $\Gamma_{\tau}^{(\ell)}(\psi)$ are equal to

$$\Gamma_{\tau}^{(1)}(\psi)=\int_{-\infty}^{\psi}(1+\lambda\cos\psi_1)^{2k-2}\sin^{\tau}\psi_1(\lambda+\cos\psi_1)^{n-\tau+1}\Pi^{3}(\psi_1)S\cdot a_0(\psi_1)d\psi_1 \tag{2.74}$$

$$\Gamma_{\tau}^{(2)}(\psi)=\int_{-\infty}^{\psi}(1+\lambda\cos\psi_1)^{2k-2}\sin^{\tau+1}\psi_1(\lambda+\cos\psi_1)^{n-\tau}\Pi^{3}(\psi_1)S\cdot a_0(\psi_1)d\psi_1 \tag{2.75}$$

This form of notation for integrals makes it possible to pass to differential equations in a similar way to the connection between (2.33) and (2.34). Consequently,

$$\Lambda\Gamma_{\tau}^{(1)}(\psi)=\frac{3(\sin\psi)^{\tau}(\lambda+\cos\psi)^{n-\tau+1}}{(1+\lambda\cos\psi)^{2(n+1)}}\Gamma(\psi), \tag{2.74'}$$

$$\Lambda\Gamma_{\tau}^{(2)}(\psi)=\frac{3(\sin\psi)^{\tau+1}(\lambda+\cos\psi)^{n-\tau}}{(1+\lambda\cos\psi)^{2(n+1)}}\Gamma(\psi)\ . \tag{2.75'}$$

As can be seen, in this case, the NDE in the differential notation contains the degeneracy property, which manifests itself in the independence of the stability analysis results from a specific value of N. Obviously, this property takes place for the corresponding stationary model [29], since for λ=0 we obtain T=1.

When λ=0, counting $a_0(\psi)\propto\exp(i\omega\psi)$, from (2.71) we find the following dispersion equation

$$\int_{0}^{\infty}e^{-i\omega\ell}P_n(\cos\ell)\cos\ell d\ell=1/3. \tag{2.76}$$

Substituting here the expansion of the Legendre polynomial in cosines of multiple arguments, we easily calculate the integral and obtain the previously known result on the complete stability of the equilibrium model [29, 13].

8b. Analysis of individual oscillation modes: Dipole-odd perturbations

Let us consider the case of large-scale disturbances at $\lambda \neq 0$. Since for volume perturbations the difference N-n>0 and is always even, we generally speaking must analyze the cases n=1, 3, ...; N=3, 5, ... and n=0, 2, ...; N=2, 4, ... But for n=0 and an arbitrary even N, the perturbations are symmetric and, therefore, individual spherical shells will pulsate synchronously, which usually does not cause instability [29–32]. Verification indeed shows the absence of instability. Therefore, of greatest interest is the large-scale type of oscillation with harmonics n=1, N=3, which displaces the kinematic center of the system and causes not only inhomogeneity, but also "ovoid" deformation (in Chandrasekhar's book [33], only homogeneous states of a liquid medium in a perturbed state are considered , in accordance with which sometimes this type of oscillation is also called "pear-shaped"). If we project the system onto the (x, y) plane (i.e., look at the model along the z axis), having previously divided the system conditionally into a set of spherical shells, then, upon the onset of egg-shaped instability, their projections will take on the shape that is obtained when a lying egg is projected onto plane z=const. Such a picture is also observed when considering the density isophotes of individual galaxies or clusters. Similarly, a number of edge-on galaxies are known to have significantly different thicknesses on both sides of the nucleus [34].

Note that the instability condition obtained below also applies to the cases n=1; N=5.7, . . . , since the quantity N does not enter into equations (2.74') and (2.75') in any way. In general, such n and N can be called dipole-odd perturbations.

Substituting n=1 into (2.74') and (2.75'), we write each of them for $\tau=0$ and $\tau=1$. Noting that $\Gamma_1^{(1)}(\psi) = \Gamma_0^{(2)}(\psi) \equiv F_2(\psi)$, and introducing the notation $F_1(\psi) = \Gamma_0^{(1)}(\psi)$ and $F_3(\psi) = \Gamma_1^{(2)}(\psi)$, we have

$$\Lambda F_\nu(\psi) = \frac{3\Gamma(\psi)}{(1+\lambda\cos\psi)^4}(\sin\psi)^{\nu-1}(\lambda+\cos\psi)^{3-\nu}, \quad (\nu = \overline{1-3}) \tag{2.77}$$

where

$$\Gamma(\psi) = (\lambda+\cos\psi)\gamma_1(\psi) + (1-\lambda^2)\sin\psi\cdot\gamma_2(\psi) \tag{2.78}$$

if

$$\gamma_j(\psi) \equiv (\lambda+\cos\psi)F_j + (1-\lambda^2)\sin\psi\cdot F_{j+1}, \quad (j = \overline{1,2}) \tag{2.79}$$

System (2.77) of three differential equations has a critical value λ, which separates the regions of stability and instability. Let's find this value analytically.

To do this, we lower the order of the system (2.77), eventually bringing it to one differential equation of the 2-nd order, which is more convenient and makes it possible to find the exact value of λ in the critical state.

First, we reduce the number of equations in (2.77) by one using identity (2.46). Considering in (2.46) the sum $U_0\{F_{j+1}\} + U_1\{F_j\}$ for $j = 1$ and 2, we obtain the connection of the first derivatives

$$\sin\psi \cdot F'_j(\psi) - (\lambda + \cos\psi)F'_{j+1}(\psi) = \sin\psi \cdot F'_{j+1}(\psi) + \cos\psi \cdot F'_j(\psi). \qquad (2.80)$$

Compiling the difference $U_0\{F_j\} - (1-\lambda^2)U_1\{F_{j+1}\}$ and using (2.79), respectively, we find

$$\frac{d}{d\psi}\left[\frac{\gamma'_j(\psi)+2H_j(\psi)}{1+\lambda\cos\psi}\right] = \frac{3\Gamma(\psi)(\sin\psi)^{j-1}}{(1+\lambda\cos\psi)^4}(\lambda+\cos\psi)^{2-j}. \qquad (2.81)$$

where $H_j(\psi) \equiv \sin\psi \cdot F_j - (1-\lambda^2)\cdot\cos\psi \cdot F_{j+1}$. It is easy to show that

$$\frac{d}{d\psi}\left[\frac{H_j(\psi)}{1+\lambda\cos\psi}\right] = \frac{1}{(1+\lambda\cos\psi)^2}[(2-\lambda\cos\psi)\gamma_j + \lambda\cos\psi\cdot\gamma'_j]. \qquad (2.82)$$

Substituting (2.82) into (2.81), we have a system of two differential equations for $\gamma_1(\psi)$ and $\gamma_2(\psi)$

$$(1+\lambda\cos\psi)\gamma''_j + 3\lambda\sin\psi\gamma'_j + 2(2-\lambda\cos\psi)\gamma_j = \frac{3\Gamma(\psi)(\sin\psi)^{j-1}}{(1+\lambda\cos\psi)^2}(\lambda+\cos\psi)^{2-j} \qquad (2.83)$$

Analysis (2.83) shows that the system has the following particular solution for arbitrary λ:

$$\tilde{\gamma}_1 = (1-\lambda^2)(\lambda + \cos\psi + \lambda\sin^2\psi), \quad \tilde{\gamma}_2 = (1-2\lambda^2-\lambda\cos\psi)\sin\psi \qquad (2.84)$$

Using this particular solution, a certain invariant relation can be deduced from (2.83) [75]. Indeed, multiplying the equations for γ_1 and γ_2 by $(1+\lambda\cos\psi)^{-4}\cdot\tilde{\gamma}_1$ and $(1-\lambda^2)\cdot(1+\lambda\cos\psi)^{-4}\cdot\tilde{\gamma}_2$, respectively, and then adding them, we take the integral on both sides over an arbitrary interval (b, g). Repeating the same calculations with the roles reversed (γ_1, γ_2) and $(\tilde{\gamma}_1, \tilde{\gamma}_2)$, we subtract one equality from the other. Then all terms that are symmetrical with respect to the replacement $(\gamma_1, \gamma_2) \Leftrightarrow (\tilde{\gamma}_1, \tilde{\gamma}_2)$ drop out and remain

$$\left[\frac{\gamma_1\gamma'_1-\gamma_1\gamma'_1+(1-\lambda^2)(\gamma_2\gamma'_2-\gamma_2\gamma'_2)}{(1+\lambda\cos\psi)^3}\right]_{\psi=b}^{\psi=g}=0 \tag{2.85}$$

for any b and g. Consequently,

$$I\equiv\gamma_1\gamma'_1-\gamma_1\gamma'_1+(1-\lambda^2)(\gamma_2\gamma'_2-\gamma_2\gamma'_2)=0 \tag{2.86}$$

is an invariant. Then we can exclude the found particular solution (2.84) from (2.83) by introducing a new function

$$\aleph=\gamma_2\gamma_1-\gamma_1\gamma_2 \tag{2.87}$$

and composing an expression like

$$\aleph''+\mu_1\aleph'-\mu_2 I\,. \tag{2.88}$$

Substituting (2.87) into (2.88) and getting rid of the second derivatives using (2.83), we select μ_j so that the coefficients at γ'_j vanish.

So we find that

$$\mu_1=\frac{\lambda\sin\psi(5-7\lambda\cos\psi)}{1-\lambda^2\cos^2\psi},\quad \mu_2=\frac{2(1-2\lambda\cos\psi)}{1-\lambda^2\cos^2\psi}. \tag{2.89}$$

After that, in (2.88) some terms remain without derivatives of γ_1 and γ_2. They can be expressed through $\aleph(\psi)$ using (2.84). Then, taking into account (2.86), we have the desired equation

$$(1-\lambda^2\cos^2\psi)\aleph''+\lambda\sin\psi(5-7\lambda\cos\psi)\aleph'+(7-17\lambda\cos\psi+12\lambda^2\cos^2\psi)\aleph=0 \tag{2.90}$$

According to the theory [26], a particular periodic solution of equation (2.90) must exist at the critical point with respect to λ. Analysis (2.90) shows that it has a periodic solution

$$\aleph(\psi)=\cos^3\psi+\frac{1}{\lambda}\cos^2\psi-\frac{5}{14}\cos\psi-\frac{13}{28\lambda} \tag{2.91}$$

on condition

$$\lambda=\sqrt{7/10}\cong 0.8366\equiv\lambda^*_{31}. \tag{2.92}$$

Therefore, the corresponding critical value of the anisotropy parameter

$$\nabla=(2<T_r>/<T_\perp>)=2[\sqrt{10/3}-1]\cong 1.6515 \tag{2.93}$$

and the critical value of the virial parameter (1.44) is equal to

$$(2T/|U|)_0=1-\sqrt{7/10}\cong 0.1634 \tag{2.94}$$

The latter is approximately twice as large as the corresponding value for ellipsoidal perturbations if we consider the region of instability of radial motions. In our opinion, the question of which of these two types of oscillation modes is more dangerous for a non-stationary system cannot be answered unambiguously in the general case. We will discuss this issue later (see § 10).

It is interesting to know the values of the instability increment for various λ. This requires a numerical calculation (2.90). Below in Table 2.2 we present the dependence of the instability increment Inc, the anisotropy parameter ∇ and the virial parameter on the pulsation amplitude $\lambda \in (\lambda_{31},\ 1)$. In this case, $< W_r >$ and $< W_\perp >$ are given in units $G \cdot M^2 R_0^2 / R_{max}^3$, and the increment - in units Ω_0.

As can be seen from this table, in the region of instability, the growth rate increases with increasing λ to λ≈0.89, and then begins to decrease and tend to zero. Consequently, at the point λ=1 there is no exponential solution, which can also be shown analytically: equation (2.90) with λ=1 has a particular periodic solution $\aleph = \sin^2 \psi \cdot (1 + \lambda \cos \psi)$. It is easy to find a corresponding one particular solution for $F_1(\psi)$: $F_1 = \mathrm{tg}(\psi / 2)$. The latter indicates that at λ=1 there is a power-law instability. Note that the limit λ=1 is special, since in this case the formula for the oscillation period in (1.30) and the principle of averaging over the period lose their meaning. Therefore, this case will be studied in detail **in Chapter 4.** It is also of interest to compare increments and egg-shaped types of instability. We discuss this issue in detail in Section 10.

Tab. 2.2

λ	Inc	∇	$W_\perp$	W_r	$(2T/\|U\|)_0$
λ^*=0.836	0	1.652	0.301	0.249	0.164
0.84	1.17	1.686	0.299	0.252	0.16
0.85	2.40	1.796	0.292	0.262	0.15
0.86	2.72	1.920	0.284	0.273	0.14
0.87	3.00	2.056	0.277	0.284	0.13
0.88	3.14	2.210	0.268	0.296	0.12
0.89	3.81	2.386	0.258	0.308	0.11
0.90	3.13	2.588	0.248	0.321	0.10
0.95	1.89	4.406	0.182	0.402	0.05
0.975	0.90	7.000	0.132	0.461	0.025

§ 9. Instabilities of a rotating pulsating models

As is known, collisionless spherical systems, in principle, can also be rotating [35, 29]. Therefore, and, in addition, if one is interested in the issues of instabilities of nonequilibrium models, it is very interesting to elucidate the role of rotation in nonstationary stages of evolution, in particular, in the state of a protogalaxy, from which, for example, an elliptical galaxy is formed. Under what conditions does rotation have a stabilizing or destabilizing effect? To what extent will the marginal state change due to the effect of rotation E, and what will be the behavior of the detected instability zones in this case? These questions require finding the corresponding NADR for rotating models.

As long as model (1.29) was non-rotating, it could be rotated arbitrarily due to the presence of spherical symmetry. This circumstance, by analogy with the results of the analysis of the stability of stationary models, allowed us each time to take simplified perturbation potentials in the form (2.11) and (2.13). In the presence of rotation, obviously, the above degree of freedom is lost and therefore, for example, instead of sectorial forms (2.11) of the perturbation potential, one should take a more general form, for example,

$$\delta\Phi = a_0(\psi)\cdot(e_1 x + e_2 y + e_3 z)^n \tag{2.96}$$

where the coefficients e_j satisfy the identity $\sum_{j=1}^{3} e_j^2 = 0$.

However, it is quite difficult to carry out theoretical calculations with the potential (2.96), which can be seen even from the analysis of the stability of stationary systems [2]. Therefore, in order to move from partial forms to more general perturbations in calculations, we will use an analytical technique associated with the rotation of the studied nonlinear model by some arbitrary angle β_0, for example, around the x axis.

Then in (1.38)

$$y \to y\cdot\cos\beta_0 + z\cdot\sin\beta_0, \quad v_y \to v_y\cos\beta_0 + v_z\sin\beta_0 \tag{2.97}$$

and to derive the non-stationary dispersion equation, we will deal with the rotated model

$$\Psi = \frac{\rho(t)}{2\pi v_b}\delta(v_r - v_a)\cdot\delta(v_\perp - v_b)\cdot[1 + \mu\frac{v_\perp}{v_b}C(\beta_0)], \tag{2.98}$$

where

$$C(\beta_0) = \cos\beta_0\sin\theta\cdot\sin\eta + \sin\beta_0(\cos\eta\cdot\cos\varphi + \sin\eta\cdot\sin\varphi\cdot\cos\theta). \tag{2.99}$$

In this case, you can temporarily work with private forms $\delta\Phi$. And to eliminate the dependence of the dispersion equation on the coordinate system, later we will move on to the vector form of the system's response to a perturbation for an arbitrary orientation of the angular velocity vector $\vec{\mu}$ relative to the z axis associated with $\delta\Phi$.

9a. “Surface” oscillations. Ellipsoidal mode

Thus, for the model (2.98), one can still take the sectorial form of perturbation (2.11), i.e., in (2.96) we temporarily consider $e_1 = 1, e_2 = i$ and $e_3 = 0$.

Then in (2.16) we calculate

$$\overline{(x_1 + iy_1)^{n-1}} = \frac{e^{i(n-1)\varphi}}{\rho} \iiint [(rH_\alpha + v_r H_\beta)\sin\theta + \\ + v_\perp H_\beta(-\cos\theta\cdot\cos\eta + i\sin\eta)]^{n-1}\Psi\cdot v_\perp dv_r dv_\perp d\eta \tag{2.100}$$

where the integral takes into account (2.8) and (2.20). We perform integration over v_r and $v_\perp$ and go from η to ξ according to the formula (2.22 '). Then, taking the number $(r\cdot\sin\theta)^{n-1}$ out of the integration, we get

$$\overline{(x_1 + iy_1)^{n-1}} = C^{\mu}_{n-1}(\psi,\psi_1)\cdot(x+iy)^{n-1}, \tag{2.101}$$

where, taking into account (2.99)

$$C^{\mu}_{n-1}(\psi,\psi_1) = \frac{1}{2\pi}\cdot\int_0^{2\pi}(H_\alpha + \frac{v_a}{r}H_\beta + i\frac{v_b}{r}H_\beta\cos\xi)^{n-1}\cdot \\ \cdot[1+\mu\cos\xi(\cos\beta_0 + i\cdot\sin\beta_0\cdot\operatorname{ctg}\theta\cdot e^{-i\varphi})]d\xi. \tag{2.102}$$

The last integral can be expressed in terms of the Legendre polynomials using (2.36). Then after some transformations we have

$$C^{\mu}_{n-1}(\psi,\psi_1) = W^{n-1}\left[P_{n-1}(\cosh) - i\mu(\cos\beta_0 + i\sin\beta_0\operatorname{ctg}\theta\cdot e^{-i\varphi})\cdot \right. \\ \left. \cdot\frac{P_n(\cosh) - \cosh\cdot P_{n-1}(\cosh)}{\sinh}\right] \tag{2.103}$$

For surface oscillations, as always, we calculate the centroid displacement $\overline{\delta r}$, first substituting (2.101) into (2.16), i.e.

$$\overline{\delta r} = \frac{1}{R} \cdot (x\overline{\delta x} + y\overline{\delta y}) = \frac{n}{R} \cdot (x + iy)^n \int_{-\infty}^{\psi} E(\psi, \psi_1) C_{n-1}^{\mu}(\psi, \psi_1) d\psi_1 \qquad (2.104)$$

Next, you need to move from $(x + iy)^n$ back to $\delta\Phi$. But first, note that the scalar product of the angular velocity vector $\vec{\mu} = (0, -\mu \sin\beta_0, \mu \cos\beta_0)$ by the vector

$$\vec{r} \times \text{grad}\,\delta\Phi = (-in \cdot a_0 z(x + iy)^{n-1}, \quad a_0 n \cdot z(x + iy)^{n-1}, \quad in \cdot a_0 (x + iy)^n)$$

gives us the identity

$$ia_0 m \cdot \left|\vec{\mu}\right| (x + iy)^n (\cos\beta_0 + i \sin\beta_0 \cdot \text{ctg}\,\theta \cdot e^{-i\varphi}) = \vec{\mu}(\vec{r} \times \text{grad}\,\delta\Phi) \qquad (2.105)$$

Therefore, (2.104), taking into account (2.103) and (2.105), can be rewritten in the form

$$\delta \vec{r} = \frac{n}{R \cdot a_0} \cdot \delta\Phi \cdot Y_{1n}(\psi) - \frac{\vec{\mu} \cdot (\vec{r} \times grad\,\delta\Phi)}{R \cdot a_0} \cdot Y_{2n}(\psi), \qquad (2.106)$$

where

$$\begin{aligned} Y_{1n}(\psi) &= \int_{-\infty}^{\psi} E \cdot T^{n-1} P_{n-1}(\cosh) d\psi_1, \\ Y_{2n}(\psi) &= \int_{-\infty}^{\psi} E \cdot W^{n-1} \cdot \frac{P_n(\cosh) - \cosh P_{n-1}(\cosh)}{\sinh} d\psi_1 \end{aligned} \qquad (2.107)$$

It is known that the displacement value $\delta \vec{r}$ corresponds to a simple layer $\rho(t)\overline{\delta r}$ and the response of the system's own potential

$$\delta\Phi = \frac{4\pi G \cdot \rho \cdot R}{2n + 1} \cdot \overline{\delta r} \qquad (2.108)$$

Here we are talking about the internal potential, and the external potential in this case may not be used to derive the dispersion equation. Therefore, in the interior of the system

$$\delta\Phi = \frac{4\pi G \cdot \rho}{2n + 1} \cdot [n \cdot \frac{\delta\Phi}{a_0(\psi)} \cdot Y_{1n}(\psi) - \frac{1}{a_0} \cdot \vec{\mu} \cdot (\vec{r} \times \text{grad}\,\delta\Phi) Y_{2n}(\psi)]. \qquad (2.108')$$

Now we can abandon the condition that $\delta\Phi$ is proportional to the sectorial harmonic. Let $\delta\Phi$ have a more general form, given by us in (2.96). This expression

can be expanded into a Fourier series (for example, in the parameter $(h_1 + ih_2)/(h_1 - ih_2)$ and, in accordance with the theory of spherical functions, the terms can be distinguished

$$\delta\Phi = a_0(\psi) \cdot r^n \cdot e^{im\varphi} \cdot P_n^m(\cos\theta) \tag{2.109}$$

where $P_n^m(\cos\theta)$ is the associated Legendre polynomial. Let us return again to the phase density in the form (1.38), i.e. let's move to the coordinate system associated with the axis of rotation of the model, after which we can use the expansion (2.96) into harmonics (2.109). Taking into account the invariance of the vector notation in (2.108'), we have

$$\vec{\mu} \cdot \left(\vec{r} \times \mathrm{grad}\delta r \right) = \mu \cdot \left(x \cdot \frac{\partial \delta\Phi}{\partial y} - y \cdot \frac{\partial \delta\Phi}{\partial x} \right) = \mu \cdot \frac{\partial \delta\Phi}{\partial \varphi} = im \cdot \mu \cdot \delta\Phi .$$

Thus, for each value of the azimuthal wave number m, the perturbation calculation will be self-consistent if the condition [23]

$$a_0(\psi) = \frac{3\Omega^2}{(2n+1)\Pi^3} \cdot [n \cdot Y_{1n}(\psi) - im \cdot \mu \cdot Y_{2n}(\psi)] \tag{2.110}$$

When deriving (2.110), the relations $\rho = \rho_0 \Pi^3$ and $\Omega^2 = 4\pi G\rho_0 / 3$ are taken into account. This equation is the NADR of the problem of the stability of the rotating model (1.38) with respect to surface perturbations. Substituting into (2.110) $\lambda = 0$, we confirm the previously known result [111] on the complete stability of the corresponding equilibrium model with rotation. However, in the presence of pulsation, instability necessarily occurs. In the case $\lambda \neq 0$, first of all, it is necessary to obtain a physical picture for ellipsoidal perturbations with n=2. Then from (2.110), taking into account (2.15) and (2.107), we have

$$\Pi^3(\psi) a_0(\psi) = \frac{6}{5} \int_{-\infty}^{\psi} (\cosh + \frac{im}{4} \cdot \mu \cdot \sinh) a_0 T \cdot S \cdot \Pi^3 d\psi_1 \tag{2.111}$$

here

$$\sinh = (1-\lambda^2)^{1/2} \cdot \frac{(\cos\psi + \lambda) \cdot \sin\psi_1 - \sin\psi \cdot (\cos\psi_1 + \lambda)}{(1 + \lambda\cos\psi) \cdot (1 + \lambda\cos\psi_1)} \tag{2.112}$$

Therefore, introducing the notation $F = (\cos\psi + \lambda)F_1 + (1-\lambda^2)^{1/2} \sin\psi \cdot F_2$, where

$$F_1 \equiv \int_{-\infty}^{\psi} a_0 (1+\lambda\cos\psi_1)^3 \cdot (\cos\psi_1 + \lambda + i\mu\frac{m}{4}(1-\lambda^2)^{1/2}\sin\psi_1) S d\psi_1 \qquad (2.113)$$

$$F_2 \equiv \int_{-\infty}^{\psi} a_0 (1+\lambda\cos\psi_1)^3 \cdot [(1-\lambda^2)^{1/2}\sin\psi_1 - i\mu\frac{m}{4}(\cos\psi_1 + \lambda)] S d\psi_1 \qquad (2.114)$$

we have the following system of 4th order differential equations [23]:

$$\Lambda F_1 = \frac{6F}{5(1+\lambda\cos\psi)^2} \cdot [\cos\psi + \lambda + i\mu\frac{m}{4}(1-\lambda^2)^{1/2}\sin\psi] \qquad (2.113')$$

$$\Lambda F_2 = \frac{6F}{5(1+\lambda\cos\psi)^2} \cdot [(1-\lambda^2)^{1/2}\sin\psi - i\mu\frac{m}{4}(\cos\psi + \lambda)] \qquad (2.114')$$

From here, one third-order differential equation for the function $F(\psi)$ can be obtained using the system order reduction method given in § 7b. Skipping intermediate calculations, we present the final equation

$$(1+\lambda\cos\psi)\frac{d}{d\psi}\left[\frac{d^2F}{d\psi^2} + \frac{3\lambda\sin\psi}{1+\lambda\cos\psi}\cdot\frac{dF}{d\psi} + \frac{14/5 - 2\lambda\cos\psi}{1+\lambda\cos\psi}F\right] + i\mu\frac{3m}{5}\cdot\frac{(1-\lambda^2)^{1/2}F}{1+\lambda\cos\psi} = 0 \qquad (2.115)$$

As can be seen, for $\mu = 0$ we have NDR (2.51) for a non-rotating system.

In (2.115), the azimuthal wavenumber m can take only three values: 0, 1, and 2. For m =0, the instability generates a biaxial ellipsoid with rotation that is flattened or extended along the z axis. The corresponding instability conditions for an arbitrary $\mu \le 1$ are the same as in the case of $\mu = 0$ (see § 7b). When m =1, we have a precessing ellipsoid, and when m =2, we have a triaxle ellipsoid. The case m=2 corresponds to an analog of a purely bar-like instability.

Equation (2.115) was solved by us in order to determine the marginal state. Figures 3a and 3b show the dependences of the initial value of the virial ratio $(2T/|U|)_0$ on the rotation parameter μ and on the instability increment. As can be seen from Figure 3, the rotation effect is destabilizing up to the value μ=0.922, and then only it starts to play a stabilizing role. The point $((2T/|U|)_0 = 1, \quad \mu = 0.922)$ is a branch point with the following properties: a) in the absence of pulsation ($\lambda = 0$) it does not appear and therefore corresponds to a stable state, but in the presence of an infinitely small $\lambda \neq 0$ it becomes unstable; b) the calculation shows at this point $d(2T/|U|)_0 / d\mu = \pm 0.887$.

Note that the stability interval found above for $\mu = 0$

$$0.084 \le (2T/|U|)_0 \le 0.127 \qquad (2.116)$$

narrows very quickly with growth μ and disappears completely when $\mu = 0.09$. This "island" of stability, as it were, separates the region of vibrational-resonant instability from the zone of instability of almost radial motions. These two types of instabilities already at small μ quickly merge. So even the zone of instability of almost radial motions at $\mu \geq 0.05$ acquires an oscillatory character.

The presence in Fig. 3 of the narrow island of stability can be explained by considering the role of the “restoring” gravitational force, which tends to return the deviation from the sphere to its previous state. This force is felt especially at the moment of the greatest contraction of the system, and at the moment of the greatest expansion it reacts least of all to the “impact”. So, if μ is small, and the initial value of the virial ratio satisfies inequality (2.116), at the moment of the greatest compression, there is a minimum, almost zero, amplitude of the perturbation.

We now present the corresponding NDE and the results of their solution for two more large-scale surface modes [34]. In the case of vibration mode N=3

$$a_0(\psi) = \frac{9}{14(1+\lambda\cos\psi)^7}\Sigma_3(\gamma_\tau), \qquad \tau = \overline{1,3} \ ,$$

$$\Sigma_3(\gamma_\tau) = (2c^2 - e^2s^2)\gamma_1 + 6cse^2\gamma_2 + e^2(2e^2s^2 - c^2)\gamma_3 +$$

$$+ \ \frac{2}{3}im\mu_1\sqrt{1-\lambda^2}\,(cs\gamma_1 - (c^2 - e^2s^2)\gamma_2 - cse^2\gamma_3)\,,$$

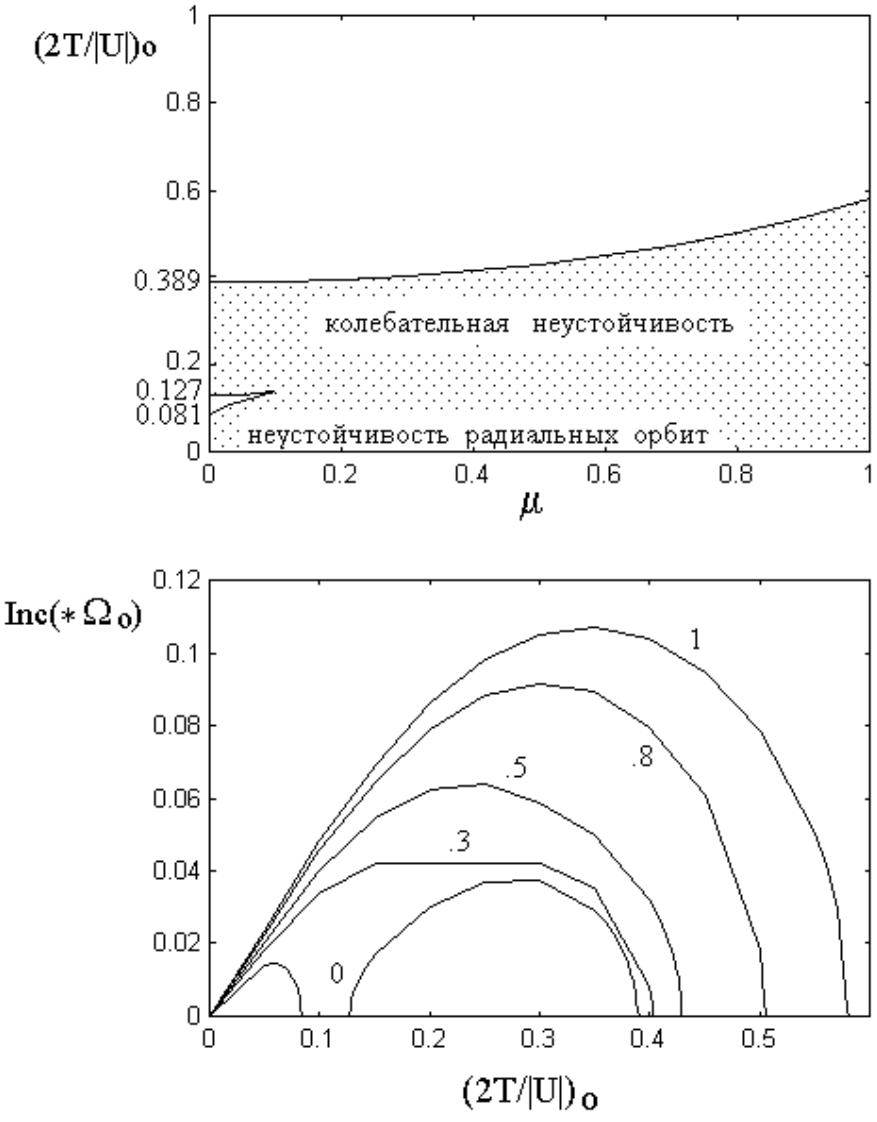

Fig. 3a. Dependences of the critical values of the initial virial parameter and dependences of the instability increments of the ellipsoidal mode; azimuth wave number m=1.

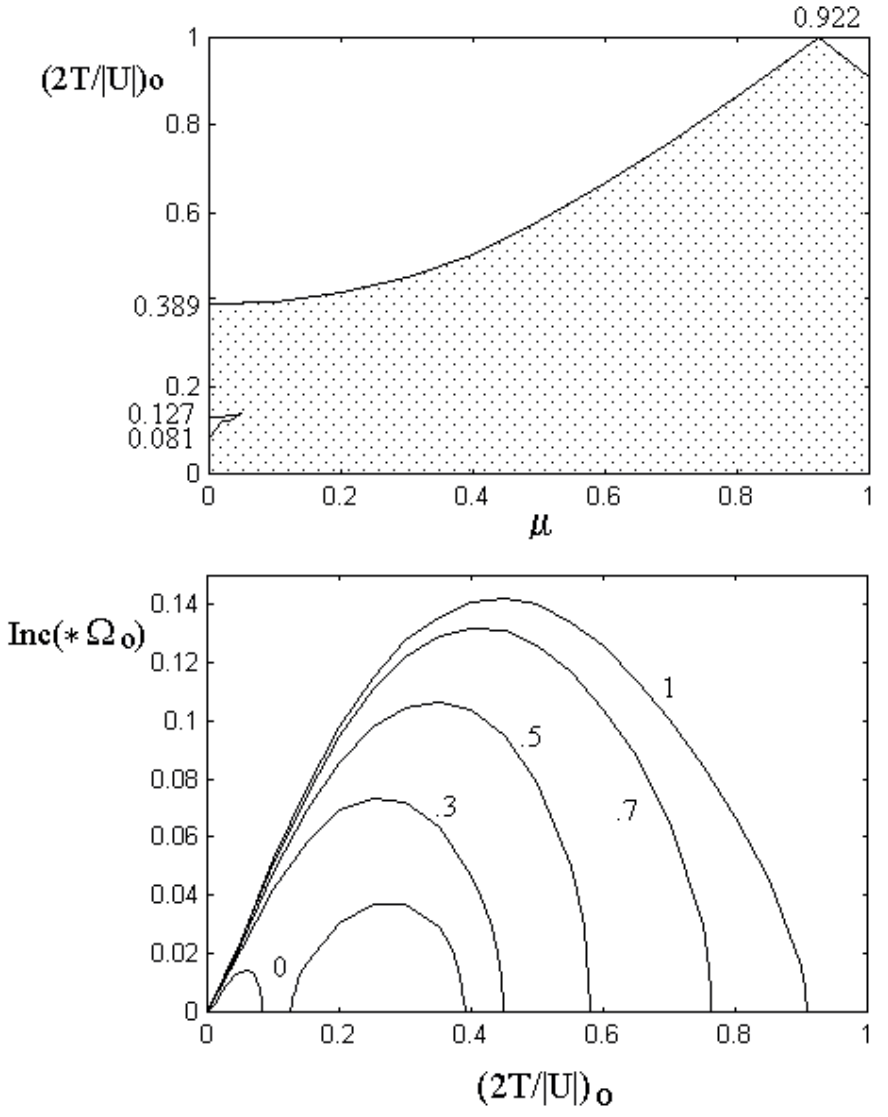

Fig. 3b. Dependences for the critical values of the initial virial parameter on the rotation parameter and the instability increments of the ellipsoidal mode on the virial parameter at azimuth wave number m=2.

where the notation is used $c = \lambda + \cos\psi$, $s = \sin\psi$, $e^2 = 1 - \lambda^2$.

Graphs are shown in Figure 4 for the values of the azimuthal wave number m=1,2,3, since the case m=0 is similar to the case $\mu = 0$. One can clearly see the "island" of stability (especially in Fig. 4(a)) inside the unstable region (shaded), which exists at small values of the rotation parameter. At $\mu = 0$, the "island" separates zones with different types of instability: in one region ($(2T/|U|)_0^* < 0.166$

) oscillatory instability prevails, in the other ($(2T/|U|)_0^* > 0.181$) is aperiodic (in the case of an ellipsoidal mode, the reverse order takes place, but, like , the increments of the region of instability of an oscillatory nature are much greater than the increments of the aperiodic one). At $\mu \neq 0$, only oscillatory instability is noted. Near $(2T/|U|)_0^* \approx 0$ we have the instability of radial orbits. The "island" decreases in size as m increases. On the graphs, its position is indicated by an arrow. Rotation also has a destabilizing character: with increasing values, μ the instability area becomes noticeably larger, reaching at $\mu = 1$ values $(2T/|U|)_0^* = 0.346$ (m=1); 0.551 (m=2) and () 0.795 (m=3). Accordingly, the increments also grow, which is clearly seen in the corresponding graphs.

For mode N=4

$$a_0(\psi) = \frac{1}{3(1+\lambda\cos\psi)^9}\Sigma_4(\gamma_\tau), \qquad \tau = \overline{1,4} \ ,$$

where

$$\Sigma_4(\gamma_\tau) = 2c(2c^2 - 3e^2s^2)\gamma_1 + 6se^2(4c^2 - e^2s^2)\gamma_2 + 6ce^2(4e^2s^2 - c^2)\gamma_3 + 2se^4(2e^2s^2 - 3c^2)\gamma_4 +$$

$$\frac{3}{8}im\mu_1\sqrt{1-\lambda^2}(s(e^2s^2 - 4c^2)\gamma_1 + c(4c^2 - 11e^2s^2)\gamma_2 + se^2(11c^2 - 4e^2s^2)\gamma_3 + ce^2(4e^2s^2 - c^2)\gamma_4) \cdot$$

The results are illustrated in fig. 5 [34]. The first thing that catches your eye is the qualitative similarity of the dependences $(2T/|U|)_0^*$ on μ and m, which allows us to formulate some regularities (which are also valid for modes up to the 10th order) [34, 23]:

(1) All considered surface modes (N=3; 4; 5; 6; 8; 10) have an "island" of stability inside the unstable region.

(2) With increasing values of the rotation parameter:

a) the region of instability grows in the sense of the onset of instability at large values of the virial parameter,

b) "island" exists for small values of μ.

Thus, the rotation acts destabilizing everywhere, while for the N=m=2 mode, with values μ, close to unity ($\mu \cong 0{,}922$), the maximum value of the parameter $(2T/|U|)_0^* = 0.999$ is observed, after which stabilizing factors begin to act.

(3) With an increase in the value of m within any one mode
a) the size of the "island" of stability decreases,
b) the instability of the model for the same values μ increases significantly.

(4) With increasing mode order N:

a) the area (on the graphs) of the region occupied by the instability decreases,

b) the length of the "island" slightly increases (this is most noticeable for m=1).

(5) When comparing the values of the instability increments (except for the ellipsoidal mode), they turn out to be the largest for the N=m=3 mode. Graphs of comparison of increments of different modes for some values of μ are shown in Figures 6a and 6b (m=1; $\mu = 0; 0.5; 1.0$) and 2.3 (m=N; $\mu = 0.1; 0.5; 1.0$). For completeness, the mode increments N=m=2 have been added here. In the case of m=1, as can be seen from Fig. 6a, almost everywhere the maximum increments are achieved for the ellipsoidal mode, and its separation from the other modes is very significant. Some exception is the case $\mu \le 0.1$, when, due to the bifurcation of the unstable region, the ellipsoidal mode, for example, for $\mu = 0$ in the range of $(2T/|U|)_0^* \in [0; 0.06]$ values, N=2 mode increments prevail over all, then to $(2T/|U|)_0^* \approx 0.15$ the “triangular” mode N=3 dominates, and then with $(2T/|U|)_0^* \ge 0.15$ only the N=2 mode reigns supreme. The smaller the mode (that is, the larger N), the smaller and smaller the increments. The curves of mode increments are evenly spaced, that is, there is no significant separation of any mode from all the others. Only with an increase in rotation does the gap between the increments of the N=3 mode and the rest increase slightly. For m=n (Figure 6b), the separation of the increments of the N=2 mode from the rest is already more moderate, but at μ close to 1.0, the N=3 mode only slightly “lags behind” the ellipsoidal mode.

Some quantitative characteristics are given in Table 2.3.

Table 2.3

N	m	island length in units μ	Island Width in units $(2T/\|U\|)_0$, $\mu = 0$
3	1	0.15	0.015
	2	0.08	

	3	0.05	
4	1	0.22	0.012
	2	0.11	
	3	0.08	
	4	0.06	
$5^{(*)}$	1	0.25	0.013
	5	0.06	
$6^{(*)}$	1	0.32	0.11
	6	0.06	
$8^{(*)}$	1	0.50	0.007
	8	0.07	
$10^{(*)}$	1	0.64	0.0058
	10	0.07	

(*): These are the results for the extreme values of m. For 1<m<N, the values of the virial ratio correspond to m=1 and m=n.

9b. Oscillations violating the density homogeneity

We could study volume oscillations against the background of a pulsating system similarly to the case $\mu=0$, setting the initial form of the potential perturbation in the form of sectorial harmonics (2.13). However, as calculations show, then you have to deal with multiple amounts, which is cumbersome and takes up a lot of space. Therefore, we will show the possibility of deriving the NDE with a simplified form of the initial perturbation

$$\delta\Phi = a_0(\psi)\cdot z^N \tag{2.117}$$

from which it is always possible to single out individual zonal harmonics.

Then

$$\mathrm{grad}(\delta\Phi) = (0,0,N\cdot a_0 z^{N-1}), \quad \overline{\delta x} = \overline{\delta y} = 0$$

and the z offset

$$\overline{\delta z} = N\cdot\int_{-\infty}^{\psi} \overline{z_1^{N-1}}\, E d\psi_1 \tag{2.118}$$

Since, according to (2.60),

$$z_1 = zH_\alpha + v_z H_\beta = r\cdot\cos\theta\cdot H_\alpha + H_\beta\left(v_r\cos\theta + v_\perp\cos\eta\cdot\sin\theta\right),$$

calculation of speed averaging from z_1^{N-1} with distribution function (2.98) leads to the following:

$$\overline{z_1^{N-1}} = \frac{r^{N-1}}{2\pi}\cdot\int_0^{2\pi}\left(a\cdot\cos\theta + b\cdot\sin\theta\cdot\cos\eta\right)^{N-1}\left(1+\mu\cdot\sin\beta_0\cos\varphi\cdot\cos\eta\right)d\eta \qquad (2.119)$$

where $a \equiv H_\alpha + v_a H_\beta/r$, $b \equiv v_b H_\beta/r$. Further, in principle, by analogy with (2.100), one can express (2.119) in terms of the Legendre polynomials, but this, unfortunately, does not make it possible to compose the NDE in an invariant form here. Therefore, we will have to use Newton's binomial in (2.119), and then only calculate the integral over η. Therefore, we have

$$\overline{z_1^{N-1}} = r^{N-1}\cdot \sum_{\substack{k=0 \\ (k-\text{четн})}}^{N-1} \frac{(N-1)!\left(a\cos\theta\right)^{N-1-k}}{(N-1-k)!\cdot k!}\cdot\left(b\sin\theta\right)^k\cdot\frac{(k-1)!!}{k!!} +$$

$$+\mu\, r^{N-2}x\cdot \sum_{\substack{k=0 \\ (k-\text{нечетн})}}^{N-1} \frac{(N-1)!\left(a\cos\theta\right)^{N-1-k}}{(N-1-k)!\cdot k!}\cdot b^k\left(\sin\theta\right)^{k-1}\cdot\frac{k!!}{(k+1)!!} \qquad (2.120)$$

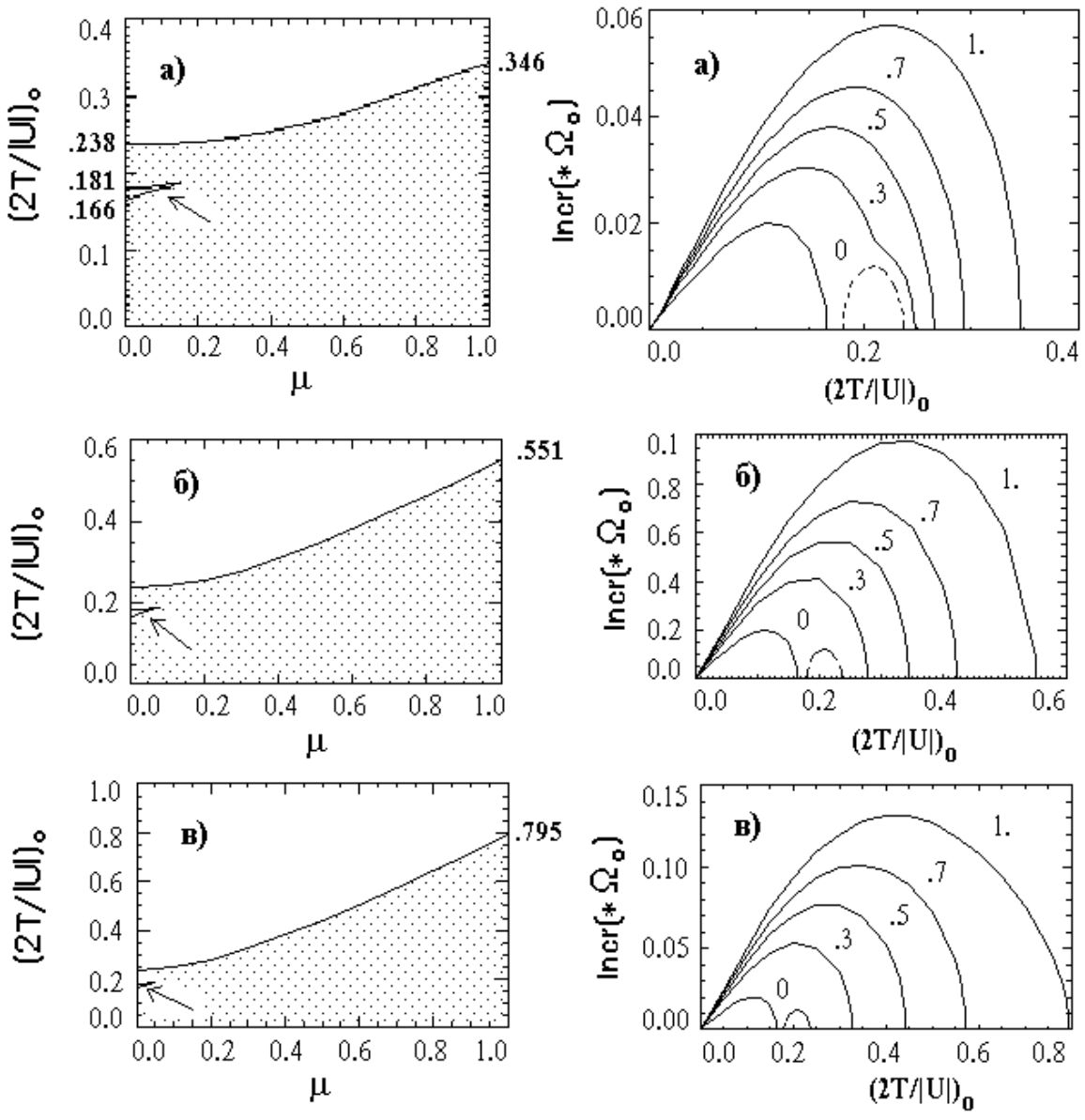

Fig. 4 Critical dependences of the initial virial parameter and dependences of the instability increments of the "triangular" mode; azimuth wave number a) m=1; b) m=2; c) m=3. The numbers next to the curved increments indicate the values of the rotation parameter.

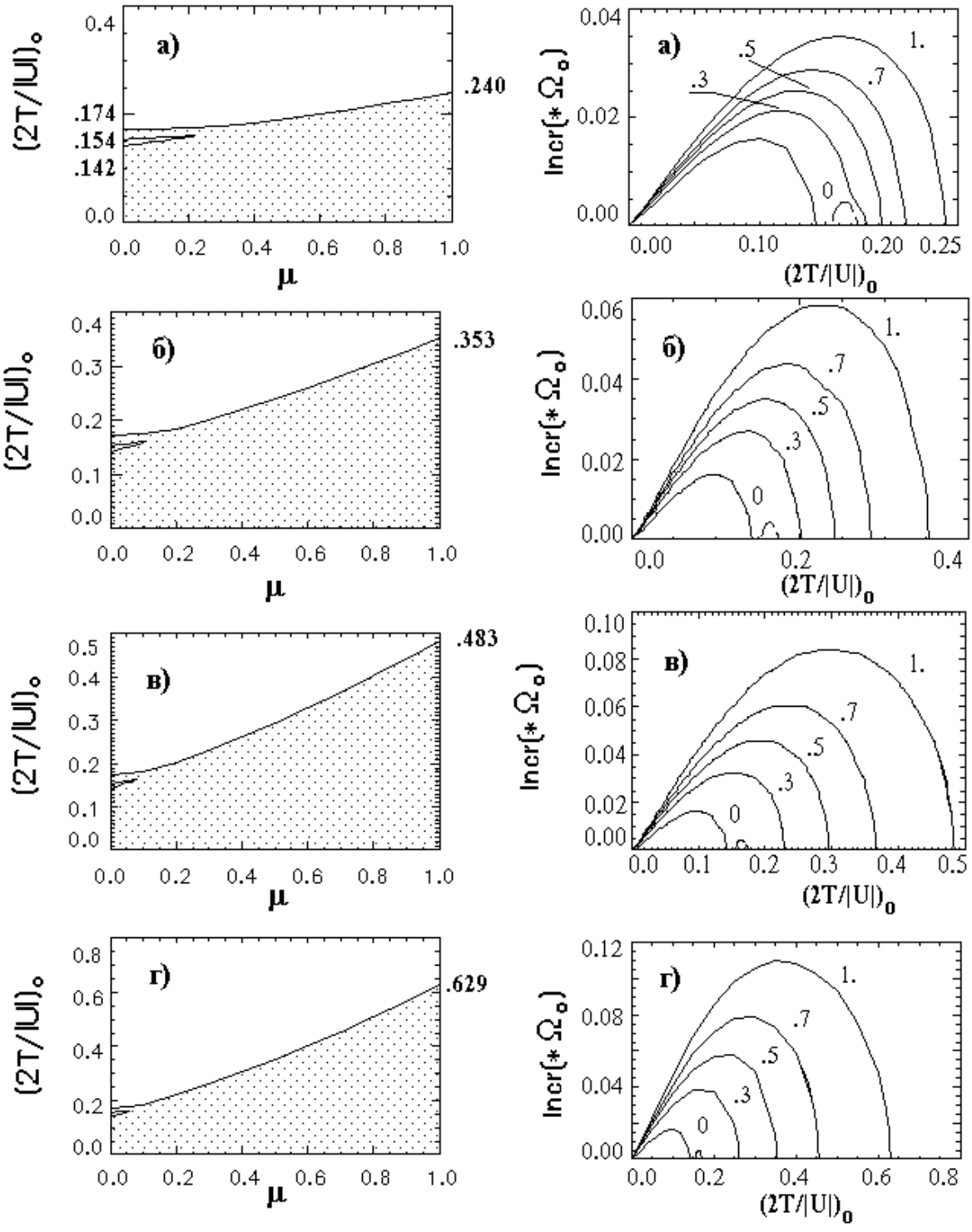

Fig. 5 Critical dependences and dependences of mode increments N=4; azimuth wave number a) m=1; b) m=2; c) m=3; d) m=4.

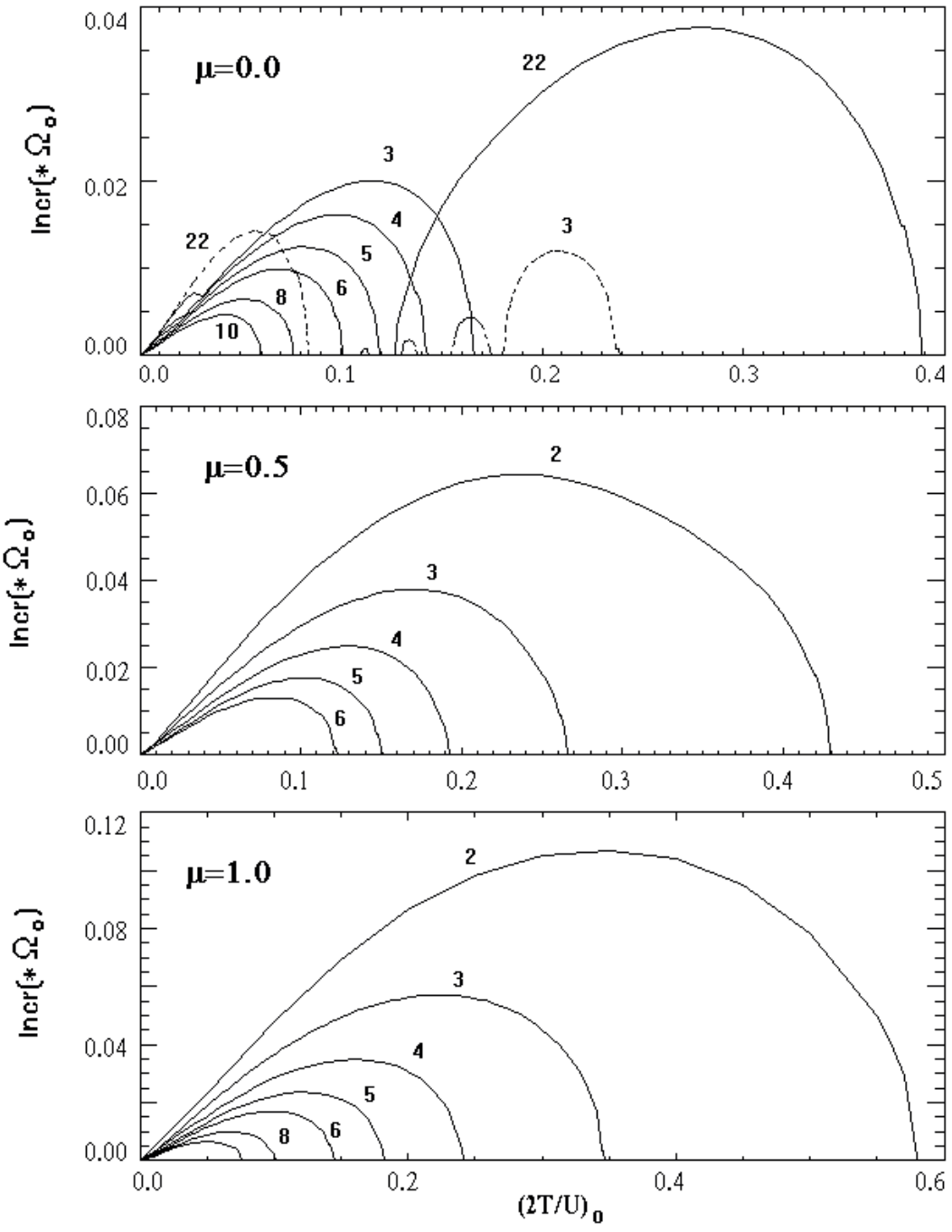

Fig. 6.a Comparison of increments of surface modes at the minimum azimuthal wavenumber m=1. The numbers next to the curves indicate the order of the mode.

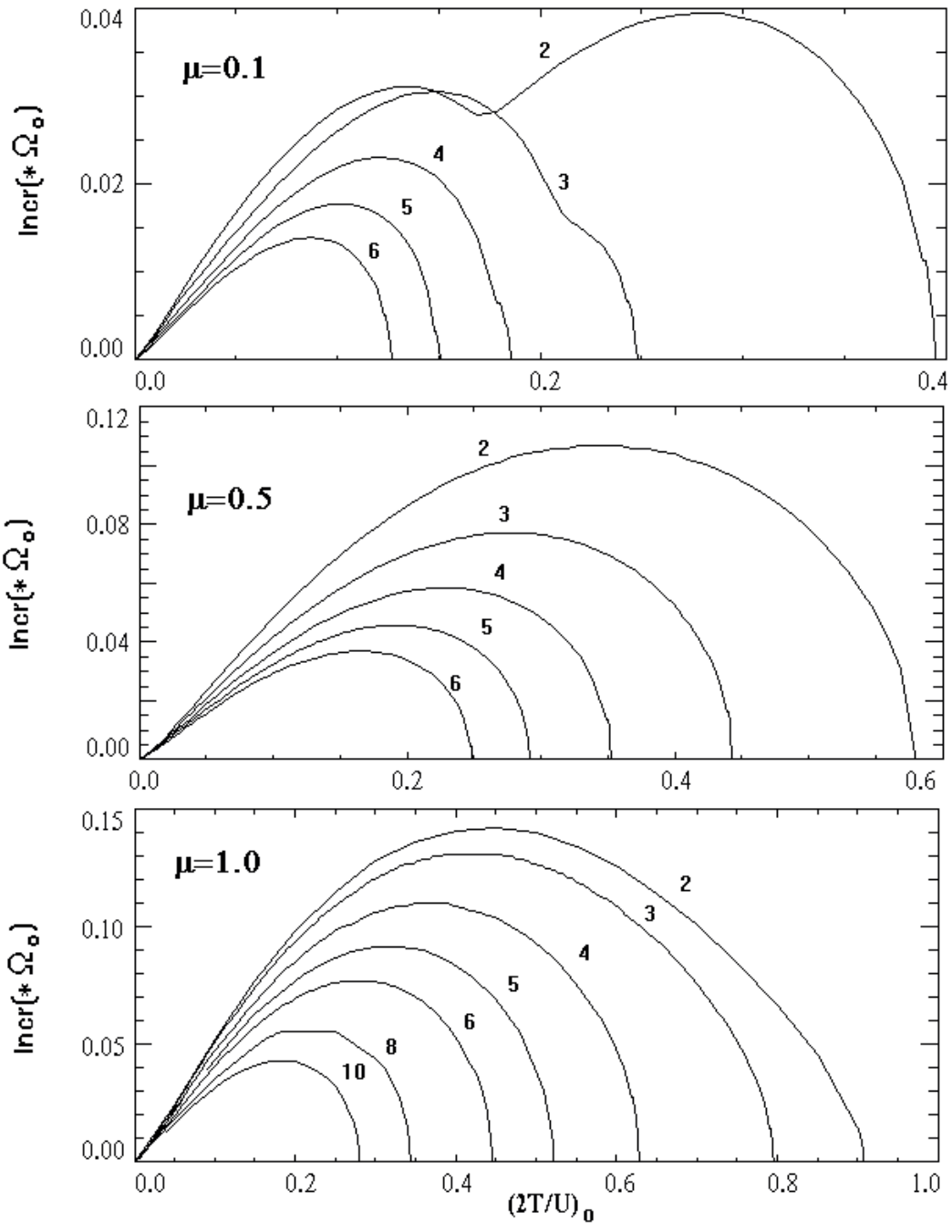

Fig. 6.b Comparison of increments of surface modes at the maximum azimuthal wavenumber m=N. The numbers next to the curves indicate the order of the mode.

We expand the functions of $\sin\eta$ also in the Newton binomial according to the formula

$$\sin^k\theta = \sum_{\nu=0}^{k/2} \frac{(k/2)}{(k/2-\nu)!\,\nu!}\cdot(-\cos^2\theta)^\nu,$$

and then, by combining powers $\cos\theta$ as $N-1-k+2\nu \equiv s$ and going all the way from $\cos^s\theta$ to $(z/r)^s$, we swap the order of summation. Substituting the result into (2.119), we have

$$\begin{aligned}\overline{\delta z} = &\sum_{s=0}^{N-1}\sum_{\substack{k=N-1-s\\(k-\text{четн})}}^{N-1} \frac{N!\,2^{-k}\,z^s r^{N-1-s}}{(k/2)![(N-1-s)/2]!}\cdot v_{ks}\,Y_k(\psi)+\\ &+\mu\cdot\sin\beta_0\sum_{s=0}^{N-2}\sum_{\substack{k=N-1-s\\(k-\text{нечетн})}}^{N-1} \frac{N![(k-1)/2]!\,x\cdot z^s r^{N-1-s}}{(k+1)![(N-2-s)/2]!}\cdot v_{ks}\,Y_k(\psi)\end{aligned} \tag{2.121}$$

where

$$Y_k(\psi)\equiv\int_{-\infty}^{\psi} a^{N-1-k}b^k E d\psi_1, v_{ks} \equiv \frac{i^{s+k-N+1}}{(N-1-k)![(s+k-N+1)/2]!}. \tag{2.122}$$

Knowing $\overline{\delta z}$, we calculate the density perturbation by the formula

$$\delta\rho = -\frac{\rho_0}{\Pi^3}\cdot\frac{\partial\,\overline{\delta z}}{\partial z}. \tag{2.123}$$

According to (2.121), on the right side of (2.123) under the sign of sums we obtain functions of the form z^{s-1} and z^{s+1}. From them, taking into account (2.117), it is necessary to go back to $\delta\Phi$ in order to obtain the NDE in an invariant form. To do this, together with even k, we apply the identity

$$a_0 z^s = \frac{s!}{N!}\cdot\Delta^{(N-s)/2}\cdot\delta\Phi, \tag{2.124}$$

and in the second sum with μ (in the case of odd k)-identity

$$a_0(\psi)\cdot\mu\cdot\sin\beta_0 x\cdot z^s = \frac{s!}{N!}\cdot\vec{\mu}\,(\vec{r}\times\operatorname{grad}\Delta^{(N-s-1)/2}\delta\Phi). \tag{2.125}$$

The validity of (2.124) and (2.125) can be easily shown by calculating the Laplace operator from (2.117) τ times and substituting the quantities (N-s)/2 and (N-s-1)/2 instead of τ.

On the other hand, according to the Poisson equations $\delta\rho = -\Delta\delta\Phi/4\pi G$. Equating the latter with (2.123), taking into account (2.124) and (2.125), we obtain an expression for $\Delta\delta\Phi$ in terms of double sums in (2.121).

Now we can abandon the original form of the potential perturbation in the form (2.117) and set it as follows

$$\Delta\delta\Phi = a_0(\psi)\cdot r^N \cdot e^{im\varphi}\cdot P_n^m(\cos\theta). \tag{2.126}$$

Such terms, in principle, can be extracted from (2.117) by means of special transformations [36]. Applying to (2.126) the Laplace operator τ times, we obtain

$$\Delta^\tau(\delta\Phi) = \frac{(N-n)!!(N+N+1)!!\cdot a_0(\psi)}{(N-n-2\tau)!!\cdot(N+n-2\tau+1)}\cdot r^{N-2\tau} e^{im\varphi} P_n^m(\cos\theta) \tag{2.127}$$

Let the direction of the vector $\vec{\mu}$ coincide with the z-axis, i.e. $\beta_0 = 0$. Then, using (2.127) in (2.125) and calculations of the right side in the expression we just found for $\Delta\delta\Phi$, we obtain the following required NDE (see also [23])

$$\frac{a_0\Pi^3}{3\Omega^2(N-n-2)!!(N+n-1)} = \sum_{s=0}^{N-1}\sum_{\substack{k=N-1-s\\(k-\text{четн})}}^{N-1}\frac{2^{-k}\,s!\cdot V_{ks}\,Y_k[N(s+1)+s-1-(n-1)]}{(k/2)![(N-s-1)/2]!\,(s-n+1)!!\cdot(s+n+2)!!} +$$

$$+ im\mu\cdot\sum_{s=0}^{N-2}\sum_{\substack{k=N-1-s\\(k-\text{нечетн})}}^{N-1}\frac{(\frac{k-1}{2})!\cdot s!\cdot V_{ks}\,Y_k[N(s+1)+2(s-1)-(n-2)(n+3)]}{(k+1)![(N-s-2)/2]!\,(s-n+2)!!\cdot(s+n+3)!!} \tag{2.128}$$

In principle, individual sums can be expressed in terms of integrals or the result of comparing (2.128) with (2.71) can be used, i.e. with case $\mu = 0$. But all this does not significantly simplify the resulting NDE as a whole.

In the particular case when N=3, n=1, from (2.128) we have

$$\frac{a_0\Pi^3}{3\Omega^2} = \int_{-\infty}^{\psi} a^2\,E\,d\psi_1 + \frac{im\cdot\mu}{2}\int_{-\infty}^{\psi} a\cdot b\cdot E\,d\psi_1 \tag{2.129}$$

Substituting our own expressions for a, b and E, we get

$$a_0 = \frac{3}{(1+\lambda\cos\psi)^7}\cdot\{(\cos\psi+\lambda)^2 F_1 + 2(1-\lambda^2)\sin\psi(\cos\psi+\lambda)F_2 +$$

$$+(1-\lambda^2)^2\sin^2\psi\cdot F_3 + i\frac{m}{2}\mu(1-\lambda^2)^{1/2}\cdot[(\cos\psi+\lambda)^2 F_2' - \tag{2.129'}$$

$$-\sin\psi(\cos\psi+\lambda)+(1-\lambda^2)\sin\psi(\cos\psi+\lambda)F_3' - (1-\lambda^2)\sin^2\psi F_2']\}$$

where the functions F_ν satisfy the following system of differential equations

$$\Lambda F_\nu = (1+\lambda\cos\psi)^3 a_0 (\cos\psi+\lambda)^{3-\nu}(\sin\psi)^{\nu-1}, \quad (\nu = 1;2;3) \tag{2.130}$$

In this case, the value m can take two values: 0 and 1. Solution (2.130) for m=0 coincides with the result of the corresponding case for $\mu = 0$ (see § 8b). The case m=1 is shown in Figure 7(a). The critical dependence shows the presence of two separate areas of instability, one of which, the main one, is larger and the critical values $(2T/|U|)_0$ increase little by little with the growth of μ; the other is much smaller and starts at about $\mu \approx 0.562$, reaching to $(2T/|U|)_0 \approx 0.899$. In the absence of rotation, there are aperiodic solutions of the characteristic equation throughout the entire unstable region.

The same figure shows the results for the N=4, n=2 mode, the NDE of which looks like this:

$$a_0 = \frac{2}{2(1+\lambda\cos\psi)^9}\Sigma_{24}(\gamma_\tau), \tau = \overline{1,4};$$

$$\Sigma_{24}(\gamma_\tau) = c(2c^2 - e^2s^2)\gamma_1 + e^2s(8c^2 - e^2s^2)\gamma_2 + e^2c(-c^2 + 8e^2s^2)\gamma_3 +$$

$$+e^4s(-c^2+2e^2s^2)\gamma_4 + im\mu_1 e\{c^2s\gamma_1 + c(c^2 - 2e^2s^2)\gamma_2 +$$

$$+e^2s(2c^2 - e^2s^2)\gamma_3 + e^4cs^2)\gamma_4\}.$$

The picture here is much simpler. Only one area of instability is observed, which increases with both μ and m. The mode is on a smaller scale, but Figures 4 and 8 show that some of its increments exceed those of the ovoid mode.

Figure 8 compares modes for some μ .

m=1 (Fig. 8.a, $\mu = 0; 0.5; 1.0$): mode (4,2) leads in terms of maximum values of increments, mode (3,1) takes second place already with $\mu = 0.1$, which in the end still yields slightly a little fashion (2,2).

m=N (Fig. 8.b) the maximum values are taken for all values of the rotation parameter also for the mode (4,2). But the ellipsoidal mode, being in the penultimate place, gradually shifts to the second place at moderate μ, and with an increase in rotation to 1, it again finds itself in the penultimate one. On the whole, comparison of the growth rates of bulk modes with each other shows a more complex picture than in the case of surface modes.

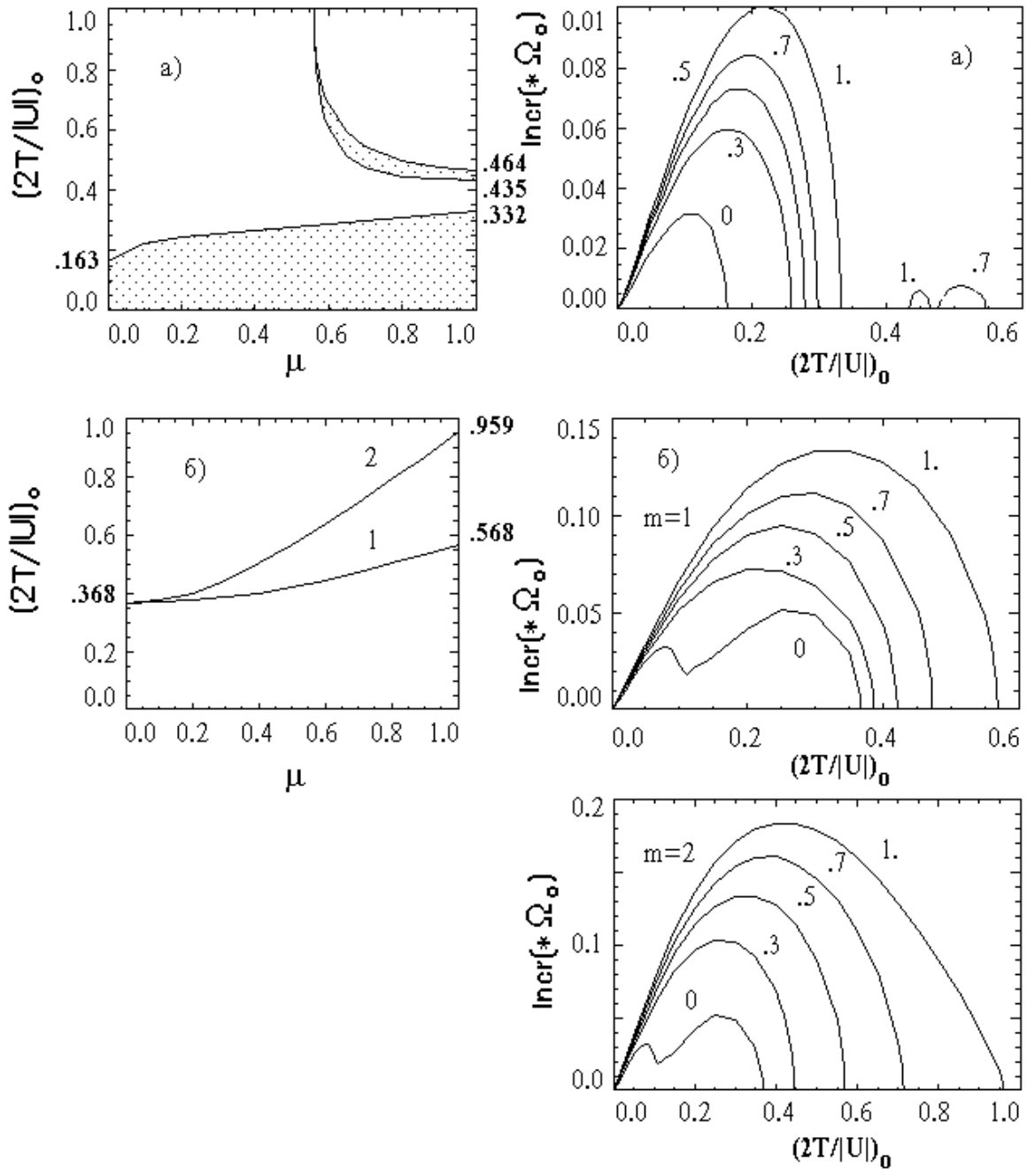

Fig. 7. Critical dependences and dependences of increments of a) ovoid and b) ring-shaped modes. The numbers next to the curves indicate the values of the rotation parameter.

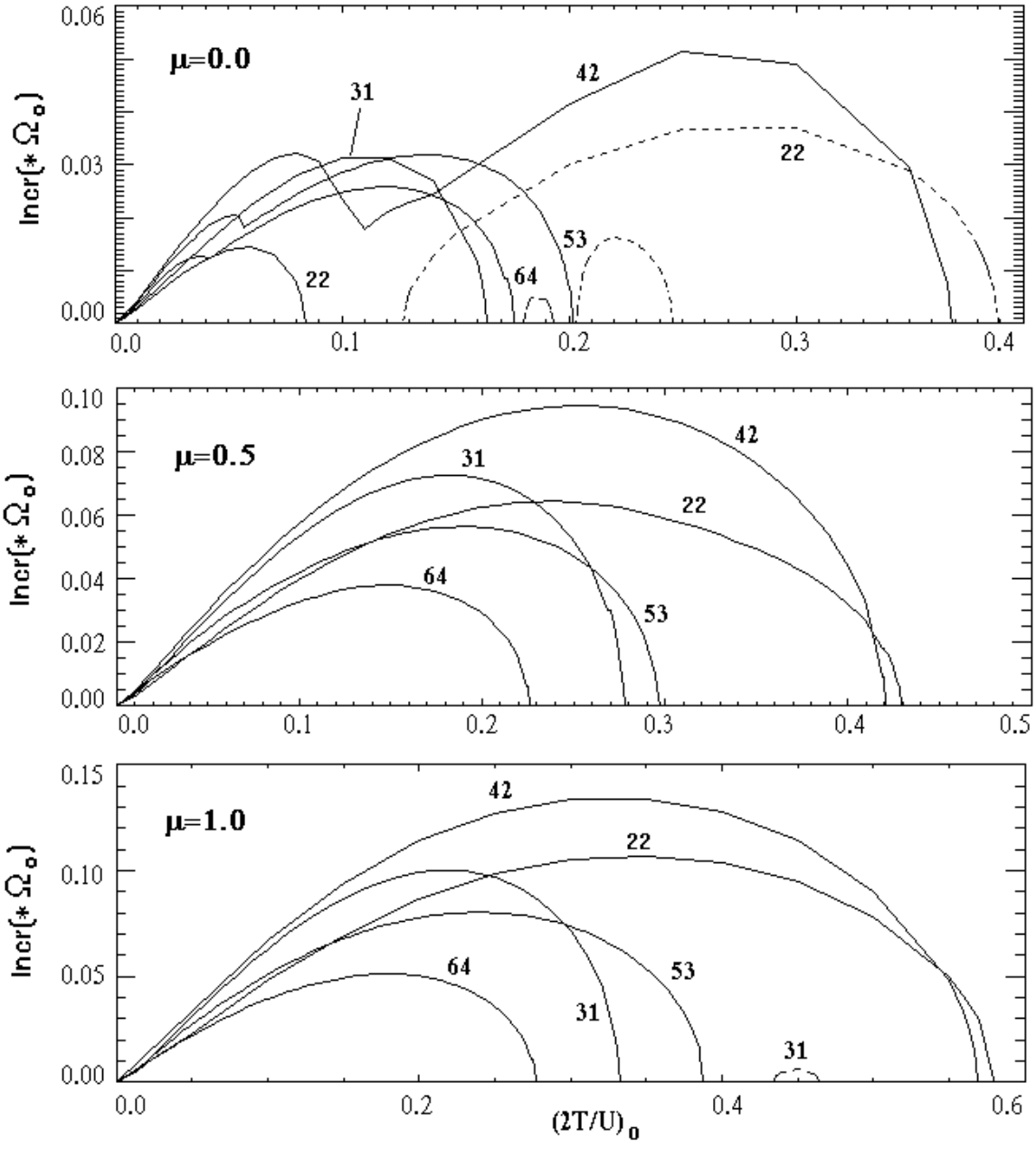

Fig. 8a. Comparison of volumetric mode increments at the minimum azimuthal wavenumber m=1. The numbers next to the curves indicate the order of the mode (N,n).

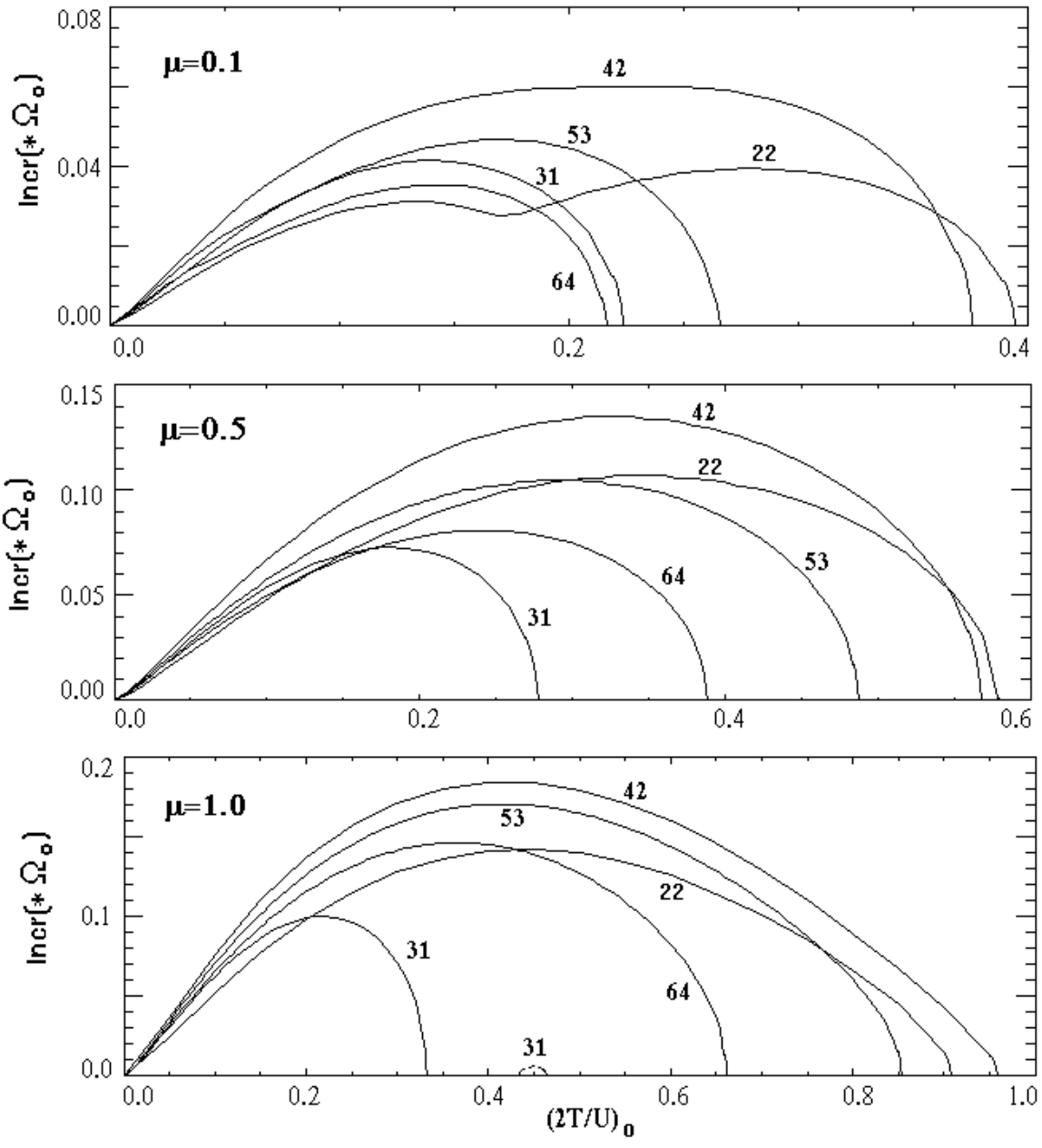

Fig. 8b. Comparison of increments of bulk modes at the minimum azimuthal wavenumber m=N. The numbers next to the curves indicate the order of the mode (N,n).

§ 10. Some remarks

So, we have obtained the exact integral and differential forms of the NDR for both non-rotating (1.29) and rotating (1.38) pulsating models separately in cases of surface deformations of volume disturbances for an arbitrary value of their oscillation index. Above, up to numerical values, the NDR of large-scale disturbances have been studied so far, although it is possible to study with the same success individual small-scale oscillations, when N and n take large values up to ∞.

Note that surface deformations of the spherical model under consideration are characterized by the presence of vibrationally resonant zones of instability and islands of stability, while this is not the case for volume disturbances. The discovered islands of stability (in particular, for n=2) quickly disappear when small rotation is turned on. For example, in the case of ellipsoidal perturbations in a non-rotating model on the scale λ there is a narrow stability zone (0.873, 0.916), which, when rotation appears, tries to become an "island", but is very imperceptible. In this case, the growth of the perturbation in the region $\lambda > \sqrt{21/5}$ is obviously due to the Jeans instability of purely radial motions.

The instability on the average of an isotropic model with the value $\lambda = \sqrt{5/3}$ is apparently associated with resonances between oscillations of individual particles and collective motions. It is interesting that as μ grows, the vibrational-resonance zone of instability quickly merges with the region of instability of radial motions. At small λ, but large μ, the region of instability is reduced due to the increasing role of Coriolis forces.

Further, we should dwell on at least the following two questions in somewhat more detail: a) on the application of the analysis of ellipsoidal perturbations; b) by comparing different types of instabilities occurring at different values of the oscillation indices.

10 a. On the question of the origin of elliptical galaxies

Although our main goal is to build accurate nonlinear nonstationary models of the early stages of the evolution of collisionless self-gravitating systems and to reveal instabilities against the background of collapse, but here we must also indicate possible applications of the results obtained. In particular, the cases of large-scale oscillation modes considered by us in § 7b and § 9a are related to the problem of the origin, for example, of elliptical galaxies, since the perturbation

itself can be considered switched on at the moment the collapse begins ($t = 0,\ \psi = 0$).

As is known [1, 2, 37], for a long time it was believed that the origin and external shape of elliptical non-spherical galaxies are due to their rapid rotation, and the observed regular distribution of luminosity and density was associated, starting with the work of Linden-Bell [38], with violent relaxation. At the same time, most authors believe (see reviews of references in [39-41] and [26]) that not far from the state of the maximum expansion of the protogalaxy (which can lead to the formation of an elliptical rather than a spiral galaxy), the process of star formation is mainly fast ends and then there is a free fall of particles - stars, leading to collapse and violent relaxation. Our nonlinear model, firstly, can describe the collapse of a collisionless system purely from dark matter, and secondly, in the case of a collapsing almost stellar system, it can start working immediately as soon as the collisionless approximation with self-gravity taken into account becomes acceptable. Such a scenario is called the non-dissipative collapse theory. Among a number of papers in this direction, the article by Gott [42] stands out, where the phenomenon of the collapse of a rotating spherical system with axial symmetry was studied in detail. As a result of the rotation effect, he obtained ellipsoidal configurations E1-E5 with isophotes and rotation curves close to some of the observed ones. However, it soon became clear that the rotation rates of the observed elliptical galaxies are very small and far from sufficient to cause the corresponding oblateness [43-45]. Then they began to carefully study the rotation curves, the laws of distribution of brightness and density, the problems of their modeling, etc. But no one had any doubts that it was the process of violent relaxation that took place at an early stage. Lynden-Bell believed that due to this collisionless relaxation, the traces of the initial non-stationary state and the "memory" of it are completely erased as equilibrium is approached, and a certain velocity distribution close to the Fermi-Dirac distribution is achieved. However, a detailed analysis shows that a lot depends on the initial state, and in the final state a distribution [46-48] is achieved that is completely different from the Lynden-Bell function, and the "memory" of strong non-stationarity does not disappear [27, 39, 48-50]. In particular, under certain conditions, a large-scale bar-like instability arises, which can significantly accelerate violent relaxation and, at the same time, give the system an ellipsoidal shape.

The condition for the onset of aperiodic instability $\lambda > \sqrt{21/5}$, (i.e. $(2T/|U|)_0 < 0.084$) was found by us long ago [14, 21] in the framework of two nonlinear models without rotation ((1.29) and (1.50)). As noted above, this instability arises due to the instability of purely radial motions. Interestingly, ellipsoidal instability also occurs in stationary systems. As was discovered by

Polyachenko and Shukhman [51], then the instability condition is determined by the ratio of the kinetic energies of motion in the radial and transversal directions, more precisely, by the condition $2\sigma_r^2/\sigma_\perp^2 > 1.6$. But this criterion is suitable for stationary models, where $2T/|U| = 1$.

During the last two decades, various computer numerical experiments have also been carried out on the subject under discussion. Among them, it is important to note the result of van Albada [52] and McGleen [53], which states that the observed density distributions in elliptical galaxies are obtained only in those cases if $2T << |U|$, i.e., when the initial state of the collisionless collapsing system is sufficiently "cold". Merritt and Aguilar [54] performed extensive numerical experiments in 1985 for three families of collapsing system models with a fairly wide set of initial conditions. In this case, the brightness profile satisfied the de Vaucouleurs law. The limiting condition of instability found by them then was expressed very approximately as $(2T/|U|)_0 < 0.2$. The authors of [54] only experimentally confirmed that only in the case of the predominance of purely radial motions of particles, a triaxial galaxy arises, and in some cases the mass distribution shows fluctuations between the states of oblate and prolate spheroids, i.e. oscillatory instability.

Ming and Choi [28] also considered an N-body experiment with the collapse of a cold system that initially has an isotropic velocity distribution and refined the result of Merritt and Aguilar [54]. By the way, we noted earlier in [24] that, on average, an isotropic analytical model (case $\lambda = \sqrt{5/3}$) is unstable with respect to ellipsoidal perturbations. Later, Aguilar and Merritt [4] also came to the conclusion that a more correct condition for ellipsoidal instability is expressed in the form $(2T/|U|)_0 < 0.1$. On fig. Figure 9 shows the results of their numerical experiment for one particular case.

The criterion (2.53) we have found means that for the occurrence of ellipsoidal instability it is necessary that at , the total kinetic energy is less than 4.2% of the potential energy. This criterion is quite well confirmed by the above numerical-experimental results, where ≈5% was obtained (see, for example, [4]). And there should not be an exact match, since in numerical experiments it is impossible to consider too many particles, there is also a machine accumulation of errors, and, in addition, the existing differences in the models, in particular, our neglect of the initial inhomogeneities in theoretical calculations densities, the role of which, on average, probably consists in destabilization. But the main thing is in determining the corresponding instability criterion at least with an accuracy of ±0.02 in terms of the virial parameter, and not with an accuracy of ±0.1, as was the

case in [54, 28, 4] in the direction of numerical experiments. Unfortunately, so far the authors of numerical experiments have not been able to reveal the zone of vibrational-resonant instability $(2T/|U|)_0 \in (0.127;0.389)$. Obviously, it should also exist in numerical experiments, if the model is not strongly inhomogeneous. In addition, these numerical experiments are still very approximate and require further improvement. Therefore, one can only regret that the results of our earlier works [14, 21, 24] were previously ignored by the authors of papers [4, 28].

The extent to which the above picture of the instability of ellipsoidal perturbations changes taking into account the effect of rotation can be seen from Fig. 3. It is noteworthy that the rotation acts in a destabilizing way up to a certain finite value μ, if we are talking about a purely bar-like instability (m=2), and then a fast rotation can just have a stabilizing effect with an increase in μ. The latter, probably, can still be associated with the effects of non-stationarity or nonlinear resonant phenomena. Thus, we can conclude that the evolution of a nonlinear system strongly depends on the relationship between the degree of its nonstationarity and rotation.

In numerical experiments, it is difficult to detect a narrow region in the form of an “island” of stability or instability, although it is also preserved in the nonlinear regime. The presence of a tiny “island” in Fig. 3 says that the instability of radial orbits acts up to a certain value λ. In this case, the island conditionally subdivides the regions of instability of different nature. It should be emphasized that already at small μ the “island” of stability begins to disappear and the regions of instability of radial motions merge with the region of vibrational-resonant instability. Unfortunately, in numerical experiments, the role of rotation in determining the criterion for the occurrence of ellipsoidal instability in the period of non-dissipative collapse has not been fully studied in order to find the marginal dependence of the virial parameter on μ.

We note that we have indicated only a possible application of some results of the previous sections, without asserting the indispensable validity of only the concept of a non-dissipative theory of collapse. Those interested in the dissipative theory of evolution can familiarize themselves with the problems there, for example, in [40, 55]. The role of dissipative processes in the form of “second viscosity” in the evolution of elliptical galaxies was studied by us for a mixed stellar-gas model [7]. We believe that the dissipative and non-dissipative concepts should in fact complement each other and cannot be opposed in order to choose one of them.

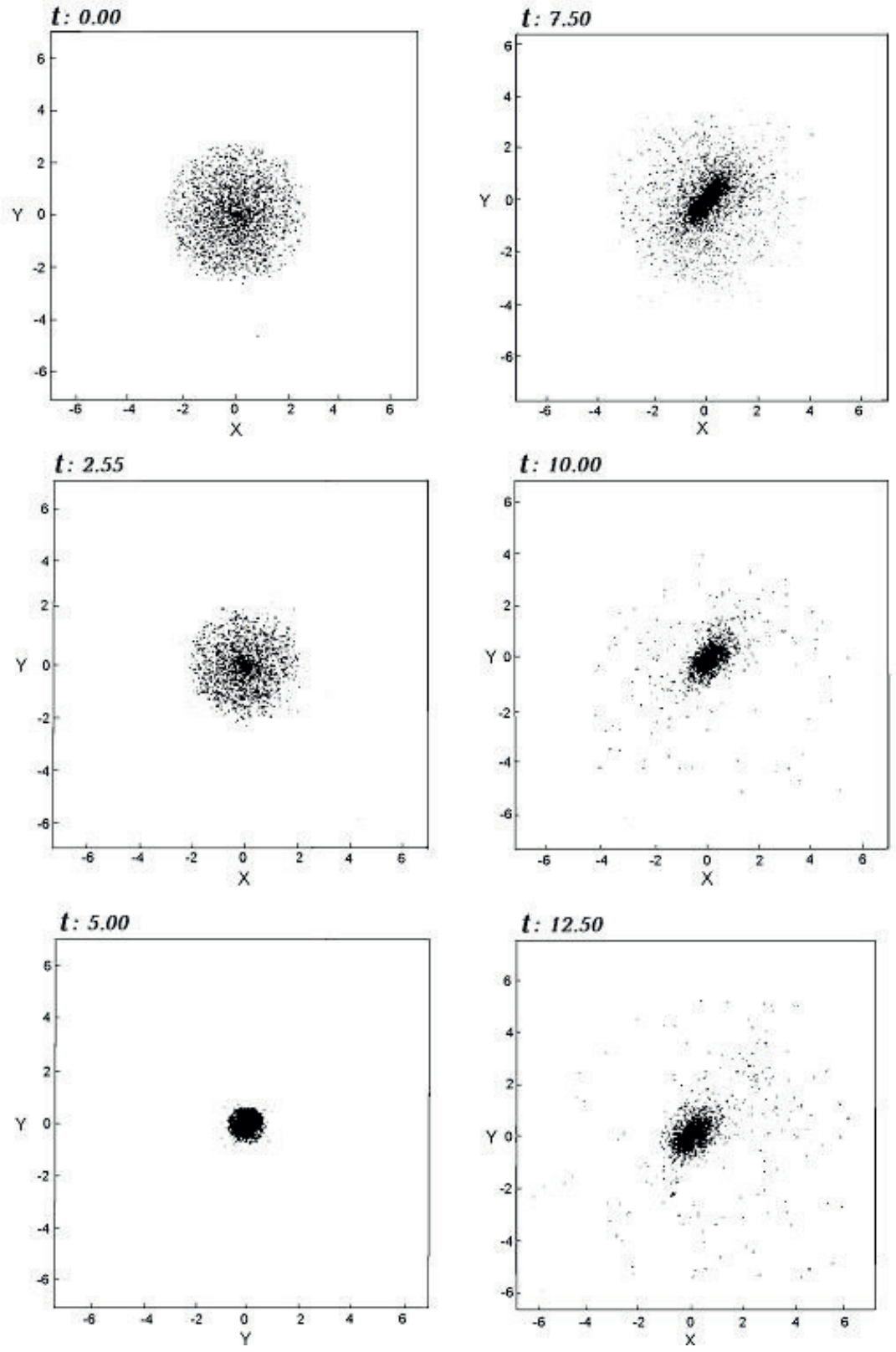

Fig.9 Collapse starting from a spherical state (2T/U)0=0.01 [4].

Note that we considered the behavior of small asymmetric perturbations against the background of a nonlinear model. In numerical experiments, although it is possible to study the problem immediately in the nonlinear case, the task of identifying the role of individual types of oscillation modes against the background of collapsing galaxies is very difficult and has not yet been completed by anyone. In particular, the predominance of the ovoid instability over the ellipsoidal one, at least at the earliest stages of evolution, has not yet been noticed. We will discuss this fact below.

10b. Which instability is more dangerous?

Probably, this question cannot be answered unequivocally when studying the stability of non-stationary models, since in the general case everything depends mainly on the initial conditions in the protogalaxy (or proto-cluster).

To be convincing, let us compare the increments of large-scale surface and bulk oscillations. On fig. 7 and 8 we present a comparison of the increments of the main types of large-scale instabilities. As can be seen, in the interval $0.01 \le (2\,T/|U|)_0 \le 0.16$ the increments of the ovoid instability are clearly larger than those of the ellipsoidal one. Therefore, if the evolution starts from the value of the virial parameter from this interval, then in the initial period before the appearance of ellipticity, a weak core arises in the system, with respect to which the spherical symmetry is lost, and the picture resembles an ovoid shape. By the way, in numerical experiments, this picture can be taken as an elliptical galaxy E1, and maybe even E2, although the ellipsoidal mode has not yet fully manifested itself. If in a purely nonlinear regime also the ovoid perturbation prevailed over the ellipsoidal one, then further, nonlinear development of the instability would lead to the birth of a satellite near the main system. However, this does not occur in numerical experiments; in the nonlinear regime, the ellipsoidal instability still becomes stronger if $(2T/|U|)_0 < 0.1$. The fact indicated here, in particular, shows that in a numerical experiment one cannot limit oneself, for example, to calculations of only a positive value of x, conditionally assuming symmetry about the y or z axis. This kind of artificial requirements just “freeze” the egg-shaped and other types of instability that give rise to an irregular shape.

Note that in the interval $0.16 < (2\,T/|U|)_0 < 0.389$ the ellipsoidal instability is oscillatory, but it has increments, on average, twice as large as the maximum value of the instability increment of almost radial motions. And in the area $(2\,T/|U|)_0 < 0.01$ the curves in Fig. 6 merge and therefore their analysis requires separate consideration.

It is clear that in reality the evolution of a non-linear self-gravitating system depends on the entire spectrum of oscillation types, and the latter interact with each other in a complex way. But until now, everyone believes that the main type of perturbation is always the bar mode, i.e. in this case, the ellipsoidal type of oscillation. This opinion remained based on the results of studying the stability of stationary models. If they take into account at least a little non-stationarity in the initial state and then study the evolution of even a small perturbation against its background, the results can change significantly. A complete analogy with the theory of stationary systems and the assumption of the largest value of the growth rate for the bar mode were recently made, for example, by the authors of [56], who calculated on a computer the critical value of the Hamiltonian for the problem of the stability of a pulsating spherical system. The critical value they found, these authors automatically attributed to the bar fashion. Since their model actually coincides with ours (1.29) (which they did not notice), it was very interesting for the author of the book to check the above-noted property of non-stationarity. Our exact calculation has shown that their main incremental instability and the value of the Hamiltonian correspond to the critical pulsation amplitude $\lambda_{cr} = \sqrt{7/10}$, which has nothing to do with the bar mode, but is related to the oscillations m=1, N=3.

It is also necessary to give an answer to the question: is it possible to express in a concrete form the general criterion of instability for a nonstationary one. pulsating spherical model and what exactly its parameters are the main ones. In order to find a more or less exhaustive answer, it is advisable to first carry out the same calculations for at least one more nonlinear model.

CHAPTER III. ANALYSIS OF THE PROPERTIES AND STABILITY OF PULSING GENERALIZATIONS OF THE CAMM MODEL

§ 11. On the properties of the perturbation of the potential and separability, simplifying the derivation of the NDE

Now that, using the example of the simplest nonlinear model, we have revealed the essence and degree of complexity of the problem of the stability of pulsating models in general, it is necessary to draw some conclusions also regarding the method of studying physically admissible states of non-stationary spherical configurations and highlight useful properties. Starting to analyze the pulsating versions of the Camm models, we note that they are inherently more complex than the non-stationary models considered in the previous chapter. Therefore, it will be useful for us to note the following properties.

11 a. Four properties of the pulsating model

1. General property of the perturbation potential. It should be emphasized that, just as for the corresponding stationary models, the choice of the initial form of the perturbation potential in the form of sectorial or zonal harmonics is indifferent to the nonstationary analogs constructed by us when deriving the NDE.

Obviously, this property is associated with the presence of spherical symmetry in the non-stationary models under study. However, the latter is violated when the rotation phenomenon is included in the model, which requires a special approach in the problem of finding the NDE.

2. Response property. For all the models considered in this paper, in particular, for models of the type (1.29) and (1.50), the response to an additional small gravitational field $\delta\Phi_n$ in the form of a polynomial of degree n creates a perturbation of the density or displacement of the boundary, which correspond to a potential $\delta\Phi_n$ with a polynomial of the same degree n.

3. Property of rotation. In the presence of rotation in a nonlinearly pulsating model, each value of the azimuthal wave number corresponds to a certain type of potential perturbation, and the latter for surface and volume fluctuations, respectively, have the form

$$r^n \cdot e^{im\varphi} \cdot P_n^m(\cos\theta), \qquad r^N \cdot e^{im\varphi} \cdot P_n^m(\cos\theta).$$

When analyzing non-rotating models, the azimuthal index m of the functions $P_n^m(\cos\theta)$ does not affect the growth rate and can be omitted when considering the functions $P_n^m(\cos\theta)$. Note that the selection of individual harmonics is completely possible for all the models we are considering, and in the general case we would have to take the sum over m.

Properties 1-3 also took place for a number of stationary [13, 29] spherical models and are proved in a similar way. But the following remarkable property necessarily requires proof.

4. Separability property of the model (1.50). For a given coordinate, for example, z, the distribution of velocities over the corresponding velocity v_z component does not depend on the other two coordinates x and y of the point where the velocity diagram is constructed, namely, for model (1.50), the formula

$$\iint \Psi dv_x\, dv_y = \frac{2\rho \cdot \Pi^4}{\pi\left(\Pi^2 - Z^2\right)^{1/2}}\left[\frac{1}{\Pi^4} - \frac{1}{\Pi^2 - Z^2}\left(v_z + \frac{z \cdot \bar{c}}{\Pi^2}\right)^2\right]^{1/2} \qquad (3.1)$$

where $\bar{c} = \lambda\sin\psi/\left(1-\lambda^2\right)^{1/2}$ and, without loss of generality, it is assumed that $\Omega_0 = 1$, $R_0 = 1$. This separability property of phase coordinates is satisfied by symmetry for any pair from (v_x, v_y, v_z). Based on (3.1), it is not difficult to show, for example, the following

$$\iint v_x \Psi dv_x\, dv_y = -\frac{2\rho\Pi^4 x\left(zv_z + \bar{c}\right)}{\pi\left(\Pi^2 - Z^2\right)^{3/2}}\left[\frac{1}{\Pi^4} - \frac{1}{\Pi^2 - Z^2}\left(v_z + \frac{z \cdot \bar{c}}{\Pi^2}\right)^2\right]^{1/2} \qquad (3.2)$$

Formula (3.2) can be called the weak separability property of model (1.50). Obviously, if we take the double integral of $v_y\Psi$, then on the right side of (3.2) instead of x there will be y.

In order to prove (3.1), we first write the model (1.50) in rectangular coordinates, and then, taking derivatives with respect to v_x, v_y of the radical expression and equating the results to zero, we obtain

$$\left(\Pi^2 - y^2 - z^2\right)v_x + x\cdot y\cdot v_y + x\cdot z\cdot v_z + \bar{c}\cdot x = 0$$

$$\left(\Pi^2 - x^2 - z^2\right)v_y - x\cdot y\cdot v_x - y\cdot z\cdot v_z - \bar{c}\cdot y = 0$$

It follows that the center of the velocity diagram for a given value v_z corresponds to the case when

$$w_x \equiv v_x + \frac{x\left(z\cdot v_z + \bar{c}\right)}{\Pi^2 - Z^2}, \qquad w_x \equiv v_y + \frac{y\left(z\cdot v_z + \bar{c}\right)}{\Pi^2 - Z^2}$$

are equal to zero, therefore

$$\Psi = \frac{\rho\Pi^3}{\pi^2}\left[h_0 - \left(\Pi^2 - y^2 - x^2\right)\cdot w_x^2 - \left(\Pi^2 - x^2 - z^2\right)\cdot w_y^2 - 2x\cdot y\cdot w_x\cdot w_y\right]^{-1/2}, \tag{3.3}$$

where

$$h_0 \equiv \frac{\Pi - r}{\Pi^2} - \frac{\Pi - r}{\Pi^2 - z^2}\left(\Pi\cdot v_z + \frac{\bar{c}\cdot z}{\Pi}\right)^2.$$

Therefore

$$\iint \Psi dw_x dw_y = \frac{2\rho\Pi^3\left(h_0\right)^{1/2}}{\pi\left[\left(\Pi^2 - r^2\right)\left(\Pi^2 - z^2\right)\right]^{1/2}}. \tag{3.4}$$

From here we obtain (3.1), which was required to be shown. For $\lambda = 0$, (3.1) implies the formula for the corresponding equilibrium model (1.50) in the case of surface perturbations. Let us show the possibility of using two methods.

11b. Methods for deriving NDE of surface perturbations

1. The method of one-dimensional functions. In contrast to the method of analysis of surface perturbations used by us for model (1.29) and in accordance with property I, we take as the initial perturbation potential a one-dimensional function of the coordinate, for example, z, i.e., $\delta\Phi \propto z^n$. Above in §9b, with the help of just such an approach, it was possible to obtain in a general form the NDE of a rotating model, for which other methods did not give the required result. If the model is non-rotating and also possesses the property of separability, then consideration $\delta\Phi$ in the form (2.117), as will be seen below, greatly simplifies the solution of the problem. This way of deriving the NDE, in view of its simplicity and elegance, can be conditionally called the method of one-dimensional functions of coordinates. In this case, two components of the displacement vector $\overrightarrow{\delta r}$ are always equal to zero $\overline{\delta x} = \overline{\delta y} = 0$, and only one component must be calculated

$$\delta z = n \int_{-\infty}^{\psi} E\left(\psi,\psi_1\right) z_1^{n-1}\, d\psi_1 , \tag{3.5}$$

where $z_1 = zH_\alpha + v_z H_\beta$. Using the separability property of the model, we obtain that

$$\overline{z_1^{n-1}} = \frac{2\Pi^4}{\pi\left(\Pi^2 - z^2\right)^{1/2}} \int \left(zH_\alpha + v_z H_\beta\right)^{n-1} \left[\frac{1}{\Pi^4} - \frac{1}{\Pi^2 - z^2}\left(v_z + \frac{\bar{c}\, z}{\Pi^2}\right)^2\right]^{1/2} dv_z \tag{3.6}$$

Applying Newton's binomial formula here gives the following:

$$\overline{z_1^{n-1}} = \frac{2}{\pi b^2} \sum_{k=0}^{n-1} \frac{(n-1)!\left(H_\beta\right)^k}{k!(n-k-1)!} \left(zH_\alpha - \frac{\bar{c}\, z}{\Pi^2} H_\beta\right)^{n-k-1} \int_{-b}^{+b} w_z^k \left(b^2 - w_z^2\right)^{1/2} dw_z ,$$

Where $b^2 \equiv \left(\Pi^2 - Z^2\right)\Big/\Pi^4$, $H_0 \equiv H_\alpha - \bar{c}\cdot H_\beta \Big/ \Pi^2$.

The last integral is

$$b^{k+2}\int_0^\pi \cos^k\xi\cdot\sin^2\xi\cdot d\xi.$$

With this in mind, you can collect the entire amount back and present the result in the form

$$\overline{z_1^{n-1}} = \frac{2z^{n-1}}{\pi}\int_0^\pi \left[H_\alpha - \frac{\bar{c}}{\Pi^2}H_\beta + i\frac{H_\beta}{\Pi^2}\left(1-\frac{\Pi^2}{z^2}\right)^{1/2}\cos\xi\right]^{n-1}\sin^2\xi\cdot d\xi \ . \qquad (3.7)$$

As mentioned above, we always follow the leading term in the perturbation expansion. Therefore, in (3.7) we can neglect the term Π^2/z^2 under the root. Further, substituting here the expression for and using (2.36), we have

$$\overline{z_1^{n-1}} = \frac{2(z\cdot W)^{n-1}}{\pi}\int_0^\pi \left(\cosh + i\cdot\cosh\cdot\cos\xi\right)^{n-1}\sin^2\xi\cdot d\xi \ , \qquad (3.8)$$

which brings us to the result

$$\overline{z_1^{n-1}} = \frac{2}{n(n+1)}(z\cdot W)^{n-1}\frac{dP_n(\cosh)}{d(\cosh)} \ . \qquad (3.9)$$

Substituting (3.9) into (3.5), we pass to the calculation of the displacement

$$\overline{\delta r} = \frac{\overline{x\cdot\delta x + y\cdot\delta y + z\cdot\delta z}}{R} = \frac{2z^n}{(n+1)R}\int_{-\infty}^{\psi} W^{n-1}\frac{dP_n}{d\cosh}E\cdot d\psi_1 \qquad (3.10)$$

Now in (3.10) from z_n back to $\delta\Phi/a_0(\psi)$ or, which is the same, from it we select the harmonics of the surface perturbation in the form

$\delta\Phi = a_0(\psi)\cdot\exp(im\varphi)\cdot P_n(\cos\theta)$ by the necessary rotations and transformations [117]. Calculating the response of the perturbation of the potential according to formula (2.108) and reducing both parts of the equation by $\delta\Phi$, we obtain the connection condition, which we call NDE

$$a_0(\psi) = \frac{6}{(n+1)(2n+1)\Pi^3}\int_{-\infty}^{\psi} W^{n-1} a_0(\psi_1)\frac{dP_n}{d\cosh}\Pi^3(\psi_1)S(\psi,\psi_1)d\psi_1 \qquad (3.11)$$

It is possible to convert this equation into a differential form by first dividing into $dP_n/d(\cos\theta)$ functions with arguments ψ and ψ_1. We perform a similar operation in the next section. And now we will show the possibility of deriving the NDE in another way.

2. Method of averaging. Let us use formula (2.21) obtained by us in the problem of stability of model (1.29), but taking into account the differences in the models under consideration. We know from Chapter I that the difference between models (1.29) and (1.50) is that in the second model the transversal velocity component $v_\perp$ does not have a specific value at each point, but fills the interval $[0, v_m]$, where $v_m = \Omega\cdot R/\Pi^2$. However, the average value of the radial component of the centroid velocity coincides with the corresponding value for the model (1.29) and is equal to v_a. Therefore, to analyze the stability of surface perturbations in model (1.50), it is necessary to first average (2.21) over $v_\perp$. To this end, we integrate the right-hand side of (2.21) with (2.22) taken into account, multiplying it first by the number of particles $2\pi v_\perp dv_\perp$ in the interval $[v_\perp, v_\perp + dv_\perp]$ and dividing by the total number of particles πv_m. Having made the change of variables $v_\perp = v_m p$, we finally have

$$\overline{(u+iv)^\tau} = K_\tau(\psi)\cdot(x+iy)^\tau \quad , \qquad (3.12)$$

where

$$K_\tau(\psi) = \frac{r^{-\tau}}{\pi}\int_0^1 p\cdot dp\int_0^{2\pi}\left(v_a + ip\cdot v_m\cos\xi\right)^\tau d\xi \qquad (3.13)$$

Here, generally speaking, one can get rid of integration over p, but as the analysis shows, this leads to some uncertainties in the subsequent basic equations. On the other hand, the integral over ξ can be expressed in terms of the Legendre polynomial, but it is easiest to leave the NDE $K_\tau(\psi)$ in the form (3.13) until the end of the derivation, and use only the expression under the sign of the integral over ξ in the calculations.

The further course of reasoning is the same as in §7a. Therefore, without giving the intermediate stages of the calculation, we write the result itself [21]:

$$a_0(\psi)=\frac{3n}{(2n+1)(1+\lambda\cos\psi)^{2n+1}}\sum_{\tau=0}^{n-1}\frac{(n-1)!}{\tau!(n-\tau-1)}\aleph_\tau(\psi)l_\tau(\psi) \quad , \qquad (3.14)$$

where

$$\aleph_\tau(\psi)=\frac{1}{\pi}\int_0^1\rho d\rho\int_0^{2\pi}\left[\cos\psi+\lambda-ip\left(1-\lambda^2\right)^{1/2}\sin\psi\cdot\cos\xi\right]^{n-\tau-1}\cdot$$

$$\left[\left(1-\lambda^2\right)\sin\psi+ip\left(1-\lambda^2\right)^{1/2}\left(\cos\psi+\lambda\right)\cos\xi\right]^{\tau}d\xi \qquad (3.15)$$

and the function $l_\tau(\psi)$ again satisfies equation (2.33) and is related to $a_0(\psi)$ by (2.34).

Consequently, we managed to write the NDE in such a way that its structure basically has the same form as in the case of model (1.29). This makes it easier to analyze the frequency types of fluctuations and compare the results with the case of a nonlinear model in the form (1.29).

If we consider the largest-scale mode with n=2, which corresponds to the ellipsoidal type of perturbations, we find that the function $a_0(\psi)$ coincides exactly with (2.43).

Hence it follows that the same critical values of the pulsation amplitude $\lambda=\sqrt{21}/5$, 0.873 and 0.611 determine the regions of stability and instability for

model (1.50). The coincidence of the results for two different models at n=2 means that in this case the evolution of ellipsoid disturbances is controlled by changing only the centroid velocity, and the difference in the velocity diagrams of the models has no effect. This was not obvious from the very beginning and is somewhat of a surprise. It turns out that the case n=2 could also be studied in a hydrodynamic way. But, obviously, starting from n=3, the NDE of these models and the results for the critical values of the pulsation amplitude will clearly differ from each other.

§ 12. Analysis of volume fluctuations

The evolution of volumetric fluctuations superimposed on pulsating models (1.29) and (1.50) proceeds in completely different ways. Therefore, their analysis is also necessary for model (1.50). In order to show explicitly the validity of the assertions of properties 1 and 2 given in the previous section, and also to have control over the results, we consider below two cases with different forms of the initial perturbation of the potential. This is also important from the point of view of the methodology and its application in similar problems.

I. Method of sectorial harmonics

Let the initial form of the perturbation potential have the form (2.13), i.e.

$$\delta\Phi = a_0(\psi) r^{N-n} (x+iy)^n . \qquad (3.16)$$

Then, to calculate the response for other characteristics, we use the formulas in (2.17) and (2.57), where now, in contrast to model (1.29), the function r_1^{2k} cannot be taken outside the averaging sign. Therefore, you must first calculate B_1 and B_2 according to the following formulas:

$$(B_1 + B_2)(x+iy)^n r^{2k} = n(x+iy) \int_{-\infty}^{\psi} \overline{(x_1+iy_1)^{n-1} r^{2k}} \cdot E d\psi_1 +$$

$$+ 2k \int_{-\infty}^{\psi} E \cdot \overline{\left(H_{\alpha} r^2 + H_{\beta} r v_r \right) (x_1+iy_1)^n r_1^{2k-2}} \, d\psi_1 \qquad (3.17)$$

$$B_2\left(x+iy\right)^{n+1} r^{2k-2} = 2k\cdot \int_{-\infty}^{\psi}\left(x_1+iy_1\right)^{n+1} r^{2k-2} E\cdot d\psi_1$$

The calculation of the averaged expressions in (3.17) will be carried out by expanding each function into a binomial series, then averaging over the space of velocities and presenting the results again in the form of finite sums. Here we use formulas (2.60) and (2.63). Therefore, in contrast to (2.18), the problem is reduced to calculating the averages of

$$J_1 = (u+iv)^{\tau}\left[\left(H_0 r+H_\beta v_r'\right)^2 + H_\beta^2 v_\perp^2\right]^k$$

$$J_2 = \left(u+iv\right)^{\tau} v_r'\left[\left(H_0 r+H_\beta v_r'\right)^2 + H_\beta^2 v_\perp^2\right]^{k-1}$$

where $v_r' = v_r - v_a$, $H_0 \equiv H_\alpha + H_\beta v_a/r$. In [23,62], we presented a method for deriving the general averaging formula. Counting in formula (A. 1) in [62] $e_1 = 1,\ e_2 = i$, we obtain $e_3 = 0$ and

$$\overline{J_1} = A_\tau^k\left(\psi,\psi_1\right)\left(x+iy\right)^{\tau} r^{2k}, \qquad (3.18)$$

where

$$A_\tau^k\left(\psi,\psi_1\right) = \frac{1}{2\pi}\int_0^{2\pi}\left(V_+^{\tau}H_+^{2k} + V_-^{\tau}H_-^{2k}\right)\cos^2\varphi\cdot d\varphi, \qquad (3.19)$$

in which connection

$$V_\pm \equiv v_a/r \pm i\sin\varphi/\Pi^2, \qquad H_\pm \equiv H_0 \pm iH_\beta\sin\varphi/\Pi^2. \qquad (3.20)$$

Based on (3.18) - (3.20), after some algebraic transformations, we obtain

$$\overline{\left(x_1+iy_1\right)^{n-1}\,r^{2k}}=K_{N-1}\left(\psi,\psi_1\right)\left(x+iy\right)^{n-1}\,r^{2k}\,. \tag{3.21}$$

Here the function

$$K_{N-1}=\frac{1}{2\pi}\int_0^{2\pi}\left(H_+^{N-1}+H_-^{N-1}\right)\cos^2\varphi\,d\varphi \tag{3.22}$$

and it is surprising that it depends only on the index N, while the dependence on the number of the spherical harmonic n disappears.

By analogy, one can get

$$\overline{J_2}=\Theta_\tau^{k-1}\left(\psi,\psi_1\right)\left(x+iy\right)^\tau\,r^{2k-1} \tag{3.23}$$

where

$$\Theta_\tau^{k-1}\left(\psi,\psi_1\right)=\frac{i\Pi^{-2}}{2\pi}\int_0^{2\pi}\left(V_+^\tau H_+^{2k-2}+V_-^\tau H_-^{2k-2}\right)\sin\varphi\cos^2\varphi\cdot d\varphi$$

Knowing (3.23), it is easy to derive the following formula

$$\overline{\left(x_1+iy_1\right)^n\,r_1^{2k-2}\left(H_\alpha r^2+H_\beta rv_r\right)}=K_{N-1}\left(\psi,\psi_1\right)\left(x+iy\right)^n\,r^{2k}\,. \tag{3.24}$$

Interestingly, (3.24) has a similar form to (3.21). Using (3.21) and (3.24) in (3.17), we find

$$B_1=n\int_{-\infty}^{\psi}E\cdot K_{N-1}d\psi_1\,,\qquad B_2=2k\int_{-\infty}^{\psi}E\cdot K_{N-1}d\psi_1\,. \tag{3.25}$$

Next, we calculate the volume density perturbation

$$\delta\rho=-\rho\left(\psi\right)\left[2k\cdot B_1+\left(2k+n+1\right)B_2\right]\left(x+iy\right)^n\,r^{2k-2}\,. \tag{3.26}$$

On the other hand, the Poisson equation for the initial perturbation of the potential gives the following expression

$$\delta\rho = -\frac{a_0(\psi)}{2\pi G}\cdot k(N+n+1)(x+iy)^n\, r^{2k-2}, \quad \left(k=\frac{N-n}{2}\right) \qquad (3.27)$$

Equating (3.26) and (3.27), taking into account (3.25), we obtain the desired NDE

$$a_0(\psi)\Pi^3(\psi) = 3\int_{-\infty}^{\psi} a_0(\psi_1)\Pi^3(\psi_1)S(\psi,\psi_1)K_{N-1}(\psi,\psi_1)d\psi_1. \qquad (3.28)$$

We note that this NDE of volume fluctuations, in contrast to the analogous equation for model (1.29), on the contrary, does not depend on the index n in any way.

In the study of special cases, the integral form of the NDE may turn out to be inconvenient. Therefore, (3.28) should be written in differential form, which requires, first of all, the separation of variables in the expression for the function $K_{N-1}(\psi,\psi_1)$. To do this, we first express $K_{N-1}(\psi,\psi_1)$ in terms of the Legendre polynomials, considering $H_0 = W\cos e, \quad H_\beta = W\cdot\Pi^2\sin e$. Then from (3.22), taking into account (3.20), we find

$$K_{N-1} = \frac{2T^{N-1}}{N\sin^2 e}\left[\cos e\cdot P_N(\cos e) - P_{N+1}(\cos e)\right] = \frac{2W^{N-1}}{N(N+1)}\frac{dP_N(\cos e)}{d(\cos e)}. \qquad (3.29)$$

If we introduce the designation

$$\frac{\cos\psi+\lambda}{1+\lambda\cos\psi} = \cos\varepsilon, \quad \frac{(1-\lambda^2)^{1/2}\sin\psi}{1+\lambda\cos\psi} = \sin\varepsilon, \quad 1 = \cos\eta, \qquad (3.30)$$

then $\cos e = \cos\varepsilon\cdot\cos\varepsilon_1 + \sin\varepsilon\cdot\sin\varepsilon_1\cdot\cos\eta$ and we have the opportunity to use the addition theorem [57] for the polynomial $P_N(\cos e)$. Therefore, we easily find

$$\frac{dP_N(\cos\varepsilon)}{d(\cos\varepsilon)}=\left[\frac{d(\cos\eta)}{d(\cos\varepsilon)}\frac{dP_N}{d(\cos\eta)}\right]\Bigg|_{\eta=0}=2\sum_{\nu=1}^{N}\frac{(N-\nu)!}{(N+\nu)!}\nu^2\frac{P_N^\nu(\cos\varepsilon)\,P_N^\nu(\cos\varepsilon_1)}{\sin\varepsilon\cdot\sin\varepsilon_1}\quad.\quad(3.31)$$

Substituting (3.29) into (3.28), taking into account (3.31), we find

$$a_0(\psi)=\frac{12(1+\lambda\cos\psi)^{1-N}}{N(N+1)\Pi^3}\sum_{\nu=1}^{N}\frac{(N-\nu)!}{(N+\nu)!}\cdot\nu^2\cdot\frac{P_N^\nu(\cos\varepsilon)}{\sin\varepsilon}\cdot L_\nu(\psi)\,.\qquad(3.32)$$

Here

$$L_\nu(\psi)=\int_{-\infty}^{\psi}(1+\lambda\cos\psi_1)^{N-1}\Pi^3(\psi_1)a_0(\psi_1)\cdot S\cdot\frac{P_N^\nu(\cos\varepsilon_1)}{\sin\varepsilon_1}d\psi_1\,.\qquad(3.33)$$

Only now, when the variables ψ and ψ_1 are completely separated, can we write down the differential form of the NDE, which follows from (3.33) and is a system of ordinary differential equations of order 2N:

$$\Lambda L_\nu(\psi)=\frac{12}{N(N+1)}\cdot\frac{P_N^\nu(\cos\varepsilon)}{\sin^2\varepsilon}\sum_{\nu=1}^{N}\frac{\nu^2(N-k)!}{(N+k)!}\cdot L_\nu\cdot P_N^\nu(\cos\varepsilon).\qquad(3.34)$$

Note that (3.34) has a special advantage over (3.28) if N>>1.

II. Method of one-dimensional functions

II.I. We are talking about the method (see § 11b), where the initial form $\delta\Phi$ was taken in a form proportional to the power function of the z coordinate. In the case of volume perturbations, we also try to take

$$\delta\Phi = a_0(\psi)\cdot z_N\,.\qquad(3.35)$$

Then by analogy with calculations (3.5) - (3.9) we have

$$\overline{\delta z} = \frac{2\,z^{N-1}}{N+1}\cdot\int_{-\infty}^{\psi} W^{N-1}E\cdot\frac{dP_N(\cos e)}{d(\cos e)}d\psi_1\ . \qquad (3.36)$$

Let us replace z^{N-1} in (3.36) by z^{N-1}, and from (3.35) select $\delta\Phi = a_0(\psi)\cdot r^N\cdot P_n(\cos\theta)$. Then the corresponding density perturbation, taking into account formula (3.29),

$$\delta\rho = -\frac{\rho_0}{\Pi^3}\cdot\frac{\Delta\delta\Phi}{a_0(\psi)}\cdot\int_{-\infty}^{\psi} W^{N-1}\cdot E\cdot K_{N-1}d\psi_1\ . \qquad (3.37)$$

Equating the latter and $\delta\rho = -\Delta(\delta\Phi)/4\pi G$, taking into account $4\pi G\rho = 3$, we obtain the NDE exactly in the form (3.28).

II. 2. The obtained identical forms of the NDE of volume perturbations give us, as it were, a hint that, in principle, the initial form of the potential could be taken as

$$\delta\Phi = a_0(\psi)\cdot P_N(z/R)\ . \qquad (3.38)$$

Then it makes sense to pose the problem of the possibility of finding the corresponding point of the form of natural fluctuations for the nonlinear model (1.50). But first we show the usefulness of considering (3.38).

Perturbation (3.38) corresponds to the displacement

$$\delta z = \int_{-\infty}^{\psi}\left[\overline{\frac{dP_N(z_1/R_1)}{dz_1}}\right]\cdot E(\psi,\psi_1)d\psi_1, \qquad \frac{z_1}{R_1} = \frac{zH_\alpha + v_z H_\beta}{R(\psi=\psi_1)}\ . \qquad (3.39)$$

Using the separability property (3.1), we have

$$\left[\overline{\frac{dP_N}{z_1}}\right] = \frac{2}{\pi\Pi_0}\cdot\int_{-\Pi_0}^{+\Pi_0}\frac{dP_N\left(z_1/R_1\right)}{dz_1}\cdot\left[1-\frac{w_z^2}{\Pi_0^2}\right]^{1/2} dw_z\ , \qquad (3.40)$$

where $\Pi_0 \equiv \left(\Pi^2 - z^2\right)\Big/\Pi^2$, $w_z \equiv v_z + \bar{c}\cdot z/\Pi^2$. Taking into account the possibility of substitution $dP_N/dz_1 = H_\beta^{-1}\cdot dP_N/dw_z$, let us perform integration by parts in (3.40). Then, introducing the notation $\cos\xi = w_z/\Pi_0$, we have

$$\left[\overline{\frac{dP_N}{dz_1}}\right] = \frac{2}{\pi H_\beta \Pi_0}\cdot\int_0^\pi \cos\xi\cdot P_N(z_1/R_1)\,d\xi\ . \qquad (3.41)$$

It is easy to show that $z_1/R_1 = \cos\aleph\cdot\cos e + \sin\aleph\cdot\sin e\cdot\cos\xi$, where $\sin\aleph = \Pi\cdot\Pi_0$, $\text{sine} = H_\beta/(\Pi^2 W)$ (see (2.36)). Therefore, in (3.41) one can apply the well-known addition theorem for the Legendre polynomial. Then it is easy to make sure that when integrating over ξ, all the terms of the sum, except for one (terms with P_N^1), make a zero contribution. As a result, we get

$$\left[\overline{\frac{dP_N}{dz_1}}\right] = \frac{2\,W^{-1}}{N(N+1)}\cdot\frac{dP_N(z/R)}{dz}\cdot\frac{dP_N(\text{cose})}{d(\text{cose})}\ . \qquad (3.42)$$

Therefore, substituting (3.24) into (3.39), taking into account (3.38), we find

$$\delta\rho = \frac{-2\rho_0}{N(N+1)}\cdot\frac{\Delta(\delta\Phi)}{a_0(\psi)\cdot\Pi^3}\cdot\int_{-\infty}^{\psi} W^{-1}\cdot E\cdot\frac{dP_N(\text{cose})}{d(\text{cose})}d\psi_1\ . \qquad (3.43)$$

Further, we assume that it has the general form (2.126). Then, comparing (3.43) with the Poisson equation for $\delta\Phi$, we obtain

$$a_0(\psi)\cdot\Pi^3=\frac{6}{N(N+1)}\cdot\int_{-\infty}^{\psi}W^{-1}\cdot a_0(\psi)\cdot\Pi^3(\psi_1)\cdot S\cdot\frac{dP_N(\cos e)}{d(\cos e)}d\psi_1\,. \qquad (3.44)$$

As can be seen, (3.44) coincides with (3.28), but there is an insignificant difference in the degree of the function T. To eliminate it, in (3.28) and (3.44) one should substitute $a_0(\psi)$ instead of $(1+\lambda\cos\psi)^N a_0(\psi)$. The nature of the function $T(\psi,\psi_1)$ is such that it does not play any role in compiling the NDE in differential form.

Let us check the special case $\lambda=0$, which corresponds to the problem of stability of the equilibrium Camm model with respect to volume perturbations with an arbitrary value of N.

Then in our notation T=Π=1, $S=\sin(\psi-\psi_1)$, $a_0(\psi)\propto\infty\exp(i\omega\psi)$. Substituting all this into (3.44) and integrating by parts,

$$i\omega\cdot\int_0^{\infty}P_N(\cos\aleph)\cdot e^{-i\omega\aleph}d\aleph=\frac{(2-N)(3+N)}{6}\,. \qquad (3.45)$$

This equation was obtained for the first time by us long ago [58] as a particular case of the NDE of the pulsating model (1.50), and then in [59] by searching for the exact form of natural fluctuations of the equilibrium model. Analysis (3.45) gives the complete stability of the equilibrium model. In doing so, we use multiplicative formulas for the representation of integrals (3.45) given in [57] for even and odd N separately. In this way, we easily notice that for even N the roots (3.45) are in the intervals (0;2), (2;4)..., (N-2;N), and for odd N they are in the intervals (0; 1), (1;3),..., (N-2;N). The same number of roots are located symmetrically with respect to the point ω=0. Note that Polyachenko [60] also derives (3.45) with mention of our result (3.45), and he uses a reduction procedure.

Finally, let us return to the question of determining the exact form of natural fluctuations for the pulsating model (1.50). Finding it is very important in the application of the results and the construction of new models for the observed specific real objects. True, all this may require delicate calculations on powerful computers. Nevertheless, this is a very interesting problem with a clear future perspective. Therefore, we indicate here our corresponding result. Namely, in

(3.38) the function $P_N(z/R)$, which is not proportional to any spherical harmonic, can be expanded into a Fourier series as follows

$$P_N(z/R) = \sum_n \chi_{nN}(r/N)\, P_n(\cos\theta)\,. \tag{3.46}$$

because $z = r\cdot\cos\theta = r\cdot\zeta, \quad R = \Pi(\psi)$. Here, in accordance with the rules of expansion in Legendre polynomials,

$$\chi_{nN} = \frac{2n+1}{2}\cdot\int_{-1}^{+1} P_n(\zeta)\cdot P_N\left(\frac{r}{\Pi}\cdot\zeta\right)d\zeta\ . \tag{3.47}$$

An integral of this type could not be found in any literary source. To find the exact form of natural fluctuations, it is sufficient to expand P_N in powers of (r/Π). Then we get some decomposition for $\chi_{nN}(r/\Pi)$, where there are no terms with $r^0 - r^{n-1}$. Therefore, it is possible to take out the bracket $(r/\Pi)^n$. Since with $r/\Pi = \pm 1$ we have $\chi_{nN} = 0$, we can also take out $(r/\Pi)^2 - 1$. Thus, we get $\chi_{nN} = r_*^n\cdot(r_*^2 - 1)\cdot\varphi_{nN}(r_*)$, where $r_* = r/\Pi$, φ_{nN} is a polynomial of degree N-n-2. Then it can be proved that

$$\int_{-1}^{+1} r_*^{n+k}\cdot(r_*^2 - 1)\cdot\varphi_{nN}(r_*)dr_* = 0\ . \tag{3.48}$$

if $n+1 \le k \le N$. It is easy to compare (3.48) with the definition of the Jacobi polynomial. As a result, it is possible to represent the sought-for exact form of eigenfluctuations in terms of the Jacobi polynomial. More precisely, after selecting one spherical harmonic, it has the form

$$\varepsilon\cdot r_*^n\cdot P_n(\cos\theta)\cdot\left[(r_*^2 - 1)\cdot P_{\frac{N-n}{2}-1}^{(n+0.5,1)}(r_*^2) + \eta_{nN}\right], \tag{3.49}$$

where η_{nN} is a constant determined from the condition of continuity of the potential at the boundary. Knowing (3.49), in principle, it can be calculated from the Poisson equation. Then, in particular, it is easy to find the corresponding nodes on the r-axis. The problem of the number of nodes is also relevant in the theory of pulsating stars [61]. Based on (3.49), we can also formulate a **theorem on the number of nodes of the fluctuational mode:** the function δΦ vanishes (N-n-2)/2 times in the interval 0< r/Π< 1 and one more time at the boundaries r=0 and r= Π.

§ 13. Egg-shaped and toroidal modes

Let us proceed to finding criteria for the instability of large-scale modes of volume fluctuations. Based on the comparison of (3.34) and (3.44), we make the following remark: in order for the right-hand sides of (3.44) to have a relatively simple and symmetric form, it is necessary to compose an equation for the functions

$$\gamma_\nu(\psi) = \int_{-\infty}^{\psi} (\lambda + \cos\psi_1)^{N-\nu} (\sin\psi_1)^{\nu-1} (1 + \lambda\cos\psi_1)^3 \cdot S(\psi, \psi_1) \cdot a_0(\psi_1) d\psi_1 . \qquad (3.50)$$

where ν=1, 2, ..., N. Then, in the general case, the system of N equations has the form

$$\Lambda\gamma_\nu(\psi) = (\lambda + \cos\psi_1)^{N-\nu} (\sin\psi_1)^{\nu-1} (1 + \lambda\cos\psi_1)^3 a_0(\psi) . \qquad (3.51)$$

It remains to substitute here each time only the expression for $a_0(\psi)$.

II. 1. Analysis of individual fluctuation modes, generally speaking, should be started with N=2. In this case, we are dealing with the case of small radial perturbations against the background of nonlinear pulsations. Therefore, stability must be preserved at 0< λ < 1. Indeed, when N=2

$$a_0(\psi) = 3(1+\lambda\cos\psi)^{-5} \gamma(\psi), \quad \gamma \equiv (\lambda + \cos\psi)\gamma_1 + (1-\lambda^2)\gamma_2 . \qquad (3.52)$$

By investigating the corresponding two equations for $\gamma_1(\psi)$ and $\gamma_2(\psi)$

$$\Lambda\gamma_1 = \frac{3(\lambda+\cos\psi)}{(1+\lambda\cos\psi)^2}\cdot\gamma(\psi), \quad \Lambda\gamma_2 = \frac{3\sin\psi}{(1+\lambda\cos\psi)^2}\cdot\gamma(\psi) \tag{3.53}$$

instead of them, one equation for $\gamma(\psi)$ can be obtained in the form

$$(1+\lambda\cos\psi)\cdot\gamma'' + 3\lambda\sin\psi\cdot\gamma' + (1-2\lambda\cos\psi)\cdot\gamma(\psi) = 0\ , \tag{3.54}$$

if we use formulas (2.46) and (2.48). One of the particular solutions (3.54) is $\sin\psi$. So, the general solution is

$$\gamma(\psi) = c_1\cdot\sin\psi + c_2\left[\cos\psi + 3\lambda + 3\lambda^2(\cos\psi + \psi\sin\psi) + \lambda^3(1+\sin^2\psi)\right]. \tag{3.55}$$

As can be seen, the fluctuation mode under consideration does not lead to instability. The presence in (3.55) of a term with the coefficient □ is associated with a small perturbation of the pulsation period itself, which entails only a progressive shift of their phase. Stability takes place at $\lambda < \lambda_{20} = 1$. If $\lambda=1$, the pulsations are replaced by a single expansion or contraction, which, of course, creates the possibility of a qualitative change in the behavior of the system from the initial small perturbation. In this case, a power-law instability arises, which is not described by solution (3.35) (see the corresponding general solution in Chapter 4).

II. 2. In the case of N=3, obviously, the wave number n must be equal to one. Then volume perturbations, violating the density homogeneity and rotational symmetry of the system, at some λ lead to the formation of a core (see § 8b), but slightly shifted from the former center, with a self-consistent change in the shape of the entire system towards “egg-shaped”. From (3.44) for N=3 it follows that

$$a_0(\psi) = \frac{3}{4}\cdot F(\psi)\cdot(1+\lambda\cos\psi)^{-7}, \tag{3.56}$$

$$F(\psi) \equiv \left[4(\cos\psi+\lambda)^2 - (1-\lambda^2)\sin^2\psi\right]\gamma_1 + 10(1-\lambda^2)\sin\psi(\cos\psi+\lambda)\gamma_2 +$$

$$+ (1-\lambda^2)\left[4(1-\lambda^2)\sin\psi - (\cos\psi+\lambda)^2\right]\gamma_3\ .$$

Consequently, for $\gamma_\nu(\psi)$ the system of equations

$$\Lambda\gamma_\nu(\psi) = (3/4)(\cos\psi + \lambda)^{3-\nu}(\sin\psi)^{\nu-1}(1 + \lambda\cos\psi)^{-4} F(\psi). \qquad (3.57)$$

moreover, it takes the form (3.34) if

$$\gamma_1 = L_1 + L_3/10, \quad \gamma_2 = \frac{2}{5}(1-\lambda^2)^{-1/2} \cdot L_2, \quad \gamma_3 = \frac{2}{5}(1-\lambda^2)^{-1} L_3.$$

Despite its relatively symmetric form, nevertheless, system (3.57) cannot be solved purely analytically in order to determine the critical value of the pulsation amplitude λ_{31}. Therefore, we integrated it numerically on a computer using the well-known method of the theory of stability of periodic solutions. It is found that $\lambda_{31} = 0.554$ and, if $\lambda > 0.554$, there are exponentially increasing solutions. The corresponding instability criterion in the language of global parameters $2T/|U|$ and ∇ for the model under consideration has the following form

$$(2T/|U|)_0 < 0.445; \quad \nabla > 0.882, \qquad (3.58)$$

Note that these conditions are weaker than the condition of ellipsoidal instability.

We also calculated the values of the instability increment for the region $\lambda > 0.554$. In [62], we presented the results of calculating these increments and the characteristic doubling time $(t_2 = \ell n\, 2 \cdot P(\lambda)/\ell n \| 1 \|)$ of the disturbance rise amplitude in units of the pulsation period, as well as the corresponding values of the ratio of the maximum radius to its nominal and global parameters. Asterisks mark those values that correspond to the complex conjugate roots of the characteristic equation and are associated with oscillatory overstability. It follows from our calculations that, as $(2T/|U|)_0$ decreases, the "egg-shaped" instability initially has the character of an oscillatory increase and then, starting from the value of $\cong 0.35$, an aperiodic, purely exponential instability sets in. Note that, on

average, a velocity isotropic model, which corresponds to λ and $\nabla = 1$, falls into the region of oscillatory instability with an asymmetric perturbation amplitude that doubles its value in $\infty 1.35^{\cdot}$P years. Obviously, with an increase in the degree of nonstationarity of the initial state, the value of the characteristic time t_2 decreases, while the values of ∇ and R_{max}/R_0 increase. Note that for the section $\lambda \in (\lambda_3; 0.70)$ we give the maximum value of the increment. In fact, there are two oscillatory solutions here, which gradually merge with increasing λ, and at a certain value of λ, an aperiodic instability arises. In other words, if the evolution of a real system due to collisionless relaxation occurs in the direction of decreasing λ, then the aperiodic instability that has arisen at an early stage of development can give rise, at some time, to two independent branches with an oscillatory nature of the instability. The further fate of the system and the question of choosing between these branches is decided only by nonlinearity.

II. 3. Consider the case N=4, which can probably also be attributed to the class of large-scale fluctuations. Since the wave number n is not included in the dispersion equations (3.34) and (3.44), the instability criterion found below for N=4 is the same for the values n=0 and n=2, i.e., the directions of evolution along the "branch" (4;0) and (4;2) turn out to be equally probable as long as we resort to a nonlinear analysis of the perturbation.

Recall that when N=4, n=0, in the unstable region $(\lambda_{40}; 1)$, a ring structure is formed either with a core or without a core. If N=4, m=2, then there is no rotational symmetry in the perturbed state, which, together with a violation of the density uniformity, leads to the following: in one meridional plane, the pattern is elongated along the equator, and in the plane perpendicular to it, elongation occurs near the polar regions, and, which is important, a ring structure of individual segments and a nucleus in the center, slightly elongated in the polar direction, are noticeable.

For N=4 the function

$$a_0(\psi) = \frac{3}{4} \cdot F(\psi) \cdot (1 + \lambda \cos\psi)^{-9},$$

where

$$\tilde{F}(\psi)=(\cos\psi+\lambda)\left[4(\cos\psi+\lambda)^2-3(1-\lambda^2)\sin^2\psi\right]\gamma_1+3(1-\lambda^2)\times$$
$$\times\{\sin\psi\left[6\cdot(\cos\psi+\lambda)^2-(1-\lambda^2)\sin^2\psi\right]\gamma_2+(\cos\psi+\lambda)\times$$
$$\times\left[6(1-\lambda^2)\sin^2\psi-(\cos\psi+\lambda)^2\right]\gamma_3\}+(1-\lambda^2)^2\sin\psi\times$$
$$\times[4(1-\lambda^2)\sin^2\psi-3(\cos\psi+\lambda)^2]\gamma_4 \quad .$$

The corresponding NDE has the form

$$\Lambda\gamma_\nu(\psi)=\frac{3\tilde{F}(\psi)}{4(\cos\psi+\lambda)^6}(\cos\psi+\lambda)^{4-\nu}(\sin\psi)^{\nu-1}. \qquad (3.59)$$

This system of differential equations of the 8th order was solved on a computer. It was found that instability occurs if $\lambda\rangle\lambda_{40}=0.6985$. Therefore, the corresponding criterion for annular instability for model (1.50) has the form:

$$(2T/|U|)_0\langle 0.3015, \quad \nabla\rangle 1.353 \qquad (3.60)$$

We note that here and in (3.58), as a criterion, we deliberately present two inequalities at once, since if we slightly modify the original nonlinear model (more precisely, consider the mixed model (1.64)), then the inequality may correspond to a completely different inequality in the virial parameter (see (discussed in §19).

In [62], the behavior of the growth rate, the value of the characteristic time, etc., is presented. The instability starts from the value λ_{40} and up to the point $\lambda\cong 0.78$ is aperiodic, and then passes into the oscillatory mode of instability, at least in the interval $\lambda\in(0.78;0.9)$. At $\lambda\rangle 0.9$, the instability is again aperiodic. It can be seen that the increments of the annular instability are much smaller than the increments of "egg-shaped" perturbations. Note that in all the cases considered above, when $\lambda\to 1$, the value of the increment explicitly tends to zero if it is calculated taking into account $P(\lambda)$ in units Ω_0 (see Fig. 7).

§ 14. Accounting for the effect of rotation

In order to elucidate the relationship between nonstationarity and rotation for the considered nonlinear model, it is necessary to investigate the stability of a rotating pulsating system with distribution function (1.60), to which we proceed further. In doing so, we need to use the separability properties (3.1) and (3.2). Therefore, we will carry out the analysis below, mainly in rectangular coordinates. Taking into account the above units $R_0 = \Omega_0 = 1$, we rewrite (1.60) in a form convenient for what follows

$$\Psi_{rot} = \left[1 + \mu\left(xv_y - yv_x\right)\right] \cdot \Psi^*, \tag{3.61}$$

where Ψ^* conventionally denotes the phase density of the nonrotating model (1.50). Just like (2.98), in order to be able to work temporarily with particular forms $\delta\Phi$ and then only generalize the result to more general types of perturbations, we are forced to use again the analytical method of rotating the model by an arbitrary angle β_0 according to (2.97). Substituting (2.97) into (3.61) gives

$$\Psi_{rot} = \{[1 + \mu(xv_y - yv_x)\cos\beta_0 + (xv_z - zv_x)\sin\beta_0]\} \cdot \Psi^*. \tag{3.62}$$

Let us start studying the behavior of the perturbation against a pulsating background (3.62)

14a. Calculation of the response by the method of one-dimensional functions

Let's try to calculate the response of an arbitrary particle to a perturbation with a potential in the form (3.38). Then, according to (3.39), we calculate

$$\left[\overline{\frac{dP_N}{dz_1}}\right] = -\frac{1}{\rho}\iiint \frac{dP_N}{dz_1}\Psi^* d\vec{v} + \frac{1}{\rho}\mu\sin\beta_0 \iiint \left(xv_z - zv_x\right)\frac{dP_N}{dz_1}\Psi^* d\vec{v}, \tag{3.63}$$

since, using (3.1) and (3.2), we have

$$\iiint \left(xv_z - zv_x\right)\frac{dP_N}{dz_1}\Psi^* d\vec{v} = 0.$$

We have already encountered the first multiple integral in (3.63) (see 3.42), and we will calculate the second integral in exactly the same way, and when integrating the terms with zv_x we use the weak separability property (3.2). Then we integrate by parts and pass to $\xi = \arccos\left[w_z\Pi^2 \Big/ \left(\Pi^2 - z^2\right)^{1/2}\right]$ (see 3.40). Then $\int_0^{\pi} \cos 2\xi \cdot P_n d\xi$ appears. Here we use the formula of the addition theorem for the Legendre polynomial. Now only the second term of the sum in this formula makes a non-zero contribution. As a result, we have

$$\left[\overline{\frac{dP_N}{dz_1}}\right] = 2W^{-1}\cdot\left[\frac{dP_N\left(\frac{z}{R}\right)/dz}{N(N+1)}\cdot\frac{dP_N(\cos e)}{d(\cos e)} + \right.$$

$$\left. + \mu\sin\beta_0\cdot\frac{(N-2)!}{(N+2)!}\cdot x\cdot\sin e\cdot\frac{d^2P_N(\frac{z}{R})}{dz^2}\cdot\frac{d^2P_N(\cos e)}{d(\cos e)}\right]. \qquad (3.64)$$

Substituting (3.64) into formula (3.39), we can very easily find the displacement of the particle at an arbitrary point $\overline{\delta z}$.

Further, it is convenient to continue the calculation for volume perturbations. Knowing $\overline{\delta z}$, we can easily calculate the density response

$$\delta\rho = -\frac{2\rho_0}{N(N+1)\Pi^3}\cdot\frac{d^2P_N(\frac{z}{R})}{dz^2}\cdot S_{1N}(\psi) -$$

$$-\frac{2(N-2)!}{(N+2)!}\cdot\frac{\mu\rho_0\sin\beta_0}{\Pi^3}x\frac{d^3P_N(\frac{z}{R})}{dz^3}S_{2N}(\psi)\,, \qquad (3.65)$$

where

$$S_{1N}(\psi)=\int_{-\infty}^{\psi}W^{-1}E\cdot\frac{dP_N(\cos e)}{d(\cos e)}d\psi_1\,,$$

$$S_{2N}(\psi)=\int_{-\infty}^{\psi}W^{-1}E\sin e\cdot\frac{d^2P_N(\cos e)}{d(\cos e)^2}d\psi_1. \qquad (3.66)$$

In (3.65) we pass from the function $P_N(z/R)$ back to $\delta\Phi$ and, comparing the results with the Poisson equation for $\delta\rho$ in general form, we obtain

$$\left[\frac{1}{6}a_0\Pi^3-\frac{S_{1N}(\psi)}{N(N+1)}\right]\cdot\Delta\delta\Phi=\frac{(N-2)!}{(N+2)!}S_{2N}(\psi)\vec{\mu}\cdot\left(\vec{r}\cdot\mathrm{grad}\Delta\delta\Phi\right), \qquad (3.67)$$

Further, it suffices to know that $\delta\Phi\propto e^{im\varphi}$ and we can ignore the dependence of $\delta\Phi$ on r/Π, since it turns out to be common for all moments of time. Then canceling both parts of (3.67) by $\Delta\delta\Phi$, we find (see, for example, [23])

$$\frac{1}{6}a_0(\psi)\cdot\Pi^3(\psi)=\frac{1}{N(N+1)}S_{1N}(\psi)+im\mu\frac{(N-2)!}{(N+2)!}S_{2N}(\psi)\,. \qquad (3.68)$$

The latter obtained by us is comparatively simpler than the analogous NDE for model (1.38). We owe this, first of all, to the properties of separability noted above. The performed calculations show that the exact form of eigenfluctuations (3.49), found by us for a non-rotating nonlinear model, remains valid also in the case of rotation.

Need to check case $\lambda=0$. Moreover, from (3.68), taking into account (3.66), we find

$$\frac{1}{N(N+1)}\cdot\int_0^{\infty}e^{-i\omega\aleph}\sin\aleph\frac{dP_N}{d(\cos\aleph)}d\aleph+$$

$$+ i\mu\mu \frac{(N-2)!}{(N+2)!} \int_0^{\infty} e^{-i\omega\aleph} \sin^2 \aleph \cdot \frac{dP_N}{d(\cos \aleph)^2} d\aleph = \frac{1}{6}, \quad (3.69)$$

where $\aleph = \psi - \psi_1$. Applying (3.69) we integrate by parts; we reduce the integral in (3.69) to

$$\int_0^{\infty} \exp(-i\omega \aleph) \cdot P_N(\cos \aleph) d\aleph .$$

Using further multiplicative representations [57] for the last integral, one can easily show that the equation has as many real roots as its degree.

14b. Analysis of the case of "surface" perturbations

For "surface" fluctuations, it is impossible to compose the NDE using the function $P_n(z/R)$, since this procedure is associated with the exact form of natural fluctuations, as we have already seen in the previous paragraph. Here, it is easier to compose the NDE in an invariant form if, immediately after calculating the response $\delta\bar{z}$, we expand the function $P_n(z/R)$ in powers of the argument and, as usual, restrict ourselves to the highest term. In other words, we pass to a perturbation of the potential of the form (3.4), assuming N=n in formula (3.64) and setting $\delta\Phi = a_0(\psi) \cdot (z/\Pi)^n$. Then, according to (3.64),

$$\overline{\delta z} = \frac{2}{(n+1)\Pi} \cdot \left(\frac{z}{\Pi}\right)^{n-1} S_{1n}(\psi) + 2\mu \sin\beta_0 \frac{x}{(n+1)(n+2)\Pi} \cdot S_{2n}(\psi) \cdot \left(\frac{z}{\Pi}\right)^{n-2} . \quad (3.70)$$

Here it is easy to pass to $\delta\Phi$ after multiplying both sides by z. And further we consider that $\delta\Phi$ has a more general form (2.109). Therefore, the radial displacement

$$\overline{\delta r} = \frac{2\delta\Phi}{(n+1)a_0(\psi)R} S_{1n}(\psi) + \frac{2S_{2n}(\psi)}{(n+1)(n+2)a_0(\psi)R} \cdot \vec{\mu}\left(\vec{r} \times \mathrm{grad}\,\delta\Phi\right). \quad (3.71)$$

Substituting (3.71) into (2.108) and returning to the previous coordinate system, taking into account (2.109), we obtain the desired NDE (see also [23])

$$a_0(\psi)\Pi^3(\psi) = \frac{6}{(n+1)(2n+1)} \cdot \left(S_{1n}(\psi) + \frac{im\mu}{(n+2)} S_{2n}(\psi) \right). \quad (3.72)$$

This result for $\mu = 0$ exactly coincides with (3.11) if in the original form the perturbation of the potential $a_0(\psi)$ is replaced by $(1+\lambda\cos\psi)^n a_0(\psi)$, which does not play any role in the NDE.

When $\lambda \neq 0$ from the point of view of application of results the most important case is n=2. In this case, from (3.72) we obtain the NDE of the ellipsoidal fluctuation mode

$$a_0(\psi)\Pi^3(\psi) = \frac{6}{5} \int_{-\infty}^{\psi} \left(\cos e + \frac{im}{4} \mu \sin e \right) \cdot W^{-1} E d\psi_1 . \quad (3.73)$$

The last equation coincides with the NDE of a similar case for the previous nonlinear model with rotation (2.111), which we have already studied in full. Thus, it turns out that the behavior of ellipsoidal perturbations is the same in both non-stationary models even in the presence of their axial rotation.

For $\lambda = 0$ we have the problem of the stability of a variant of the well-known equilibrium Camm model with respect to surface perturbations. For this case $a_0(\psi) \approx \exp(i\omega\psi)$ and (3.72) will give us

$$\int_0^\infty e^{-i\omega\varkappa}\sin\varkappa\frac{dP_n}{d(\cos\varkappa)}d\varkappa+\frac{im\mu}{n+2}\cdot\int_0^\infty e^{-i\omega\varkappa}\sin^2\varkappa\frac{d^2P_n}{d(\cos\varkappa)^2}d\varkappa=$$

$$=\frac{(n+1)(n+2)}{6},$$

what can be brought to mind

$$i\cdot\left[\frac{m(n^2+n-2\omega^2)}{n+2}\cdot\mu-\omega\right]\cdot\int_0^\infty e^{-i\omega\varkappa}P_n(\cos\varkappa)d\varkappa=$$

$$=\frac{(n+1)(2n+1)}{6}-\frac{2m\mu}{n+2}\cdot\omega-1. \qquad (3.74)$$

Then we can proceed in the usual way, using multiplicative formulas for the known integral, and prove stability.

Next, we consider two more surface modes [68].

Mode N=3:

$$a_0=\frac{9}{28(1+\lambda\cos\psi)^7}K_3(\xi_\tau),\quad \tau=\overline{1,3},$$

$$K_3(\xi_\tau)=(4c^2-e^2s^2)\xi_1+10cse^2\xi_2+e^2(-c^2+4e^2s^2)\xi_3+$$

$$+\ 2im\mu_2\sqrt{1-\lambda^2}\{cs\xi_1-(c^2-e^2s^2)\xi_2-cse^2\xi_3\}.$$

Mode N=4:

$$a_0=\frac{1}{3(1+\lambda\cos\psi)^9}K_4(\xi_\tau),\quad \tau=\overline{1,4},$$

$$K_4(\xi_\tau)=c(4c^2-3e^2s^2)\xi_1+3se^2(6c^2-e^2s^2)\xi_2+3ce^2(-c^2+6e^2s^2)\xi_3+se^4(-3c^2+4e^2s^2)\xi_4+$$

$$0.5im\mu_2\sqrt{1-\lambda^2}\{s(6c^2-e^2s^2)\xi_1-c(6c^2-15e^2s^2)\xi_2-se^2(15c^2-6e^2s^2)\xi_3-ce^2(-c^2+6e^2s^2)\xi_4\}.$$

The critical dependences of the initial virial ratio on and increments for these modes are shown in Fig. 10. The role of the parameter μ and the wavenumber m affects the behavior of the critical dependences of surface modes in a similar way to model (1.38), with the exception of: there is only one region of instability, which has aperiodic solutions for μ=0. Figures 11a and 11b compare the increments of different. Here, too, the maximum values are reached for the N=m=3 mode (if, again, the ellipsoidal mode is not taken into account). In the case of m=1 (Figure 11a), everywhere (except for small $\mu \le 0.1$) the N=2 mode increments prevail over all. The mode increments also decrease as N increases, but, in contrast to model (1.38), the larger μ, the stronger the separation of N=2 from the other modes. In addition, the increments of the N=3 mode are always more distant from the other modes, as if separating themselves from them. In the case of m=N (Fig. 11b), the detachment of the N=2 mode is not as strong as for m=1, but closer to $\mu = 1.0$, the maximum values of the N=3 mode increments are almost equal to the values of the ellipsoidal mode increments.

Figure 12 compares the increments of both models (1.38) and (1.60). Graphs for $\mu = 0, 0.5$ и 1.0 values are given. The solid lines indicate the increments of the model (1.38), the dotted line is the model (1.60). For m<n, model (1.38) is always more unstable than model (1.60). But for m=n, somewhere for $\mu \approx 0.8$ and more, model (1.60) overtakes and surpasses model (1.38). This is best seen when looking at the composite model (Chapter 5).

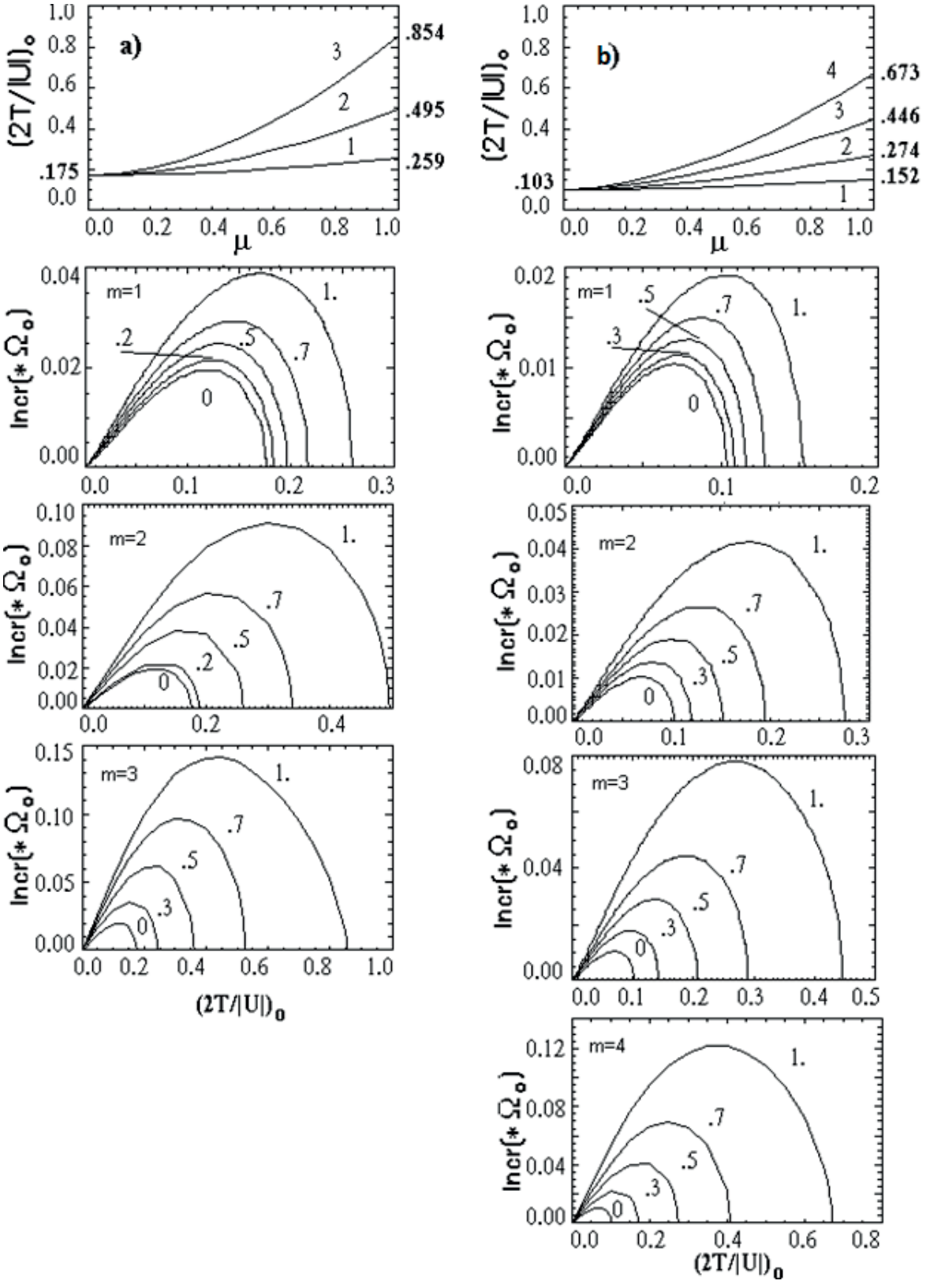

Fig. 10. Critical dependences of the values of the initial virial ratio and dependences of the instability increments for the N=3 (a) and N=4 (b) modes.

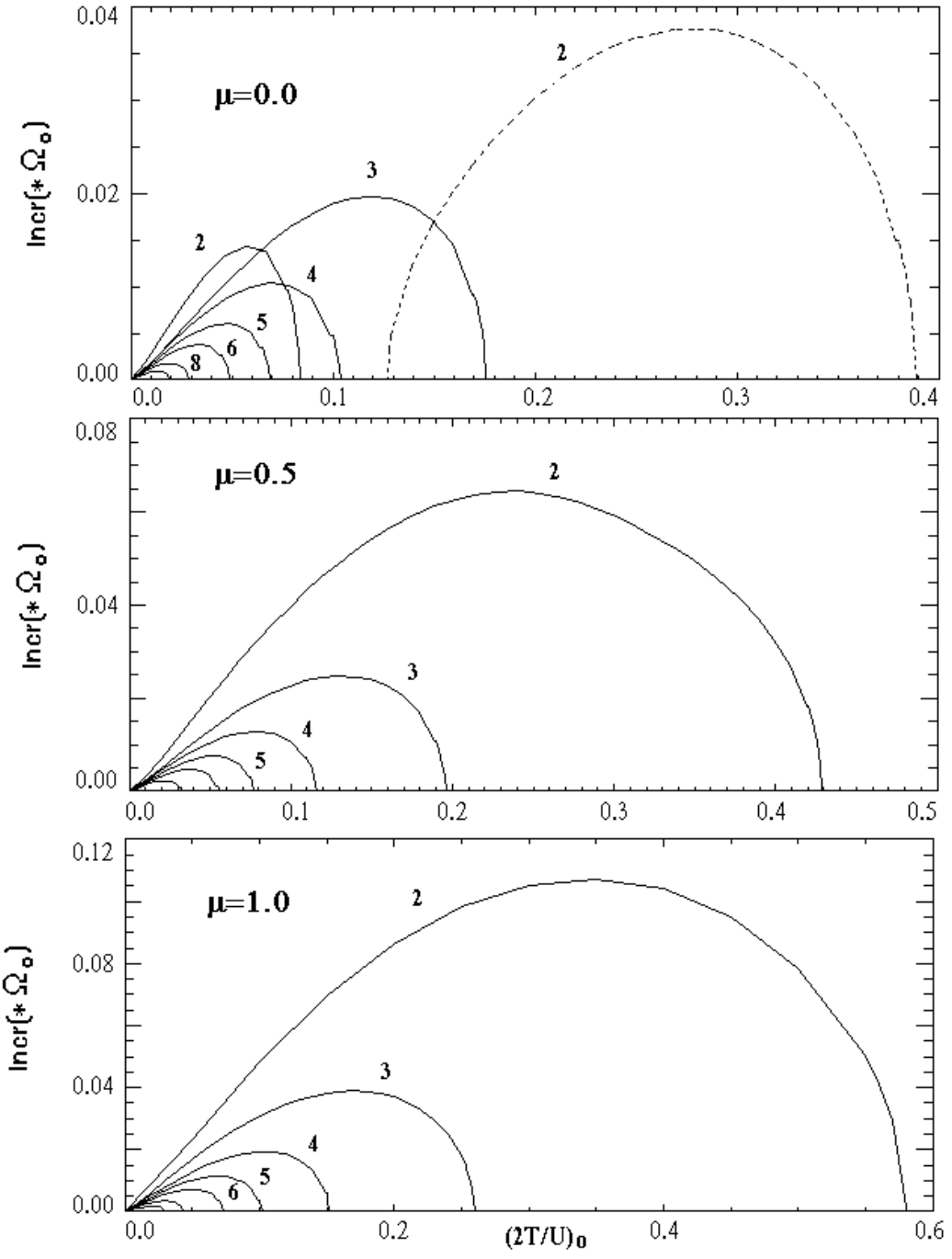

Fig. 11a. Comparison of increments of surface modes at the minimum azimuthal wavenumber m=1. The numbers next to the curves indicate the order of the mode.

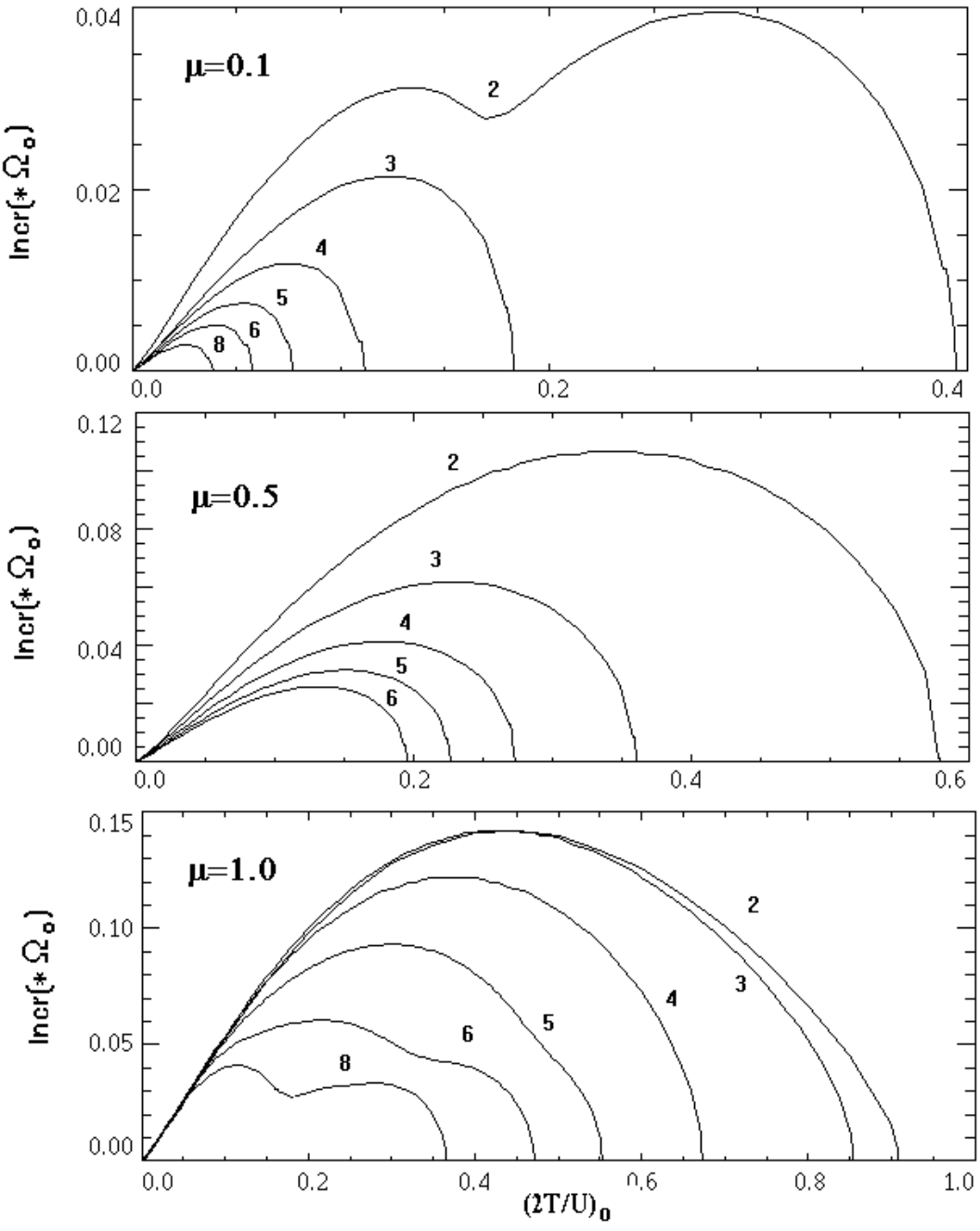

Fig.11b. Comparison of increments of surface modes at the maximum azimuthal wavenumber m=N. The numbers next to the curves indicate the order of the mode.

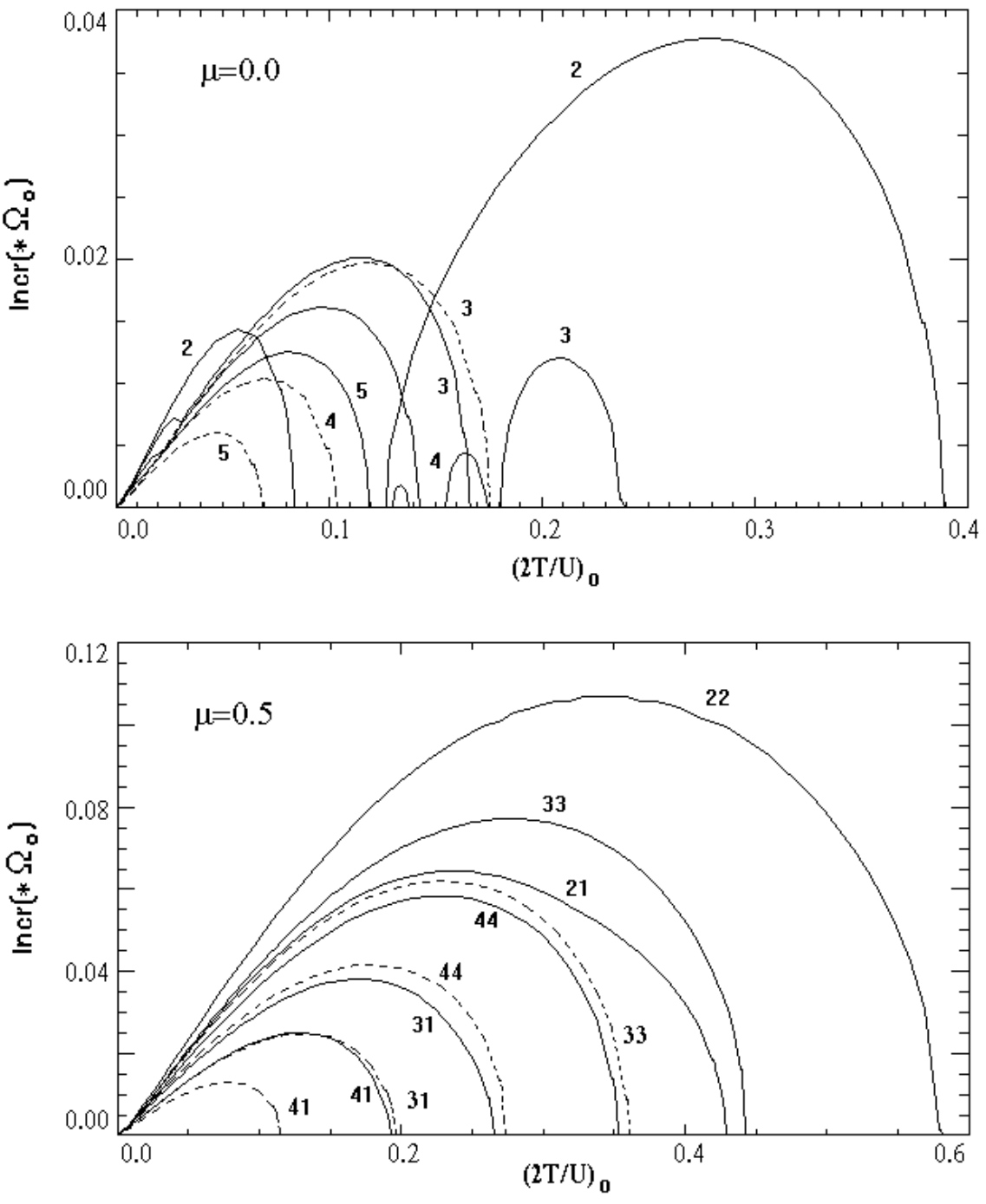

Fig.12. Comparison of increments of surface modes of nonequilibrium versions of Einstein balls (solid lines) and Camm balls (dashed line). The numbers next to the curves indicate the order of the mode N (Nm).

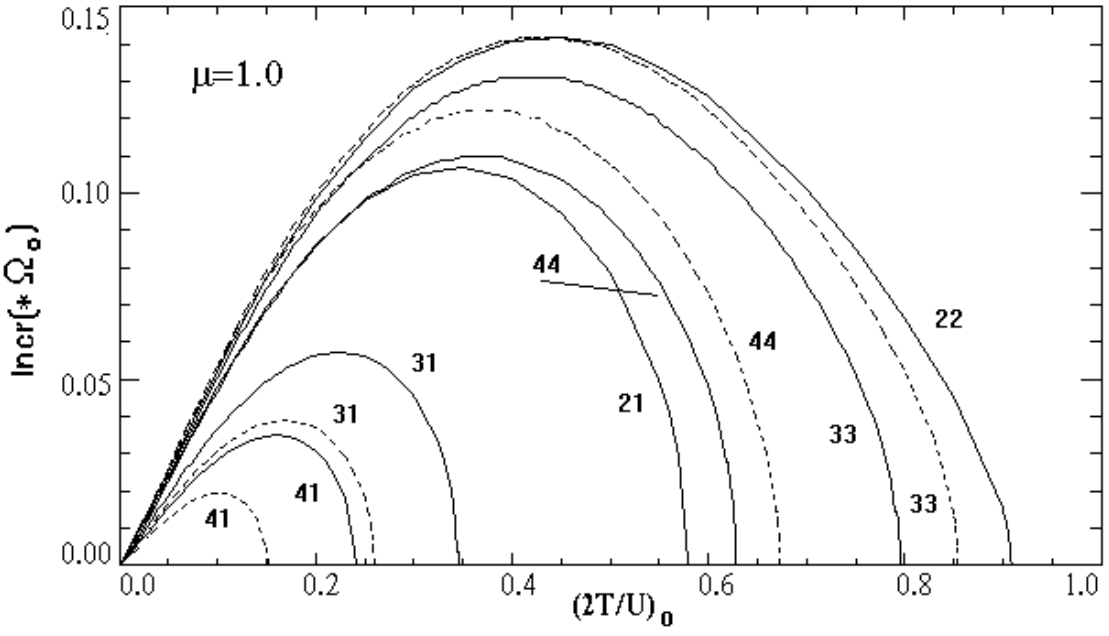

Fig. 12. Continuation

14 c. Analysis of the case of "volume" pertubations

Let us write down the NDE of the "egg-shaped" mode n=1, N=3:

$$a_0(\psi) = \frac{3}{4(1+\lambda\cos\psi)^7} K_{13}(\xi_\tau), \quad \tau = \overline{1,3},$$

$$K_{13}(\xi_\tau) = (4c^2 - e^2s^2)\xi_1 + 10sce^2\xi_2 + e^2(4s^2e^2 - c^2)\xi_3 +$$

$$im\mu_2 e\{sc\xi_1 - (c^2 - e^2s^2)\xi_2 + sce^2\xi_3\}$$

and toroidal mode n=2, N=4:

$$a_0 = \frac{3}{4(1+\lambda\cos\psi)^9} K_{24}(\xi_\tau), \quad \tau = \overline{1,4},$$

$$K_{24}(\xi_\tau) = c(4c^2 - 3e^2s^2)\xi_1 + 3se^2(6c^2 - e^2s^2)\xi_2 +$$

$$3ce^2(-c^2 + 6e^2s^2)\xi_3 + se^4(-3c^2 + 4e^2s^2)\xi_4 +$$

$$+ \frac{5im\mu_2 e}{6}\{s(6c^2 - e^2s^2)\xi_1 - c(6c^2 - 15e^2s^2)\xi_2 +$$

$$+se^2(15c^2 - 6e^2s^2)\xi_3 - ce^2(-c^2 + 6e^2s^2)\xi_4\}.$$

The results of studying the stability of equations are shown in Figure 13 [Gainullina, 2000]. In the case of an egg-shaped model, it has one region of instability, but bifurcating, starting from the value $\mu \approx 0.552$, its increments, despite the bifurcation, continuously increase with μ. The picture for the toroidal mode already resembles model (1.38) in the case of surface fluctuation modes, but the stability "island" is longer and reaches $\mu \approx 0.58$ (m=1) and $\mu \approx 0.32$ (m=2). In contrast to model (1.38), the instability region grows with much more slowly, and the increments are, on average, 3 times smaller than the increments of the egg-shaped mode.

Figures 14a and 14b compare the increments of volume modes. m=1 (Fig. 14a, $\mu = 0; 0.5; 1.0$) - starting from $\mu = 0$, the increments of the mode (3,1) are noticeably higher than the increments of the mode (2,2), although to $\mu = 1.0$ modes (2.2) and (3.1) seem to divide the area of influence: up to $(2T/|U|)_0 \approx 0.34$ "dominates" the egg-shaped mode, after - the mode (2,2). The rest of the modes are noticeably smaller. m=N (Fig. 14b, $\mu = 0.1; 0.5; 1.0$) - the mode (3,1) exceeds the mode (2,2) for $\mu < 0.5$ on all $(2T/|U|)_0$, but starting from $\mu \approx 0.5$, the maximum increments of the mode (2,2) exceed the maximum mode increments (3,1), and the further, the more noticeable, although not on the entire interval $(2T/|U|)_0$. Figure 15 compares the model increments of both models (1.38) and (1.60). Here, for small and moderate values of the rotation parameter, only large modes (2.2), (3.1), (4.2) are shown, and for the maximum value of rotation - μ and smaller modes (5.3), (6.4) to clearly illustrate that the increments of small-scale modes with large azimuth numbers during strong rotation are greater than the increments of individual large-scale modes. Graphs are given for three values of the rotation

parameter $\mu = 0; 0.5; 1.0$. The dotted line again denotes the model (1.60). The curves are labeled with numbers denoting N,n,m. The graphs clearly show that the mode (3,1) of the model (1.38) begins to lead, and with $\mu = 0.3$ it yields to the mode (N,n,m)=(4,2,2) of the model (1.60), which retains its leadership to end. It can also be seen that there is no such property as that of surface modes (Fig. 17): for any m, for all μ, model (1.38) is more unstable than model (1.60) (with the exception of only mode (3.1)). On the other hand, smaller-scale modes, in particular, modes (5.3) and (6.4) of model (1.38), compete with larger-scale modes, in particular (3.1) and (4.2). As a result, it turns out that at large rotations, among volume modes, the N=4 n=m=2 and N=5 n=m=3 modes of model (1.38) have the advantage in increments, only then do all the other modes go along with the ellipsoidal one.

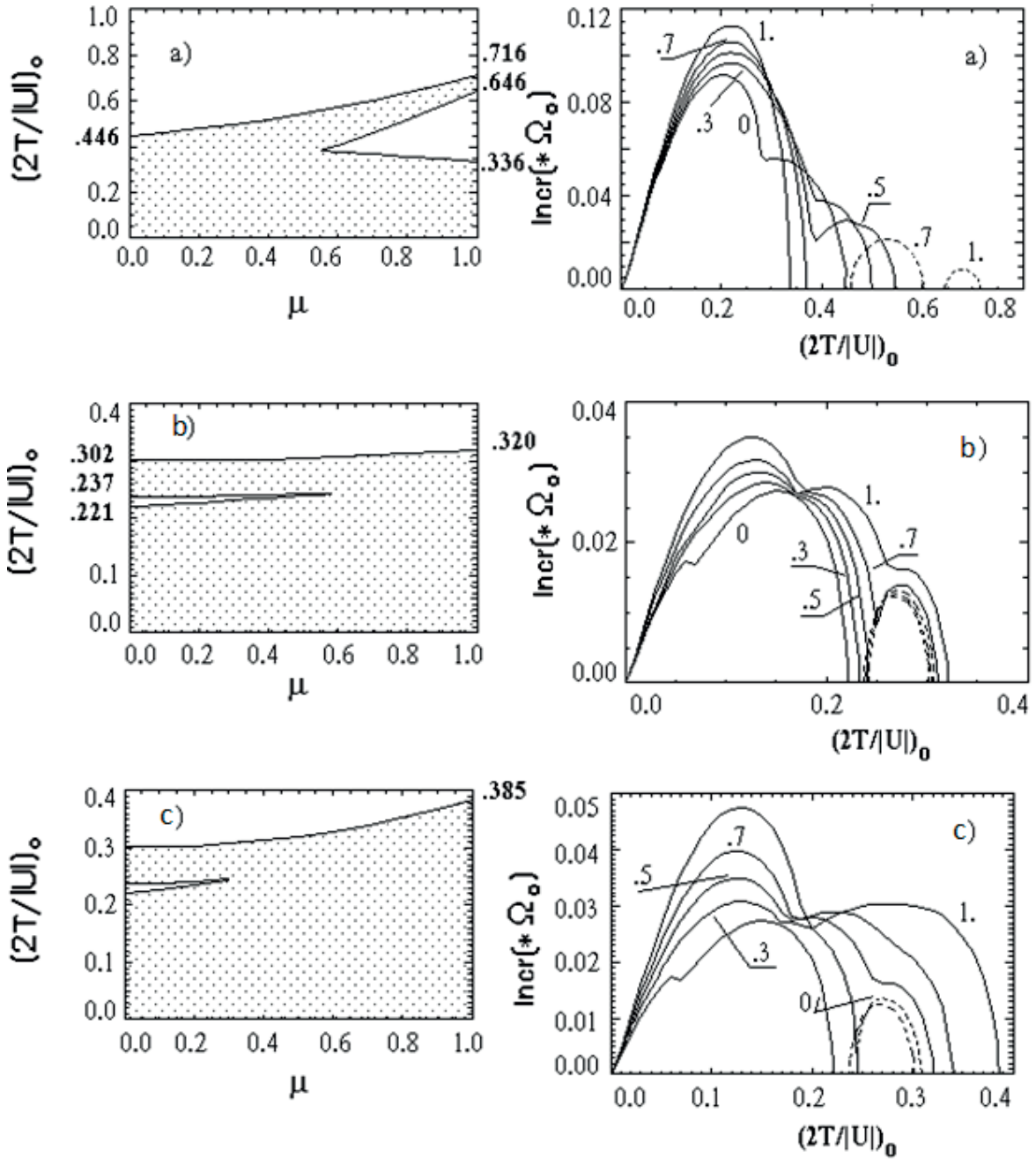

Fig. 13 Critical dependences of the initial virial ratio and dependences of the instability increments for a) egg-shaped and b, c) annular modes (m=1, m=2).

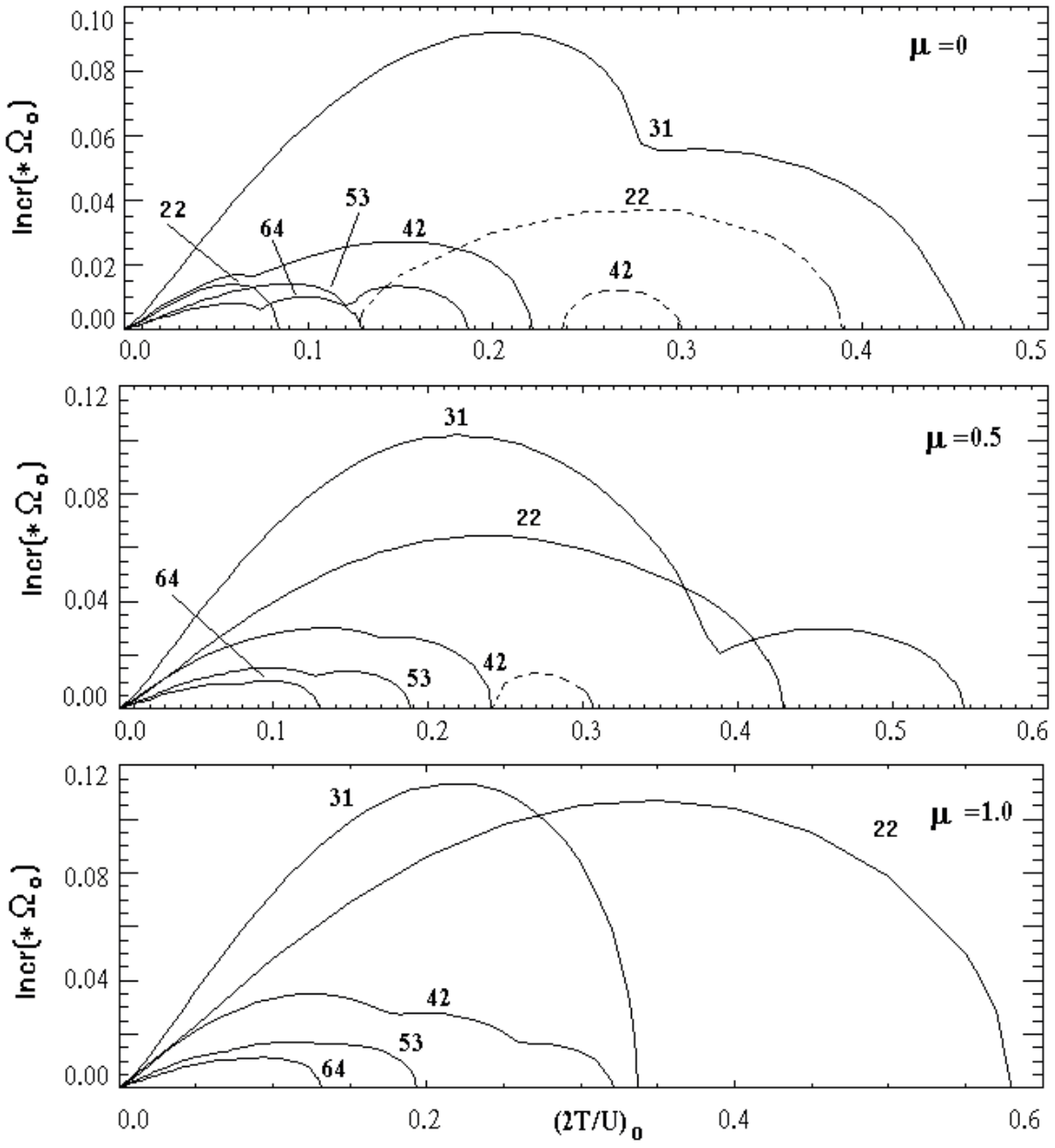

Fig. 14a. Comparison of volumetric mode increments at the minimum azimuthal wavenumber m=1. The numbers next to the curves indicate the order of the mode.

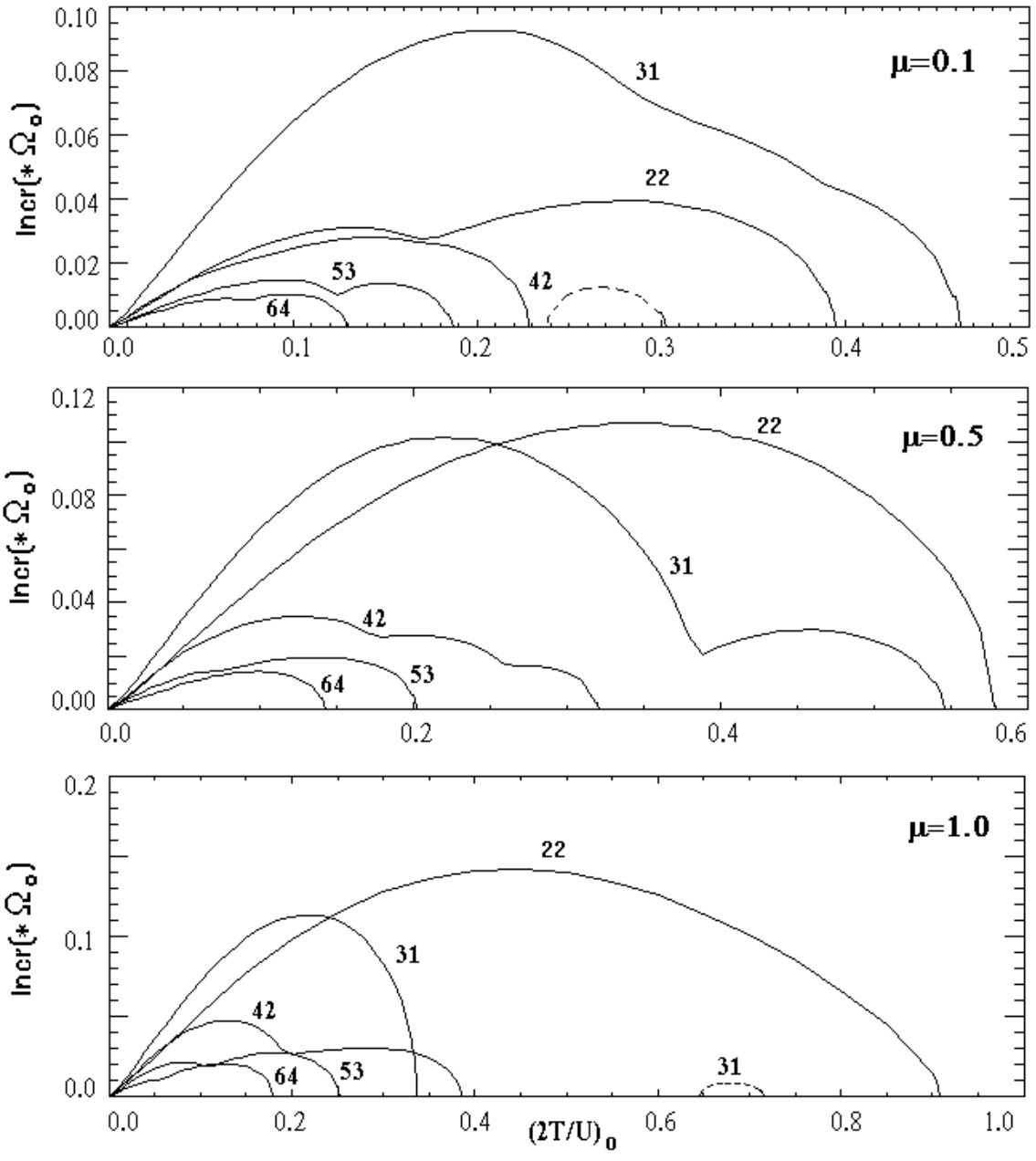

Fig. 14b. Comparison of volumetric mode increments at the maximum azimuthal wavenumber m=N. The numbers next to the curves indicate the order of the mode.

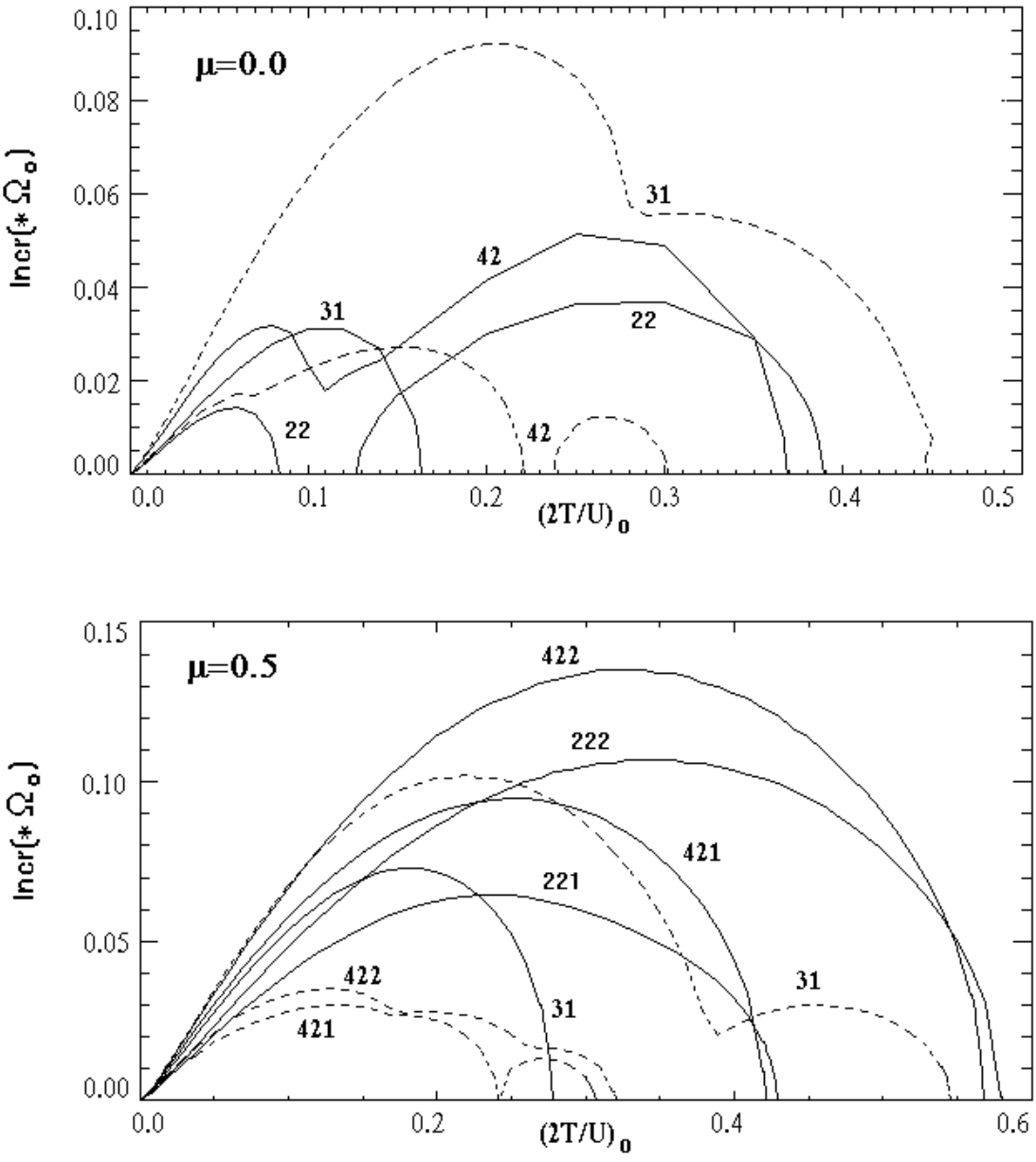

Fig.15. Comparison of increments of volume modes of nonequilibrium versions of Einstein balls (solid lines) and Camm balls (dashed line). The numbers next to the curves indicate the order of the mode Nn (Nnm).

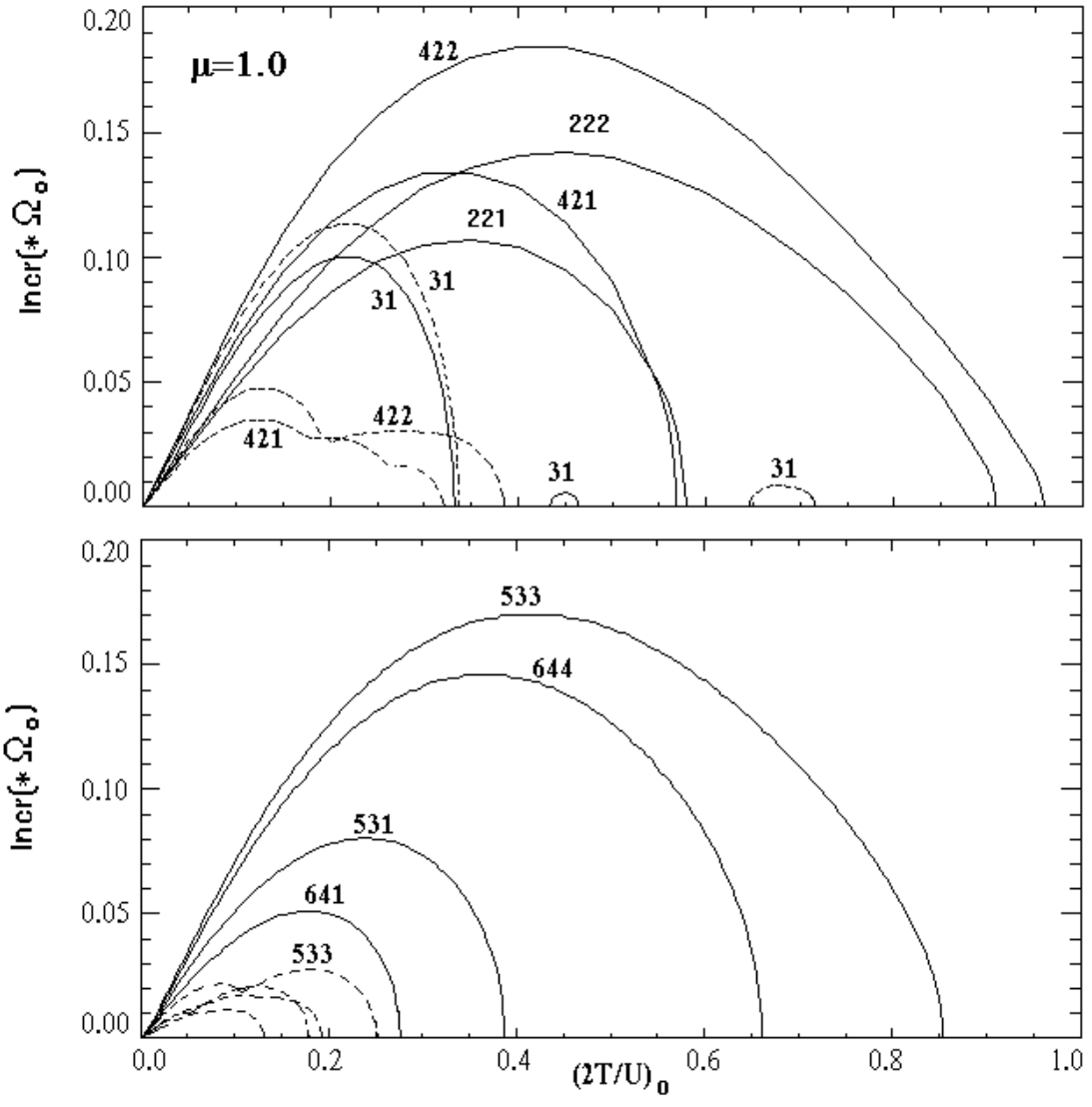

Fig. 15. Continuation

CHAPTER IV. INSTABILITY OF PURE RADIAL MOTIONS IN NON-STATIONARY MODELS

§ 15. On the problem and the perturbation nature

From the analysis of the problems and results of the previous chapters, it follows that the considered nonlinear models with a pulsation amplitude $\lambda=1$ are a special case, since then the system consists of purely radially moving particles and lose their meaning, at least, concepts like the pulsation period $P(\lambda)$ and averaging over it. This is on the one hand, and on the other hand, at $\lambda\to1$, the virial parameter $\left(2T/|U|\right)_0$ characterizing the initial state tends to zero and, accordingly, the increments of various instabilities (see Fig. 5) almost merge with each other and behave in a somewhat complicated way, which does not allow a clear preference for any of them. Finally, this case is also of particular interest for Newtonian cosmology and may find its application in questions of evolution, for example, of dust clouds, clusters of galaxies, and some subsystems of the galaxies themselves. Note that in theoretical terms, if we are limited to the Newtonian approximation, most authors were interested mainly in either stationary models from radially moving orbits [63], or collapsing ones, but mainly with infinite dimensions [41, 8], not counting some works on numerical experiment for interstellar clouds, which are only similar in nature to the topic discussed here. Thus, the instability of purely radial motions, which has long been known in cosmology, also becomes important for systems with a finite size. As noted above, for the first time the existence of such an instability in the theory of stability of stationary systems was partially indicated in [64], and it was proved exactly for the first time by Antonov [63], then by Polyachenko [65]. It should be emphasized that if the original collisionless model consists of only radial orbits and does not change its size in time, then it is Jeans unstable with exponential behavior. An example is the Agekyan model [66]. If, on the other hand, a system consisting only of radially moving particles expands or collapses due to non-observance of the virial theorem, then such a collisionless model takes a completely opposite position compared to the previous one. As will be seen from the results of this chapter, in the latter case there is also instability, but it is always of a power-law nature. In this case, the exponent certainly depends on the initial model and perturbation parameters, and therefore it can differ greatly from the classical case studied by Bonnor [67].

Let us begin our analysis of the problem by studying the stability of a non-stationary model with phase density (1.74). Let $\delta\Phi$ again mean the perturbation of the potential, and δx, δy, δz are the displacements of the particle that occupied the

position (x, y, z) at φ=0 (t=0). Obviously, these displacements depend not only on φ, but also on the position of this point. Taking into account the potential $\delta\Phi$ of a small perturbation on the right side of equation (1.69) and the transition from t to φ leads us to the equation

$$(1+\cos\psi)\frac{\partial^2 \delta\vec{r}}{\partial\psi^2}+\sin\psi\frac{\partial^2 \delta\vec{r}}{\partial\psi^2}+\delta\vec{r}=\frac{1}{g^2}(1+\cos\psi)^3\frac{\partial\delta\Phi}{\partial\vec{r}},\quad\left[g=\left(\frac{8GM}{R_0^3}\right)^{1/2}\right]. \tag{4.1}$$

Note that equation (4.1) is similar in form to (2.3) for λ=1, but the right side of (2.3) contains a singularity in the denominator. Here we have eliminated this feature by deriving (4.1) independently on the basis of § 4.

Before proceeding to the solution (4.1) for a given form $\delta\Phi$, let's pay attention to the trivial, so-called "permutation" type of perturbation. For this, let, in particular, the displacements $\delta\vec{r}$ be such that the density distribution does not change, i.e., $\mathrm{div}\left(\delta\vec{r}\right)=0$. We also require that the boundaries be preserved, namely, when $r^2=R_0^2$

$$x\delta x+y\delta y+z\delta z=0.$$

Then the solution of equation (4.1) has the form

$$\delta\vec{r}=\cos^2(\psi/2)\delta_1\vec{r}+\sin\psi\delta_2\vec{r}, \tag{4.2}$$

where the vectors $\delta_1\vec{r}$ and $\delta_2\vec{r}$ describe the contribution from the perturbation and are constant in time. When the above two conditions for (4.2) are satisfied, we can assume that self-consistency of the type is achieved when the particles are displaced, but the total field does not change. The two conditions specified for this can be written in terms of $\delta_1\vec{r}$ and $\delta_2\vec{r}$ as follows

$$\operatorname{div}_r \delta_1 \vec{r} = \operatorname{div}_r \delta_2 \vec{r} = 0, \quad \vec{r}\,\delta_1 \vec{r} = \vec{r}\,\delta_1 \vec{r} = 0, \quad \left(\left| \vec{r} \right| = R_0 \right). \qquad (4.2')$$

We note that permutation perturbations have no physical meaning in reality, but they must be able to isolate them when analyzing solutions of equations for perturbations in individual problems.

Let us pass to perturbations of a general form. We represent the initial vector $\delta_1 \vec{r}$ as the sum of $\left(\delta_1 \vec{r}\right)_0$ satisfying (4.2) and another vector $\tilde{\delta}_1 \vec{r}$ that is the gradient of some function $\theta(x,y,z,\varphi)$, i.e., $\tilde{\delta}_1 \vec{r} = \operatorname{grad}\theta$. Substituting $\left(\delta_1 \vec{r}\right)_0 = \delta_1 \vec{r} - \tilde{\delta}_1 \vec{r}$ in (4.2) gives

$$\Delta\theta = \operatorname{grad}_r \delta_1 \vec{r}, \quad R_0 \frac{\partial \theta}{\partial r} = x\left(\delta_1 \vec{r}\right)_x + y\left(\delta_1 \vec{r}\right)_y + z\left(\delta_1 \vec{r}\right)_z, \qquad (4.3)$$

where Δ is the Laplace operator. Therefore, the definition of the function θ is the well-known Neumann problem, and the condition for its solvability, by virtue of (4.3), is automatically satisfied.

We perform a completely similar construction for the vector $\delta_2 \vec{r}$. As a result, an arbitrary perturbation (at t=0) splits into two parts: 1) the “trivial” or “permutable” part, which does not violate the density and therefore splits into perturbations of individual particles; 2) the “potential” part, for which, in particular, $\delta_1 \vec{r} = \partial\theta \big/ \partial \vec{r}$. For the second part, due to self-gravity, the laws of evolution will already be different, $\delta_1 \vec{r}$ and $\delta_2 \vec{r}$ now depend on ψ, but retain the meaning of the initial conditions, i.e., φ=0, according to (4.2).

$$\delta_1 \vec{r} = \delta \vec{r}, \quad \delta_2 \vec{r} = \partial\left(\delta \vec{r}\right) \big/ \partial\psi \quad (\psi = 0). \qquad (4.4)$$

Consideration of the general evolution equation (4.1) shows that conditions (4.2) and (4.4) will be satisfied all the time, and not only for $\psi = 0$, if $\delta_2 \vec{r} = \partial^2 \theta / \partial \psi^2$. Then the evolution equation for small perturbations (4.1) takes the form

$$\left(1 + \cos\psi\right)\frac{\partial^2 \theta}{\partial \psi^2} + \sin\psi \frac{\partial \theta}{\partial \psi} + \theta = 2 \cdot \frac{\left(1 + \cos\psi\right)^2}{g^2} \cdot \delta\Phi \ . \qquad (4.5)$$

Since the system is limited and homogeneous, then, as in the previous chapters, it is necessary to further distinguish again two types of perturbations: “surface” and “volumetric”.

§ 16. Instability of purely radial motions in non-stationary model

II.1. We begin our consideration with surface perturbations. Due to spherical symmetry, it is sufficient to describe them in the form

$$\theta = A_0(\psi) \cdot (x + iy)^n, \quad (n = 1,2,...) \ . \qquad (4.6)$$

In this case, the density perturbation proportional to $\Delta\theta$ vanishes and only the perturbation of the outer surface remains. Since $\delta \vec{r} = \partial\theta / \partial \vec{r}$, then the offset value

$$\delta \vec{r} = \frac{x}{R_0} \cdot \delta x + \frac{y}{R_0} \cdot \delta y + \frac{z}{R_0} \delta z = \frac{n}{R_0} \cdot \theta \ . \qquad (4.7)$$

taking into account (4.6). It is easy to show that a layer with surface density

$$\rho(t)\delta r = \frac{n}{R_0}\cdot\rho(t)(x+iy)^n A_0(\psi)\,. \qquad (4.8)$$

corresponds to the internal potential

$$\delta\Phi = \frac{3n}{2n+1}\cdot\frac{GM}{R_0R^2}\cdot(x+iy)^n A_0(\psi)\,. \qquad (4.9)$$

Substituting (4.6) and (4.9) into (4.5), we obtain

$$(1+\cos\psi)\cdot\frac{d^2A_0}{d\psi^2}+\sin\psi\cdot\frac{dA_0}{d\psi}-\frac{n-1}{2n+1}\cdot A_0(\psi)=0\,. \qquad (4.10)$$

Passing from ψ to a new variable $\tilde{\psi}=\mathrm{tg}(\psi/2)$, we have

$$\frac{1}{2}\cdot\frac{d}{d\psi}\left[\left(1+\tilde{\psi}^2\right)\cdot\frac{dA_0}{d\tilde{\psi}}\right]+\tilde{\psi}\cdot\frac{dA_0}{d\tilde{\psi}}-\frac{n-1}{2n+1}A_0=0\,. \qquad (4.11)$$

Further, counting $A_0=d\tilde{A}_0/d\tilde{\psi}$ and integrating equation (4.11) once, we reduce it to the following form:

$$\frac{d}{d\tilde{\psi}}\left[\left(1+\tilde{\psi}^2\right)\cdot\frac{dA_0}{d\tilde{\psi}}\right]-\frac{6n}{2n+1}\cdot\tilde{A}_0=0\,. \qquad (4.12)$$

Finally, if we pass from $\tilde{\psi}$ to $i\tilde{\psi}$, then (4.12) takes the form of an equation for the Legendre function. In this case, except for the case of a trivial displacement of the system as a whole (n=1), for other n>1 the index of the Legendre function is non-integer. Then the solution of equation (4.12) in the form of Legendre functions

of the 1st and 2nd kind on the real axis $\tilde{\psi}$ has a singularity $\tilde{\psi}=\infty$, which corresponds to the value and $\psi=\pi$ can lead to power-law instability, i.e., it is necessary to check the asymptotics.

First, it is important to note the following. Earlier, in [75], we obtained, in particular, equation (4.12) and the result on power-law instability by direct analysis of the NDE of surface fluctuations of pulsating models (1.29) and (1.50) at $\lambda=1$, since in this particular case both nonlinear models behave in exactly the same way. Indeed, for example, substituting $\lambda=+1$ into (2.37) and (2.38), we have $\cosh=1$, $P_{n-1}(\cosh)=1$,

$$a_0(\psi)=\frac{3n}{2n+1}\cdot\int_{-\infty}^{\psi}a_0(\psi_1)\cdot S\cdot W^{n-4}d\psi_1 \ . \qquad (4.13)$$

what does the differential equation correspond to

$$\Lambda a_0(\psi)=\frac{3n}{2n+1}\cdot a_0(\psi) \ . \qquad (4.14)$$

Hence, taking into account the form of the operator Λ for $\lambda=1$, we arrive at the equation for $a_0(\psi)$ in the form (4.10). This means that the results for the model (1.29) coincide. And for the model (1.38) one should consider the NDE (3.11). Since for $\cosh=1$ we have $dP_n/d(\cosh)=n(n+1)$, (3.11) for $\lambda=1$ takes the form (4.13), which was required to be shown.

On the basis of the results obtained, it is not difficult to find an asymptotic law for the growth of the perturbation near the collapse moment t_0. To do this, we will carry out a linearization everywhere, considering $\psi=\pi-\delta\psi$, where $\delta\psi<<1$. Then we have

$$\delta\psi\propto(t_0-t)^{1/3},\quad R(t)\propto(t_0-t)^{2/3} \ . \qquad (4.15)$$

If we accept that in (4.12)

$$\frac{6n}{2n+1} = \nu(\nu+1), \qquad \nu > 0 \ . \tag{4.16}$$

then, according to (4.6), (4.7), (4.12) and (4.15), the growth law of surface perturbations near the moment has the form

$$\frac{1}{R} \cdot \delta r_\infty (t_0 - t)^{-(\nu+1)/3} \ . \tag{4.17}$$

For example, ellipsoidal fluctuations with n=2 correspond to $\nu \cong 1.128$, and the exponent in (4.17) is -0.709. From (4.16) it also follows that for $n \to \infty$ the value is $\nu \to 1.303$. **Result (4.17) is not found in the literature, although it may be of some interest, for example, for dust clouds or clusters of galaxies.**

II.2. We now turn to a discussion of volumetric fluctuations. To consider perturbations violating spatial homogeneity, it suffices to generalize (4.6) as follows:

$$\theta = (x+iy)^n [A_0(\psi) + (x^2+y^2+z^2)^k \cdot A_k(\psi)] \ . \tag{4.18}$$

(κ=1,2,…). Then the radial displacement of the particle

$$\delta r = \frac{(x+iy)^n}{R_0} \cdot \left[n A_0(\psi) + (n+2k) r^{2k} A_k(\psi) \right] . \tag{4.19}$$

while the volume density perturbation

$$\delta\rho = -\frac{4k\rho}{1+\cos\psi} \cdot (2n+2k+1) \cdot (x+iy)^n \cdot A_k(\psi) \ . \tag{4.20}$$

The equation for the perturbation of the potential has the form

$$\Delta\delta\Phi=-2\pi G\rho(1+\cos\psi)\cdot\Delta\theta\ . \qquad (4.21)$$

Internal and external potentials, respectively, are equal

$$\delta\Phi_i=-2\pi G\rho(1+\cos\psi)\theta+\ \tilde{k}_i R^{-n}(x+iy)^n\ , \qquad (4.22)$$

$$\delta\Phi_e=\tilde{k}_e R^{n+1}(x+iy)^n\cdot r^{-(2n+1)}\ , \qquad (4.23)$$

where $\tilde{k}_e$ and $\tilde{k}_i$ are some functions of ψ. The continuity condition for the potential at the boundary gives

$$\tilde{k}_e = \tilde{k}_i - 2\pi\pi G\rho R_0^n(1+\cos\psi)\cdot[A_0(\psi)+R_0^{2k}A_k(\psi)]. \qquad (4.24)$$

Therefore, the internal perturbation potential is equal to

$$\delta\Phi_i = \frac{3}{2}g^2(1+\cos\psi)^{-2}\left[-\frac{n}{2n+1}\cdot A_0(\psi)+\left(\frac{n+1}{2n+1}\cdot R_0^{2k}-r^{2k}\right)A_k\right]\cdot(x+iy)^n. \qquad (4.25)$$

Substituting (4.18) and (4.25) into (4.5), we find the following two equations:

$$(1+\cos\psi)\cdot\frac{d^2A_0}{d\psi^2}+\sin\psi\frac{dA_0}{d\psi}-\frac{n-1}{2n+1}\cdot A_0 = -\frac{3(n+1)}{2n+1}\cdot R_0^{2k}A_k\ . \qquad (4.26)$$

$$(1+\cos\psi)\cdot\frac{d^2A_k}{d\psi^2}+\sin\psi\frac{dA_k}{d\psi}-2\cdot A_k=0\ . \qquad (4.27)$$

The first of them confirms that in (4.18) it was impossible to ignore the term with $A_0(\psi)$. Equation (4.27) has the following general solution (see, for example, [23]):

$$A_\kappa(\psi)=c_{1\kappa}\cdot tg(\psi/2)+c_{2\kappa}\cdot[3\psi\cdot tg(\psi/2)-\cos\psi+5]\ , \qquad (4.28)$$

where c_{1k} and c_{2k} are arbitrary constants. Analysis of (4.26) with allowance for (4.28) shows that

$$A_0(\psi)=-R_0^{2k}\cdot A_\kappa(\psi)\ . \qquad (4.29)$$

and therefore

$$\theta=(x+iy)^n\cdot(r^{2\kappa}-R_0^{2k})\cdot A_\kappa(\psi)\ . \qquad (4.30)$$

This shows that in the case of volume perturbations on the surface $r=R_0$, the tangent part of the displacement vanishes.

Result (4.28) should also follow from the analysis of the NDE of volume perturbations of pulsating models. Indeed, substituting $\lambda = 1$, cosh =1, for example, in NDE (3.44), we have $dP_N/d\cosh = N(N+1)/2$ and

$$a_0(\psi)\cdot\pi^3(\psi)=3\cdot\int_{-\infty}^{\psi}W^{-1}\cdot a_0(\psi_1)\cdot S\cdot\pi^3(\psi_1)d\psi_1\ . \qquad (4.31)$$

From this follows the equation

$$(1+\cos\psi)\cdot\frac{d^2a_0}{d\psi^2}+\sin\psi\frac{da_0}{d\psi}-a_0=3a_0(\psi)\ . \qquad (4.32)$$

As can be seen, we have obtained an equation in the form (4.27) and, consequently, the solution for $a_0(\psi)$ will have the form (4.28).

Volume perturbations in the collapsing model, as well as surface perturbations, are unstable according to a power law. Using linearization (4.15), we find that

$$A_0(\psi) \propto A_k(\psi) \propto \delta r \propto (t_0 - t)^{-1/3} . \qquad (4.33)$$

Further, since $\rho \propto (t_0 - t)^{-2}$, the volume density perturbation

$$\delta\rho \propto (t_0 - t)^{-3} . \qquad (4.34)$$

and the rate of development of the perturbation does not depend on the indices n and k. This was also true for those small-scale perturbations with which Newtonian cosmology operates. Indeed, (4.34) coincides with the result known for the case of a shrinking infinite model of the Universe [41]. It is interesting to compare the particle displacements δr of the two types of perturbations considered. As can be seen from the comparison of (4.17) and (4.34), taking into account (4.15), for $n \geq 1$, the value of δr is always greater in the case of volume fluctuations than in the case of surface fluctuations.

§ 17. Instability of the cosmological expansion, attached to an Einstein ball with rotation

We are talking about the behavior of the process of unlimited expansion for a self-gravitating model with a finite volume in the Newtonian approximation. Let us analyze the instability of the expanding model with rotation (1.78). As we saw in the previous section, in such cases it suffices to study the general NDE for the corresponding approximation in λ. And when constructing the nonlinear model (1.78), we assumed that $\lambda = -[1-(\delta\lambda)^2]^{1/2} \approx -1+(\delta\lambda)^2/2$, and revealed the existing features in the NDE of the pulsating model. Similarly, and taking into account (1.77), in particular, we find that

$$\cosh = \frac{(1-\psi^2)(1-\psi_1^2+4\psi\psi_1)}{(1+\psi^2)(1+\psi_1^2)}, \qquad \sinh = 2\cdot\frac{(1-\psi^2)\psi_1-\psi(1-\psi_1^2)}{(1+\psi^2)(1+\psi_1^2)} \tag{4.35}$$

Based on the results of the previous chapters, it can be seen that further we can restrict ourselves to the study of the two largest fluctuation modes: ellipsoidal (N=n=2) and dipole-odd modes (or, in particular, “egg-shaped” with N=3 and N=1).

The considered model expands all the time and, therefore, taking into account (1.77) at $t\to\infty$, $\psi\to\infty$ and the radius $R\to\infty$. Therefore, below we will be interested in the asymptotic behavior of perturbations at $\psi\to\infty$. Here we study the case of ellipsoidal perturbations, and in the next section we consider “egg-shaped” perturbations in order to compare the growth rates of deviations.

Substituting (1.77) and (2.111) and deriving the notation

$$L_\tau(\psi) = \int_{-\infty}^{\psi} \psi_1^{1-\tau}(1-\psi_1^2)^\tau\, a_0(\psi_1)\cdot S\cdot\left[\frac{1+\psi_1^2}{1+\psi^2}\right]^3 d\psi_1 \tag{4.36}$$

(τ=0 ;1), we get the following two equations

$$\Lambda L_0 = \frac{6\psi}{5\left(1+\psi^2\right)^2}\cdot L(\psi), \qquad \Lambda L_1 = \frac{6\left(1-\psi^2\right)}{5\left(1+\psi^2\right)^2}\cdot L(\psi). \tag{4.37}$$

where the operator:

$$\Lambda = \frac{1+\psi^2}{2}\cdot\frac{d^2}{d\psi^2} - \psi\cdot\frac{d}{d\psi} + 1 \tag{4.38}$$

and the function

$$L(\psi) = (1-\psi^2)L_1 + 4\psi L_0 + \frac{im}{2}\cdot\mu\cdot\left[(1-\psi^2)L_0 - 4\psi L_1\right] \tag{4.39}$$

The system of differential equations of the 4th order (4.37) must have only four pairs of solutions in L_0 and L_1. To find them, we first assume that the functions L_0 and L_1 have the same order as $\psi\to\infty$. Then (4.37), taking into account (4.39), takes the form

$$\Lambda_\psi L_\tau \equiv \frac{\psi^2}{2}\cdot\frac{d^2 L_\tau}{d\psi^2} - \psi\cdot\frac{dL_\tau}{d\psi} + L_\tau = \frac{6}{5}\cdot\left(L_1 + \frac{im}{2}\cdot\mu L_0\right)(-\psi)^{\tau-1} \qquad (4.40)$$

Comparing the equations in (4.40) with $\tau=0$ and $\tau=1$ with each other, we conclude that L_0 and L_1 can have the same order, unless

$$L_1(\psi) + \frac{im}{2}\cdot\mu L_0(\psi) = 0 \qquad (4.41)$$

Under the condition that (4.41) is satisfied, the equations in (4.40) have the following two pairs of solutions

$$L_{\tau 1}(\psi) = \ell_\tau\,\psi, \qquad L_{\tau 2}(\psi) = \tilde{\ell}_\tau\,\psi^2 \qquad (4.42)$$

which are, respectively, the highest terms in two pairs of solutions of the original system of equations (4.37), the coefficients ℓ_τ and $\tilde{\ell}_\tau$ satisfy the relations

$$\ell_1 + \frac{im}{2}\cdot\mu\,\ell_0 = 0, \qquad \tilde{\ell}_1 + \frac{im}{2}\cdot\mu\,\tilde{\ell}_0 = 0. \qquad (4.43)$$

To complete the “picture”, solutions (4.42) should be generalized in the form:

$$L_{\tau 1} = \ell_\tau\,\psi + p_{\tau 0} + p_{\tau 1}\cdot\frac{1}{\psi} + p_{\tau 2}\cdot\frac{1}{\psi^2} + \ldots, \qquad (4.44)$$

$$L_{\tau 21} = \tilde{\ell}_\tau\,\psi^2 + c_\tau\psi + b_{\tau 1}\cdot\frac{1}{\psi} + \ldots, \qquad (4.45)$$

Substituting (4.43) into (4.37) and equating the coefficients at the same powers of ψ, we find the unknown constants $p_{\tau i}$ from the relations

$$p_{01} = \frac{2}{5}\cdot\left(4\ell_0 - p_{10} - 2\,im\mu\,\ell_1\right), \quad p_{10} = \frac{6}{11}\cdot\left[\frac{im}{2}\cdot\mu\left(p_{02} + 4\ell_1\right) - 4\ell_0\right],$$
$$p_{11} = \frac{im}{3}\cdot\mu\left(p_{01} + 4p_{10}\right), \quad p_{02} = -\frac{1}{5}\cdot\left[p_{11} + \frac{im}{2}\cdot\mu\left(p_{01} + 4p_{10}\right)\right] \tag{4.46}$$

and so on, and $P_{00}=0$. A separate substitution of (4.45) into (4.37) gives, in particular, the following unknowns

$$c_1 = 4\tilde{\ell}_0 - \frac{im}{2}\cdot\mu(c_0 + 4\tilde{\ell}_1), \qquad b_{00} = \frac{6}{5}\cdot[4\tilde{\ell}_0 - c_1 - \frac{im}{2}\cdot\mu(c_0 + 4\tilde{\ell}_1)],$$

$$b_{01} = \frac{2}{5}\cdot[4\,c_0 - b_{10} - \frac{im}{2}\cdot\mu(b_{00} + 4\,c_1)], \qquad b_{10} = 6\cdot[4\,c_0 - \frac{im}{2}\cdot\mu(b_{00} + 4\,c_1)],$$

$$b_{02} = \frac{1}{5}\cdot[3\,c_1 + 4\,c_0 - 8\tilde{\ell}_0 + 4\,b_{00} - b_{11} + \frac{im}{2}\cdot\mu(3\,c_0 - 4\,b_{10} - b_{01} + 8\tilde{\ell}_1)],$$

$$b_{11} = -2\cdot[4(c_0 + c_1 + b_{00} - 3\tilde{\ell}_0) + \frac{im}{2}\cdot\mu(4\,c_0 - b_{01} - 4\,b_{10} + 12\tilde{\ell}_1)]. \tag{4.47}$$

It remains to find two more pairs of solutions to system (4.37). To do this, according to the nature of the equations in (4.37), it is necessary to consider the case when the functions $L_0(\psi)$ and $L_1(\psi)$ have different orders in ψ, exact $L_1/L_0 \to\infty$ as $\psi\to\infty$. Then for $\psi\to\infty$ from (4.37) we have

$$\Lambda_\psi L_0 = -\frac{6}{5\,\psi}\cdot L_1, \qquad \Lambda_\psi L_1 = \frac{6}{5}\cdot L_1\,. \tag{4.48}$$

The second equation is rewritten as

$$\frac{1}{2}\cdot\psi^2\,\frac{d^2L}{d\psi^2} - \psi\cdot\frac{dL}{d\psi} - \frac{1}{5}\cdot L_1 = 0 \tag{4.49}$$

and is solved by the assumption $L_1(\psi) = c\psi^\kappa$. From here we find $k_1 = 3.1279$, $k_2 = -0.1279$, and c is an arbitrary constant. Therefore, from (4.48) we have

$$L_0(\psi) = 12c\psi^{\kappa_1^{-1}} / [5(3-k)(k-2)] \qquad (4.50)$$

The last two pairs of solutions are supplemented by subsequent terms by analogy with (4.44) and (4.45), and then the unknown constants are easily found from (4.37). As a result, we obtain four pairs of independent solutions to the system of equations (4.37). For each pair $L_\tau(\psi)$ there is its own expression for the function $a_0(\psi)$ and the perturbation of the potential is defined as follows:

$$a_0(\psi) = \frac{6}{5\left(1+\psi^2\right)^2}\left\{\left(1-\psi^2\right)L_1(\psi) + 4\psi L_0(\psi) + \frac{im\mu}{2}\left[\left(1-\psi^2\right)L_0 - \psi L_1\right]\right\},$$
$$\delta\Phi_{22} = \frac{r_0^2 a_0(\psi)}{4}\cdot\left(1+\psi^2\right)^2\cdot e^{im\varphi}\cdot P_2^m(\cos\theta), \qquad (4.51)$$

where $r(\psi) = \Pi(\psi)r_0$ is taken into account. From (4.51), taking into account the above solutions, it follows that for $\psi \to \infty$, the perturbation of the potential behaves as

$$\delta\Phi_{22} \propto \psi^{k_1+2} \propto t^{\left(k_1+2\right)/3} \qquad (4.51')$$

In a similar way, one can analyze and find the corresponding expression $\delta\Phi$ for model (1.78) in the case of dipole-odd fluctuation modes, when m=1, and N takes odd values (starting from N = 3). However, in accordance with the results of §15, it is more interesting to compare the growth rates $\delta\Phi$ within the framework of model (1.79), which is a special case of model (1.60). For this model, the results found in this section also remain valid. Therefore, let us pass to the case of the model (1.79).

§ 18. Rotating non-stationary version of the Camm model

The model (1.79) expanding indefinitely from a finite volume is the limiting case for (1.60). Therefore, to analyze stability (1.79), one can proceed from the NDE model (1.60). Since the most important type of surface fluctuations has already been considered in the previous section, below it is sufficient to study the

large-scale mode N = 3, m = 1 based on the NDE of volume fluctuations (3.68). The latter for the above particular case has the form

$$a_0\Pi^3 = \frac{3}{4}\cdot\int_{-\infty}^{\psi} W^2 E\cdot\left[5\cos^2 h - 1 + im\mu\cdot\sinh\cdot\cosh\right]d\psi_1 \qquad (4.52)$$

Substituting here (4.35) and introducing the notation

$$L_\tau(\psi) = \int_{-\infty}^{\psi}\psi_1^{2-\tau}\left(1-\psi_1^2\right)^\tau a_0(\psi_1)\cdot S\cdot\left[\frac{1+\psi_1^2}{1+\psi^2}\right]^3 d\psi_1 . \qquad (4.53)$$

we have

$$\Lambda L_\tau(\psi) = \frac{3\psi^{2-\tau}\left(1-\psi^2\right)^\tau}{\left(1+\psi^2\right)^4}\cdot\tilde{L}(\psi)\quad(\tau=0;1;2) \qquad (4.54)$$

where

$$\tilde{L}(\psi) = \left[(1-\psi^2)^2-\psi^2\right]L_2 + 10\,\psi(1-\psi^2)\,L_1 + \left[16\,\psi^2-(1-\psi^2)^2\right]L_0 +$$

$$+\frac{im}{2}\cdot\mu\cdot\left\{\left[(1-\psi^2)^2-4\,\psi^2\right]L_1 + 4\,\psi(1-\psi^2)\,L_0 - \psi(1-\psi^2)\,L_2\right\} \qquad (4.55)$$

The system of differential equations (4.54) has the sixth order. Therefore, it is necessary to find 6 groups of its solutions. We should be primarily interested in the highest term in ψ for each type of movement. We apply the method used in the previous paragraph, considering at the beginning the case $\psi\to\infty$.

In this case, instead of the system of equations (4.54), we have

$$\Lambda_\psi L_\tau(\psi) = 3(-\psi)^{\tau-2}\left(L_2 - L_0 + \frac{im}{2}\cdot\mu L_1\right) \qquad (4.56)$$

(cp. c (4.40)). This shows that the functions $L_\tau(\psi)$, in particular, can have the same order in ψ if

$$L_2(\psi) - L_0(\psi)\frac{im}{2}\cdot\mu L_1(\psi) = 0 \qquad (4.57)$$

Under this condition (4.56) has solutions of the form (4.42) known to us, i.e.,

$$L_{\tau 1}(\psi) = g_{\tau 1}\psi, \quad L_{\tau 2}(\psi) = g_{\tau 2}\psi^2, \quad (\tau = 0;1;3) \qquad (4.58)$$

According to (4.57), the constants $g_{\tau 1}$ and $g_{\tau 2}$ satisfy the relation

$$g_{21} - g_{01} + \frac{im}{2}\cdot\mu g_{11} = 0, \quad g_{22} - g_{02} + \frac{im}{2}\cdot\mu g_{12} = 0, \qquad (4.59)$$

The subsequent terms following the terms in (4.58) can be easily found from (4.54) by analogy with (4.44) and (4.45).

We find the third and fourth groups of solutions by assuming that the ratios L_2/L_0 and L_2/L_1 tend to infinity as $\psi\to\infty$. Then from (4.56) we obtain the system of equations

$$\Lambda_\psi L_\tau(\psi) = 3(-\psi)^{\tau-2} L_2(\psi)\,. \qquad (4.60)$$

Of these, the equations for $\tau=2$

$$\frac{\psi^2}{2}\cdot\frac{d^2L_2}{d\psi^2} - \psi\cdot\frac{dL_2}{d\psi} - 2L_2(\psi) = 0$$

has solutions

$$L_{23}(\psi) = g_{23}\psi^4, \quad L_{24}(\psi) = g_{24}\psi^{-1} \qquad (4.61)$$

The remaining solutions can be easily found from (4.60) with $\tau=0$ and 1. Further, in exactly the same way, one can obtain the fifth and sixth groups of solutions, assuming that first $L_1(\psi)$ contains a higher degree than other functions, and then it is function $L_0(\psi)$. However, there is no need to waste time on them, so that in (4.61) we have already obtained the solution ($\sim\psi^4$), in which the corresponding perturbation response grows faster than in the case of the bar mode (4.51′).

Indeed, for “egg-shaped” perturbations

$$\delta\Phi_{31} = a_0(\psi)\cdot r^3\cdot e^{i\varphi}\cdot P_1^1(\cos\theta) = a_0(\psi)\left[\frac{1+\psi^2}{2}\right]^3 r_0^3 e^{i\varphi} P_1^1(\cos\theta) \qquad (4.62)$$

where $a_0(\psi)=3L(\psi)/(1+\psi^2)^4$. The solution $L_2\sim\psi^4$, in accordance with (4.55), leads us to the dependence $\widetilde{L}\sim\psi^8$. Substituting all this (4.62), we find

$$\delta\Phi_{31}\sim\psi^6\sim t^2, \qquad (4.63)$$

which is clearly higher in growth rate than (4.51′). Exactly the same result would be obtained if we calculated $\delta\Phi_{31}$ for the model considered in the previous paragraph.

CHAPTER V. ANALYSIS OF INTERMEDIATE STATES BETWEEN NONLINEAR MODELS

§19. Search for New Nonlinear Models: Composite Model

Note that the collapse of protogalaxies before the formation of the galaxies themselves takes a number of stages of globally nonstationary evolution. Unfortunately, these stages are still unknown to anyone. That is why, step by step, it is necessary to build analytically solvable new nonlinear models of individual early stages of the evolution of galaxies. First of all, it would be interesting to build weakly inhomogeneous models, as well as models with a central core, in order to accurately estimate their effect during the collapse. However, this is a very, very difficult task.

On the other hand, we must also study the intermediate states between the nonlinear models constructed above. Therefore, we will conclude this book with a chapter that we will devote to the analysis of the physics of intermediate states between the considered nonlinear models, introducing the concept of a composite configuration. More precisely, we call a composite model an early-stage model whose phase density is (see Chapter 1) a linear superposition of two other non-linear non-stationary rotating configurations (1.38) and (1.60) (hereinafter models 1 and 2):

$$\Psi_s(\vec{r},\vec{v},\mu_1,\mu_2,\lambda,\nu,t)=(1-\nu)\Psi_1(\vec{r},\vec{v},\mu_1,\lambda,t)+\nu\Psi_2(\vec{r},\vec{v},\mu_2,\lambda,t) \tag{5.1}$$

The composite model (5.1) will allow us to explore intermediate states in order to capture the broader possible initial conditions at an early stage at the moment of the beginning of the collapse. It depends, in general, on four parameters: ripple amplitude λ, rotation parameters μ_1, μ_2 and superposition parameter ν. It is not difficult to obtain physical characteristics for the model before the perturbation is applied.

We indicate the following most basic characteristics:

a). The velocity dispersion components:

$$\sigma_r^2=\frac{1}{\rho}\int(\bar{v}_r-v_r)^2[(1-\nu)\Psi_{1\mu_1}+\nu\Psi_{2\mu_2}]d\vec{v}=$$
$$=(1-\nu)\sigma_{1r}^2+\nu\sigma_{2r}^2=\nu\frac{R_0^2\Omega_0^2}{4\Pi^2}\left[1-\frac{r^2}{R^2}\right], \tag{5.2}$$

$$\sigma_{\perp}^2 = \frac{1}{\rho}\int (\bar{v}_{\perp} - v_{\perp})^2 [(1-\nu)\Psi_{1\mu_1} + \nu\Psi_{2\mu_2}]d\vec{v} =$$
$$(1-\nu)\sigma_{1\perp}^2 + \nu\sigma_{2\perp}^2 = \frac{\Omega_0^2}{\Pi^2}\left[\frac{\nu}{2}R_0^2 + (1-\nu)r_0^2\right], \qquad (5.2')$$

The root-mean-square velocity components:

$$\overline{v_r^2} = \frac{1}{M}\int d\vec{r}\int v_r^2[(1-\nu)\Psi_{1\mu_1} + \nu\Psi_{2\mu_2}]d\vec{v} = (1-\nu)\overline{v_{1r}^2} + \nu\overline{v_{2r}^2} =$$
$$= \frac{R_0^2 q^2}{5(1+\lambda\cos\psi)^2}\left[\frac{\nu}{2}(1-\lambda^2) + 3\lambda^2\sin^2\psi\right] \qquad (5.3)$$

$$\overline{v_{\perp}^2} = \frac{1}{M}\int d\vec{r}\int v_{\perp}^2[(1-\nu)\Psi_{1\mu_1} + \nu\Psi_{2\mu_2}]d\vec{v} = (1-\nu)\overline{v_{1\perp}^2} + \nu\overline{v_{2\perp}^2} =$$
$$= \frac{R_0^2 q^2(1-\lambda^2)}{5(1+\lambda\cos\psi)^2}\cdot\frac{6-\nu}{10} \quad . \qquad (5.3')$$

c). The kinetic energy components and their values averaged over the pulsation period:

$$T_r = \frac{M}{2}[(1-\nu)\overline{v_{1r}^2} + \nu\overline{v_{2r}^2}] = \frac{Mq^2R_0^2}{10(1+\lambda\cos\psi)^2}[\frac{\nu}{2}(1-\lambda^2) + 3\lambda^2\sin^2\psi], \qquad (5.4)$$

$$T_{\perp} = \frac{M}{2}[(1-\nu)\overline{v_{1\perp}^2} + \nu\overline{v_{2\perp}^2}] = \frac{Mq^2R_0^2(1-\lambda^2)}{20(1+\lambda\cos\psi)^2}(6-\nu),$$

$$< T_r >= (1-\nu) < T_{1r} > + \nu < T_{2r} >= \frac{Mq^2R_0^2}{20}[6 + (\nu-6)\sqrt{1-\lambda^2}], \qquad (5.5)$$

$$< T_{\perp} >= (1-\nu) < T_{1\perp} > +\nu < T_{2\perp} >= \frac{Mq^2 R_0^2 \sqrt{1-\lambda^2}}{20}(6-\nu),$$

d). The global anisotropy parameter:

$$\widetilde{\Delta}(\lambda) = \frac{2 < T_r >}{< T_{\perp} >} = 2\frac{6+(\nu-6)\sqrt{1-\lambda^2}}{(6-\nu)\sqrt{1-\lambda^2}}. \qquad (5.6)$$

To derive the NDE, we use the same approach described in the previous chapters. As a result, in the case when the phase density function of the composite model is taken in the form (5.1), the NDE is obtained in the form [68]:

$$a(\psi) = (1-\nu)a_1(\psi) + \nu a_2(\psi) \qquad (5.7)$$

§20. Analysis of surface perturbation

In accordance with (5.7), the NDEs of the composite model for individual modes are as follows [68, 69, 34]:

N=3:

$$a(\psi) = \frac{9}{14(1+\lambda\cos\psi)^7}\left[(1-\nu)\Sigma_3(\gamma_\tau) + 0.5\nu K_3(\xi_\tau)\right],$$

N=4:

$$a(\psi) = \frac{1}{3(1+\lambda\cos\psi)^9}\left[(1-\nu)\Sigma_4(\gamma_\tau) + \nu K_4(\xi_\tau)\right],$$

N=5:

$$a(\psi) = \frac{15}{88(1+\lambda\cos\psi)^{11}}\left[(1-\nu)\Sigma_5(\gamma_\tau) + \nu K_5(\xi_\tau)\right],$$

N=6:

$$a(\psi) = \frac{18}{13(1+\lambda\cos\psi)^{13}}\left[(1-\nu)\Sigma_6(\gamma_\tau) + \nu K_6(\xi_\tau)\right],$$

N=8:

$$a(\psi) = \frac{3}{34(1+\lambda\cos\psi)^{17}}\left[(1-\nu)\Sigma_8(\gamma_\tau) + 0.25\nu K_8(\xi_\tau)\right],$$

N=10:

$$a(\psi) = \frac{5}{448(1+\lambda\cos\psi)^{21}}\left[0.5(1-\nu)\Sigma_{10}(\gamma_\tau) + \nu K_{10}(\xi_\tau)\right].$$

Formulas and expressions for functions here in square brackets have a cumbersome appearance and therefore we will not give them. The corresponding expressions were given in detail in [68, 69].

20a. Non-rotating model.

For simplicity, we will consider a special case when the rotation parameters of models 1 and 2 are the same. Since it makes no sense to consider a composite model for the N=2 mode, the results are given for the N=3 modes; four; 5; 6; eight; 10 [68]. Figure 16 shows that the surface modes here also show a qualitative similarity between the critical dependences. All considered modes have an "island" of stability, but now it is quite long and very narrow, extending on average to values $\mu \approx 0.8$. Summing up the calculation results, it can be seen that with the growth of N the following happens:

a) the area of the region of instability decreases, and the width of the "island" also decreases;
b) the length of the "island" of stability gradually, almost imperceptibly, decreases;
c) comparing the values of the increments (Fig. 16), we find that at N=3 models 1 ((ν=0) and 2 ((ν=1) do not differ much in the degree of instability, and starting from N=4 model 1 becomes significantly " more unstable" for all other values of ν.
d) if there are no “islands” of stability or any other features at the boundary values (ν=0 and 1.0, then there are none when considering intermediate states, that is, nothing “by itself” arises.

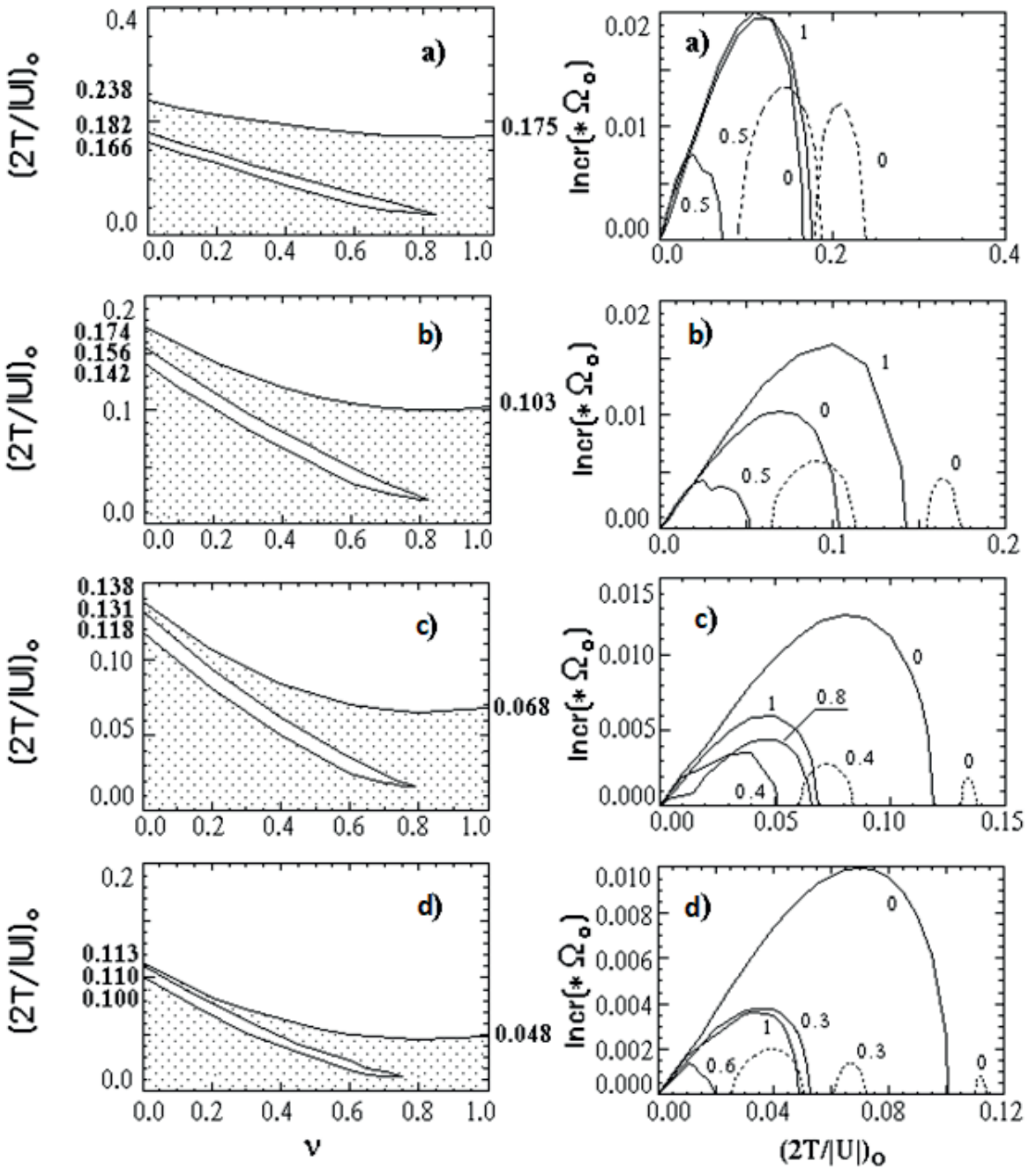

Fig. 16 a. Critical dependences of the initial virial ratio and dependences of the increments of instability of the composite non-rotating model for modes a) N=3, b) 4, c) 5, d) 6, e) 8, f) 10.

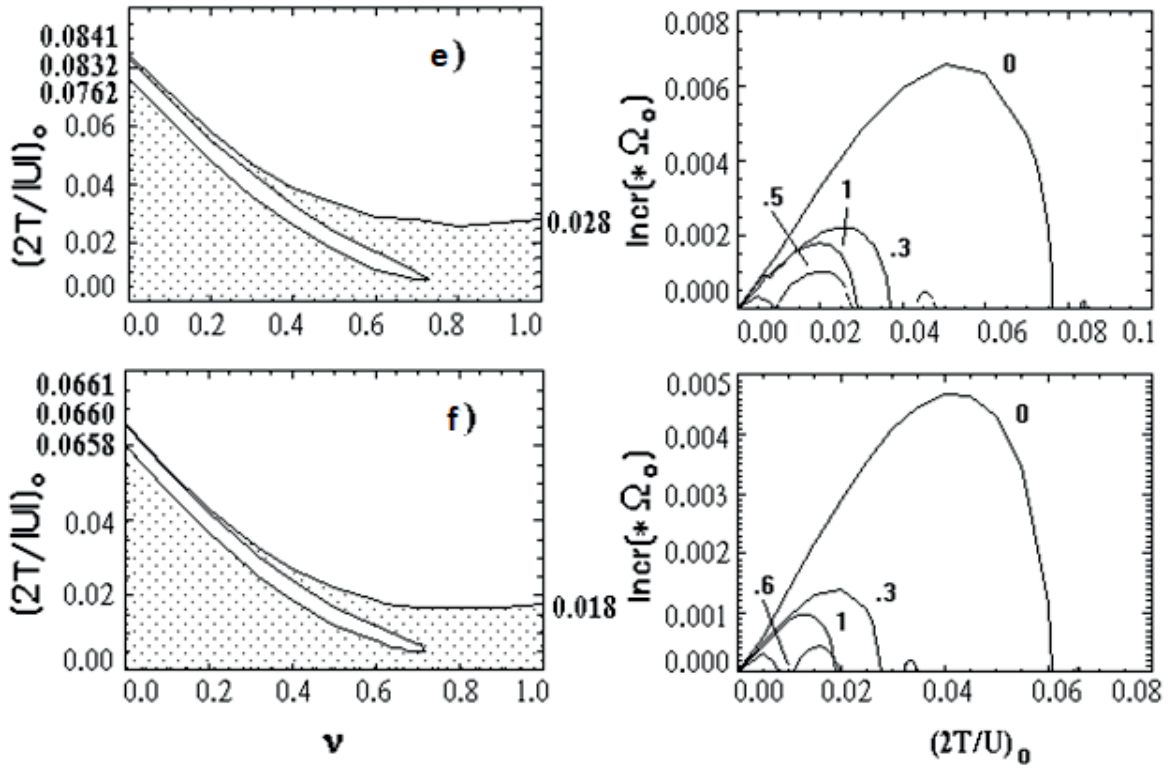

Fig 16 b. Continuation fig. 16 a.

In the bottom Table. 5.1 given the change in the length of the "island" in units of ν.

Tab. 5.1.

N	length of the island in units. ν	N	length of the island in units. ν
3	0.835	6	0.750
4	0.801	8	0.732
5	0.779	10	0.711

In general, turning to the role of the superposition parameter, we note that here there is a fairly smooth transition from model 1 to model 2 without any surprises.

On fig. 17 compares the mode increments for three values of the superposition parameter.

20 b. Rotating model.

The results of calculations of two large modes N=3 and N=4 for individual ones are shown in Figures 18 and 19. Let us formulate the patterns that are found in the study of this composite model (for smaller-scale modes, see the work of Gainullina and Nuritdinov [68]).

(1) For a given mode N:

a) with an increase in the values of the "island", in comparison with the previous case ($\mu = 0$), it becomes even narrower and shorter, until it completely disappears. The value of μ, at which this occurs, is determined by the value μ, up to which the "island" is still observed in model 1.

b) there is a phenomenon that can be seen even when comparing the increments of models 1 and 2, namely: for m<n, model 1 is more "unstable" than model 2 for all values of μ (see, for example, Fig. 18 a ,b); when m=n, as μ approaches 1.0, the instability region at ν=1 (model 2) begins to slightly exceed the unstable region at ν=0 (model 1). This is even better illustrated in Fig. 20.

(2) As the value of N increases, the areas of "unstable" regions decrease, as it was before.

(3) The action of rotation here is also destabilizing everywhere.

(4) The role of the superposition parameter is small: model 1 (ν=0) smoothly passes into model 2 (ν=1).

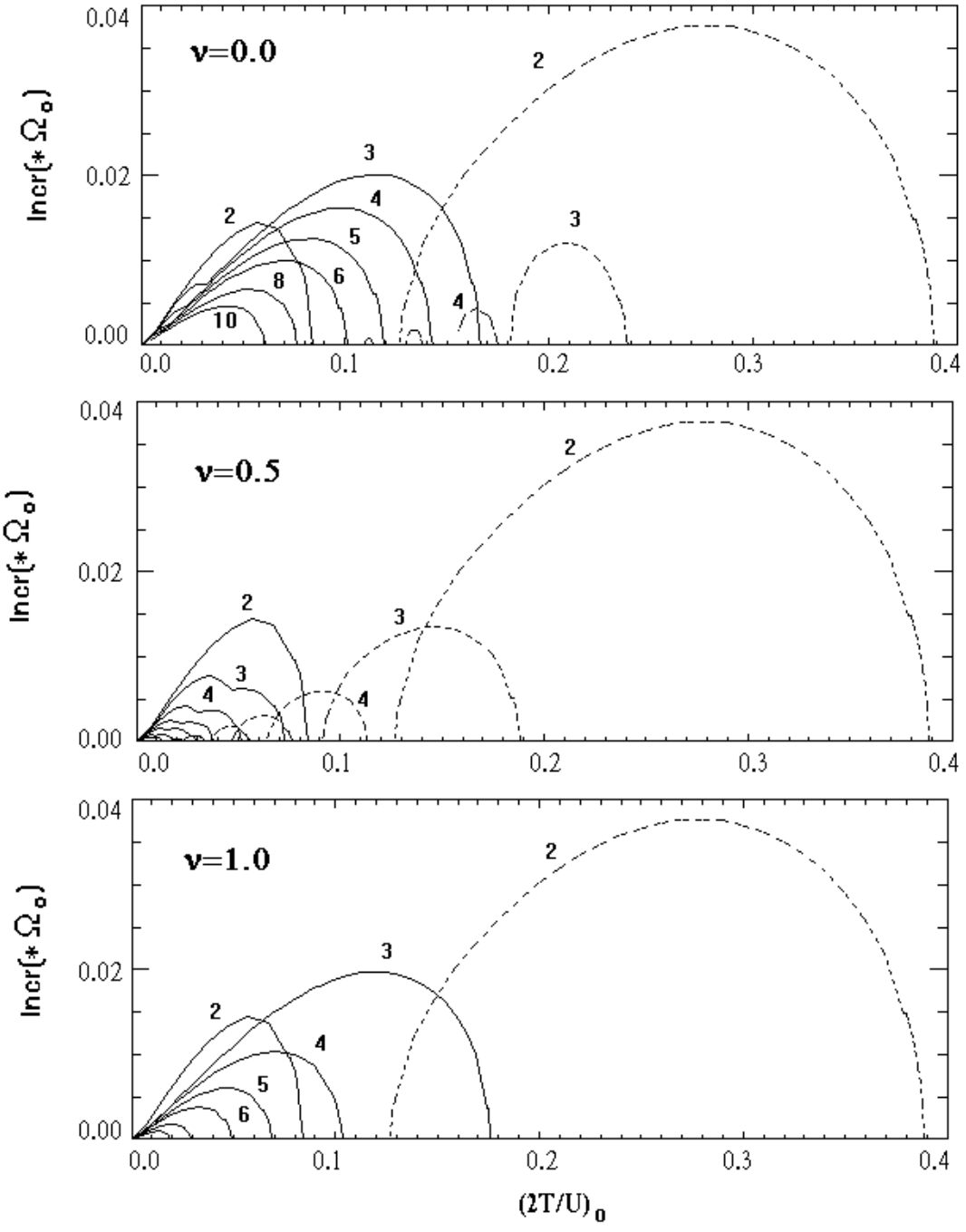

Fig. 17 Comparison of the mode increments of a composite non-rotating model. The numbers next to the curves indicate the mode order N.

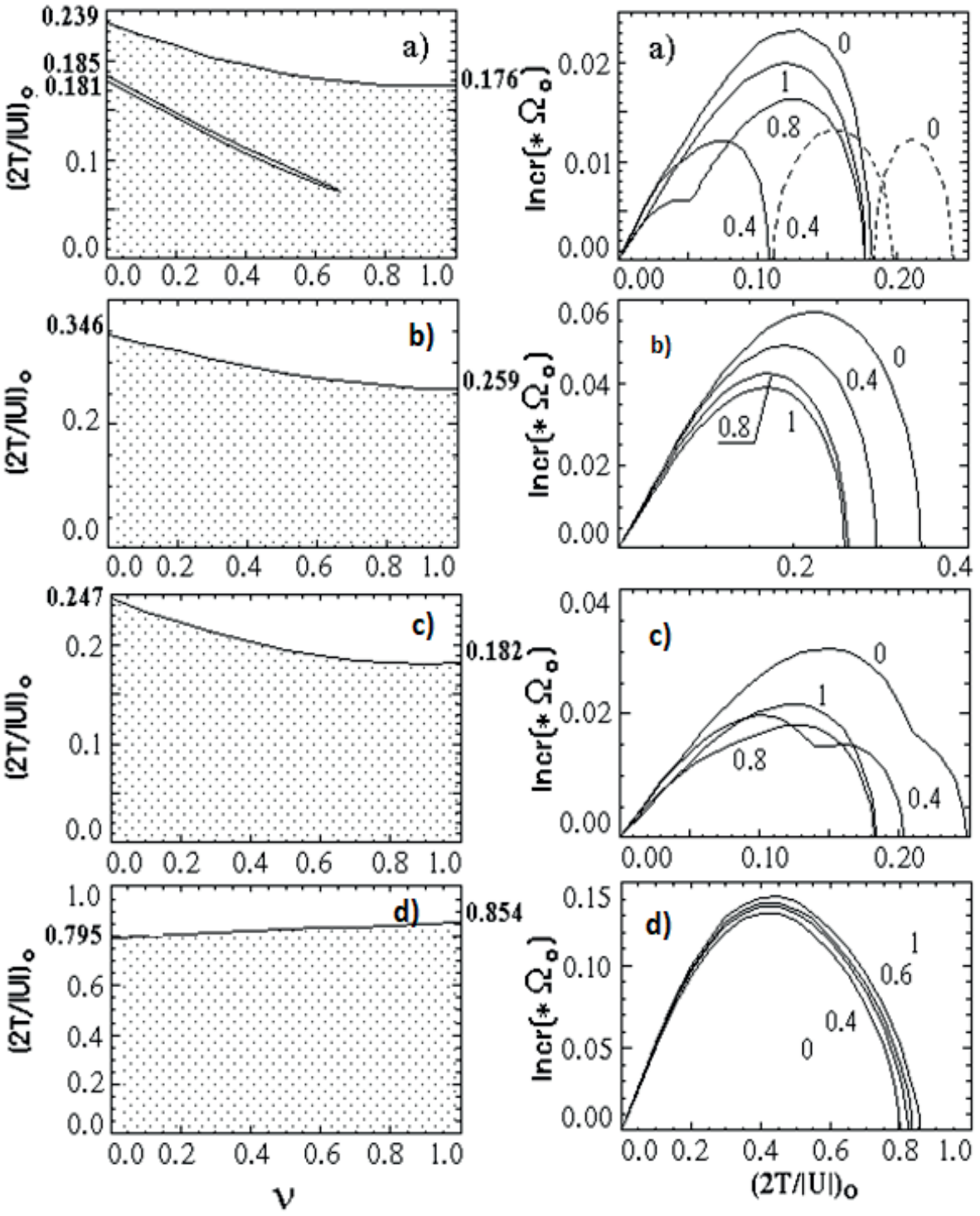

Fig. 18. Composite Model. Mode N=3. a, b) m=1; c, d) m=3; a, c) μ=0.1; b, d) μ=1.0.

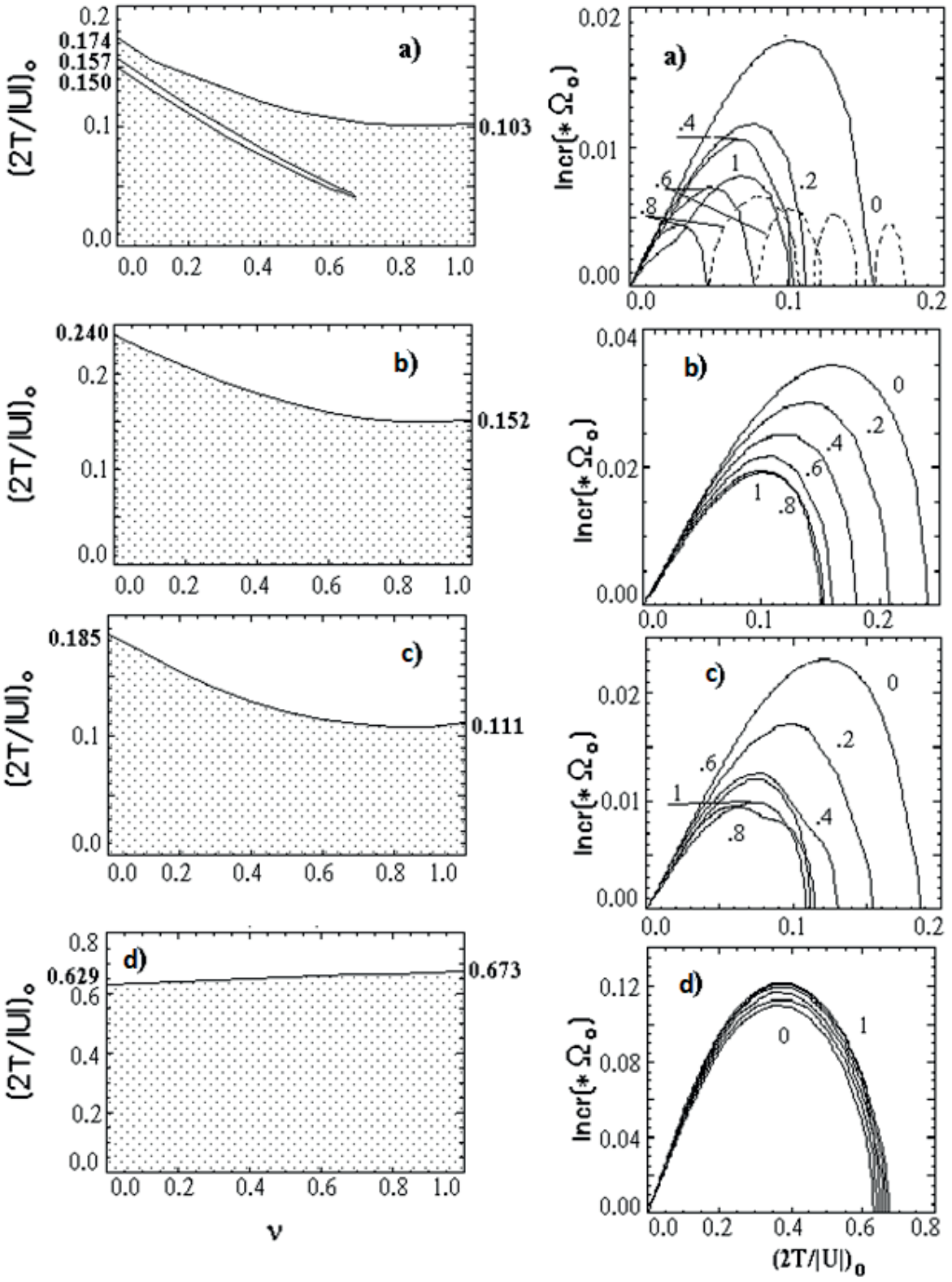

Fig. 19. Mode N=4 composite model. a, b) m=1; c, d) m=4; a, c) μ=0.1; b, d) μ=1.0.

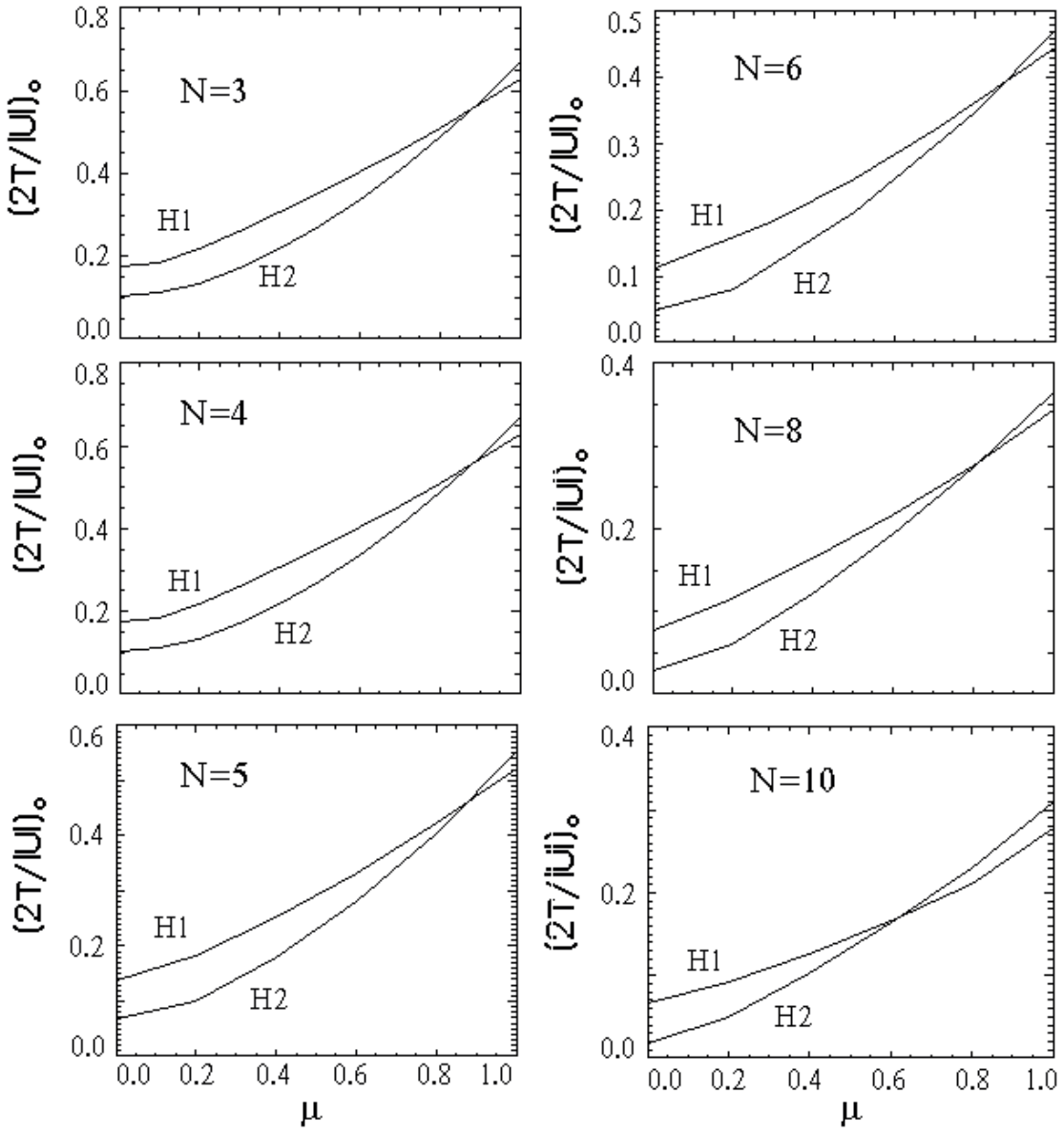

Fig. 20. Comparison of instability regions of non-equilibrium versions of Einstein (H1) and Camm (H2) balls for the maximum azimuthal wave number m=N.

(5) “Islands” of stability take place only when they exist either in the case of $\nu = 0$, or when $\nu = 1$, that is, nothing “by itself” arises at intermediate values of the superposition parameter.

It is easy to guess what will happen if we consider a more general case $\mu_1 \neq \mu_2$: we will have all possible combinations of existing dependencies.

§21. Analysis of volume perturbations

Thus, the study of the role of the superposition parameter in the case of surface perturbations did not lead to anything unexpected. When considering intermediate, between states 1 and 2 ($0<\nu<1.0$), the critical values of the initial virial ratio occupied an intermediate position, that is, there was a smooth transition from model 1 to model 2. Even when analyzing non-rotating models, it was found that the increments of the egg-shaped mode of the perturbation superimposed on the pulsating model (1.50), turned out to be much larger than the N=2 mode increments [23, 24]. Later it was shown that the increments of the N=4, n=2 mode of model (1.29) also exceed the mode N=2, although they are smaller than the increments of the egg-shaped mode of model (1.50). And the increments of the egg-shaped mode for (1.29) and the N=4 n=2 mode of model (1.50) exceed the increments of the zone of aperiodic instability and instability of the radial orbits of the ellipsoidal mode. These results show the importance of volume perturbations in the early nonequilibrium stages of the evolution of spherical self-gravitating systems.

Let us present non-stationary dispersion equations for the composite model and study the stability with respect to four volume modes.

n=1, N=3: $$a(\psi)=\frac{3}{(1+\lambda\cos\psi)^7}\left[(1-\nu)\Sigma_{13}(\gamma_\tau)+\frac{\nu}{2}K_{13}(\xi_\tau)\right]$$

n=2, N=4: $$a(\psi)=\frac{3}{(1+\lambda\cos\psi)^9}\left[(1-\nu)\Sigma_{24}(\gamma_\tau)+\frac{\nu}{4}K_{24}(\xi_\tau)\right]$$

n=3, N=5: $$a(\psi)=\frac{3}{(1+\lambda\cos\psi)^{11}}\left[(1-\nu)\Sigma_{35}(\gamma_\tau)+\frac{\nu}{8}K_{35}(\xi_\tau)\right]$$

n=4, N=6: $$a(\psi)=\frac{3}{(1+\lambda\cos\psi)^{13}}\left[(1-\nu)\Sigma_{46}(\gamma_\tau)+\frac{\nu}{8}K_{46}(\xi_\tau)\right]$$

We begin our analysis again with the case without rotation.

21a. Non-rotating model

The results of a numerical study of these equations of the composite model [68] are illustrated in Fig. 21. Even a cursory glance shows a variety of dependences, in contrast to surface perturbation modes. The dependence for the N=3, n=1 mode (Fig. 21(a)) demonstrates the role of the ν parameter, which is fundamentally different from all other studied modes, both surface and volume. Namely, the superposition of two models led to the emergence of a certain resonance effect, as a result of which the instability region from $(2T/|U|)_0 \in (0; 0.164)$ increased to $(2T/|U|)_0 \in (0; 0.993)$, $(\nu \approx 0.357)$, occupying almost the entire range of possible values taken by the virial ratio (the deviation of the model from the equilibrium state by only 0.7% leads to Having reached the maximum value $(2T/|U|)_0 \cong 0.9931$ at $\nu \cong 0.3575$, the instability region gradually decreased to the interval $(2T/|U|)_0 \in (0; 0.446)$ $(\nu = 1)$. To the left and to the right of this peak, “outgrowths” (similar to horns) extend from the main region of instability.of instability.

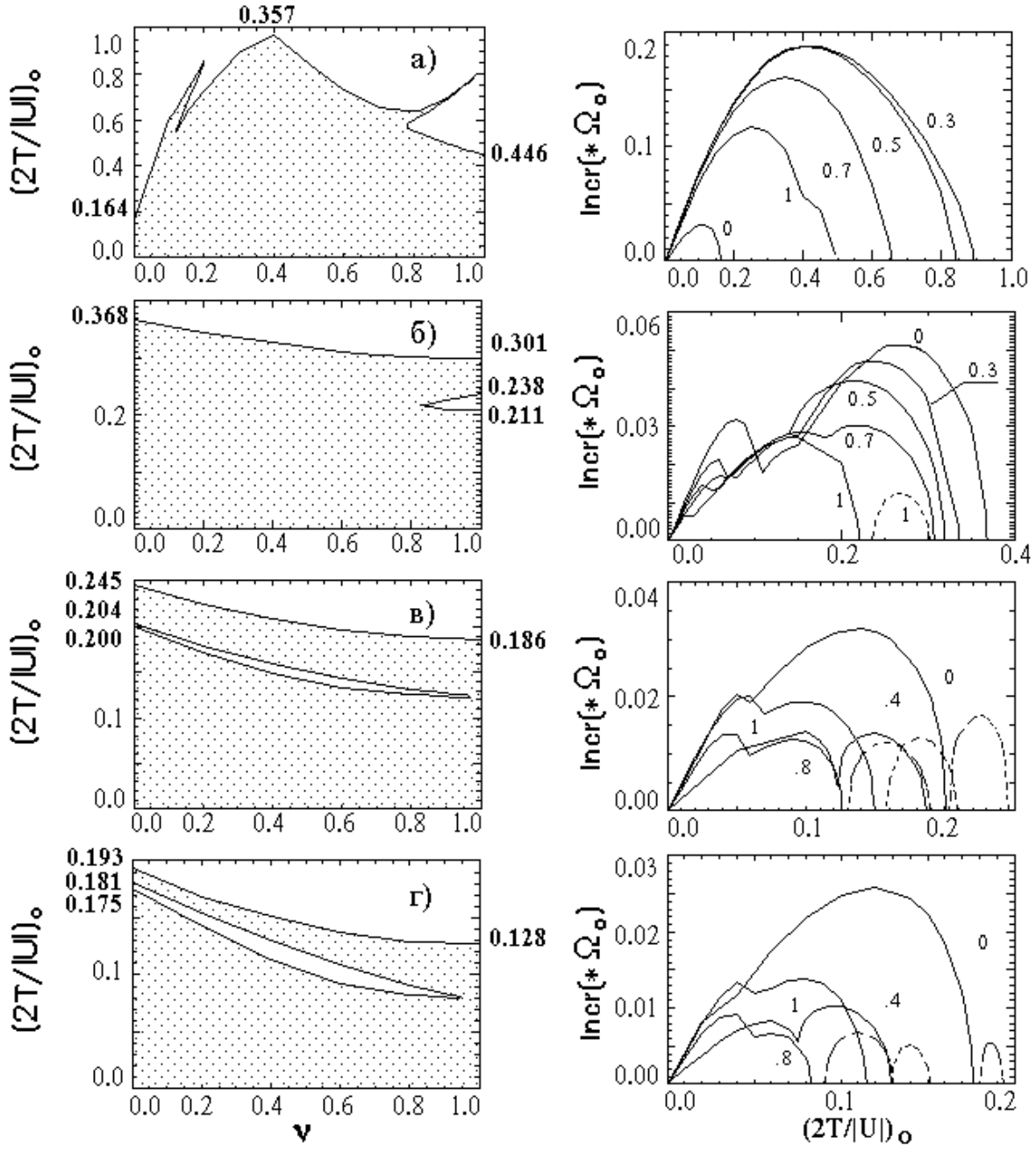

Fig. 21. Critical dependences of the initial virial ratio and dependences of the instability increments of the composite model for volume modes a) N=3, n=1; b) N=4, n=2; c) N=5, n=3; d) N=6, n=4.

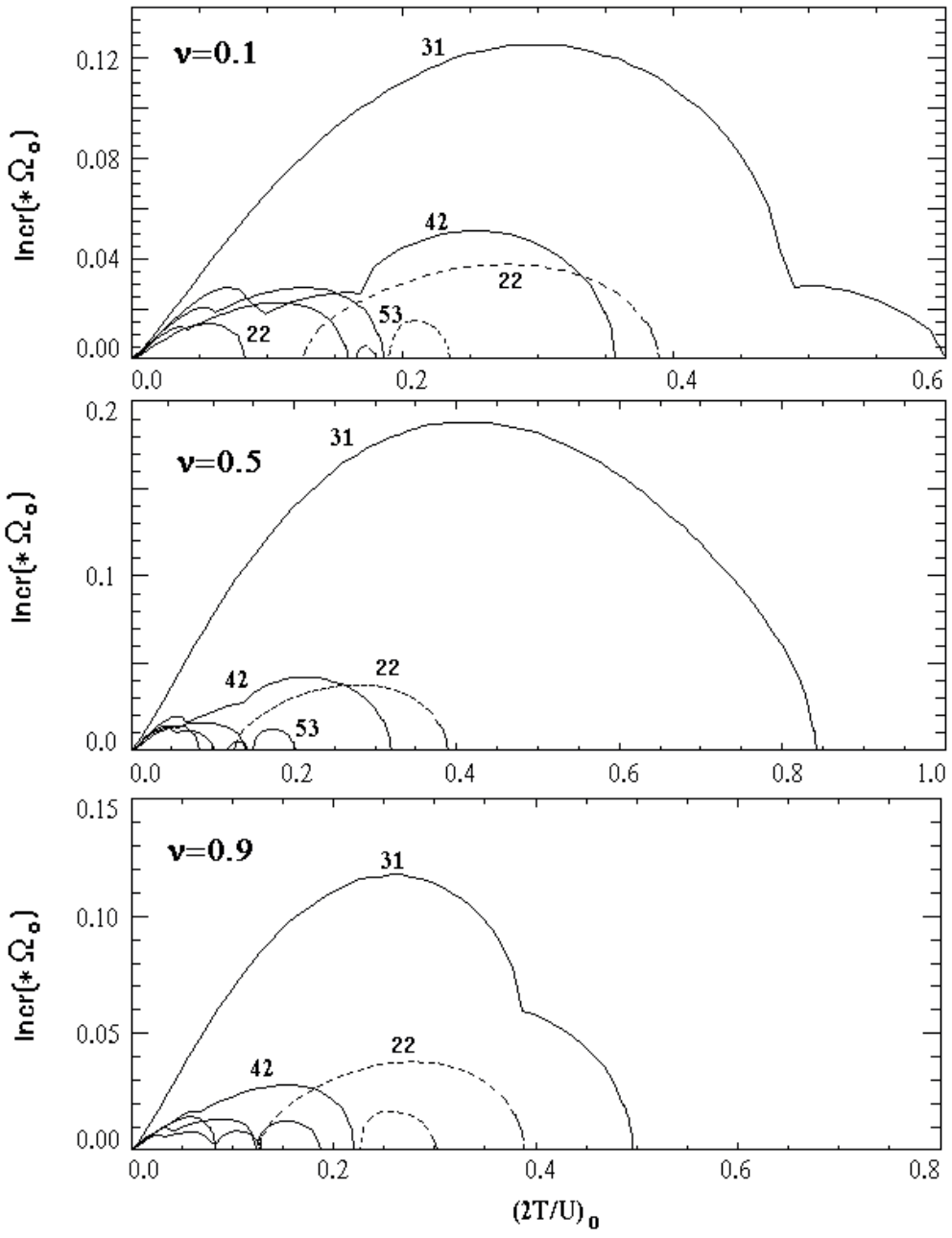

Fig. 22. Comparison of increments of volume modes of the composite model: **μ=0**

The remaining three modes, like the previously surface ones, do not show anything unusual, except for a smooth transition from model 1 to model 2. It is only worth noting that the smaller-scale modes (N=5, n=3 and N=6, n=4) are very similar to the dependences of surface modes with a slight difference: the "islands" of stability slightly expand (thicken) at moderate ν and continue to values (that is, there are actually two separate regions of instability) and $\nu \approx 0.95$, respectively.

Figure 22 compares the increments of a composite non-rotating model. Everywhere, the undisputed leader is the mode (3.1), which is significantly ahead of the mode increments (4.2) and (2.2).

21 b. Rotating compound model

Here we consider only the two largest-scale modes and briefly mention the results obtained for the other two modes [34].

Mode N=3, n=1. The results of the numerical analysis of the instability are shown in Figure 23. The combination of the dependencies in Figs. 8(a), fig. 13(a) and fig. 21(a) gave some very bizarre pictures. Against the background of general instability, there are various "offshoots" that at first look like "horns", and later turn into "peninsulas" and isolated "islands"; both those and other details are modified, reduced, completely, however, without disappearing (Fig. 23.A). The "peak", where the instability is maximum, slightly shifts (moves) to the left (to smaller ν) with increasing μ. Since the "outgrowths" only slightly distort the overall picture, the dependences of the increments are given for only one value μ (Fig. 23.B).

Mode N=4, n=2. There is nothing unexpected here (see Fig. 24). And dependences 24a and 24c are identical, since their products $\mu = 0.2$ are the same in this case.

Modes N=5, n=3 and N=6, n=4. As noted above, there is a "return" to surface modes here.

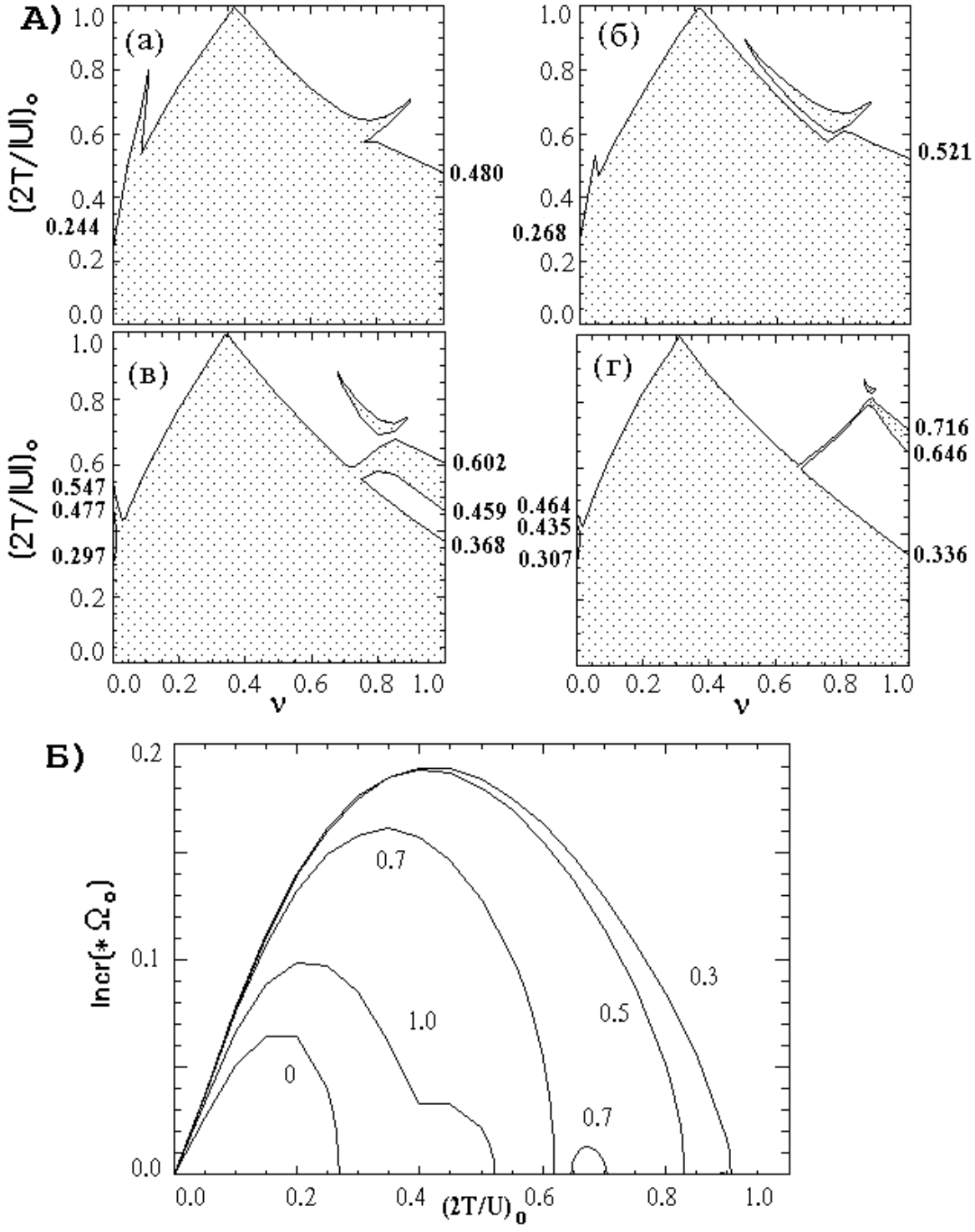

Fig. 23 A. Critical dependencies of the composite model for the egg-shaped mode: a) μ=0.2; b) μ=0.4; c) μ=0.7; d) μ=1.0. B. Dependences of increments for the value of the rotation parameter μ=0.4. The numbers next to the curves indicate the values of the superposition parameter.

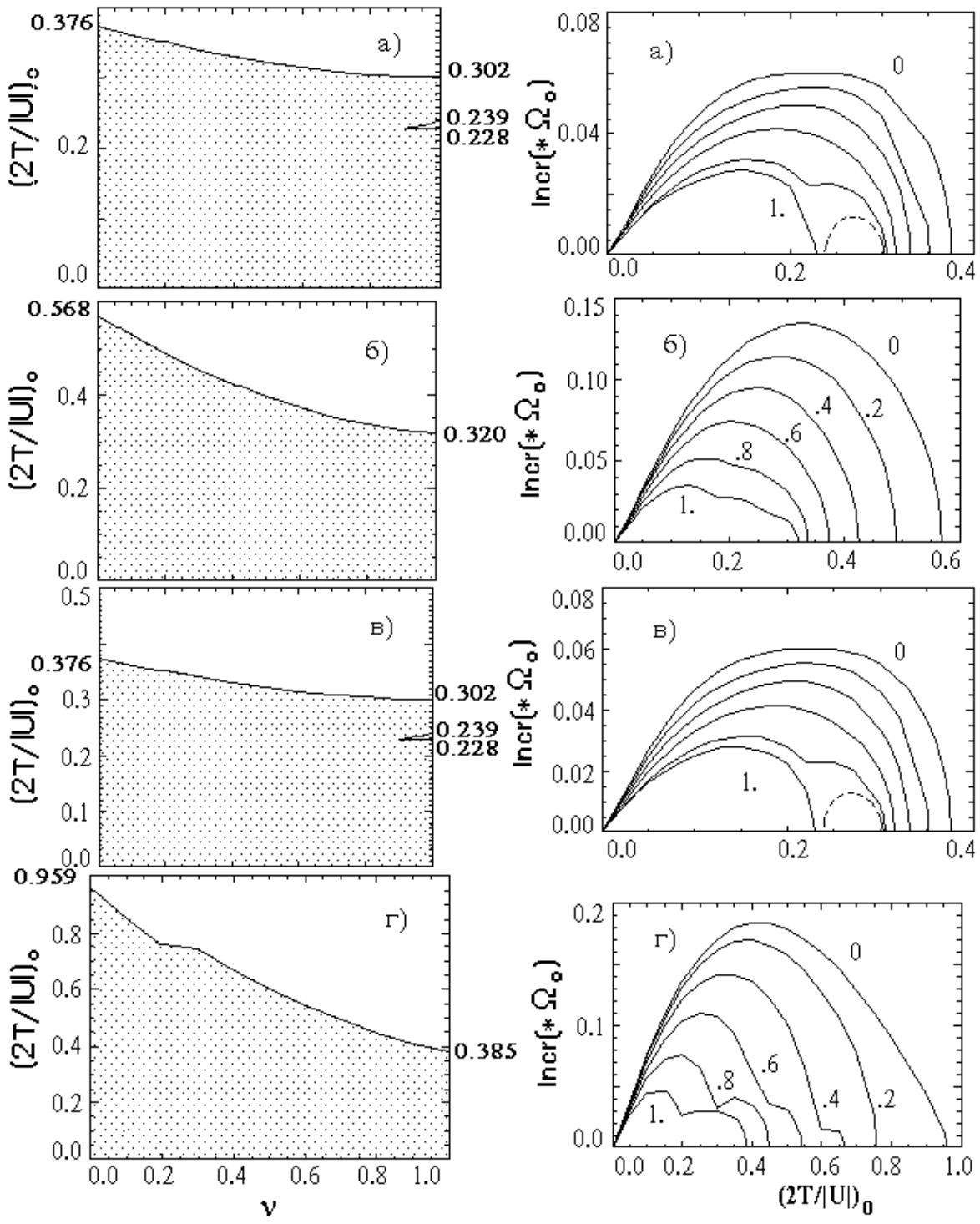

Fig. 24 Critical dependences and dependences of the composite model increments for the mode N=4, n=2; m=1: a) μ=0.2; b) μ=1.0; m=2: c) μ=0.1; d) μ=1.0.

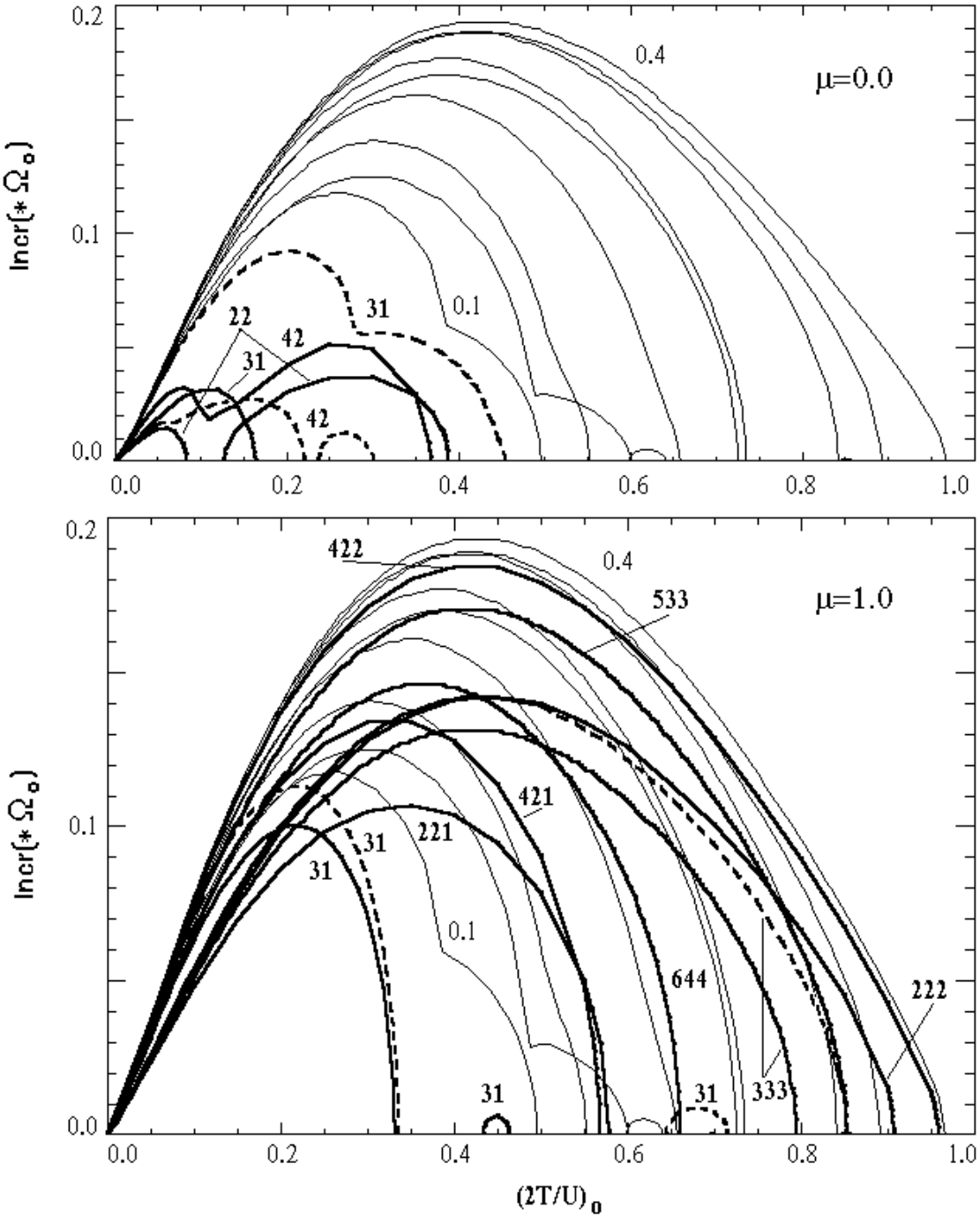

Fig. 25 Comparison of increments of non-equilibrium versions of Einstein balls (solid lines) and Camm balls (dashed line) with the egg-shaped mode of the composite non-rotating model (thin lines).

It seems that small-scale volume modes behave similarly to surface modes.

Figures comparing the modes of the composite rotating model are not given, since they will take up too much space, and this is not advisable, since for modes, in addition to (3.1), the increments of the intermediate ones also occupy an intermediate position. Finally, Figure 25 shows the volumetric mode increments for models 1 and 2 compared to the egg-shaped mode increments of the composite non-rotating model.

Thus, in the case of volume perturbation modes, it is impossible to formulate any regularities that would describe the behavior of all considered modes at once. It is only possible, on the basis of the available results, to assume a qualitative similarity between surface modes and volume modes, starting from N=5 n=3 (and to be even more precise, from N=6 n=4). Volume modes do not have the phenomenon that surface modes have and is shown in Fig. 20. The increments of volume modes with increasing order (increasing N) are not as uniform as those of surface modes (that is, the larger N, the smaller the increments), but show a more complex picture.

Thus, we have completely covered all possible states between the constructed two nonlinear models of the early stages of the evolution of rotating collapsing galaxies and studied interesting large-scale and small-scale modes of fluctuations against their background.

CHAPTER VI. COLLISIONLESS AND COLLISIONAL STELLAR SYSTEMS

§22. Collision term

Any deviation of the phase density function $\Psi\left(t, \overrightarrow{R}, \overrightarrow{V}\right)$ from purely collisionless conditions is described by the collision term $\left(\frac{\partial \Psi}{\partial t}\right)_{coll}$ which takes into account the effects due to velocity variations emerged by two-particle stellar encounters. When considering dynamic processes in stellar systems, in most cases we can neglect the effects of close stellar encounters on the time evolution of the phase density function, since under normal conditions (low concentration of stars, high relative velocities) the mean free path of the test star between two successive encounters by many orders of magnitude exceeds average interparticle distance and even the size of the stellar system. One of the key kinetic characteristics of the stellar field is the impact parameter of close encounter $d_{90} = \frac{G \cdot (m + m_f)}{V_0^2}$, where the vector of relative velocity of two approaching stars is deflected by 90°; here *G*, the gravitational constant; *m* and m_f, the masses of the test and field star respectively, and V_0, the magnitude of the relative velocity vector. The second important parameter is the characteristic mean interstellar distance, $\bar{d} \approx 0.554 \cdot \nu^{-1/3}$, where ν is the stellar number concentration. It is easy to show that in the galactic disk ($\nu \sim 0.1\, pc^{-3}, V_0 \sim 30\, km \cdot s^{-1}$) $d_{90} \approx 10^{-5}\, pc \sim AU, \bar{d} \approx 1\, pc$. In open star clusters ($\nu \sim 1\, pc^{-3}, V_0 \sim 1\, km \cdot s^{-1}$) $d_{90} \approx 10^{-2}\, pc \sim 10^3 AU$, $\bar{d} \approx 0.3 - 0.5\, pc$. In globular star clusters we deal with broader interval of the parameters ($\nu \sim 10 - 10^3\, pc^{-3}, V_0 \sim 5 - 10\, km \cdot s^{-1}$), and $d_{90} \approx 10^{-4}\, pc$, $\bar{d} \approx 0.05 - 0.1\, pc$. As can be seen, in realistic stellar systems typical impact parameter which provides noticeable change of the velocity, is much less than the average interstellar distance. This means that encounters leading to significant changes in the velocity of stars are extremally rare under normal conditions, and their short-term effect can be neglected. Nevertheless, it is stellar encounters, leading to the dissipation of mass and total energy, that ensure the long-term evolution of quasi-stationary and non-stationary stellar systems.

Due to the low frequency of stellar encounters, their effect is usually described within the framework of the theory of random forces arising during stellar encounters. There are two distinct ways to describe their action. The first considers the cumulative (that is, total) effect of successive random stellar encounters, each of which leads to a very small change in the spatial velocity of the star. This process is of a diffusion nature, and the logical development of this approach leads to an expression for the collision term of the Fokker-Planck form [71, 72]. Within the framework of an alternative approach, we introduce the probability of stellar collision, which leads to a given finite change in velocity (or

kinetic energy). Successive changes in velocity are described in terms of a purely discontinuous random process, and the collision term is written in the form of the Kolmogorov-Feller integral equation [73, 74].

There is a fundamental difference between these approaches. The Fokker-Planck approximation describes the process of stellar diffusion in velocity space (random walk) and uses calculations of linear and quadratic diffusion coefficients $\langle \Delta \boldsymbol{V_i} \rangle, \langle \Delta \boldsymbol{V_i} \cdot \Delta \boldsymbol{V_j} \rangle$. When calculating the diffusion coefficients, the results of successive independent two-particle encounters of a test star with field stars with different approach geometries, different values of impact parameters and relative velocities are summed up. Diffusion assumes that the speed of the test star changes with time in an almost continuous manner; therefore, leaving the system with almost a critical speed, the star does not carry away part of the energy of the system, and the dynamic evolution of the system proceeds with the conservation of the total energy. The Kolmogorov-Feller approximation does not have this disadvantage, because there is a non-zero probability of a significant change in the velocity of the test star, which in this case can abruptly overcome the critical velocity, carrying away part of the kinetic energy. The loss of the energy tend to accelerate dynamical evolution of the system and leads to decrease of the lifetime of stellar clusters.

All estimates of the rate of the velocity and kinetic energy change usually yield quite similar values for the characteristic time scale of these kinetic processes, which is usually identified with the collisional relaxation time. A characteristic feature of standard diffusion coefficients and relaxation time estimates is the logarithmic divergence, which arises at the upper integration limit of the cumulative effect of two-particle encounters over impact parameter. It has the form of the term $\boldsymbol{\Lambda = \ln \frac{d_{max}}{d_{90}}}$ – a close analog of the so-called Coulomb logarithm in plasma physics – that appears in the formulas for the diffusion coefficients. Here $\boldsymbol{d_{max}}$ is the upper limit of impact parameter. The problem of the upper limit of impact parameter has been raised repeatedly by many authors in their studies of stellar dynamics during past 100 years. Thus Williamson and Chandrasekhar [76] and Parenago [77] pointed out that in the frame of two-particle encounters the natural upper limit for the impact parameter should be equal to the average interparticle distance, $\boldsymbol{\bar{d}}$, because all the weaker encounters with the impact parameter $\boldsymbol{p \gtrsim \bar{d}}$ are actually simultaneous and multiple, implying that integration over all $\boldsymbol{p}$ overestimates their combined effect. By treating these distant encounters as involving only two particles, we actually incorporate into the resulting diffusion coefficients not only the effect of irregular forces, but also, to a certain extent, the effect due to the regular component of the gravitational field.

From the other side, Ambartsumyan [78], Ogorodnikov [79], King [80], Binney and Tremaine [1] and some other authors mentioned in the latter monograph [1], on the contrary, believe that d_{max} should be set equal to the characteristic size of the entire stellar system (the radius of the cluster, thickness of the galactic disk etc.) or the radius of the regular stellar orbit. Note that the precise knowledge of the upper integration limit is by no means critical for practical purposes (estimation of the relaxation time and computation of the diffusion coefficients), because the rather weak (logarithmic) divergence cannot change significantly the estimates of the above quantities whatever be a realistic choice of the maximum impact parameter. Indeed, we have for the solar neighborhood in the Galaxy $\boldsymbol{\bar{d} \approx 1\, pc}$, $\boldsymbol{d_{90} \approx 1 - 2\, AU}$, and $\boldsymbol{\Lambda \approx \ln \frac{\bar{d}}{d_{90}} \sim 11 - 12}$. Adopting $d_{max} \sim H_z \approx 100$ pc as the upper limit increases the "Coulomb logarithm" $\boldsymbol{\Lambda}$ to $\boldsymbol{\Lambda \sim 15 - 16}$, i.e., only by 40-50%, with no radical effect whatsoever on our estimates. However, the problem of choosing the upper limit for impact parameter has another aspect, which is directly associated with the physical basis of collisional kinetics of stellar systems, and we believe that a more in-depth understanding of the physics of such phenomena and attempts to describe them in a noncontroversial way is a task of fundamental importance and leads to deeper understanding of nature of random forces in stellar systems.

§23. On the multiplicity of stellar encounters

As was noted above, Agekyan [73] developed and implemented a probabilistic approach to account for stellar encounters, and derived analytical formulas for the probability $\Phi(V^2, h)$ of a stellar encounter producing the given change in the velocity of the test star in some special cases. Here $h = \frac{\Delta V^2}{V^2}, \Delta V^2$ is the change in the squared velocity of the star. The weak point of Agekyan's approach is the divergence of the probability for small changes of velocity, $\Phi(V^2, h) \sim h^{-3}$, which, in particular, prevented the computation of the average change in the star's energy. It is evident that this divergence is directly associated with the multiplicity of distant encounters mentioned above, which results in small velocity changes in the computation of the cumulative effect. To attenuate the divergence, Agekyan [81] introduced a factor accounting for the multiplicity of encounters (Agekyan's *λ-factor;* although in previous chapters of this book the symbol λ denoted the amplitude of radial pulsations, in this chapter, in order to preserve the historical original designation used by Agekian, we decided to use the same symbol λ for the reduction factor). This factor is equal to the ratio of the magnitude of the random force $\left|\delta \vec{F}\right|$ acting on the test star and produced by all stars within a thin spherical layer to the arithmetic sum of the magnitudes of the

forces $\sum\left|\vec{F}_i\right|$ acting on the test star and produced by all these stars, i.e., $\lambda(p) = \frac{|\delta\vec{F}|}{\sum|\vec{F}_i|} < 1$.

This problem was later discussed by Kandrup [82], who used simplified approach and suggested that the forces from distant stars effectively cancel each other. Detailed quantitative description of an irregular force field in locally homogeneous stellar field was presented in very important paper of Kandrup [83]. He was the first to note that the diffusion coefficients in the Fokker-Planck approximation do not diverge on the upper limit of integration over the impact parameter.

Agekyan's λ-factor has a simple physical meaning. In fact, the actual change in the velocity of the test star (within unit time interval) due to stellar encounters with impact parameters in the *(p, p+dp)* interval is determined by the magnitude of random force, $\left|\delta\vec{F}\right|$, i.e., by the geometric sum of the forces produced by all stars in the spherical layer. The use of the arithmetic sum of forces arising in two-particle encounters instead of the random force, as is the case in the calculations of the cumulative effect, results in substantially overestimated values of both the irregular force and the effect of encounters. The need to take into account the attenuation of the effect of distant encounters becomes absolutely clear if one recalls Newton's theorem about a spherically symmetric distribution of external masses. Uniform discrete distribution of gravitating material points evidently has similar properties at large distances from the test particle because particles are distributed practically uniformly over all angles. Scattering centers – i.e., field stars – are distributed randomly and uniformly with average number density (concentration) υ, and therefore the vectors of their forces acting onto the test star cancel out. This results in the effect of sui generis total *levelling* of the random force of two-particle encounters already at several interparticle distances. *Agekyan's factor* allows us to compensate the overestimation of the effect of distant encounters. To compute *λ(p)*, Agekyan [81] used the technique earlier employed by Chandrasekhar [84] to derive Holtsmark's distribution for random gravitational force, and obtained the following formula

$$\lambda(p) = \frac{4}{\pi}\int_0^\infty \frac{x-\sin x}{x^3}\exp\left(-a\frac{4\pi}{3}\nu\, p^3 x^{3/2}\right)\, dx, \qquad (6.1)$$

where $a = \frac{2}{5}\sqrt{2\pi} \approx 1.00265$.

Taking into account that $\frac{4\pi}{3}\nu\, p^3 \equiv N(p)$ – average number of stars inside the sphere of radius *p*, where *p* is the impact factor of the encounter under consideration – we can rewrite (6.1) in the equivalent form, treating *λ-factor* as a function of *N = N(p)*:

$$\lambda(N) = \int_0^{\infty} \frac{x - \sin x}{x^3} exp\left(-a\, N\, x^{3/2}\right) dx$$

Thus *Agekyan's λ-factor* is fully determined by the average number of stars located inside the sphere of radius equal to the impact parameter of the encounter considered. We will use this form of the *λ-factor* throughout the text. Function *λ(p)* cannot be expressed in terms of elementary functions, however, at large *N* is has the well-known asymptotic behavior $\sim N^{-2/3} \sim p^{-2}$ and rapidly decreases with increasing impact parameter. Fig. 6.1 shows the *Agekyan's λ-factor* as a function of the impact parameter expressed in the units of average interparticle distance, $\boldsymbol{p' = p/\bar{d}}$. As is evident from the Fig. 6.1, the effect of stellar encounters is overestimated by one order of magnitude even at two average interparticle distances from the test star. Thus Agekyan quantitatively confirmed the intuitive conclusion that within the framework of 3D-Poisson model of the stellar medium the immediate neighborhood of the test particle is the main contributor to the random gravitational force.

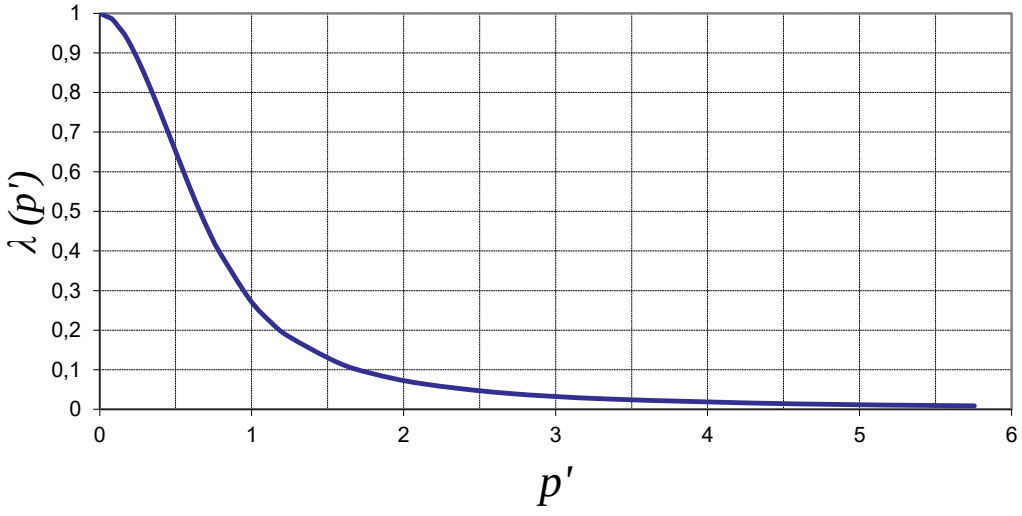

Fig. 6.1. *Agekyan's λ-factor* as a function of the impact parameter *p'* expressed in the units of average interparticle distance $\bar{d}$.

Agekyan's λ-factor cannot be expressed in terms of elementary functions and therefore we must use piecewise analytical approximations to estimate the diffusion coefficients. First, we consider *Agekyan's λ-factor* to be a function of $n = N/N_0$, where $N_0 \approx 0.7122$ is the average number of stars inside the sphere of radius equal to the average interparticle distance $\bar{d}$. We thus naturally introduce $\bar{d}$ as a scale parameter of the stellar field. We established with simple computations that *Agekyan's λ-factor* can, up to about 2-3%, be approximated by the following simple analytical formulas

$$\lambda(n) \approx \begin{cases} a \cdot exp[-b \cdot n^c] + d, n \leq 1 \\ e \cdot n^{-2/3}, \qquad\qquad n > 1 \end{cases}, \tag{6.2}$$

Where the constants *a≈0.863±0.001, b≈2.281±0.002, c≈0.616±0.0002, d≈0.141±0.002, e≈0.235±0.001* (at a significance level of 95%). This accuracy is more than sufficient for our estimates of integrals.

The current values of the impact parameter and average number of stars in the sphere of the corresponding radius are connected by the following evident relation,

$$p = \bar{d} \cdot \left(N / N_0 \right)^{1/3} = \bar{d} \cdot n^{1/3} \tag{6.3}$$

This approximation will be used to integrate the diffusion coefficients over the impact parameter up to infinite limit.

§24. Rigorous calculation for the diffusion coefficients

We will follow the paper of Rastorguev, Utkin and Chumak [75] who have explicitly shown that the consistent usage of Agekyan's reduction factor leads to convergent expression for the diffusion coefficients. We take as a basis the derivation of the diffusion coefficients described in the monograph by Binney and Tremaine [1], Fig. L.6. Initial expressions for first and second order components of the diffusion tensor for a test star averaged over only the orientation of the plane of relative orbit have the form:

$$\langle \Delta V_i \rangle = -\Delta V_{\parallel} \left(\vec{e_i} \cdot \vec{e_1'} \right), \tag{6.4}$$

$$\langle \Delta V_i \cdot \Delta V_j \rangle = (\Delta V_{\parallel})^2 \left(\vec{e_i} \cdot \vec{e_1'} \right) \left(\vec{e_j} \cdot \vec{e_1'} \right) + \\ + \frac{1}{2} (\Delta V_{\perp})^2 \left[\left(\vec{e_i} \cdot \vec{e_2'} \right) \left(\vec{e_j} \cdot \vec{e_2'} \right) + \left(\vec{e_i} \cdot \vec{e_3'} \right) \left(\vec{e_j} \cdot \vec{e_3'} \right) \right], \tag{6.5}$$

where $(\vec{e_1}, \vec{e_2}, \vec{e_3})$ – are the orts of the laboratory coordinate system; $\left(\vec{e_1'}, \vec{e_2'}, \vec{e_3'} \right)$ – are the orts of the coordinate system connected with the field star, such that the vector $\vec{e_1'}$ is directed along the vector of the relative velocity of approaching stars (see Fig. L.1 in [1]). The variations of the parallel and transverse velocity components transformed to the laboratory coordinate system and appearing in formulas (6.4), (6.5) for the diffusion coefficient are equal to ([1], Fig. L.7)

$$\Delta V_{\parallel} = \frac{2Gm_f p_{90}}{V_0 (p^2 + p_{90}^2)}, \; \Delta V_{\perp} = \frac{2Gm_f p}{V_0 (p^2 + p_{90}^2)}, \tag{6.6}$$

where m_f, V_0, p are the mass of the field star, magnitude of the relative velocity of approaching stars, and the impact parameter, respectively.

The variation in the velocity component, $\Delta V_{\parallel}$, is computed for unit time interval, i.e., it can be treated as an acceleration of the test star due to (stochastic) irregular forces. It therefore seems absolutely logical to multiply $\Delta V_{\parallel}$ before the integration by $\lambda(p)$, reduction factor of the force. From the other side, $(\Delta V_{\parallel})^2$ and $(\Delta V_{\perp})^2$ can be treated as the changes of the kinetic energy per unit time and, therefore, these changes are proportional to the *power of random force*, and these terms should also be multiplied by $\lambda(p)$, when we further integrate formulas (6.4) and (6.5) over impact parameters. Note that this is entirely equivalent to the alternative Agekyan's interpretation, that the reduction factor describes also decreasing effective concentration of field stars.

As usual, we integrate the above expressions over impact parameter with the weight $dN(p) = 2\pi\nu V_0 p dp$ equal to the number of test-star encounters with field stars with relative velocity V_0 and impact parameters in the $(p, p + dp)$ interval over unit time interval. We focus only on the integration over impact parameters, because the subsequent integration over the velocity distribution of field stars yields Rosenbluth potentials [85] like in classical stellar dynamics studies. It is easy to see that, taking into account the Agekyan's asymptotics for large values of the impact parameter, $\boldsymbol{\lambda}(p) \sim p^{-2}$, the expressions for the diffusion coefficients converge and no longer show logarithmic divergence. Let's calculate, within the framework of this approach, the exact values of the diffusion coefficients, taking into account analytical approximation for the reduction factor (6.2), shown above.

The computation of the diffusion coefficients consists in integrating velocity changes $\Delta V_{\parallel}, (\Delta V_{\parallel})^2, (\Delta V_{\perp})^2$ over impact parameters:

$$\langle \Delta V_{\parallel} \rangle = \pi\nu V_0 \cdot \int_0^{\infty} \Delta V_{\parallel} \cdot \lambda\,(p) \cdot d(p^2) \tag{6.7}$$

$$\langle \Delta V_{\parallel}^2 \rangle = \pi\nu V_0 \cdot \int_0^{\infty} (\Delta V_{\parallel})^2 \cdot \lambda\,(p) \cdot d(p^2) \tag{6.8}$$

$$\langle \Delta V_{\perp}^2 \rangle = \pi\nu V_0 \cdot \int_0^{\infty} (\Delta V_{\perp})^2 \cdot \lambda\,(p) \cdot d(p^2) \tag{6.9}$$

It is evident that $\langle \Delta V_{\parallel}^2 \rangle \ll \langle \Delta V_{\perp}^2 \rangle$, because integral (6.8) converges in "classical" computations of the diffusion coefficients, and the convergence is even more evident in our case where the integrand is multiplied by a rapidly decreasing function of impact parameter. That is why we do not consider diffusion coefficient (6.8) below.

We now use formula (6.3) and pass from integration over impact parameter to integration over the relative number of stars *n* by transforming formula (6.7) to the form

$$\langle \Delta V_{\parallel} \rangle = \frac{2\pi G^2 m_f (m+m_f)\nu}{V_0^2} \cdot \int_0^{\infty} \frac{\lambda(p)\, d(p^2)}{(p^2+p_{90}^2)} = \frac{2\pi G^2 m_f (m+m_f)\nu}{V_0^2} \cdot K^2 \cdot \int_0^{\infty} \frac{\lambda(t)\, dt}{1+K^2 t} =$$

$$= \frac{2\pi G^2 m_f (m+m_f)\nu}{V_0^2} \cdot I_1(K) \qquad (6.10)$$

where $K = \bar{d}/p_{90}$ is the ratio of two scale lengths of the stellar field and the new integration variable is $t = \left(N/N_0\right)^{2/3}$. We similarly derive the following formula for the quadratic diffusion coefficient,

$$\langle \Delta V_{\perp}^2 \rangle = \frac{4\pi G^2 m_f^2 \nu}{V_0} \int_0^{\infty} \frac{\lambda(p)\, p^2\, dp}{(p^2+p_{90}^2)^2} = \frac{4\pi G^2 m_f^2 \nu}{V_0} \cdot K^4 \cdot \int_0^{\infty} \frac{\lambda(t)\, t\, dt}{(1+K^2 t)^2} =$$

$$= \frac{4\pi G^2 m_f^2 \nu}{V_0} \cdot I_2(K), \qquad (6.11)$$

where the dimensionless functions

$$I_1(K) = K^2 \cdot \int_0^{\infty} \frac{\lambda(t)\, dt}{1+K^2 t}, \quad I_2(K) = K^4 \cdot \int_0^{\infty} \frac{\lambda(t)\, t\, dt}{(1+K^2 t)^2} - \qquad (6.12)$$

that appear in the expressions (6.10) and (6.11) for the first- and second-order diffusion coefficients, respectively, depend only on scale factors ratio *K*.

To illustrate quick convergence of the diffusion coefficients, we computed the dimensionless functions in (6.12) by numerically integrating the corresponding integrands for a wide range of scale factor ratios $1 < K < 10^5$. Note that the upper boundary of parameter *K* corresponds to rather low star number density of the order of 0.1 pc^{-3}, which resembles the conditions in the solar neighborhood. Fig. 6.2 shows the behavior of integral I_1 with increasing upper integration limit for the scale factor ratio of $K = \bar{d}/p_{90} = 1000$. It is evident from the figure that the function levels off already at relatively small *t* values demonstrating the total absence of logarithmic divergence. We now recall that $t = \left(d_{max}/p_{90}\right)^2$ to see that the integral "saturates" and the test star becomes practically "shielded" from distant encounters at distances as small as 2–3 average interparticle distances, $\bar{d}$.

Fig. 6.3 shows the behavior of dimensionless integral I_2 as a function of the upper integration limit for the same scale ratio $K = \bar{d}/p_{90} = 1000$. It is evident from the figure that this integral converges even faster, and the test star becomes actually "shielded" from distant encounters at the distances as small as about 1–2 average interparticle distances. This is no surprise given the very rapid decrease of

Agekyan's λ-factor with impact parameter of the encounters.

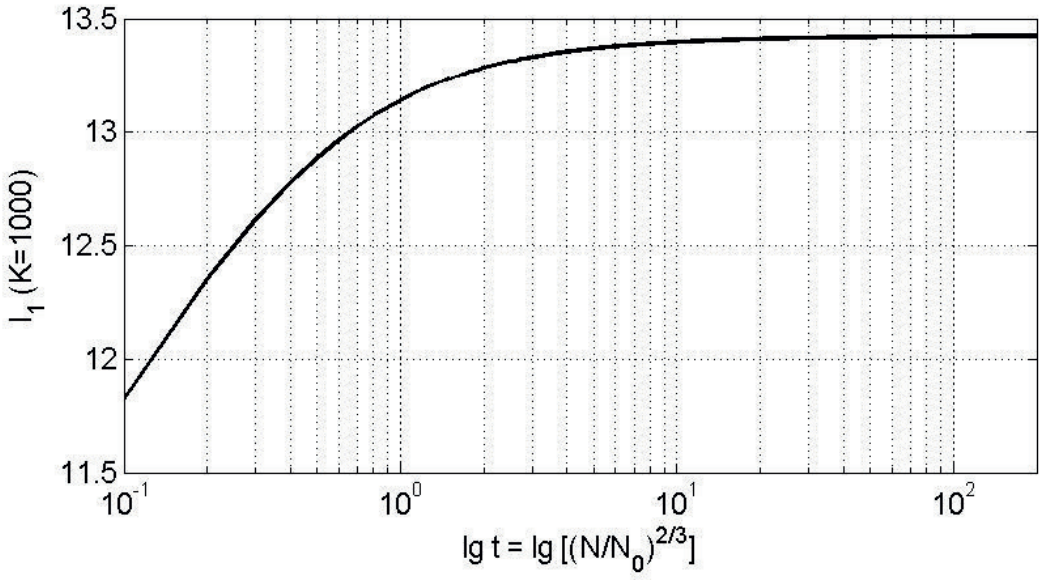

Fig. 6.2. Behavior of integral $I_1(K = 1000)$ in (6.10) as a function of the upper integration limit, t_{max}.

The parameters of linear dependences I_1 and I_2 on $lg\ (K^2)$ for sufficiently large parameter values, $K > 10$, can be easily derived from the results of our computations.

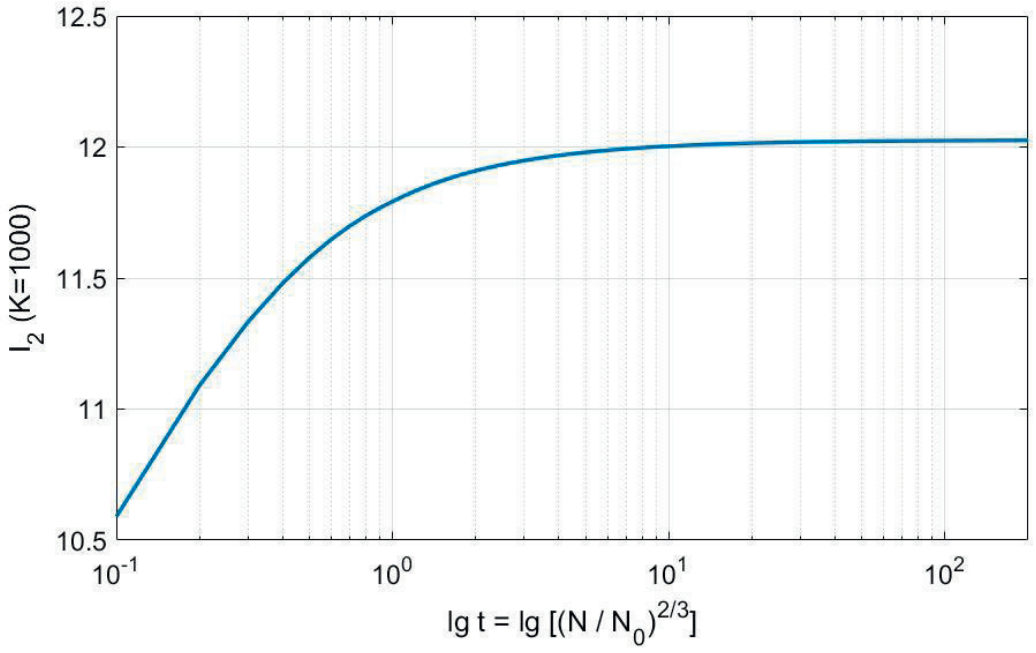

Fig. 6.3. Behavior of integral $I_2(K = 1000)$ in (6.11) as a function of increasing upper integration limit, t_{max}.

From calculated final values of dimensionless functions in (6.12), we derived simple linear approximations

$$I_1(K) \approx (2.306 \pm 0.01) \cdot lg(K^2) - (1.070 \pm 0.03) \approx 2 \cdot ln\left({K}/{1.7}\right) \qquad (6.13)$$

$$I_2(K) \approx (2.302 \pm 0.04) \cdot lg(K^2) - (2.224 \pm 0.02) \approx 2 \cdot ln\left({K}/{3.0}\right), \qquad (6.14)$$

where ln symbol is used for natural logarithm. We now substitute equations (6.13) and (6.14) into equations (6.10) and (6.11), respectively, to obtain the final expressions for the diffusion coefficients with the allowance for gravitational "shielding" of distant two-particle encounters:

$$\langle \Delta V_{\parallel} \rangle \approx \frac{4\,\pi G^2 m_f (m+m_f)\nu}{V_0^2} \cdot ln\left({\bar{d}}/{1.7 \cdot p_{90}}\right), \qquad (6.15)$$

$$\langle \Delta V_{\perp}^2 \rangle \approx \frac{8\,\pi G^2 m_f^2 \nu}{V_0} \cdot ln\left({\bar{d}}/{3.0 \cdot p_{90}}\right) \qquad (6.16)$$

The coefficients at logarithm in (6.13-6.14) are wery close to 2; we are sure that for more accurate approximation for Agekyan's factor these values will be equal exactly to 2.

Let us now compare our computed diffusion coefficients with the results of the "classical" computations with the effect of distant encounters intuitively cut off at the average interparticle distance $\bar{d}$ (see, e.g., [71]):

$$\langle \Delta V_{\parallel} \rangle \approx \frac{4\,\pi G^2 m_f (m+m_f)\nu}{V_0^2} \cdot ln\left({\bar{d}}/{p_{90}}\right), \qquad (6.17)$$

$$\langle \Delta V_{\perp}^2 \rangle \approx \frac{8\,\pi G^2 m_f^2 \nu}{V_0} \cdot ln\left({\bar{d}}/{e \cdot p_{90}}\right) \qquad (6.18)$$

First, given that we are concerned only with estimating the effect of binary stellar encounters, it is safe to say that the use of formulas (6.15) and (6.17), (6.16) and (6.18) for practical computations of diffusion and the time scales does not bring any large discrepancies. Second, from Fig. 6.2 and Fig. 6.3 it becomes absolutely clear that the effective maximum impact parameter in the frame of the two-particle encounter concept should indeed be not significantly larger than 1–2 average interparticle separations, and all the more distant encounters contribute mostly to the regular force component or to large-scale fluctuations. We thus actually corroborated intuitive point of view of the researchers who consider it necessary to restrict the effect of irregular forces calculated in the frame of binary encounters by the average interparticle distance. Strictly speaking, encounters with $p \geq (5 - 10)\,\bar{d}$ do not contribute to the random irregular force at all.

Third, and most important, both our expressions and those proposed in classical works contain the logarithmic factor. However, in our approach it has a fundamentally different physical meaning. We show that the reduction factor effectively cuts multiple distant encounters and allows avoiding the divergence of integrals at the upper limit. **In our case, the logarithmic factor appears naturally and is due to the fact that any stellar medium is characterized by two totally independent scale lengths: the average interparticle separation, $\bar{d} \approx 0.554 \cdot \nu^{-1/3}$, which is related only to the concentration of stars, and the parameter of close encounter, $p_{90} = \frac{G(m+m_f)}{V_0^2}$, which reflects the dynamics of the stellar medium (it is determined by the masses and characteristic velocities of stars).** It should be noted that these parameters become directly related only under the conditions of virial equilibrium.

Nearly the same result was obtained earlier by Kandrup [82, 83] who analyzed kinetic processes in a locally homogeneous stellar media (e.g. homogeneous over distance comparable to the local mean interparticle spacing). Using the distribution of random forces analogous to Holtsmark, he was able to derive rigorous expressions for the diffusion coefficients very similar to classic expressions for uniform infinite stellar field. He also emphasized that the Coulomb logarithm in these expressions does reflect the ratio of two characteristic scales rather than logarithmic divergence. Finally, we must note that two different methods used by us and by Kandrup [82, 83] to calculate the contribution of random forces to the diffusion in the velocity space, lead to the same conclusion about very effective shielding of distant encounters, which results in the convergence of diffusion coefficients, in contrast to classical artificial cut-off of distant encounters. Our technique seems to be more simple and straightforward.

Agekyan's λ-factor was derived based on the Holtsmark distribution for infinite static uniform stellar medium. In real stellar systems the size of spatial irregularities (density fluctuations) is significantly greater than the average interparticle separation, and therefore the estimates of the range of *irregular forces* produced by stars obtained here are, in our opinion, quite applicable to nonuniform systems as well, as was also noted by Kandrup [82, 83]. It is evident that the influence of spatial irregularities may show up as collective effects in the gravitating medium, including the effects due to the fractal structure of the medium. We believe that the passage to the limit in the computation of kinetic coefficients in the case of fractal medium also allows us to ignore the effect of irregularities located beyond several *intercluster* distances.

REFERENCES

1. **Binney J., Tremaine S.** Galactic dynamics – Princeton Univ. Press, 2008, 733pp
2. **Silchenko O.K.** Origin and evolution of galaxies. Fryazino. 2017, 224cc
3. **Miller R.H., Smith B.F.** Six collapses // Astroph. J., 1979, v. 227, p. 407-414
4. **Aguilar L., Merritt D.** The structure and dynamics or galaxies formed by cold dissipationless collapses // Astrophys. J., 1990, v. 354, p. 33-51
5. **Barnes J., Grodman J., Hut P.** Dynamical instabilities in spherical stellar systems // Astrophys. J., 1986, v. 300, p. 112-131
6. **Nuritdinov S.N.** Nonlinear stationary waves. I. Strong waves in a homogeneous self-gravitating system // Astrophysics, 1975, v. II, p. 135-144
7. **Antonov V.A., Nuritdinov S.N.** Oscillations and stability of a mixed star-gas ellipsoidal system // Kinematic and dynamic characteristics of individual stellar systems. – Tashkent: Fan, 1978, p. 122-141
8. **Zeldovich Y.B., Novikov I.D.** Structure and Evolution of the Universe. – Moscow: Nauka, 1975
9. **Zeldovich Y.B.** Decay of homogeneous matter into parts under the action of gravity // Astrophysics, 1970, v. 6, p. 319-335
10. **Nuritdinov S.N.** Nonlinear oscillations of some homogeneous models of stellar systems. II // Bulletin of Leningrad State University, 1977
11. **Antonov V.A., Nuritdinov S.N.** Nonlinear non-radial oscillations of two-dimensional models of stellar systems // Reports of the USSR Academy of Sciences, 1977, v. 232, № 3, p. 545-547
12. **Einstein A.** Collected papers. Volume 2 – Moscow: Nauka, 1967, p.514-531
13. **Fridman A.M., Polychenko V.L**… Physics of gravitating systems – New York: Springer, 1984
14. **Antonov V.A., Nuritdinov S.N**… Instability of a nonlinearly pulsating model of a stellar system: Einstein's sphere // Sov.Astron., 1981, v.25, p.659-663
15. **Synakh V.S., Fridman A.M., Shukhman I.G**… Stability of a model of a spherical cluster of stars with a non-zero moment of rotation // Rep. the USSR Academy of Sciences, 1971, v.201, p.827-830
16. **Nuritdinov S.N**… A new series of non-stationary models of galactic subsystems: accounting for rotation // Astron. Tsir., 1992, №1553, p.9-10
17. **Nuritdinov S.N**… Non-linear models of non-stationary self-gravitating systems and their stability problem // A.Ap.Trans., 1995, v…7, p…307-309
18. **Ostriker J.P., Peebles P.J.T**… A numerical study of the stability of flattened galaxies: or can cold galaxies survive // Astrophys.J., 1973, v.186, p.467-480
19. **Camm C.L**… Self-gravitating star systems // Mon.Not.RAS., 1952, v.112, p.115-176
20. **Malkov E.A**… Stability of a pulsating rotating model of a stellar system // Astrophysics ,1986 ,v.24 ,p.416-420
21. **Nuritdinov S.N.** Instability of a nonlinearly pulsating model of a stellar system // Sov. Astron. , 1983, v.27, p.24-26

22. **Nuritdinov S.N.** Rotational-symmetric oscillations of a gravitating ellipsoid of rotation with a corona // Sov.Astron., 1978, v.22, p.21-23
23. **Nuritdinov S.N.** Nonlinear models and physics of instability of non-equilibrium collisionless self-gravitating systems. Author's abstract of doctoral dissertation, St. Petersburg, 1993;
24. **Nuritdinov S.N.** Instability of a nonlinearly pulsating model of a stellar system: Volume perturbations on the background of a non-equilibrium version of Einstein's sphere // Sov. Astron., 1985, v.29, p.293-299
25. **Shukhman I.G.** On the theory of stability of gravitating systems with respect to surface perturbations // Astron.Zh, 1973, v.50, p. 651-653
26. **Babakov I.M.** Theory of oscillations – Moscow: Nauka, 1968, 560 pp.
27. **Aguilar L.A.** Violent relaxation, dynamical instabilities and the formation of elliptical galaxies // Mexic Astron. Astroph., 1990, v. 21, p. 89-98
28. **Min K.W., Choi Ch.S.** Cold collapse of a spherical stellar system // Mon. Not. RAS, 1989, v. 238, p. 253-259
29. **Polyachenko V.L., Fridman A.M**… Equilibrium and stability of gravitating systems – Moscow: Nauka, 1976, 447 pp.(Russian)
30. **Antonov V.A.** Figures of equilibrium // Itogi nauki, ser. Astron., 1975, v.10, p.7-60 (Russian)
31. **Nuritdinov S.N., Mirtadjieva K.T., Sultana M.** Instabilities in a nonstationary model of self-gravitating disks. I. Bar and ring perturbation modes // Astrophysics, 2008, v. 51,, p.410-423
32. **Fridman A.M.** Equilibrium and stability of collisionless gravitating systems // Itogi nauki, ser. Astron., 1975, v. 10, p. 61-159 (Russian)
33. **Chandrasekhar S.** Ellipsoidal figures of equilibrium. Yale Univ., 1973, 288pp
34. **Gainullina E.R.** Instabilities of the early evolution stage of E-galaxies and globular clusters. Author's abstract of dissertation, Tashkent, 2001.
35. **Lynden – Bell D.** Can spherical clusters rotate? // Mon. Not. RAS, 1960, v. 120, p. 204-213
36. **Vilenkin N.Ya.** Special functions and the theory of group representations. Moscow: Nauka, 1991, 576 pp. (Russian)
37. **Hodge P.W.** Galaxies. Cambridge; Harvard Univ. Press, 1986
38. **Lynden-Bell D.** Statistical mechanics of violent relaxation in stellar systems // Mon. Not. RAS, 1967, v. 136, p. 101-121
39. **White S.D.M.** Dissipationless formation of elliptical galaxies // Structure and dynamics of elliptical galaxies. IAU Symp. 127, 1986, p. 339-351
40. **Jones B., Rees M**. The epoch of galaxy formation // Large-scale structure of the Universe, IAU Symp.79 ,1981 ,p.416-428
41. **Peebles P.J.E.** The large-scale structure of the Universe.1983, 408 pp.
42. **Gott J.R.** Dynamics of rotating stellar systems: collapse and violent relaxation // Astrophys. J., 1973, v. 186, p. 481-500
43. **Binney J.** Is the flattening of elliptical galaxies necessary due to rotation? // Mon. Not. RAS, 1976, v. 177, p. 19-29

44. **Illingworth G.** Rotation in 13 elliptical galaxies // Astrophys. J., 1977, v. 218, p. 143-147
45. **Surdin V.G.** Structure and dynamics of elliptical galaxies IAU Symp.127 // AstronZh, 1988, v.65 ,p.1112-1113
46. **Merritt D., Tremaine S., Johnstone D.** Models of violently relaxed galaxies // Mon. Not. RAS, 1989, v. 236, p. 829-841
47. **Fridman A.M.** Development of views on relaxation processes in the Galaxy in the works of V.A. Ambartsumian // Soobshe. Byurakan Observatory, 1985, v.55 ,p.46-51(Russian)
48. **Polyachenko V.L**… On the nature of the universality of the structure of elliptical galaxies //Pis'ma v AZh, 1991, v.17 ,p.691-697
49. **Nuritdinov S.N**… A possible way of Elliptical formation: an analytical model with rotation // IAU Symp.153 ,Galactic bulges ,1992 ,p.27
50. **Madsen J**. On the applicability of the statistical mechanical theories of violent relaxation // Astroph.J., 1987, v.316, p.497-501
51. **Polyachenko V.L., Shukhman I.G**… Investigation of the stability of collisionless spherical-symmetric systems // AstronZh, 1981, v.58, p.933-948
52. **Van Albada T.** Dissipationless galaxy formation and the r1/4 law// Mon. Not. RAS, 1982, v. 201, № 3, p. 939-956
53. **McGlynn T.A.** Dissipationless collapse of galaxies and initial conditions // Astroph. J., 1984, v. 281, p. 13-30
54. **Merritt D., Aguilar L.** A numerical study of the stability of spherical galaxies // Mon. Not. RAS, 1985, v. 217, p. 787-804
55. **Silk J**. Birth of galaxies //Astroph. Ages and Dating Methods.1996, p.467.
56. **Sridhar S., Nityananda R.** Undamped oscillations of collisionless stellar systems: spheres, spheroids and discs // J. Astrophys. Astron., 1989, v. 10, p. 279-293
57. **Gradshteyn I.S., Ryzhik I.M**. et al. Tables of integrals, sums, series and products – Moscow: Nauka, 2016 , 1108 p.(Russian)
58. **Nuritdinov S.N**. Non-stationary models of spherical star clusters and their stability // Star clusters. Ural State University, 1987, p.121-125
59. **Antonov V.A., Nuritdinov S.N**… Exact form of eigen oscillations of the phase model of Camm spherical star cluster // Astron. Tsir., 1990, №1545 ,p.3-4
60. **Polyachenko V.L**… Stability of spherical gravitational collisionless systems // Astroph.,1987 ,v.27, p.296-309
61. **Cox J.P**… Theory of stellar pulsations – Moscow: Mir, 1983, 326 pp
62. **Nuritdinov S.N**… Instability of a nonlinearly pulsating model of a stellar system: Volume perturbations: Camm model // Sov. Astron., 1991, v.35, p.377-383
63. **Antonov V.A**… On the instability of stationary spherical models with purely radial motion // Dynamics of galaxies and star clusters Alma-Ata: Nauka ,1973 ,p.139-143(Russian)
64. **Polyachenko V.L., Shukhman I.G**… Investigation of the stability of collisionless systems with quadratic potential I, II //Preprint SibIZMIR SO AN USSR ,1972 ,№1-72 ,31pp.(Russian)

65. **Polyachenko V.L.** On the analytical theory of instability of radial orbits // Astron. Tsir.,1991 ,№1551, p.1-2(Russian)
66. **Agekyan T.A.** Spherical systems of stars and galaxies at early stages of evolution // Vestnik of Leningrad State University ,1962, №1, p.152-161
67. **Bonnor W.B.** Jeans' formula for gravitational instability // Mon.Not.RAS., 1957, v.117, p.104-117
68. **Gaynullina E.R., Nuritdinov S.N.** Towards the theory of early evolution stage of galaxies // Uzbek Journal of Physics, 2000 ,v.2, №3, p.185-193
69. **Gaynullina E.R., Nuritdinov S.N.** On the instabilities in the composite model of collapsing galaxy // Izvestiya RAN, series physical,1998, v.62, №9, p.1738-1742
70. **Gaynullina E.R.** Stability analysis of the non-stationary composite model of spherical stellar system: volume oscillations // Stellar Dynamics: from classic to modern. S.-Petersburg, 2001, p.391-394
71. **Spitzer L., Schwarzschild M.** The possible influence of interstellar clouds on stellar velocities // Astrophys. J., 1958, v.114, p.385
72. **Spitzer L. Harm R.** Evaporation of stars from isolated clusters // Astrophys. J., 1958, v.127, p.544
73. **Agekyan T.A.** The probability of a stellar approach with a given change of the absolute velocity // Sov. Astron., 1959, v.3, p.46
74. **Agekyan T.A.** The velocity distribution function and the rate of dissipation in systems of gravitational bodies // Sov. Astron., 1959, v.3., p.280
75. **Rastorguev A.S., Utkin N.D., Chumak O.V.** The effect of the multiplicity of stellar encounters and the diffusion coefficients in a locally homogenious three-dimensional stellar medium: Removing classical divergence // Astron. Lett., 2017, v.43, p.536
76. **Williamson R.E., Chandrasekhar S.** The time of relaxation of stellar systems. II // Astrophys. J., 1941, v.93, p.305
77. **Parenago P.P.** // Kurs zvezdnoi astronomii (A course of Stellar Astronomy), 1954, Moscow: Gos. Izd. Tekhn.-Teor. Lit.
78. **Ambartsumyan V.A.** // 1938, Uch. Zap. Leningr. Univ., Issue 22, 19, 1938 (in Russian)
79. **Ogorodnikov K.F.** // Dinamika zvezdnykh sistem (The Dynamics of Stellar Systems), 1958, Moscow: Gos. Izd. Fiz.-Mat. Lit. (in Russian)
80. **King I.R.** // Vvedenie v klassicheskuyu zvezdnuyu dinamiku" (An introduction to the classical Stellar Dynamics), 2002, Moscow: URSS (in Russian)
81. **Agekyan T.A.** Correction for multiple encounters in a fluctuating force field // Sov. Astron, 1962, v.5, 809
82. **Kandrup H.E.** Stochastic problems in stellar dynamics // Thesis (PhD), 1980, The University of Chicago, USA

83. **Kandrup H.E.** Stochastic gravitational fluctuations in a self-consistent mean field theory // Physics Reports, 1980, v.63, pp.1-59
84. **Chandrasekhar S.** Stochastic problems in physics and astronomy // 1943, Rev. Mod. Phys., v.15, Issue 1, pp.1-89
85. **Rosenbluth M.N., MacDonald W.M., Judd D.L.** Fokker-Planck equation for an inverse-square force // Phys. Rev., 1957, v.107, p.1

About the authors:

Salahutdin N. Nuritdinov – Dr.Sci, Professor, Chair of the Astrophysical Laboratoty, Physics Faculty, Mirzo Ulugbek National University of Usbekistan, 100174, Universitet street 4, Olmazor district, Tashkent, Uzbekistan Republik

Alexey S. Rastorguev – Dr. Sci., Professor, Chair of the Experimental Astronomy Division, Physics Faculty, Lomonosov Moscow State University, 119991, Leninskie Gory 1, bld. 2, Moscow, Russian Federation

Book cover:

Three-colour composite image of NGC 628 (M 74) galaxy, taken by James Webb Space Telescope (NASA)."